UTS UNIVERSITY OF TECHNOLOGY SYDNEY

Essays in electricity market design and semi-structural price modelling

by Krisztina Katona

Thesis submitted in fulfilment of the requirements for the degree of

Doctor of Philosophy

under the supervision of Assoc. Prof. Christina Sklibosios Nikitopoulos, Prof. Erik Schlögl and Dr. Julius Susanto

University of Technology Sydney
UTS Business School (Finance Discipline Group)
January 2024

Certificate of original authorship

I, Krisztina Katona, certify that the work in this thesis has not been previously submitted for a degree nor has it been submitted as a part of the requirements for any other degree.

I also certify that this thesis has been written by me. Any help that I have received in my research and in the preparation of the thesis itself has been fully acknowledged. In addition, I certify that all information sources and literature used are quoted in the thesis.

This research is supported by the Australian Government Research Training Program.

Krisztina Katona

9 January, 2024

Abstract

Electricity market designs are complex, diverse and constantly evolving frameworks of policies with multidisciplinary theoretical work underpinning them. The fast transforming landscape of the electricity sector, driven by the global commitment to meet emission goals, calls for a constant re-evaluation of market designs around the world. To this end, the economic equilibrium models aiding market oversight should also be adapted to the reality of power markets. The current thesis contributes to this discussion.

The first chapter describes the general features of electricity markets, focusing on the theory of price formation on security-constrained economic-dispatch (SCED) principles. The equivalence of obtaining price as the dual of the energy balance constraint from an SCED optimisation to the standard economic equilibrium argument is shown under certain conditions. The application of this argument to electricity markets using the merit order rule to infer supply and demand curves from the bid data is also demonstrated from first principles. This equilibrium framework is then extended with the typical features of power markets, such as storage fuel activity and physical constraint effects.

The second chapter contributes an in-depth survey of Australia's National Electricity Market (NEM) with numerical examples that untangle several typical price outcomes from the central dispatch data. A wide array of industry publications are summarised to comprehensively describe how the market works and how the price is set in the NEM, including the reliability mandate, the timeline of dispatch and the security constraints in the NEM Dispatch Engine. This survey reveals a number of additional market design features that have a price impact and should be incorporated into the economic equilibrium argument.

The third chapter presents a novel economic equilibrium approach for price modelling that replaces the widely used exponential supply function with a hyperbolic one to permit price negativity. The previously identified market design factors that are compatible with the assumed supply curve construction mechanics are also incorporated into this model. Renewable and

storage fuels in the fuel mix, capacity limits, inter-regional trade, network constraint effects and disorderly bidding are thus included in the proposed semi-structural price model. The distributional fit of this approach is verified in a multi-regional empirical study.

The fourth chapter infers the supply curve of a particular market by approximating the price result of the market clearing process for different levels of demand. This is performed for three real-world market designs around the world – the Pennsylvania-New Jersey-Maryland Interconnection (PJM) in the United States, the Balancing Market (BM) in Great Britain and the NEM in Australia – to investigate the monotonicity property of the implied supply curves. A small-scale case study compares supply curves and welfare across these market designs. Non-monotonicity of supply is confirmed owing to fixed cost by slow-start units in the PJM and minimum loading and dynamic interconnector losses in the NEM. A detailed discussion is presented on welfare outcomes, underscoring the primacy of the PJM market design in social surplus.

Acknowledgements

I am most grateful to Assoc. Prof. Christina Sklibosios Nikitopoulos and Prof. Erik Schlögl at the University of Technology Sydney for their excellent supervision and encouragement over the years. Thank you! I also deeply appreciate the contributions of my external supervisor, Dr. Julius Susanto.

I thank my mentor from the Industry Mentoring Network in STEM (IMNIS) programme, Bill Jackson, for having taken a barrage of questions about electricity systems and having helped me since the early days.

I would also like to say thanks to Prof. Michael Pollitt at the Energy Policy Research Group at the University of Cambridge for the inspiring discussions during my academic visit.

I appreciate the comments around the wide-spread use of bidding software from anonymous practitioners. I thank Dr. Les Clewlow for their insights on electricity price modelling. I am grateful to Dr. Alan Rai for helping with the NEM market design. I wish to express my genuine respect to Nicholas Gorman for having created Nempy. I thank Allan O'Neil for their detailed explanation of the strange price setter cases that I would not have unravelled otherwise. I would like to express my gratitude to my fellow student Dr. Muthe Mwampashi for being an inspiration on dedication. I also thank Benjamin Fram for guiding me through the PJM-land. I am grateful to Francisco Celis Andrade for doing the same for the BM. Last, thank you, Dr. Marton Benedek, for asking me to formalise some facts mathematically.

I am also grateful to the seminar participants at the Energy Finance Italia 6 Workshop, the International Conference on Sustainability, Environment and Social Transition in Economics and Finance, the 6th Commodity Markets Winter Workshop and the KTI Summer Workshop. I also thank the Quantitative Social and Management Sciences research group at the Budapest University of Technology and Economics for the constructive feedback during my academic visit.

This thesis would not have been possible without the support I received from the University of Technology Sydney (UTS). I am delighted to have been awarded the UTS International Research Scholarship, the UTS President's Scholarship as well as conference funds as part of the Finance Research Training Program Funding and the Vice-Chancellor's Conference Fund.

I also thank the administrative staff at the UTS Business School, who always assisted me in the most helpful manner.

Last but not least, I could not be more grateful to my friends and family for their enduring motivation. My final thanks goes to them.

Contents

Certificate of original authorship i

Abstract ii

Acknowledgments iv

List of figures viii

List of tables ix

Acronyms and abbreviations xi

1 Introduction 1

1.1 Motivation 1

1.2 Literature review 3

1.3 Thesis outline 17

2 Market design in electricity markets 19

2.1 Introduction 19

2.2 Market participants and governance goals 21

2.3 Security-constrained least-cost pricing 24

2.4 Differences in market design and fuel mix 35

2.5 Financial markets along electricity markets 37

2.6 Conclusion 38

3 A survey of the Australian National Electricity Market 40

3.1 Introduction 40

3.2 Overview . . . 41
3.3 Dispatch . . . 50
3.4 Price settlement . . . 71
3.5 Conclusion . . . 82

4 A hyperbolic supply function approach to price modelling 84

4.1 Introduction . . . 84
4.2 Description of the hyperbolic electricity price model . . . 86
4.3 Model implementation . . . 116
4.4 Model results . . . 133
4.5 Conclusion . . . 139

5 Supply function non-monotonicity and welfare under different market designs 140

5.1 Introduction . . . 140
5.2 Algorithms for price and welfare . . . 143
5.3 Non-monotonicity of supply . . . 159
5.4 Case study . . . 168
5.5 Implications . . . 189
5.6 Conclusion . . . 193

6 Conclusion 195

6.1 Limitations and further research . . . 196

References 198

List of figures

2.1 **Market bid stack** 29

3.1 **FCAS trapezium** 64

4.1 **Modelled paths: A full-range view** 136

4.2 **Distributional results: A mid-range view** 138

5.1 **The NEM fuel mix and supply curve** 175

5.2 **The PJM fuel mix and supply curve** 176

5.3 **The BM fuel mix** 177

5.4 **Consumer surplus** 178

5.5 **Producer surplus** 179

5.6 **Social surplus** 180

5.7 **Cost of energy and frequency balancing** 182

List of tables

2.1 **Market bid stack with two-way fuel activity** 28

2.2 **Price effect of two-way fuel activity** 30

3.1 **Market systems** 42

3.2 **Fuel mix in the NEM** 46

3.3 **Constraint sets in the NEM** 56

3.4 **Ancillary services** 62

3.5 **Capacity indicators** 67

3.6 **Price settlement: An as-bid $\lambda_N^{c,l} := \lambda_i$ setting** 72

3.7 **Price settlement: FCAS effects in a $\lambda_N^{c,l} := \lambda_N^c$ setting** 73

3.8 **Price settlement: Loss effects in a $\lambda_N^{c,l} := \lambda_N^l$ setting** 75

3.9 **Price settlement: marginal load in a $\lambda_N^{c,l} := \lambda_i$ setting** 76

3.10 **Price settlement: High price in a $\lambda_N^{c,l} := \lambda_N^{c,l}$ setting** 77

3.11 **Price settlement: Low price in a $\lambda_N^{c,l} := \lambda_N^{c,l}$ setting** 79

3.12 **Price settlement: Mid price in a $\lambda_N^{c,l} := \lambda_N^{c,l}$ setting** 81

4.1 **The fuels in the example** 104

4.2 **Market view** 105

4.3 **Subset result** 108

4.4 **Input data** 117

4.5 **Regional fuel sets – January 2022** . . . 119

4.6 **Regional fuel sets – May 2022** . . . 120

4.7 **Regional fuel sets – October 2022** . . . 121

4.8 **Fuel bid curve parameters** . . . 123

4.9 **Gamma $\gamma_{\cdot,t}$ formula inputs – January 2022** . . . 125

4.10 **Gamma $\gamma_{\cdot,t}$ formula inputs – May 2022** . . . 126

4.11 **Gamma $\gamma_{\cdot,t}$ formula inputs – October 2022** . . . 127

4.12 **Solar availability formula inputs** . . . 129

4.13 **Wind availability formula inputs** . . . 130

4.14 **Constrained-on/off X_t formula inputs** . . . 131

4.15 **Generation G_t formula inputs** . . . 132

4.16 **Wasserstein distances** . . . 135

5.1 **Specifications in the real-time electricity supply curve** . . . 141

5.2 **Welfare calculation** . . . 158

5.3 **Supply non-monotonicities due to indivisibilities in energy** . . . 161

5.4 **Loss factor and loss calculations** . . . 167

5.5 **Price calculations** . . . 168

5.6 **Summary of the assumptions** . . . 170

5.7 **'Convexifying' the bids** . . . 172

5.8 **Welfare summary** . . . 178

Acronyms and abbreviations

AEMC	Australian Energy Market Commission
AEMO	Australian Energy Market Operator
AER	Australian Energy Regulator
AGC	Automatic Generation Control
APC	Administered Pricing Cap
APF	Administered Pricing Floor
ASEFS	Australian Solar Energy Forecasting System
ASX	Australian Securities Exchange
AUD	Australian dollar
AWEFS	Australian Wind Energy Forecasting System
BM	Balancing Market
CfD	Contract for differences
CPT	Cumulative price threshold
CO_2	Carbon dioxide
CVP	Constraint violation penalty
DC	Direct current
DSO	Distribution system operator
DUID	Dispatchable Unit Identifier
EAAP	Energy Adequacy Assessment Projection
EMMS	Electricity Market Management Systems
EPEC	Equilibrium program with equilibrium constraints
ER01-04	Eraring Power Station
ESB	Energy Security Board

ESOO	Electricity Statement of Opportunities
ETS	Emissions Trading Scheme
FCAS	Frequency Control Ancillary Services
FCP	Fixed configuration pricing
FERC	Federal Energy Regulatory Commission
FPN	Final physical notification
FSIP	Fast-Start Inflexibility Profile
FTR	Financial transmission rights
GELF	Generator Energy Limitation Framework
HPRL1	Hornsdale Power Reserve
Hz	Hertz
IRSR	Inter-regional settlements residue
ISP	Integrated System Plan
KKT	Karush-Kuhn-Tucker
L6SE	FCAS Contingency Fast Lower 6 second
L60S	FCAS Contingency Slow Lower 60 second
L5MI	FCAS Contingency Delayed Lower 5 minute
L5RE	FCAS Regulation Lower
LGC	Large-scale generation certificate
LHS	Left hand side
LIMOSF21	Limondale Solar Farm 2
LP	Linear programming
LMP	Locational marginal pricing
LOR	Lack of Reserve
LOYYB1-2	Loy Yang B Power Station
LRC	Low Reserve Condition
LRIC	Long-run incremental cost
LYA1-4	Loy Yang A Power Station

MCP	Mixed complementarity problems
MILP	Mixed integer linear programming
MIP	Mixed integer programming
MLF	Marginal loss factor
MNSP	Market Network Service Provider
MPEC	Mathematical program with equilibrium conditions
MW	Megawatt
MMS	Market Management System
MP1-2	Mt Piper Power Station
MT PASA	Medium Term Projected Assessment of System Adequacy
NC	Non-Conforming
NEM	National Electricity Market
NEMDE	National Electricity Market Dispatch Engine
NER	National Electricity Rules (aka the Rules)
NIL	System normal condition
NLAS	Network Loading Ancillary Services
NOS	Network Outage Scheduler
NRM	Negative Residue Management
NSCAS	Network Support and Control Ancillary Services
NSW	New South Wales
NTEM	Northern Territory Electricity Market
NUMURSF1	Numurkah Solar Farm
OCD	Over-Constrained Dispatch
OPF	Optimal power flow
OTC	Over-the-counter
PASA	Projected Assessment of System Adequacy
PJM	Pennsylvania-New Jersey-Maryland Interconnection
POAT220	Poatina Power Station

QLD	Queensland
R6SE	FCAS Contingency Fast Raise 6 second
R60S	FCAS Contingency Slow Raise 60 second
R5MI	FCAS Contingency Delayed Raise 5 minute
R5RE	FCAS Regulation Raise
RAC	Reliability Assessment and Commitment
RERT	Reliability Emergency Reserve Trader
RHS	Right hand side
ROC	Rate of change
ROP	Regional original price
RRN	Regional reference node
RRP	Regional reference price
SA	South Australia
SCADA	Supervisory Control and Data Acquisition
SCED	Security-constrained economic-dispatch
SDC	Semi-dispatch cap
SFE	Supply function equilibrium
SOS2	Type 2 Special Ordered Set
SRA	Settlement Residue Auctions
SRAS	System Restart Ancillary Services
SRMC	Short-run marginal cost
SSFR	Static Firm Frequency Response
ST PASA	Short Term Projected Assessment of System Adequacy
TARONG#1	Tarong Power Station
TUNGATIN	Tungatinah Power Station
UIGF	Unconstrained Intermittent Generation Forecast
USE	Unserved energy
VIC	Victoria

VOLL	Value of lost load
WEM	Wholesale Electricity Market
WEMENSF1	Wemen Solar Farm
Wh	Watt-hour

Chapter 1

Introduction

1.1 Motivation

The simplifying arguments of economic theory in Parkin and Bade (2016) elucidate several key concepts for understanding markets in general. Importantly, the unit price of a good or a service is determined by the equilibrium of supply and demand. In efficient markets, the demand curve captures the marginal benefit of obtaining another unit, which decreases as the available quantity increases. Consumer surplus is also calculated from this demand curve. In contrast, the supply curve captures the marginal cost of producing an additional unit. By the law of supply, this curve or function is increasing in that marginal cost increases as quantity increases. The supply curve also determines producer surplus. The sum of consumer surplus and producer surplus, known as social surplus, is a common measure of welfare.

These standard economic arguments can be applied to wholesale electricity markets using auction bids to specify the supply and demand curves. Price and welfare are then obtained by aggregating the bids following the assumptions of the general case. This is in line with the merit order rule, whereby bids are filled in increasing order of price, starting from the lowest price bid.

However, the thus assumed mechanics of bid aggregation ignore a number of complicating factors characteristic to power markets. These either relate to the physical nature of electricity, such as operational limits and network safety constraints, or are elements of the electricity market design, such as bid language, and thus impact the way equilibrium is obtained. Adapting the economic equilibrium argument to the reality of power markets provides improved clarity on how prices are formed and what welfare results eventuate.

Most real-world market designs are constantly being probed by industry groups and the public and are re-evaluated by regulators to endorse efficiency and reliability while transitioning

to low-carbon systems. As a result, market designs in different parts of the world have developed to operate based on vast and varied adequacy planning and dispatch rules. Some markets rely on a multi-stage security-constrained dispatch algorithm, known as integrated pool markets; others work on an exchange basis. Some organise a mix of day-ahead, intra-day and real-time trading, whereas others use 5-minute real-time settlement only. Some co-optimise operating reserves, whereas others trade those separately from the energy market. Overall, the market methodologies can vary significantly from country to country and have important implications for price formation.

Focusing on a particular market design, once endowed with a good understanding of the dispatch rules and the required data, price formation in practice can be recovered in numerical detail. In integrated pool markets this highlights the disparities between the fully-fledged engineering models and the theoretical economic equilibrium arguments and provides valuable insights into what factors are required for improving the equilibrium interpretation for any given market.

The modelling of electricity price is an important research topic. It is central to investment and asset valuation – including physical power investments, commercial licences, clean energy certificates, debt and equity claims, and financial derivatives – as projecting the cash flows of these types of assets usually requires the expected value of the electricity price. The optimal control and financial risk management involved in using these types of assets are no less dependent on the electricity price evolution. These applications require a price model that recovers the common empirical features of the spot price path, including negativity and spikes, with distributional accuracy at the minimum. In addition, the price impact of planned market design changes is often of interest in regulatory oversight favouring a more structural approach to price modelling.

Different interpretations of the equilibrium argument are inherent in a large body of semi-structural modelling literature (see Barlow (2002); Howison and Coulon (2009); Aid et al. (2009); Carmona et al. (2013); Aid et al. (2013); Carmona and Coulon (2014); Ware (2019)). Most of these studies assume perfectly inelastic demand and a monotonically increasing functional form to the supply curve. A new interpretation that closely reflects the market design of the NEM and incorporates the factors deemed relevant after recovering the price formation in

the engineering model is proposed along these lines for a novel price model.

However, the monotonically increasing form of the supply curve breaks down owing to non-convexities and other factors in the security-constrained dispatch model. To show this, the mathematical formulation of the multi-stage dispatch algorithm of a market is used in this thesis to compute prices at different levels of demand. In this way, an implied supply curve can be obtained, which may exhibit decreasing prices as quantity increases.

Lastly, computing welfare taking a much wider array of factors into consideration than just the bids provides a good vantage point for comparing different market designs in terms of efficiency.

1.2 Literature review

This thesis makes contributions to two strands of the literature: electricity market design and semi-structural price modelling. Literature reviews on both strands are detailed below.

1.2.1 Electricity market design

The academic literature on electricity market design comes in five flavours. Some papers focus on reporting about market design around the world such as Mayer and Trück (2018). Others describe certain markets historically and at present, e.g., Cramton (2017), Liu et al. (2022) and Csereklyei and Kallies (2022). Another strain of the literature discusses the more recent issues around electricity market design, such as the 'missing money' or the 'missing policy' conundrum (Newbery (2016); Simshauser (2019*a*)) the emergence of new ancillary service side markets (Mountain and Percy (2020)), etc. In addition, textbooks have been written about the economics of power systems for those studying either economics or electrical engineering, such as Biggar and Hesamzadeh (2014) and Wood et al. (2013). Last, some authors are attempting to characterise a socially optimal – ideal – electricity market design in low-carbon settings, as, for example, Newbery et al. (2018).

1.2.1.1 Standard theory

The standard theory of efficient spot pricing using direct current (DC) flow approximation by Schweppe et al. (1988) depicts a mostly unregulated, centrally dispatched, energy-only, nodal

system with liquid forward markets, as in Simshauser (2019*a*). However, this market design has not become a reality since the inception of the framework in the 1980s because the theory assumes short-term demand price elasticity. Even today, consumers are seldom able to react to spot price signals instantaneously as real-time metering is fairly uncommon (Hirst and Hadley (1999); Stoft (2002); Bidwell and Henney (2004); De Vries (2005); Joskow (2008)). Demand is highly inelastic; therefore, relatively high levels of demand can threaten blackouts: the market fails to clear an equilibrium because supply and demand never match, in which case the spot price tends to infinity (Stoft (2002); Finon and Pignon (2008); Cramton et al. (2013)). Such absurd spikes seldom arise under the ideal market design, but price caps must be used to avoid them in practice (De Vries (2005)). Indeed, a second-best social solution is found by Stoft (2002), who modify this market design by setting the price cap at the dollar amount that consumers would agree to pay on average to avoid blackouts, called the value of lost load (VOLL). This optimum does not eliminate rolling blackouts; it optimises their duration, assuming that the administratively set VOLL is indeed an accurate measure of the disutility value (Cramton et al. (2013)). The blackouts and the potential network collapses they might trigger are optimised by managing the reliability of the system, which includes long-term resource adequacy and short-term security (De Vries (2005); Cramton et al. (2013)).

Should the price cap fall short of the VOLL, either thanks to political pressure to set the price cap below the VOLL or due to uncertainties in the value of VOLL, scarcity pricing fails, hindering the profit recovery of generation investments to ensure resource adequacy, known as the 'missing money' problem (Bidwell and Henney (2004); Hogan (2005); Newbery et al. (2018)). If generation and storage units bid on a cost basis, the uncapped spot price then reflects the marginal cost of the incrementally or decrementally dispatched plant, rather than its long-run incremental cost (LRIC). It follows that infra-marginal plants are better able to recover their long-run costs during scarcity events – when peaking plants with higher marginal costs set the price – than peaking plants that only receive their own marginal costs (below their LRIC) or the sub-VOLL price cap (Bidwell and Henney (2004); Joskow (2008)). Consequently, and because of the lagged nature of investment cycles preventing timely entry, electricity markets and peaking plants in particular are often 'withering' off equilibrium (Bidwell and Henney (2004); De Vries (2005); Simshauser (2019*a*)). Profitability is further eroded when expensive plants are

used for out-of-market dispatch by the system operator to resolve scarcity without the spot price reflecting the utility value provided by these plants or if various ancillary services are insufficiently remunerated (Hogan (2005); Roques (2008); Joskow (2008); Hogan (2014); Newbery (2016)). However, imperfect future information, regulatory uncertainty, construction permits, and risk aversion also contribute to the 'missing money' problem (Schweppe et al. (1988); Littlechild (1992); De Vries (2005); Joskow (2008)). Consequently, markets with these measures often break with the energy-only design and establish capacity mechanisms to encourage generation investments for resource adequacy or they permanently increase their operating reserves (Bidwell and Henney (2004); Hogan (2005); Finon and Pignon (2008); Cramton et al. (2013); Simshauser (2018)).

As the standard theory on efficient spot pricing has significant flaws, workarounds to ensure the satisfaction of several stakeholder groups became necessary in practice. These have led to significantly different market designs. These are briefly explored in the present thesis before providing an in-depth review of the NEM market design.

1.2.1.2 The case for the NEM

The Australian NEM has an energy-only market design with a relatively high price cap that is currently at a VOLL of $15,500/MWh (AEMC (2023)) and uses bilateral out-of-market reliability reserves (AEMO (2020*g*)). Whereas Stoft (2002), De Vries (2005), Hogan (2005) and Cramton et al. (2013) argue that a price cap at or above the fair value of the VOLL is desirable to achieve a clearer price signal and sufficient generation investments through the wealth transfer from consumers to generators in a way that the 'missing money' problem vanishes, some also stress the significant market power concerns in connection to high prices, most notably the tactics whereby generators withhold capacity to exploit scarcity pricing or use their isolated locations to unilaterally game system congestion, both of which reduce reliability. However, as mentioned above, price caps are not always binding during scarcity events owing to out-of-market mechanisms in dispatch. Indeed, Simshauser (2008), Tómasson et al. (2020) and Holmberg and Ritz (2020) assert that capacity mechanisms are often needed to close off the equilibrium gap towards a socially more optimal outcome, even with a price cap at the correct estimate of the VOLL.

A few further comments are also important regarding the NEM market design. First, it allows price-based bidding and re-bidding, which can be disorderly: bids do not have to match marginal costs and may be revised any number of times before the start of every 5-minute trade interval (AEMC (2021*c*); AEMO (2021*s*)). Second, the only means by which slow-start units can inform the market operator of their plant status is their price–quantity bids (no multi-part bidding), and after bidding, they must legally abide by the dispatch targets issued for them by the central engine. Third, there is a market price floor at -$1000 (as per Clause 3.9.6 in AEMC (2021*c*)), and negative prices are common. Fourth, a period of administered pricing commences if the cumulative sum of the spot prices reaches a certain threshold (AEMO (2019*a*)). As a result, the bidding behaviour of the units is geared towards a complex, if not completely unregulated, game theoretical setting where strategic bidding and the ability to unilaterally move prices are a function of technological flexibility, input costs, grid location and the adoption of software for automated bidding. For example, units often bid at negative prices to avoid competition within a network constraint and secure dispatch. It is unclear if this state of affairs helps resolve the 'missing money' conundrum, or, alternatively, whether it promotes investments into storage fuels such as battery and hydro.

In addition, endorsements for non-generation investments promoting short-term system security, such as interconnectors, grid forming storage, inverters, capacitors and retrofitted synchronous condensers, are important for adequate market design, especially for high-renewable markets with greater intermittency (Cramton et al. (2013); Newbery (2016); Mountain and Percy (2020)). Security typically involves various products and services, including (fast) frequency balancing, system restart, voltage control, transient and oscillatory stability, ramping, as well as system strength and inertia, and less conventionally also carbon capture (Newbery (2016); AEMO (2021*k*)). Failing to efficiently price any of these is known as the 'missing markets' problem, which also perpetuates the 'missing money' problem through remunerative deficiencies. Owing to the NEM market design that co-optimises frequency balancing into the spot market, concerns with regard to the bilateral, non-market procurement of the rest of the security services have revived in Australia, after the last coal plant of the high-renewables South Australia region exited in mid-2016 (Simshauser (2018); AEMO (2021*k*); Department of Industry, Science, Energy and Resources (2022)).

The lack of perfect forward markets, another assumption of the socially optimal spot price theory, is also often considered to be part of the 'missing markets' problem. In the NEM, near-term forward markets for energy are only liquid enough up to three years, whereas they are non-existent for the capacity or quantity of service products. These aspects are problematic for project financing and adverse because of the incentive reduction effect of forward markets to gaming the spot market (Newbery (2016); Simshauser (2018); Ahlqvist et al. (2018)). The forward market conditions have only deteriorated in recent years, due to the loss of hedge capacity for energy by the exiting coal plants, the large-scale variable generators entering via government-supported contracts for differences (CfD), certificate side-markets, and the 'missing' climate change policy continuity (Simshauser (2018, 2019*a*,*b*, 2021*a*)).

With no nuclear generation, the aspirations for sustainability through decarbonisation and electrification envisage ever greater increases in the share of renewables and storage technologies (including hydro) in Australia. However, incentivising variable renewables comes at the cost of increased security service provision in addition to the direct subsidy costs and the implied costs of forward market distortions (Simshauser and Gilmore (2020); Simshauser (2021*b*)). Nevertheless, transitional fuels, such as natural gas, and firming technologies offer complementary properties to maintain the physical security of high-renewables systems, given also the susceptibility of aging coal plants to technical failures (Pollitt and Anaya (2016); Newbery et al. (2018); Simshauser (2021*a*); Nelson et al. (2023)).

The challenges of moving towards a socially optimal NEM market design are heightened by criticisms of the short-run efficiency of the theoretical nodal marginal spot price and by the fact that the NEM operates with a spatially less granular zonal (regional) rather than with a nodal locational marginal price (LMP). Early on, Littlechild (1992) warns that the continuity, differentiability, and convexity of the cost, demand, and loss functions required to obtain the short-run social optimum do not hold in electricity systems and remarks that the power-engineering literature explained why mixed integer programs should be used for efficiency. Today, uplift payments are often used to compensate for the capital losses from the market-clearing solutions that ignore unit commitment decisions (Hogan (2014); Ahlqvist et al. (2018)).[1] Strikingly,

[1] Uplift payments compensate units so that they do not incur any losses over their costs when following dispatch targets.

however, fast-start unit commitment pre-processing in the NEM uses mainly linear constraints to pre-empt infeasible outcomes (AEMO (2021*j*)), and the lumpy start-up and shut-down costs of plant economics mostly remain with the plants to bid upon, not with the system operator to optimise. Uplifts are typically not paid in the absence of intervention. Furthermore, the NEM is a regional market that does not expressly price congestion: it usually relaxes all but the tie-break constraints until a violation cost of nil, and constrains plants on or off without either a locational compensation in the spot price or a bid-price guarantee (Hogan (2005); Leslie et al. (2019)). Thus, prices may reflect binding security constraints far away on the grid, and counter-price flows through cross-regional interconnectors are part of the norm (Biggar and Hesamzadeh (2014)). By contrast, nodal prices are usually preferred in the literature as a more efficient way of transitioning to higher levels of renewables (Newbery et al. (2018); Ahlqvist et al. (2018); Wolak (2019)).

This thesis adds to this literature by explicating the workings of the optimisation routine used for dispatch and pricing in the NEM to explicate the prevailing market design in conceptual and mathematical detail. Many price-relevant features of market design and the key sources of non-price data are identified. This creates an extensive repository of industry publications, which might be useful to those who wish to learn more about the mentioned aspects of market design.

1.2.1.3 The general case

There is a growing consensus that the electricity dispatch and pricing problem is non-convex in both nodal and zonal settings, which is attributable to the discrete costs and decisions inherent in the problem, including but not limited to fixed costs and minimum loading requirements (Liberopoulos and Andrianesis (2016)). It follows that using linear programming (LP) to solve for the dispatch targets and the price result does not support the competitive equilibrium condition, i.e., profit-maximising units would sometimes prefer to deviate from their assigned dispatch targets given the price signals under LP (Wang et al. (2023)). Moreover, although MIP is readily available to solve dispatch, the duals (or dual functions) in MIP cannot be interpreted as shadow prices, as in Pachkova (2004): these models lack an economically sensible way of calculating prices. The seminal idea of O'Neill et al. (2005) is that separating the MIP in a first step to obtain the optimal values for the integer constraints, and running an LP optimisation with

those constraint values fixed allows for computing prices. However, the prices from their model are not consistent with the competitive equilibrium, unless complemented by uplift payments, which they also compute.

Similar two-step methodologies are widely used in electricity pool markets today (Eldridge et al. (2019)). However, even markets with the same core two-step methodology differ in terms of market design settings, such as bid language, and on whether they pay uplift, include slow-start plants in the MIP run, co-optimise ancillary services, use minimum operating level relaxation, etc. In contrast, exchange-based (self-dispatch) markets tend to vary from the two-step methodology even more (Ahlqvist et al. (2018)).

The assumptions for obtaining the supply curve (marginal cost curve) are equally heterogeneous, but the use of fixed configuration pricing (FCP) is an intuitive starting point in the pool market literature. FCP corresponds to the two-step methodology above, but without the uplift payments, to construct the implied supply curve, as in Byers and Hug (2023). They also state that FCP is often considered the non-convex analog of LP marginal pricing, as it takes the slope of the total cost curve, when defined, to obtain the price. Indeed, Hogan and Ring (2003), Gribik et al. (2007), Bjørndal and Jörnsten (2008), Ruiz et al. (2012) and Byers and Hug (2023) have observed that price is not a monotonically increasing function of output quantity under FCP and other FCP-style models, mainly owing to start-up costs.

The last essay of the thesis starts by fine-tuning the FCP approach to an extended set of market design assumptions to construct and analyse supply curves in different markets. This involves time-sequential and discretionary aspects of the market as well as bid language and out-of-market payments. We show that certain market design elements explicitly dampen energy-linked supply curve non-monotonicity compared with the baseline case with multi-part bids. By contrast, we also posit that unmitigated non-monotonicities may appear due to dynamic losses under bid price negativity. The main objective in this regard is drawing out a small-scale but conceptually detailed numerical example where the degree of non-monotonicity[2] can be illustrated and welfare can be quantified across the market designs of three real-world electricity markets.

[2]Note that the aggregate inverse supply curves and not the supply curves of the individual units lose monotonicity. The supply curve aggregation mechanism of the dispatch and pricing, particularly the application of security constraints, is responsible for most monotonicity distortions.

1.2.2 Semi-structural price modelling

There has been a renewed interest in modelling the electricity price in such a way that the price effects of certain market factors such as the capacity changes of the regional fuel mix or the cross-regional interconnectors are traceable. These features open any price model to scenario analysis, commonly used in, for example commissioning and capacity planning, system constraint cost pricing, investigating interconnector arbitrage and setting the regulatory price thresholds by the market operator and in regulatory oversight. The replication of the available capacity variation, including ramping speed, must-run amounts, shut-down periods, etc., and the intricate link between intermittent generation and the price, as found in empirical studies by Paraschiv et al. (2014), Csereklyei et al. (2019), Maciejowska (2020), Mwampashi et al. (2021) and Mwampashi et al. (2022), are sources of detailed modelling assumptions in recent years. These often also have considerable data support, providing more accurate modelling frameworks that are often highly specific to the fuel mix (see, for example, Moazeni et al. (2016); Benth and Ibrahim (2017); Deschatre and Veraart (2017); Gianfreda and Bunn (2018)). Such models, which aim to reflect the way prices are formed in the market, are typically called 'structural', as opposed to 'reduced–form' models, which simply assume a particular stochastic dynamic for prices.[3]

1.2.2.1 Bid stack modelling context

The supply function (bid stack) model literature – starting with Barlow (2002), who retrieve the stochastic microeconomic market structure of Föllmer and Schweizer (1993) and write the spiky electricity price as a non-linear transformation of a jumpless diffusion process for demand – typically maintains a characteristic, fundamental set of assumptions about the pre-existing supply–demand and auction schema relations. Most bid stack models still at least implicitly retain this characteristic market structure with perfect demand inelasticity and frictions (Carmona and Coulon (2014)). Further, to obtain the price, the different parametric bid stack models provide different forms of the aggregate supply function – that is, the market bid stack function – as appropriate in the local context. These differentiations highlight the various instances of the

[3]For reduced-form models see Clewlow and Strickland (2000), Lucia and Schwartz (2002), Cartea and Figueroa (2005) and, more recently, Gudkov and Ignatieva (2021).

largely typical market structure. The rationale is that the price formation cannot significantly detach from the equilibrium mechanism as long as end-user demand is assumed inelastic and electricity is not economically storable. In what follows, this thesis presents a generic overview of wholesale price settlement from the Australian perspective, which demonstrates that any strict non-storability assumption is already untenable at the operational level. The market structure underpinning the usual bid stack framework can easily be adjusted for storability.

Electricity is typically cleared as a homogeneous commodity in an automated multi-unit and often also uniform price auction (Krishna (2009)). The wholesale price is typically determined from the participants' bids based on economic principles under the physical constraints of the electric system, using constrained linear optimisation programs, such as the NEM Dispatch Engine in the NEM as per AEMC (2021*c*). Simply put, this program collects the bids in the maximum registered capacity of the units, discards the ones that are physically infeasible (constrained-off), enforces those that cannot be omitted for feasibility reasons (constrained-on), and returns the least-cost price from the marginal prices at the optimum solution (AEMO (2021*g*)).

*Bid*s are a series of price–quantity pairs offered by a unit as terms of trade. There are two basic types of bids. *Generator bids* are placed by generator units of any fuel type – e.g. coal, gas, solar, battery, hydro, etc. – to sell electricity. Regardless of their availability, the units partition their full capacity into quantity blocks. They assign the lowest price that they would ask for producing every quantity block to each block. These are the price–quantity pairs, i.e., the generator bids. They submit as many bids as there are blocks, and that number is usually capped by the market operator. *Load bids* are placed by load units of any fuel type – e.g. battery, hydro – to buy electricity. Regardless of their availability, the units also partition their full capacity into quantity blocks. They then assign the highest price that they would offer for purchasing every quantity block to each block. These are the price–quantity pairs or the load bids. The units submit as many bids, as there are blocks, and that number is usually capped by the market operator.

For market price settlement, the generator bids are pooled and arranged in ascending order of price – that is, in *merit order*. The *generator bid stack* is the cumulative sum of the bid quantities in merit order, at or below every price in the complete set of bid prices in ascending order from

the regulatory price floor to the regulatory price cap. It is agnostic to the fuel type behind the bids. The generator bid stack is a left-continuous, step-wise relation, that resembles the implied aggregate inverse supply. As such, the bid stack is typically plotted with the quantity along the horizontal axis and the price along the vertical axis. With fully inelastic end-user demand, the price at demand – where the vertical demand line intersects the generator bid stack – is the market price. It is the price of the last bid in merit: the price of the most expensive generator bid still needed to fill the demand in full.

Similarly, load bids are pooled and arranged in descending order based on price – that is, in merit order. The *load bid stack* is the cumulative sum of the bid quantities in merit order, at or above every price in the complete set of bid prices in descending order from the regulatory price cap to the regulatory price floor. The load bid stack is a right-continuous, step-wise relation that resembles the implied inverse demand of the load units. Market price settlement is not complete without coalescing the load bid stacks with the generator bid stacks in the equilibrium mechanism. The load bids that are eventually granted uptake in addition to end-user demand are the ones at or above the market price. Consequently, in the presence of loading, aggregate demand is higher and becomes slightly elastic compared with the generation-only market structure.

Above, in stating that the bid stacks of the two basic bid types resemble implied inverse supply and implied inverse demand, respectively, we are assuming that there exist appropriate parametric formulae for transforming the bid information to supply and demand functions within a mostly typical stochastic market structure. For generator bids and the implied inverse supply curve, this is a fundamental assumption in the parametric bid stack model literature (Carmona and Coulon (2014)). For load bids and the implied inverse demand curve, however, this is a new assumption.[4]

Supply function (bid stack) models that emulate the above mechanism make extensive and varied assumptions about what constitutes aggregate supply under the operational constraints of

[4]When using parametric bid curve formulae, the variable quantities are usually estimated from the appropriate non-price data, as the equilibrium formulation has a way of converting the non-price data into the expected value of the price. This is valuable for modelling the electricity price in scenarios that are in some way unprecedented, e.g. in anticipating the highest rates of green generation on record, or shutting down a historically relevant coal plants. Furthermore, the model can then be tested on historical price data, without having to split the price data between calibration and testing, as explained in Eydeland and Wolyniec (2003).

the electric system,[5] mostly through the capacity variation effect, which concerns the removal of unavailable capacity (Burger et al. (2004); Cartea and Villaplana (2008); Coulon et al. (2013)) or, similarly, the scarcity effect, which captures sudden capacity depletion (Howison and Coulon (2009), Aid et al. (2013)) as well as through the merit order dynamics – that is fuel bid curve aggregation – when the fuel types are differentiated (Howison and Coulon (2009); Aid et al. (2009); Carmona et al. (2013); Aid et al. (2013)). The models propose different functional forms of the aggregate inverse supply function, but usually omit two-way (i.e. storage) fuels with loads. Moreover, some are more explicit about the underlying market structure than others (Ware (2019)). The diversity of the model literature also shows that the geographic and the commercial wholesale environment has a profound impact on the spot price trajectory.

Indeed, as wholesale electricity is traded almost immediately after it is produced, and always locally, the main features of the local market, such as the fuel mix, the network sparsity, and the rules and regulatory requisites of the automated auction algorithm, all tend to factor into price discovery to some extent (Eydeland and Wolyniec (2003)). This thesis argues that the properties of the local market routinely determine the correct modelling assumptions and heavily restrict the functional form of the aggregate supply function.

1.2.2.2 Applicability to the NEM

Surprisingly, the well-known bid stack models with fuel-type differentiation mentioned above encounter difficulties at the model assumption level when simulating the NEM power price owing to the following peculiarities of the local market: the already high and increasing renewable penetration, the ongoing two-way fuel expansion, the price effects of binding network constraints, the price-based auction mechanism, and the resulting frequent price negativity. The seminal model by Carmona et al. (2013) has an attractive merit order dynamic, which the present thesis retrieves and adapts in five directions to propose an improved approach that better reflects the NEM.

In the NEM, the fuel mix is increasingly high in solar, wind, and hydro generation (Department of Industry, Science, Energy and Resources (2022)); therefore, the model cannot rely on

[5] See Carmona and Coulon (2014) for a summary of bid stack models.

the spot and futures prices of the input fuels, such as gas and coal, as closely as the existing literature suggests (Carmona et al. (2013); Carmona and Coulon (2014); Aid et al. (2013)). Given, however, that the NEM has a price-based auction mechanism – that is, the participants can bid at any price within the regulatory price thresholds with no obligation to justify their price on a cost basis according to AEMC (2021*c*) – the proposed model can establish the fuel-specific bidding behaviours by fitting a time-dependent fuel bid stack function to the different fuel bid data with fuel-specific variables. Using the fuels, or explicitly evaluating the relationship between the bidding behaviour and the input fuel prices by fuel type, then provides the implied inverse supply curves in reduced form without tying the fitted functions to the production costs or the utility equations of the individual plant (thus making the model 'semi-structural' in this sense). In any liberalised market, this is applicable to all fuels for which the individual operators engage in bidding, including renewables.

Although the model for fitting the functions to the fuel bid data can be easily adapted to different fuel types, the physically available capacity of the fuels cannot be readily captured by the same formulation. In the NEM, individual participants bid in their full capacity (AEMC (2021*c*)); this is the bid data. They also provide other real-time technical data, such as ramp rates, renewable forecast measurements, etc., from which the available quantities can be centrally ascertained. Drawing on the same data set, rather than introducing a 'hidden' variable for average capacity variation (Burger et al. (2004); Cartea and Villaplana (2008); Coulon et al. (2013)) or a scarcity effect (Howison and Coulon (2009); Aid et al. (2013)), the proposed model makes use of the technical data for approximating what constitutes the available aggregate capacity under the operational constraints.

The NEM also has considerable pumped hydro generation and a rapidly growing battery fleet, as described by the Department of Industry, Science, Energy and Resources (2022). These two-way fuels enter on both sides of the market by placing two distinct sets of generator and load bids, and thus open the typical market structure to demand elasticity with an evident effect on the electricity price. Therefore, the suggested equilibrium formulation that extends to two-way fuels is a new contribution to the bid stack modelling literature.

Furthermore, dispatch scheduling and price settlement in the NEM are subject to a myriad of security constraints. When some of these constraints bind, some bids are forced on

(constrained-on) and others are consequently curtailed (constrained-off), depending on the constraint coefficients of the participating units placing the bids. Accordingly, the market bid stack, or more simply and equivalently (as we show) the demand quantity, must be adjusted to reflect these constraint effects on quantity. This is not a case of increased scarcity when the constrained-on quantities are considered, but a new feature we suggest incorporating into the usual market bid stack formulation.

Finally, the regulatory market price floor is $-\$1000$ in the NEM, and negative prices, including negative price spikes, are common. This requires a model that evaluates the positive and the negative price outcomes much the same way. Whereas the existing bid stack models present elaborate mechanisms for positive prices, they only provide probabilistic overlays (Carmona et al. (2013); Carmona and Coulon (2014)), if anything, for negative prices. More commonly, they disallow (Howison and Coulon (2009); Ware (2019)) or disregard (Aid et al. (2009, 2013)) price negativity. In contrast, our approach assigns a hyperbolic form to the fuel bid stack functions and preconditions the negative price outcomes the same way as the positive ones, as long as the bid data records negative bids. This hyperbolic feature is akin to the spread adjustment method of Ward et al. (2019), who apply this to the short-term marginal cost of thermal technologies: both approaches clearly identify what puts prices under downward pressure near the negative end of the price spectrum, and use a hyperbolic feature to reproduce that.

1.2.2.3 Other recent developments

For completeness, note other more recent papers that model the electricity price via an equilibrium between supply and demand curves. These models are thus structural to some degree. However, the more refined (the more structural) a model, the more likely it is to reflect the settings of a specific exchange or wholesale market. A day-ahead market model in Europe might have very different ingrained assumptions, such as sequential arbitrage, stable offer capacity over time and lack of real-time balancing constraints, compared with the requirements of a wholesale real-time market model for the NEM in Australia. In addition, negative prices are relatively large and common in some regions in the NEM, which is why the standard assumption of an exponential supply curve is not adequate in this setting without adjustments. Therefore, the applicability of the models below to the Australian NEM is limited.

The *X-model* proposed by Ziel and Steinert (2016) and further improved by Kulakov (2020) first creates a small number of price classes, that is price ranges that are sub-segments of the full price range. The authors then stochastically model the bid volume within every price class, whereby the correlation structure of the bids is also retained. Finally, the bid volumes are probabilistically reassessed for every discrete price within every price class. This is referred to as price curve reconstruction. The original model in Ziel and Steinert (2016) reconstructs both supply and demand, whereas Kulakov (2020) reworks the supply curve so that it contains the elastic negative supply bids from the demand curve, allowing for the demand curve to be perfectly inelastic. The latter thus models the supply curve with multiple price classes but the demand curve with only one price class. The name of the approach comes from the fact that in equilibrium, the curves appear as the letter X. This approach would be problematic for Australia without first adjusting the bid-in data to the available capacity and constrained-on/off volumes. Moreover, the computational burden of the entire exercise would be relatively high for the NEM, because more price classes would be required in that setting, since market prices might take any value in the range [-A$1000, A$16000] in the NEM and not only in the range of [-€50, €3000].

Buzoianu et al. (2012) suggest an exponential supply curve function that incorporates temperature and seasonality effects, and distinguishes between gas-fuelled and non-gas generation. In addition, they formulate a linear demand function with an autoregressive component to equilibrate the two. Rassi and Kanamura (2023) use a stochastic power transform to map excess supply quantity minus liquefied natural gas volume to the price using a closed-form expression. Their model admits a near-exponential shape for the supply curve when implemented on Japan Electric Power Exchange data. Neither of these models is likely to admit negative prices and they are most suitable for markets or price regions with a high share of natural gas.

Beran et al. (2019) assume a piece-wise linear supply curve, bidding at marginal cost by fuel type and a level of must-run combined heat and power capacity. They apply fuel-specific available capacity truncation as well before obtaining the price at the intersection of supply and demand. This approach is well-developed in terms of fuel specification, but the assumption that fuels bid at marginal cost is problematic for the Australian market. In Australia, disorderly bidding away from marginal cost and shadow bidding, i.e., submitting more than one price–

quantity bid pairs, are allowed.

Mahler et al. (2019) tackle the pricing problem as an optimisation, where the objective function minimises the sum of the parameterised marginal prices times residual generation quantities by production type. The authors make special adjustments for nuclear and hydroelectric plants. The parametric stack function for the marginal prices is linear. This model is also well-developed in terms of fuel availability, but the linear assumption limits the model's ability to predict positive and negative price spikes.

Pinhão et al. (2022) posit a polynomial form for the so-called price sensitivity curve, which is obtained by subtracting the supply curve from the demand curve. The root of this curve gives the price. The parameters of the curve are updated over time using a vector autoregressive model with harmonic components. This method does not attempt to isolate fuel-specific properties in the bid stack; therefore, similar to Ziel and Steinert (2016) and Kulakov (2020), one would need to first adjust the fitted bid-in data for availability and constrained-on/off quantities. Otherwise, the supply and demand curves cannot capture the true volumes owing to physical network constraints. These are, however, inevitably present in every real-time wholesale electricity market.

1.3 Thesis outline

The arc of the thesis is described as follows. The first essay is about market design in general – as much as market design across the world can be generalised – with a focus on the merit order principle and the standard bid stack framework, which is also extended to better capture the properties of real-life markets. The second essay unveils the NEM market design by collating information from a wide array of sources with an interest in price formation.[6] A screening of the academic literature for a fitting semi-structural price hypothesis or price model – preferably a bid stack model – reveals that most of the existing models build their assumptions on European or North American market design principles. Therefore, in the third essay, we propose a novel bid stack–style price model that better reflects the underlying assumptions and the required stylised features of regional electricity prices in the NEM. However, an obstacle to using these types of models for the Australian context is – as we soon discover – that the NEM

[6]No descriptive summary of this sort is found in the academic literature as of late 2023.

supply curve is not always monotonically increasing. This property and welfare are investigated internationally in a small-scale numerical example in the last essay. That, in turn, opens a window into a critical assessment of several key market design features.

Accordingly, this thesis comprises four essays under the following titles:

- Chapter 2: Market design in electricity markets;
- Chapter 3: A survey of the Australian National Electricity Market;
- Chapter 4: A hyperbolic supply function approach to price modelling;
- Chapter 5: Supply function non-monotonicity and welfare under different market designs.

Chapter 2

Market design in electricity markets

2.1 Introduction

Electricity is a heavily traded commodity in most markets around the world. Unlike most commodities, however, electricity is neither globally transferable, nor economically storable. Infrastructural developments such as network extensions and storage technologies hold the potential to overcome these restrictions in the near future. At present, however, electricity is exchanged almost always instantaneously at local or sometimes coupled markets.

Local markets typically adopt one of the two dominant market models, the integrated pool model or the exchange model, as classified by Cramton (2017) and Mayer and Trück (2018). The integrated model finds the price as the equilibrium result of a security-constrained dispatch optimisation using actual system information. Pricing is ex-post or dispatch-based; therefore, it aptly reflects the true grid economics given the security constraints. In contrast, the exchange-based model obtains the equilibrium solution from voluntary bid participation via self-dispatch, similar to financial markets. Pricing is therefore ex-ante; it is not based on actual dispatch and may lack validity.[7]

This chapter provides an overview of electricity markets in the integrated pool model. These markets might handle bid offer curves, virtual bids, and forward contracts simultaneously in the market value maximising central dispatch algorithm (Ott (2003); Cramton (2017)). The simple bid offer curves recording competitive price–quantity bids per unit are relatively widespread. However, because the cost function of the market value maximisation often exhibits non-convexities (lumpiness) due to start-up costs, must-run times, unit commitment (online/offline status), etc., other more involved multi-part bid curves are also fairly common (Hogan (2014); Cramton (2017)). Multi-part bid curves – as we refer to them here – internalise

[7] Mayer and Trück (2018) explain that "As the market is balanced only based on the price, technical limitations can sometimes make it impossible to physically fulfill the trades.".

the fixed energy economics of the plants by including fixed costs in the bid language. Moreover, contrary to the simple and the multi-part bid offer curves, which usually involve physical amounts, virtual bids are financially settled bids offered into the physical market (Ott (2003)). According to Cramton (2017), virtual bids have been found particularly useful in resolving cost non-convexities and other spot market frictions by providing liquidity. Furthermore, forward contracting – that is, bilateral transactions into the spot market – have been shown to help disincentivise strategic bidding (gaming).

Energy is the main commodity in the various bid offers, but there is reserves trading too, in most dispatch-based markets, to promote reliable non-stop supply. Energy and reserves are more or less identical in material substance, with delivered quantity measured in watt-hours (Wh)[8], but they have very different roles in the system. As suggested by Cramton (2017), 'operating reserves' is a broad area covering a number of ancillary services. In general, the installed capacity on standby in various ancillary services is potentially co-optimised with energy, but an installed capacity on standby earning scarcity rent through the capacity markets may not be. Further, the contracted demand response before involuntary load[9] shedding and the contracted reliability unit commitment are mostly also not co-optimised out-of-market operations, as detailed in Hogan (2014) and Cramton (2017) for the North American regulatory context.

Exploring the similarities between pool markets worldwide with an emphasis on price discovery reveals two main shared facets between most wholesale markets in the integrated model. First, because the economic objectives of the agents are virtually indistinguishable and the transmission networks acting as the distribution channel have similar physical constraints, the sets of market participants and governance goals are broadly the same. Second, as long as the price solutions constitute uniform prices so that every megawatt (MW) power is sold at the same price to some – albeit varying – degree of price locality, that is at a locational marginal price, but not without security constraints, the security-constrained utility maximising price protocols will perforce bear some resemblance.

This chapter discusses how electricity prices are set by specifying the bid aggregation as-

[8]Watt-hours is a unit of energy obtained as a unit of average power (in Watts) multiplied by a unit of time (in hours).

[9]We use the terms load and demand interchangeably within the wholesale context.

sumptions in line with the above similarities to retrieve the equilibrium price. Storage fuel units and physical constraint effects are also assumed to be reflected in the extended economic framework, which is presented from the ground up. Numerical examples are used to emphasise the effects of these extensions on the price.

Finally, alternative forms of electricity exchange have significantly proliferated in recent decades. Some examples include bilateral contracts such as power purchase agreements, behind-the-metre batteries, non-integrated hybrid utilities, such as wind farms combined with battery storage, distributed energy resources, e.g., rooftop solar panels, and decentralised demand response activities. These solutions are all viable but are usually small-scale or increasingly integrated into wholesale trading. In this chapter, we only discuss these alternative forms of exchange as relevant to the wholesale spot price.

The remainder of the chapter is organised as follows. After this brief introduction, Section 2.2 explores some common characteristics of electricity markets. Then, Section 2.3 explicates ex-post marginal pricing in the integrated pool model and expands the equilibrium pricing framework to storage fuel and network constraint effects. Section 2.4 highlights some features that distinguish different market designs within the pool model, and Section 2.5 discusses the role of financial markets. Finally, Section 2.6 concludes the chapter.

2.2 Market participants and governance goals

Owing to the natural monopolistic setting, perhaps the most overt similarities between the pools at different geographic locations are the similar sets of governance goals and market participants. This section presents the four most general governance goals and the usual market participants involved on the operative side of market conduct.

The rule maker sets market regulations in four important directions. The rules promote short- and long-run reliability, equitability, and sustainability through generation, storage and transmission investments, market power mitigation, efficient equilibrium price approximation, and efficient hedge markets.[10] First, the market design incentives for new investments aim to meet the dual goal of having sufficient long-term generation capacity and adequate operating

[10] See Cramton (2017) for a global overview of electricity market governance objectives and AEMC (2018*a*) (pages 56-59) for a discussion of particular issues in efficient equilibrium price approximation.

reserves to manage the short-run scarcity risk. Second, market power mitigation is necessary to ensure that the agents are unable to unilaterally move the prices, to maintain an equitable market environment and consumer welfare (Cramton (2017)). Third, drawing from the arguments put forward by Hogan (2014), the efficiency of the dispatch-based price outcome – that is, market price quality – is of interest while aiming to keep the uplift payments at a minimum[11] so that the spot prices determined at the efficient grid equilibrium better reflect the costs of capacity investments. Finally, liquid and efficient hedge markets are beneficial for participants to continually manage the price risk, basis risk, and dispatch risk involved in their physical and financial positions. Price risk arises out of spot price volatility, whereas basis risk denotes the zonal[12] or nodal price differentials between the prices at different locations due to losses and congestion (AEMC (2018*a*), page 56). Dispatch risk involves the lack of financial firmness in dispatch;[13] it is the risk of not being dispatched – for example, being curtailed due to security-constraint costs in spite of bidding price competitively.[14]

The distribution system operator (DSO), or so-called market operator, is the central entity mandated to plan out the processes for orchestrating optimal power flow (OPF) and spot pricing, and to operate the market in real-time, in agreement with the above outlined governance goals. Besides these core functions, market operators may or may not own and manage assets and hold responsibilities in facilitating auxiliary functions, such as forward contracting, financial rights trading and capacity trading, while maintaining some degree of their independence (Cramton (2017); Hogan (2014)). Whether there is one system-wide DSO, or many operators perform these functions at the same time through coaction, depends on the jurisdiction and the governance choices, as do many other settings (Eydeland and Wolyniec (2003), pages 5-6). However, it follows from the discussion in Cramton (2017) that the independence of the market operator is generally preferred for market power concentration reasons.

---

[11] Every aspect of market settlement can rarely be covered in one central dispatch. Therefore, uplift payments are also often needed. Common examples include the make-whole payments that compensate for the non-convex costs that are not funded by the spot price and the compensation payments for firm access, e.g. when nominally low-priced quantities are curtailed in the dispatch outcome. These are typically socialised with no effect on the spot price (Hogan (2014)). For further discussions about uplift, see Hogan (2014) and Cramton (2017). Note further that NERA (2013) (pages 13-16) provides an assessment for the possible curtailment of nominally low-priced quantities.

[12] We use the terms zonal and regional interchangeably.

[13] Financial firmness is the volumetric certainty about the contracted transfer.

[14] Following the definition of dispatch risk in AEMC (2018*a*) (pages 57-59).

The generator and load units are the main body of bidders. Generator units produce and sell electricity. They may be powered by thermal, renewable or nuclear fuels. Or, they can be the energy injection legs of integrated two-way units – that is, units endowed with storage capabilities such as a pumped hydro or battery plants. In contrast, load units buy electricity from the grid. They can be load-only industrial demand response providers or the energy withdrawal legs of storage units (Cramton (2017)). The fuel or resource mix of a market describes the relative magnitudes of different fuels in the system typically by nameplate capacity or by some historical throughput measure.

The transmission network and distribution network providers maintain the closely monitored electric network that connects the units and the end users, as detailed in AEMC (2022*a*). They maintain the high voltage transmission lines, the substations with voltage transformers, the low voltage distribution lines, and the various grid forming and phase control equipment in stable and secure operating conditions. The lines have secure flow limits constraining throughput, and telemetry instruments including weather scanners are installed to ensure that OPF is being directed within these limits at all times, even during extreme events. Moreover, transmission and distribution lines inevitably incur electric losses due to resistance.[15]

The interconnectors are the actively maintained transmission lines that carry capacities between the regions if a market has multiple interconnected price regions (AEMO (2021*c*), page 5). Similar to the intra-regional lines, interconnectors, too, have physical capacity limits and incur transmission losses.[16] According to AEMO (2015*a*) (page 7), these can be directed lines under the market operator's management or market interconnectors that participate by placing bid offer curves.

Finally, retail utility providers are entrusted with representing the end users in accessing volumes of electricity from the wholesale market. They ensure that the demand of the consumers is being met at the flick of a switch. However, the 2000-2001 crisis of the California market also illustrates the case for efficient hedge markets benefitting retailers.[17]

[15] Personal communications with Bill Jackson (ElectraNet) Oct 28, 2021.

[16] The calculation of interconnector losses is detailed in AEMO (2009) (pages 3-4).

[17] A detailed account of the California market crisis is set forth in Cramton (2017).

2.3 Security-constrained least-cost pricing

Energy is typically cleared as a homogeneous commodity in multi-unit auctions, which is an umbrella term including discretionary price, uniform price and Vickery auctions.[18] Any of these settings could apply to electricity pools (Hinz (2004)). In this essay, we focus on (automated) electricity auctions adhering to uniform price principles. These trade every megawatt (MW) of delivered quantity at the same price within the price locality, such as a price region.

In integrated market models, the real-world uniform price auction protocols maximise the economic utility of the consumers under security constraints. The uniform price is set as low as possible, given the bid-in quantities (MW offers) in merit order,[19] using three important notions. First, stacking the bids from the bid offer curves in the most basic way develops some implied supply and demand curves, the equilibrium of which defines the price. Second, these implied curves for energy remain well understood in the marginal pricing framework as long as we assume simple bid curves and not multi-part bids. Third, the physical constraints of the interconnected networks have price effects.

2.3.1 Merit order principles in pricing

Biggar and Hesamzadeh (2014) show that under certain conditions, centrally optimised generator-only wholesale electricity dispatch adheres to pricing on merit order principles (also see page 115 in Wood et al. (2013)). These conditions involve unit-level capacity limits but no network constraints. Their argument is as follows.

Given a set of generators N_j at a single bus j, let generator $i \in N_j$ have a constant cost c_i for all of its quantity served Q_i within its capacity limits $0 \leq Q_i \leq K_i$.

Let us define the objective function of this economic dispatch problem as $\min \sum^I c_i Q_i$, where $C_i(Q_i) = c_i Q_i$ for $0 \leq Q_i \leq K_i$. The objective function is then subject to the following constraints: $\sum^I Q_i = Q(\leftrightarrow \lambda)$, $\forall i$, $Q_i \leq K_i(\leftrightarrow \mu_i)$ and $Q_i \geq 0(\leftrightarrow \nu_i)$. These can be respectively re-expressed as $Q - \sum^I Q_i = 0(\leftrightarrow \lambda), \forall i, Q_i - K_i \leq 0(\leftrightarrow \mu_i)$ and $-Q_i \leq 0(\leftrightarrow \nu_i)$.

The Lagrange function can be formed as $\mathcal{L} = \sum^I c_i Q_i + \lambda(Q - \sum^I Q_i) + \sum^I \mu_i(Q_i -$

[18] For auction theory, we refer the reader to Krishna (2009).

[19] We interpret the merit order concept based on Hinz (2004).

$K_i) + \sum^I \nu_i(-Q_i)$. Then, the Karush-Kuhn-Tucker (KKT) conditions give for $\forall i$ that $\frac{\partial \mathcal{L}}{\partial Q_i} = c_i - \lambda + \mu_i - \nu_i = 0$, from which $c_i = \lambda - \mu_i + \nu_i$, and that $\forall i$, $\mu_i \geq 0$ and $\mu_i(Q_i - K_i) = 0$, $\forall i$, $\nu_i \geq 0$ and $-\nu_i Q_i = 0$. Therefore, $\mu_i = 0$, $\nu_i = 0$ and $c_i = \lambda$ if the dispatch quantity values are within the capacity limits. We can say that λ is both the marginal value of the demand balance constraint and the system marginal cost at this bus. If a unit is dispatched at its upper capacity K_i, then $c_i + \mu_i = \lambda$ for $\mu_i \geq 0$; that is λ is at or above c_i. Otherwise, if a unit is undispatched, then its costs are at or above λ, as $c_i = \lambda + \nu_i$ for $\nu_i \geq 0$. Therefore, firms with the lowest c_i are dispatched first: the dispatch follows merit order.

This result substantiates the basic results in bid stack–based pricing where quantities are dispatched on merit order principles while ignoring network constraints and losses.

2.3.2 Market bid stack framework

The as-bid bid offer curves are a series of price–quantity bids offered by the bid-eligible units to indicate their preferred terms. The standard unit of measurement for the bids is dollar per megawatt hour ($/MWh). These rates are later converted into the sustained rate of dispatch in megawatt hours, which can then be apportioned to the duration of the trade period, e.g. to five minutes. In most markets, units may change their bids over time; therefore, the merit order is dynamic over time. Alternatively, should the majority of the bidders use the same bids for days or longer, i.e., not change the term structure of their offers, perhaps owing to a market-specific rule, then the merit order of the bids could be described as non-dynamic (Carmona et al. (2013)).

To obtain the uniform price, the market operator first sorts the cumulative price-quantity blocks of generators in ascending order based on price (in merit order) and sums the energy quantities offered at or below every price. This gives the as-bid implied inverse supply curve of the generator units; the total generation is expressed as a function of the price. The step-wise view thereof is the inverse of the generator bid stack function, as in Chapter 1. In the mainstream structural modelling literature, the generator bid stack function – that is, the step function that expresses the price as a function of the total generation without load activity – is the as-bid market bid stack function.[20] The market operator may then assume that demand is

[20]The mainstream bid stack price modelling literature mostly but not exhaustively comprises Barlow (2002),

inelastic and that the least-cost price is set at the dollar level at which the demand line intersects the market bid stack. Identically, the marginal system cost of energy is the price of the last bid in merit, i.e., it is the most expensive bid still needed to meet demand.

Two-way fuel units simultaneously offer negative supply (demand) on their load legs and positive supply on their generation legs. The negative supply offers to buy electricity are the load bids. The construction of the market bid stack function is not fundamentally different in the presence of two-way fuel units, except that the negative energy quantities are summed with negative signs. The load bid stacks are coalesced with the generator bid stacks in the market by summing the offered negative and positive quantities, respectively, at every price over the full price range. The elastic implied demand curves of the two-way fuel units or the load-only activity (with positive quantities, i.e. the mirror images of the load bid stacks along the y-axis) are then implicit in the market bid stack[21] by construction. The market operator may use this modified market bid stack to read the price off at the price-quantity point at which the supposedly inelastic demand line intersects it or may by other means find the last available bid.

The assumptions for establishing the merit order market price as the marginal system cost of energy from bidding are direct developments from economic theory. At market level, the uniform price bid stack mechanism we describe is akin to the standard supply–demand mechanism in microeconomics. That is, we let aggregate market demand be fully inelastic and conjecture, based on the mainstream bid stack modelling literature, that the inverse market bid stack represents the aggregate market supply. Also, the merit order corresponds to trade utility maximisation on the basis of price competition under simplified conditions, as in Biggar and Hesamzadeh (2014). At unit level, in stating that the bid stacks of generators resemble an implied inverse supply relation, we are affirming a fundamental assumption from the parametric bid stack model literature. For loads, however, the implied inverse demand representation is a new assumption, as load units have not been included in the bid stack modelling literature in this way. The price impact of such an embedded elastic negative supply curve is examined in Table 2.2.

Howison and Coulon (2009), Aid et al. (2009), Carmona et al. (2013), Aid et al. (2013), Carmona and Coulon (2014), Ware (2019).

[21] The market bid stack is commonly shown with quantity along the x-axis and price along the y-axis.

Furthermore, the notion that the last bid in merit, rather than the next unused bid, sets the price, is based on the principle proposed in Hua et al. (2019) that a commercial dispatch solver would price the last MW.[22] The left-continuity assumption for the generator and load bids follows from the last MW premise as well.

The above discussion of the price discovery process and the example below demonstrate the mechanics of the implied supply and demand curves and the price calculation with the two types of energy bids. However, the now presented framework is relatively simple in the sense that it omits reserve bids, security constraints, losses and interconnectors from the price setting context, which we shall later include. The following example shows the basic construction of the market bid stack step function with and without two-way fuel activity.

Example 2.1. *The uniform price is calculated on merit order principles to illustrate the price effect of the two-way fuel activity in the market. The two-way loads are assumed to use a generic strategy, whereby they bid considerably lower to buy than they bid to sell.*

Let a market receive three generator bids – 20 MW at \$100, 70 MW at \$1000, and 10 MW at \$10 – and no load bids at first. The merit order can then be written as (10 MW, \$10) → (20 MW, \$100) → (70 MW, \$1000), in increasing order on price.[23] *It follows that the generator bid stack, the cumulatively increasing generation offers* ① *(10 MW, \$10) →* ② *(30 MW, \$100) →* ③ *(100 MW, \$1000) is the as-bid market bid stack. It is also left-continuous. Note the implications of left-continuity. At every bid price, the generation quantity goes up to the full bid quantity (inclusive), which implies the possibility of complete dispatch. However, zero dispatch is impossible given the left-continuous definition of the first bid in merit order. Also, should the price fall between two bid prices, the associated quantity is the lower one at the lower*

[22] This relates to the problem of dual degeneracy in the marginal price when it is determined as the dual variable of the demand balance constraint (as in Section 2.3.3). If one was to write a simple linear example for security-constrained least-cost dispatch as a two-band minimisation problem in its Lagrange equation form, such that both bands were completely dispatched, seeking to determine the price as the Lagrange multiplier, one would find that the price cannot be uniquely determined without an assumption about whether the last MW or the next hypothetical MW is used to set the price (Wood et al. (2013), page 114). This pre-assumption case leaves infinite price solutions within the price range defined by the marginal costs considering the last MW and the next MW at the end points of the range, i.e., a problem of dual degeneracy within the range, for the given edge case when both bid bands are fully utilised. Hogan (2012), Ela and O'Malley (2015) and Biggar and Hesamzadeh (2022) reach the same conclusion for more general settings and explain that the problem is due to the (piece-wise) linearity of the solver's objective function and that it implies the time inconsistency of the trade value maximising price outcome.

[23] In this notation, (10 MW, \$10) refers to 10 MW of energy being supplied at \$10 or more until it is superseded by the next bid, (20 MW, \$100) supplying an additional 20 MW at minimum \$100.

price: suppliers do not offer to sell additional quantities at prices below the next bid price, which makes economic sense. For example, at \$900 that falls on $[\$100, \$1000)$*, the generator bid stack takes 30 MW as at* $\$100$ *and not 100 MW as at* $\$1000$*. Therefore, in the inverse view in Table 2.1,* ① *(10 MW, \$10) is 10 MW on* $[\$10, \$100)$*,* ② *(30 MW, \$100) is 30 MW on* $[\$100, \$1000)$ *and* ③ *(100 MW, \$1000) is 100 MW on* $[\$1000, \infty)$*.*

The market operator may then assume that demand is inelastic and use the economic notion that the least-cost price is set at the dollar level at which the demand line intersects the market bid stack. Identically, the least-cost price can also be found as the price of the last bid in merit. For the price calculation, let pool demand be 50 MW. Because 30 MW is not sufficient to fill 50 MW in full, the last bid used for setting the price at the marginal system cost would be the third in merit order: (70 MW, \$1000). To the same effect, the market operator could just evaluate the last rung of the market bid stack at the demand quantity, ③ *(100 MW, \$1000), to get the unit price of the incremental 1 MW energy at 50 MW. The generation-only price is 1000 \$/MWh both ways, as in Table 2.2.*

Table 2.1 : **Market bid stack with two-way fuel activity**

The table coalesces the positive generator bid stack and the negative load bid stack in the market at every price. This gives the market bid stack as ① (5 MW, \$10) → ② (25 MW, \$100) → ③ (30 MW, \$900) → ④ (100 MW, \$1000) → ⑤ (135 MW, \$2000).

Price level	Generation fuels: generator bid stack (MW, \$)			Two-way fuels: generator and load bid stack (MW, \$)				Market bid stack (MW, \$)
	① (10, \$10)	② (30, \$100)	③ (100, \$1000)	④ (135, \$2000)	① (-25,-\$100)	② (-5,-\$10)	③ (0, \$900)	
-\$100	+0 MW				-25 MW			Negative MW
-\$10	+0 MW					-5 MW		Negative MW
\$10	+10 MW						-5 MW	① (5, \$10)
\$100		+30 MW					-5 MW	② (25, \$100)
\$900		+30 MW					-0 MW	③ (30, \$900)
\$1000			+100 MW				-0 MW	④ (100, \$1000)
\$2000				+135 MW			-0 MW	⑤ (135, \$2000)

Now consider adding one positive load bid of 35 MW at \$2000 and three negative load bids of -20 MW at -\$10, -10 MW at -\$100 and -5 MW at \$900 to the market for the two-way fuels, which sum to zero MW overall. The bid on the generation leg can be appended to the previous generation bid stack (positive supply), and the load leg can be treated as negative supply. First, the load merit order is (-10 MW, -\$100) → (-20 MW, -\$10) → (-5 MW, \$900) in increasing price order. Then, the load bid stack ① *(-25 MW, -\$100) →* ② *(-5 MW, -\$10) →* ③ *(0 MW, \$900) is the cumulatively increasing energy load in merit order that is left-continuous. Note the*

implications of left-continuity. The load fuels can never be dispatched in the full bid volume, but they can go to nil easily. Also, should the price fall between two bid prices, the associated quantity is the more negative one at the lower price: buyers offer to buy more quantities at prices below a given bid price. For example, the load bid stack at \$10 that falls on $[-\$10, \$900)$ *takes -5 MW as at* $-\$1$ *and not 0 MW as at* $\$900$*). In this way,* ① *(-25 MW, -\$100) is -25 MW on* $[-\$100, -\$10)$*,* ② *(-5 MW, -\$10) is -5 MW on* $[-\$10, \$900)$ *and* ③ *(0 MW, \$900) is 0 MW on* $[\$900, \infty)$ *in Table 2.1.*

In addition, the generation leg of the two-way fuel unit gives the last rung of the combined generator bid stack ① *(10 MW, \$10)* → ② *(30 MW, \$100)* → ③ *(100 MW, \$1000)* → ④ *(135 MW, \$2000) as 135 MW on* $[\$2000, \infty)$ *due to the left-continuity on the inverse.*

Figure 2.1 : **Market bid stack**

The figure shows the aggregate market bid stack that coalesces both generator and load bids, as in Example 1.

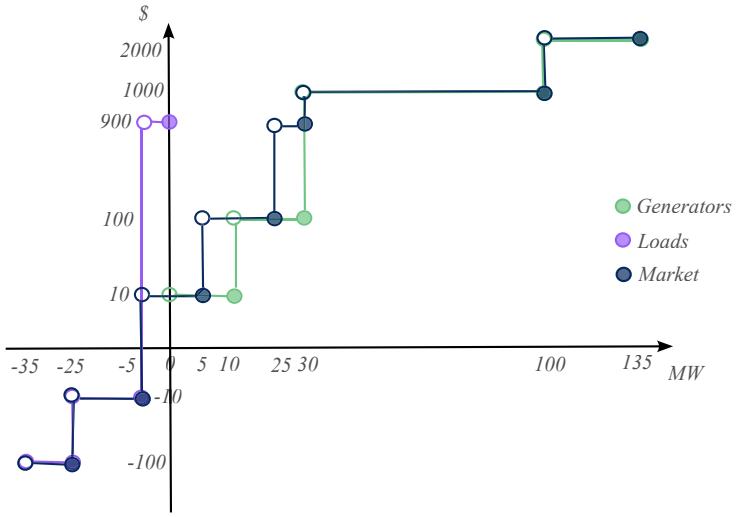

For the price calculation with load bids, the load-adjusted market bid stack coalesces the positive generator bid stack and the negative load bid stack quantities at every price in the market. As shown in Table 2.1 and Figure 2.1, meshing the generator and the load bid stacks gives the load-adjusted market bid stack as ① *(5 MW, \$10)* → ② *(25 MW, \$100)* → ③ *(30 MW, \$900)* → ④ *(100 MW, \$1000)* → ⑤ *(135 MW, \$2000). This ordering can then be used to determine the system cost price at 50 MW demand. Because 30 MW is not sufficient to meet the 50 MW demand, the last rung of the market bid stack,* ③ *(100 MW, \$1000), would be used for setting the price. That gives a price of 1000 \$/MWh for the last 1 MW.*

In edge cases – that is, at quantities at full bid amounts – the price is still that at the aggregated market bid curve. For example, 30 MW demand is an edge case, because the first two generator bids in merit order sum to 30 MW, whereas the offset from the load bid is zero MW, as shown in Figure 2.1. Here, the price would have been $100 in the absence of load activity (green), but with loads, the price is $900. Note that because of left-continuity, this value is consistent with any quantity over the last 1 MW, i.e., on the range of (29 MW, 30 MW]. In this example, at 29 MW, there is 1 MW load activity and 30 MW dispatched generation, after which the load is shed at 30 MW over the incremental change; hence, it is the price of the load bid that sets the price.

Table 2.2 : **Price effect of two-way fuel activity**

The table shows the merit order price effect of adding two-way loads to the market (right) compared to the generator-only setting (left). Price differentials arise between 5-10 MW and 25-30 MW.

Demand	Generator-only	With two-way fuels
[0 MW, 5 MW]	$10	$10
(5 MW, 10 MW]	$10	$100
(10 MW, 25 MW]	$100	$100
(25 MW, 30 MW]	$100	$900
(30 MW, 100 MW]	$1000	$1000
(100 MW, 135 MW]	$2000	$2000

To evaluate the price effect of the two-way fuel activity, i.e., the embedded elastic negative supply curve, we show an illustrative breakdown for different levels of demand in Table 2.2. As one might expect, the load legs of the loads absorb supply at low prices, which contracts the implied inverse supply curves if demand is low. As a result, the load effect results in higher prices at lower levels of demand – that is, a price of $100 between 5 and 10 MW instead of $10 and $900 between 25 and 30 MW instead of $100, as in Table 2.1. In summary, when loads follow a broadly typical buy low sell high strategy, the price effect results in a price increase at lower quantities and a quantity increase at high prices at higher quantities.

2.3.3 Marginal pricing principles

The market price is thus determined as the marginal system cost of energy, i.e. the cost of an incremental 1 MW load, which is typically given as the dual variable of the demand balance

constraint of the LP central dispatch program.[24] Locational marginal pricing (LMP) principles are now introduced for a more complete treatment of security-constrained least-cost marginal price discovery in a general DC load flow model, in line with the work of Schweppe et al. (1988).

There are two frequent settings of LMP: nodal and zonal. The nodal model uses every substation bus (source) separately as an injection point to obtain the gradient of the total system cost for marginal demand withdrawals at the reference node[25] ex-post, given the dispatch solution (Ott (2003)). It computes many different market prices at a multitude of locations for the same network area. It follows that nodal LMP can comprehensively price congestion, as it considers various transmission routes separately (AEMC (2020), pages 18-22)). In the zonal setting, in contrast, the market price is calculated as the gradient of the total system cost for a change in the demand at a single reference node of the network area (swing bus or sink), ex-post, after the dispatch result is known. Therefore, there is only one zonal price per network area. The zonal setting is usually viewed as an approximation of the full-fledged nodal LMP design (AEMO (2012*c*), page 10).

Most commonly, nodal prices can be decomposed into the bid-in marginal system cost, the locational marginal loss and the locational marginal congestion. A simpler representation of nodal prices in Ott (2003) omits marginal losses, whereas the more general form in Hogan (2014) accounts for both the co-optimised reserve requisites and losses. We can express the price p_i at node i for all k in the binding constraint set B as

$$p_i = \lambda_N^{c,l} - \sum_{\forall k \in B} A_{i,l,k} S_k, \tag{2.3.1}$$

where $\lambda_N^{c,l}$ denotes the marginal cost of energy for a unit change in MW injection at node i withdrawn at the reference node N, co-optimised with reserves (upper index c) and after losses (upper index l),[26] which can be collapsed to the as-bid marginal system cost of energy as $\lambda_N^{c,l} := \lambda_i$

[24] "Economic theory derives the fact that marginal cost pricing is optimum in a social welfare sense. This can be viewed as a way to introduce spot prices which causes the customer to choose a value for demand which satisfies the social optimality conditions for the demand at the time." as in AEMO (2012*c*) (page 9).

[25] We use the terms node and bus interchangeably.

[26] Equation (2.3.1) restates the first equation on page 534 in Ott (2003).

while neglecting reserves co-optimisation and losses. Then, $A_{i,l,k}$ denotes the constraint coefficient, the power flow change over network element (link) l for a unit increase in MW injection at node i and withdrawal at node N. Furthermore, S_k denotes the shadow price (marginal value) of the constraint: the cost of a unit increase in the constraint coefficient with respect to constraint k. Note that $S_k = 0$ for all non-binding constraints. Therefore, p_i at all locations i collapses to the same system price $\lambda_N^{c,l}$ if there are no binding constraints. When there is a binding constraint over any link l, however, this affects every nodal price with a non-zero constraint coefficient $A_{i,l,k}$ for l anywhere in the network.[27]

Hogan (2014) warns that dispatch-based LMP is built on the actual dispatch solution, which is an imperfect approximation of the optimal outcome, and that therefore the accuracy of the constraint coefficients might deviate from the optimal flows in the presence of reliability unit commitment or other lumpy system requirements. Indeed, sometimes not all binding constraints are used; for example, contingency constraints may be left out (Ott (2003)). Similarly, based on Cramton (2017), the constraints that are non-competitive by some market concentration or constraint violation measure may be removed to mitigate market power anomalies.

In contrast, the zonal price at reference node N breaks down into the bid-in marginal cost with reserves co-optimisation and losses as

$$p_N = \lambda_N^{c,l}, \tag{2.3.2}$$

because $A_{ik} = 0$ at N as in Biggar and Hesamzadeh (2014) (page 154). The shadow price of the constraints (congestion) is no longer explicit in (2.3.2) compared with (2.3.1).[28]

2.3.4 Security-constraint price effects

Although the security-constraint bottlenecks are not explicit in the zonal price in (2.3.2), the physical limitations are present in the network; they inevitably influence the viable set of

[27] As Hogan (1999) states for non-radial networks, "A single transmission constraint in an electric network can produce different prices at every node. Simply put, the different nodal prices arise because every location has a different effect on the constraint. This feature of electric networks is caused by the physics of parallel flows." Otherwise, the constraints over the links only apply for neighbouring nodes.

[28] The nodal structure better disentangles the shadow price of line congestion at least in radial systems. By contrast, the zonal design without nodal price differentials tends to export the price effects of local line limits to entire regions (AEMC (2019*a*); Leslie et al. (2019); NERA (2020); AEMC (2020)).

MW offers for dispatch and therefore the market price outcome. What bid or bids turn out to be marginal and in what quantity depends both on the demand level and the underlying constraint topography.[29]

Two price channels are associated with the physical constraints that can modify the merit-order-based marginal bid selection for computing the marginal system cost of energy before losses λ_N^c in (2.3.2). First, the bid-in quantities are constrained-on or constrained-off in out-of-merit interventions.[30] Second, quantity offsets due to binding constraints over the marginal 1 MW are fairly common. Both price effects stem from pre-empted constraint violation.

First, the constrained-on quantities are nominally high-priced MW offers that must run either because of binding technical limitations such as a ramp-down rates or to relieve system gridlocks by buying, for example inertia or system strength counterflows. Analogously, the constrained-off quantities are nominally low-priced MW offers that are curtailed due to binding technical limitations, such as thermal constraints, ramp-up rates, the lack of system strength, or any other constraint. Although these quantities appear uneconomic and economic, respectively, in a nominal sense, before considering any security-constraint non-bid factors, they are in fact feasible and unfeasible in the least-cost solution given the opportunity costs of breaching the physical limits of the network. On the supply side, constrained-on quantities are appended to the merit order, whereas constrained-off quantities are blocked out and not included in the merit order. Translating that into the equivalent effect on inelastic demand, constrained-on quantities decrease demand, whereas constrained-off quantities increase it. These modifications indirectly affect the marginal bid set and the price result.

Second, sometimes network elements must reduce throughput to relieve an otherwise violating constraint or to change quantities (decision variables) within a binding constraint to permit the incremental 1 MW power flow increase on the grid. Although the net amount of reduction and increase would equal 1 MW, these forced changes most probably involve targets summing to more than 1 MW that directly affect the marginal bid set and the price result.

Expanding on Example 2.1, the price impacts of these direct and indirect security constraint

[29] Including the effects of security constraints relaxes the 'as-bid' assumption and replaces it with an 'as-feasible' view of the market bid stack.

[30] The scenarios shown in AEMC (2018*b*) (pages 242-254) and AEMC (2018*a*) (page 57) detail the conditions for constraining quantities. See also AEMO (2021*d*) (pages 6-7).

effects are demonstrated in greater detail in the following example.

Example 2.2. *As earlier, on a hypothetical grid with no security constraints, the unit price of the incremental 1 MW power at 50 MW demand is evaluated as 1000 $/MWh using the as-bid market bid stack with two-way fuel activity, ① (5 MW, $10) → ② (25 MW, $100) → ③ (30 MW, $900) → ④ (100 MW, $1000) → ⑤ (135 MW, $2000). Similarly, price is $100 at 15 MW demand.*

Relaxing the no-constraint assumption, first, the constrained-on quantities are bid-in volumes that must run despite having offered a price in their bids that is above the market price (in the absence of constraints) – that is, a price above 100 $/MWh at 15 MW demand. Assume that 12 MW offered at $2000 is constrained-on. This will see a negative demand adjustment of 12 MW. The demand after adjustment is 15-12 = 3 MW. The cost of the last MW supply from 2 MW to 3 MW is obtained as follows. Because 2 MW $\leq$ 5 MW and 3 MW $\leq$ 5 MW, the price is 1 $\times$ 10 $/MWh using the adjusted demand and the original market bid stack. This shows that constrained-on quantities decrease the market price.

Second, the constrained-off quantities are bid-in volumes that are curtailed despite having offered a price in their bids that is at or below the realised market price, which is $100 at 15 MW load. This constrained-off amount pops off of the market bid stack, and the remaining market bid stack contracts leftwards. Equivalently, demand is adjusted upwards by 12 MW. For 15 MW demand, the demand after adjustment is 15+12 = 27 MW, and the market bid stack stays as is. Then, the cost of the last MW supply from 26 MW to 27 MW is obtained as follows. Because 26 MW $\geq$ 25 MW and 27 MW $\leq$ 30 MW, the price is 1 $\times$ 900 $/MWh. This shows that constrained-off quantities increase the market price.

Moreover, when a network bottleneck reduces MW flows on some nodes and increases them on others, so that the net as seen in dispatch-based pricing is always (approximately[31]) 1 MW, we might observe the following at 50 MW demand. The incremental 1 MW power is subject to a binding constraint $1 \times q_A + 0.8 \times q_B \leq 10$*, where* q_A *and* q_B *are the node-level decision variables. If this constraint is already binding, i.e.,* $1 \times q_A + 0.8 \times q_B = 10$*, then the changes in these decision variables must be such that the constraints on the left hand side (LHS) do not increase*

[31] Ignoring losses in this discussion.

above zero ($1 \times \Delta q_A + 0.8 \times \Delta q_B \leq 0$), but their sum increases by 1 MW ($\Delta q_A + \Delta q_B = 1$). In the solution, $-\Delta q_A = 4$ MW power is removed from the node that serves the quantities from 45 to 49 MW in the market bid stack, and $\Delta q_B = 5$ MW is supplemented from the node dispatching 49–54 MW in the market bid stack. This will see no demand adjustment and no change in the original market bid stack but only a significant 'multiplier change' in the price calculation. For 50 MW demand, because 44 MW $\geq$ 30 MW and 54 MW $\leq$ 100 MW, the price is -4 $\times$ 1000 + 5 $\times$ 1000 = 1000 $/MWh using the original market bid stack.

A small variation to the above example would be the removal of 4 MW power from the node that serves the quantities from 16 to 20 MW in the market bid stack, if that corresponds to $-\Delta q_A = 4$ MW, as a way of relieving the binding constraint and causing the price effect. In addition, $\Delta q_B = 5$ MW is supplemented from the generation node dispatching 49–54 MW in the market bid stack. In combination, the reduction and the increase result in a net 1 MW incremental change in quantity. Then, the price becomes -4 $\times$ 100 + 5 $\times$ 1000 = 4600 $/MWh using the original market bid stack, giving rise to a price increase relative to the price ignoring the security constraints.

2.4 Differences in market design and fuel mix

Here, the key differences across market designs are discussed within the integrated pool model. As related to price discovery, the number of prices per market, the timing of the trade intervals, the regulatory price thresholds, the basis for bidding, the extent to which the reserves are co-optimised and the fuel mix are the main differences within the category of integrated pool auctions around the world.

First, the market prices are published per price node in nodal markets and per price region in zonal markets (Eydeland and Wolyniec (2003) (page 11); Cramton (2017)). As regions involve multitudes of nodes, there are only a handful of prices in regional markets but hundreds in nodal pools (PJM (2022*b*)). Other markets operate in a single-price setting, where there is only one price per country (Mayer and Trück (2018)).

Secondly, pools specify the dispatch and the trade intervals for the day-ahead, real-time or multi-settlement schedules usually at 5-minute, 30-minute or hourly resolution, which impact the timing of the trade intervals. The dispatch interval determines the periodicity for dispatch

target allocation, and the trade interval is the recurrence of price settlement. These may be aligned for a single schedule, or they may differ. The two kinds of schedules, day-ahead and real-time. The day-ahead market is a form of forward market into the dispatch and trade intervals of the next trading day. Plants may plan their delivery both physically and financially using the day-ahead market, according to Ott (2003), as is common in many countries in Europe (Mayer and Trück (2018)). In contrast, bidding into real-time markets inevitably gives less predictable quantity outcomes as these are settled directly in the dispatch and trade intervals of the trading day. Real-time markets without day-ahead markets are common in Canada and Australia (Mayer and Trück (2018)). Nodal markets in North America tend to have both day-ahead and real-time schedules in combination. The purpose of this multi-settled design is to enhance the efficiency of the equilibrium price approximation for capacity decisions mainly through arbitrage between the day-ahead and the much more volatile real-time market.[32] Indeed, Ott (2003) shows for such a market that day-ahead and real-time prices strongly converge.

Third, using a regulatory price band consisting of a price floor and a price cap, as mentioned in Barlow (2002), is a common technique for maintaining the market price in a particular band. Although these price thresholds are typically imposed at vastly different levels in different countries, the trade-off between a more restrictive and a less restrictive policy is well-understood. A narrower price band promotes price stability and impedes exercising market power, whereas a wider price band rewards private investment into generation and storage infrastructure.[33] The regulatory choice between the two works towards either mitigating or aggravating the positive and potentially negative price spike events.

Fourth, some pools adopt a cost-based approach to bidding, whereas others accept price-based bids. In the cost-based approach, the bids must reflect the bidder's audited production costs based on the short-run marginal costs of production (SRMC), as discussed in Munoz et al. (2018) and Ward et al. (2019). In the price-based (bid-based) setting, bidders are not limited on a cost basis (Munoz et al. (2018)), although regulatory price thresholds may still apply.

Moreover, as energy is aimed to meet end user consumption as precisely as possible, in principle, throughput follows centrally scheduled target directives: the units receive targets in

[32]The advantages of the spot-forward arbitrage are detailed in Cramton (2017), Ott (2003) and Hogan (2014).

[33]Personal communications with Bill Jackson (ElectraNet) Oct 28, 2021.

every dispatch interval. However, because the scheduled demand by the end of the dispatch interval is necessarily a prediction, disparities will arise between the scheduled targets and instantaneous consumption. In response, ancillary-type reserves can be kept on standby to safely balance the electric frequency of the system within a band around, for example, 50 hertz (Eydeland and Wolyniec (2003) (pages 8-9); Cramton (2017)). Energy pools are often augmented by ancillary-type reserves trading, although the details of synchronising energy and reserves are often extremely dissimilar. One end of the spectrum is when price settlement for energy and reserves is mostly joint (co-optimised), and the other end is when the two are fully separate – that is, when all reserves receive out-of-market payments. There are many configurations in between. Different market designs can be developed to include some ancillary-type reserves in the co-joint processes, such as frequency balancing, but not others, such as voltage stability or system restart services, as is the Australian experience (AEMC (2021*c*)).

Finally, the fuel mix plays an important role in market design owing to a few reasons. One aspect why the fuel mix must be a balanced mix of different resources is MW reliability to avoid short-run scarcity. Renewable energy, particularly wind generation, is highly intermittent and requires quick-response high-reliability complements such as hydro generation, battery throughput or industrial demand response. Another challenge to the market design in allowing high penetration of renewables that are inverter-based is that these resources do not provide inertia. Turbine generators that do, such as gas and coal, are in this case required in the fuel mix. Finally, depending on the dispatch formulation, some fuels are more likely than others to create lumpy costs in the network; for example definite must-run conditions apply for coal-based generation in Cramton (2017), which might make a stronger argument for a mixed integer dispatch solver as part of the market design.

2.5 Financial markets along electricity markets

Electricity markets today are often complemented by derivatives markets for price, congestion and scarcity risk hedging. They trade firm instruments on a fixed MW of electricity flow as the underlying asset to manage the spot price volatility of physically or financially binding firm positions (ASX (2020)). There are also products more specific to congestion-linked difficulties, such as the basis risk and the dispatch risk. Point-to-point financial transmission rights

(FTR) trading is common in nodal markets, which also provides financial firmness on the quantity (Cramton (2017)). Similarly, flowgate and other solutions have existed in zonal markets to provide firm access to hedge the dispatch risk associated with security constraints.[34]

Furthermore, capacity markets are annual forwards auctions for electricity trading during scarcity periods based on Cramton (2017). These aim to solve the dual problem of scarcity risk and suppressed spot prices that are insufficient to cover the costs of new generation investment by introducing another source of revenue for generators that are willing to reserve some of their capacity for reliability response in exchange of some forward-type payments as in Hogan (2014).

Any of these financial contracts are either physically settled, in which case the underlying commodity is physically transmitted, or cash settled, in which case it is not. As trade with physical delivery requires transmission infrastructure, electricity market operators are in a unique position to facilitate trade or act as a counterparty in short-term (for example hourly or daily) derivative contracts with physical settlement if that is permitted by the applicable legislation (Deng and Oren (2006); Cramton (2017)). If not facilitated by the main market operator, physical settlement is either conditional on the cooperation of a private operator according to Eydeland and Wolyniec (2003) (pages 5-6), or off-grid purchase agreements can be struck if the generator is in the immediate vicinity of the buyer, and if the parties can set up a private transmission line (Broom (2020)). Once established, trade with physical settlement has a direct impact on price discovery, as it effectively removes both capacity and demand from the wholesale market.

In contrast, cash settlement makes financial contracts much more accessible, which implies higher liquidity for convenience-related financial reasons. These markets potentially also impact spot price formation, most directly by influencing the participants' bidding decisions.

2.6 Conclusion

The fact that electricity price formation heavily depends on market rules motivates this chapter on electricity market design. In terms of similarities and dissimilarities across market

[34] For an international review on creating congestion compensation and firm access, see NERA (2013) (pages 13-23).

designs around the world, the sets of market participants and government goals – as well as dispatch optimisations, to a lesser degree – can be viewed as relatively similar. However, a number of other aspects exist from which market designs significantly vary, including the timing of the trade intervals, the regulatory price thresholds, the bid language, the extent to which the reserves are co-optimised and the fuel mix.

After unravelling the different aspects of market design, an emphasis is placed on the link between price formation based on constrained optimisation and economic bid aggregation principles. Importantly, an equivalence of the two is shown under limiting conditions. Some important conceptual background is also built on bid stack–based pricing by extending the standard bid aggregation framework to storage fuels and network constraint effects. This reveals that by consuming at incrementally lower rates, storage fuels too can set the electricity price. Moreover, constrained-on and constrained off quantities are shown to take effect by shifting the inelastic demand line, which is also not without a price impact.

Note that the current essay aims to set the scene for Chapter 3 about the Australian market design by deciphering the most commonly used nomenclature of the field.

Chapter 3

A survey of the Australian National Electricity Market[35]

3.1 Introduction

Electricity market designs comprise the rules for market operations in response to the 'energy trilemma' that states that markets should manage the trade-offs between achieving affordability, security and sustainability through policy and planning (Newbery (2016)). This complicated multi-interval problem usually results in very specific local market designs.

Precisely expressing how such a market operates enables the identification of the key factors that impact price formation within that setting. Therefore, this chapter presents an in-depth survey of the market design of the Australian NEM to build knowledge for an improved price hypothesis over the extended equilibrium framework presented in Chapter 2. A descriptive summary of the prevailing regulations (AEMC (2021*c*)), the available technical reports and implementation software (Gorman et al. (2022)), and some insights from practitioners and relevant data are set forth. The main contribution is the unravelling of the constrained dispatch optimisation formulation of the NEM Dispatch Engine (NEMDE) within the broader market context. This allows recovering how the electricity price is set by NEMDE. Worked numerical examples are also provided to analyse actual price outcomes using the historical solver solution data.

Multi-regional interconnectedness, network losses, wholesale load activity, co-optimised ancillary services, and congestion effects surface in this analysis as highly relevant to pricing. Some of these factors can be integrated into theoretical equilibrium frameworks, whereas others unveil the limitations of the economic equilibrium argument for electricity markets. The present survey might be useful to those interested in the nexus between these factors and the price or in the NEM market design in general.

[35]This chapter is largely based on the paper Katona et al. (2023*b*) with Christina Sklibosios Nikitopoulos and Erik Schlögl contributing in a supervisory capacity.

The rest of the chapter is organised as follows. Section 3.2 summarises the NEM across the market design features mentioned in Chapter 2. Section 3.3 discusses the optimisation procedure of the NEMDE focusing on dispatch, and Section 3.4 presents price formation in that setting. Section 3.5 concludes the chapter.

3.2 Overview

This overview of the Australian NEM begins with the sheer size of the grid. Spanning about 5,000 km end to end and counting 6 interconnectors and over 55 GW nameplate capacity along the east coast of Australia, the NEM is the longest interconnected market in the world (AEMC (2022*a*)). Its length is paired with what is colloquially known as a chilli shape. The rest of Australia belongs to the Northern Territory Electricity Market (NTEM) and the Wholesale Electricity Market (WEM) in Western Australia (AEMO (2023*e*,*f*)).

3.2.1 Institutions

The responsibilities around the orderly operation and effective oversight of the NEM are held by the following institutions. First, the Energy Security Board (ESB) oversees that the evolving market design honours the NEM's commitment to efficiently integrating competitive new technologies and reducing the system's carbon footprint while maintaining strong system adequacy (ESB (2020), pages 15-28). Second, the Australian Energy Market Commission (AEMC) presides over rule making to promote the long-run interests of consumers as in AEMC (2022*b*). The AEMC establishes and amends the National Electricity Rules (NER, the Rules[36]) under the National Electricity Law (as per Rule 1.2 in the Rules). Finally, the Australian Energy Regulator (AER) enforces the Rules made by AEMC as in AEMC (2022*b*).

Furthermore, according to AEMC (2022*b*), the Australian Energy Market Operator (AEMO) is the sole, independent market operator that establishes, reviews and executes procedures to fulfil extensive operative obligations in secure and reliable dispatch and price settlements under 3.2.1 in the Rules.[37] The AEMO automates the security-constrained least-cost auction mecha-

[36]The present chapter is written using version 175 of the Rules, which is referenced in AEMC (2021*c*).

[37]The AEMO does not facilitate physically settled bilateral agreements, and it is impartial to resolving current market issues.

nism in a linear solver framework, the NEM Dispatch Engine (NEMDE),[38] which co-optimises the dispatch of energy and market-based ancillary services, such that interconnector flows, too, are synchronised over the five price regions in real time (see 3.9.2 in the Rules). For the market to operate with the least amount of intervention as per 3.1.4 (a) in the Rules and AEMO (2020*d*) (page 5), supply–demand and bid analysis both by the market operator and by individual bidders heavily rely on telemetry, price (AEMO (2022*j*,*c*)), demand and supply adequacy forecasts, and other information sources administered by AEMO. Many of these resources are also disseminated to registered market participants to inform their bidding and potentially re-bidding actions on the minute, as per 3.1.4 (a.2) in the Rules. Some are also publicly available on the NEMWeb (AEMO (2022*h*)).[39] Finally, the different systems supporting the NEMDE are shown in Table 3.1.

Table 3.1 : **Market systems**

The table lists the different AEMO data systems that underpin real-time dispatch by delivering pre-calculated values to the NEMDE.

System		Function
Automatic Generation Control	AGC	Communications tool for sending out dispatch instructions (as per 3.8.21 (d) in the Rules) including frequency balancing Regulation targets electronically (AEMO (2021*g*), page 9).
Australian Solar Energy Forecasting System	ASEFS	Solar forecast algorithm for intermittent output (UIGF) feeds to the NEM Dispatch Engine (AEMO (2023*c*), pages 4-5).
Australian Wind Energy Forecasting System	AWEFS	Wind forecast algorithm for intermittent output (UIGF) feeds to the NEM Dispatch Engine (AEMO (2023*c*), pages 4-5)
Electricity Market Management Systems	EMMS	Portal and API interface for submitting bids and intermittent plant availability (AEMO (2017*c*), page 1), (AEMO (2022*d*), pages 10-11).
Market Management Systems Data Model	MMS Data Model	Data model for providing data to market participants (AEMO (2021*h*)).
Market data NEMWeb	NEMWeb	Public website for historical data based on MMS Data (AEMO (2022*h*)).
Network Outage Scheduler	NOS	Planned outage calendar for informing the medium-term adequacy process (AEMO (2018), pages 9-10), (AEMO (2020*d*), page 12).
Supervisory Control and Data Acquisition	SCADA	Telemetry system (metering) for informing higher level applications (AEMO (2021*g*), pages 8, 14).

[38] An open-source reference implementation of NEMDE is also available thanks to Gorman et al. (2022).

[39] Indeed, a number of publicly available data sources underpin the present survey, including the 'Register of all current Market Participants' (3.2.1 (b) in the Rules) in AEMO (2022*f*), the bid submission files of AEMO (2022*i*) as part of the MMS Data Model in AEMO (2021*h*), and the NEMDE outcome data in AEMO (2021*p*).

3.2.2 Market settings

The NEM operates in a zonal market design. There is one locational reference node, i.e. price node, for each of the five regions in the market – New South Wales (NSW), Queensland (QLD), South Australia (SA), Tasmania (TAS), and Victoria (VIC) – roughly corresponding to the administrative divisions of the country. Therefore, five market prices are issued by in the NEMDE per trade interval.[40] Note further that the nodal LMPs are also calculated in the NEM at every market connection point (bus) as a congestion information resource on mis-pricing as per 3.4.1 (3) and 3.7A (b.2) in the Rules to better understand the costs of security constraints. These costs are, however, not directly expressed in the five zonal spot prices.[41]

Since 1 October 2021, both the dispatch interval and trade interval are 5 minutes, in contrast with the earlier methodology with 30-minute trade intervals but 5-minute dispatch intervals, where six preliminary 5-minute prices had been averaged for every half-hourly price (AEMO (2021*i*), page 3). Therefore, the prices are single real-time (5-minute intra-day) prices, as there is neither multi-settlement nor market coupling in Australia apart from the import–export between the price regions. The switch to 5-minutes settlement prevents exercising market power through certain gaming strategies to bidding[42] and promotes price transparency.

Moreover, the NEM market design ascertains the following regulatory price threshold settings. A regulatory price floor is administered at $-\$1000$ per MW and the price cap is at \$15,100 per MW as of October 2021.[43] The price cap is also indexed to inflation based on AEMO (2021*i*) (page 3). This is a relatively unrestrictive policy compared with the stricter regulatory thresholds in other markets worldwide.

[40] See the RegionID and BandCost fields in the PriceSetting tab of the AEMO (2021*p*) data.

[41] From a price quality perspective, explicitly priced congestion effectively recovers the security constraint costs (the shadow price) at different points on the grid. Whereas the cost of congestion is directly expressed in nodal markets, the price only contains vague information about congestion in zonal markets.

[42] One such strategy involved bidding high to move the prices to the market price cap in the first 5-min interval and bidding low for the rest of the 30-minutes to collect the resulting relatively high price (after averaging) in large quantities.

[43] In line with the AEMC reliability standards (as per 3.9.4 in the Rules) AEMC (2021*a*), respectively.

3.2.3 Bidding rules

Bidding is price-based in the NEM. Bidding away from the verifiable costs, often by means of bidding software, called disorderly bidding, is fully consistent with the Rules. One implication of this, and the fact that the prices are not suppressed between strict regulatory price thresholds, is the lack of limitation on market power concentration: exercising market power through strategic bidding is evidently encouraged. However, the lack of limitation reinforces price results closer to the costs of capacity investments that better pay for new investments.

The bid-eligible units fall under the three categories: energy bidders (as per 3.8.6 and 3.8.7 in the Rules), reserves bidders (as per 3.8.7A in the Rules) and market interconnectors, i.e. Market Network Service Providers (MNSPs) (under 3.8.6A in the Rules). The standard bid type involves ten price–quantity pairs, but there are a few more bid types within some bidder categories. First, for energy bidders, generators and loads[44] are warranted the standard ten and twice ten price–quantity bid slots every trade interval (as per 3.8 in the Rules), respectively, much like in the example in Section 2.3.2. An upcoming rule change may, however, replace the twice ten bid bands by 20-bid single trader submissions for the two-way fuels (AEMC (2021*b*), pages 2-4). In addition, all energy bidders can use fixed bids when they intend to act as price takers and secure trade amounts that might not be otherwise allotted to them in the auction.[45] Second, reserves bidders include two groups of service providers: the market-based ancillary services and the non-market scarcity reserves providers. The market ancillary services bids – that is, the Frequency Control Ancillary Services (FCAS) bids (AEMO (2021*o*), page 6) – are co-optimised with energy in the NEM. There are a number of different FCAS bid types for the different FCAS services, which are all standard 10-slot bids (see Section 3.3.5.2). Furthermore, non-market reserves occasionally enter the market calculations through placeholder bids for scarcity and distributed capacities, such as Reliability Emergency Reserve Trader (RERT) bids,[46] as per 3.20.7 (d) in the Rules and AEMO (2020*g*) (pages 4-11), and Distributed Generation bids.[47] Third, market interconnectors, too, use the ten standard price–quantity bands

[44] Two-way fuels and hybrid plants are registered as generators and loads separately within each category based on AEMO (2021*l*) (page 5) and AEMO (2022*f*). Load-only units are registered as loads only.

[45] See the FIXEDLOAD field definition of the AEMO plant commitment (bid) data (AEMO (2022*i*)).

[46] RERT is an example of out-of-market payments.

[47] See the RT_ and DG_ prefixes, respectively, under the DUID field in the AEMO (2022*i*) data.

to express their MW offers under 3.8.6A in the Rules.[48] Finally, the units are obliged to provide technical information about their availability in accord with their registration profiles to complete their bid submissions (AEMO (2022*i*)).

Re-bidding is another facility provided to the bid-eligible market members under 3.8.22 in the Rules. The previously submitted bid quantities can be revised any number of times during the day until the start of the relevant trade interval; there is 'no gate closure' for changing the bid quantities other than the start of the trade interval based on AEMC (2015) (page ix) and AEMO (2021*s*) (page 6). Prices, too, can be modified in re-bidding but only until the start of the trading day, as there is only one price submission per day.[49] There are various valid reasons for re-bidding, but in each case, particularly for late re-bids, regardless of the disclosed re-bid explanations, bidders are obliged to act with fidelity (in good faith) in changing their commitments as per 3.8.22A in the Rules.[50]

3.2.4 Fuel mix

Table 3.2 shows the regional breakdown for the NEM generation fuel mix. The fuels most dominant in at least one region are listed on top. Coal-fired plants are the most common in NSW, QLD, and VIC, and hydro is the most prevalent in TAS. SA is the most diverse region in terms of fuel mix, with natural gas and renewable generation in almost 50%–50% proportion. The load fuel breakdown at the bottom of Table 3.2 only shows battery and omits pumped hydro. Again, SA has the largest battery capacity of all NEM regions.

According to the modern market design principle, the fuel mix should present a reliable and environmentally sustainable fuel combination. Renewable energy generation, including solar and wind generation, is unmistakably paving the way to meeting the up-to-date CO_2 targets in the NEM; however, these methods, particularly wind generation, are highly intermittent. They require complementary quick-response FCAS by gas turbines, hydro generation, battery throughput, or industrial demand response for MW reliability. Because FCAS is fully co-optimised with spot energy in the NEMDE, it is already streamlined for the highest opti-

[48] Basslink is the only MNPS is the NEM currently under two DUID fields, BLNKVIC and BLNKTAS AEMO (2022*f*)

[49] See the OFFERDATE field for the price rows with BIDDAYOFFER_D) in the AEMO (2022*i*) data.

[50] Personal communications with Bill Jackson (ElectraNet) Oct 28, 2021.

Table 3.2 : **Fuel mix in the NEM**

The table shows the regional generation fuel mix breakdown for the NEM market with data from calendar year 2010-21. The interconnector count is shown as of 2021, with a new SA-NSW line (through VIC) called EnergyConnect also underway as of the writing of this chapter (ElectraNet (2021)). Source: Table O9 for calendar year 2021 in % terms in Department of Industry, Science, Energy and Resources (2022), Table O12 for calendar year 2020 in Department of Industry, Science, Energy and Resources (2021), and AEMO (2017*e*) (pages 4-8).

	NSW	VIC	QLD	SA	TAS
Generator fuels (%/year)					
Hydro	4.0%	5.5%	1.5%		80.6%
Black coal	69.7%		65.1%		
Brown coal		63.0%			
Natural gas	2.8%	3.2%	14.2%	33.8%	1.0%
Wind	7.6%	16.3%	2.5%	41.2%	15.9%
Solar	13.8%	10.2%	13.2%	23.3%	2.1%
Biomass	1.5%	1.4%	1.8%	0.7%	0.3%
Oil products	0.5%	0.3%	1.5%	1.0%	0.2%
Load fuels (GWh/year)					
Battery		51.4		64.3	
Interconnectors (6)	3	4	2	2	1

misation efficiency. Another challenge in allowing a high penetration of renewables including distributed energy such as rooftop solar panels that are inverter-based, is that these resources do not provide inertia. Turbine generators that do, such as gas and coal, are in this case required in the fuel mix. On the other hand, grid forming storage solutions can provide fast frequency response, despite being inverter-based.

3.2.5 Hedge markets

Finally, the NEM pool is in contact with the Australian Securities Exchange (ASX) that offers financial risk management products. First, the ASX trades financially settled contingent products on spot electricity[51] as the underlying flow asset with continuous delivery (ASX (2020)). These are used to hedge price risk. Second, in terms of the basis risk, the regional NEM has fewer price differentials than markets in the nodal design; it only has the five regional prices. Thus, there is neither FTR trading nor any flowgate-based congestion rights solution; there are no auction- or exchange-traded financial products to hedge the regional price differentials. Third, with regard to the dispatch risk implicitly covering the congestion rent in zonal settings, hedge markets should provide a form of firm access to hedge the risk of being

[51] Referencing the five regional prices obtained in the NEMDE.

constrained-off or constrained-on. However, no such contracts are currently available in the NEM outside perhaps 'over–the–counter' (OTC) deals. Fourth, utilities and eventually market participants are sometimes exposed to the elevated costs of importing from higher price regions. According to AEMC (2014) (page 13), "currently there is no mechanism available to market customers to be able to hedge against the negative IRSR [inter-regional settlements residue] cost". Finally, physical contracts are not traded either at the ASX or at any centralised auction or clearing house (non-OTC), and there are no capacity markets alongside the NEM to help manage the scarcity risk. In summary, the ASX only offers hedge products against the price risk.

3.2.6 Reliability planning

The trade schedule issued at every 5-minute dispatch/trade interval marks the culmination of months if not years of market planning. This point is illustrated by elaborating the long-term to short-term to real-time considerations in capacity planning and system upgrades.[52]

Reserves and system upgrades planning is centred on "the reliability standard, set by the NER, [that] specifies that a region's maximum expected unserved energy (USE) should not exceed 0.002% of energy consumption per year" (AEMO (2020*c*), page 21). The AEMO must take every reasonable endeavour to achieve this rate and to monitor other reliability and sustainability proxies in the interim to mitigate the scarcity risk.[53] The AEMO undertakes annual reviews of several forecasting and planning assessments on an ongoing basis, including both long-term capacity models and medium- and short-term and security-constrained time-sequential LP reliability models, while also making provisions for the immediate nature of continuous system stability remediation, especially during extreme events, under up-to-date future scenario assumptions.[54]

The Integrated System Plan (ISP) is a comprehensive forward-looking roadmap for market upgrades (AEMO (2021*n*), pages 6-7). Drawing from AEMO (2021*n*) (pages 6-7, 58),

[52] Note that there is no day-ahead market in the NEM and therefore no day-ahead information about the next day's scarcity risk. This makes robust real-time adequacy planning a more challenging task in general.

[53] A more detailed record of these success indicators can be found in AEMO (2015*b*) (pages 4-15) and AEMO (2020*c*) (page 21).

[54] As stipulated in AEMO (2020*c*) (pages 15-31, 49) and AEMO (2021*b*) (pages 4-8).

although the integrated methodologies used in the report (a suite of interlinked market models) are primarily aimed at system development analysis while minimising capital expenditure, the future constraints they formulate on first principles are often also practicable later at higher time resolutions. The ISP model group accommodates weather and climate effects, gas supply, outage simulations, thermal capability, stability, system strength, inter-regional limitations, unit commitment, inter-temporal plant limits in two-way fuels and bid profiles that depart from the SRMC, to name but the main features of this comprehensive security-constrained LP framework, in quantitative detail.[55]

The Electricity Statement of Opportunities (ESOO) is a 10-year-ahead evaluation of supply adequacy and a reserve requirement breakdown for the USE goal using a system-constrained market simulation over larger time blocks as per 3.13.3A in the Rules and AEMO (2021*a*) (pages 13-20). Preparing this assessment is inseparable from producing reliable minimum, maximum and mean demand forecasts (AEMO (2021*a*), pages 21-29), which later form the basis of a cascading sequence of wholesale, distributed (e.g. rooftop solar) and retail (residential and business) consumption projections (AEMO (2021*f*), pages 12-22). The supply adequacy calculations use the up-to-date Pre-dispatch constraints and projected network constraints to forecast the USE over the 10-year window (AEMO (2015*b*), pages 7-9).

The Energy Adequacy Assessment Projection (EAAP) is a 2-year-ahead probabilistic assessment of the available supply capabilities for satisfactory USE results in line with 3.7C in the Rules and AEMO (2020*a*) (pages 4, 7). The security-constrained EAAP solver considers daily generation limits and replenishment information in all relevant fuel types, including reservoir storage and pump generation (AEMO (2020*a*), pages 8-19), using the resource-constrained Generator Energy Limitation Framework (GELF) declarations submitted by the scheduled generators (AEMO (2014*a*), page 4-5).

In addition, the AEMO administers two granular security-constrained Projected Assessment of System Adequacy (PASA) procedures using LP in line with 3.7.1 in the Rules, AEMO (2015*b*) (pages 11-12) and AEMO (2012*b*) (pages 8-9). These are the weekly Medium Term PASA (MT PASA) up to two years with a daily resolution, and the two-hourly Short Term PASA (ST PASA), which is six trading days ahead with 5-minute granularity (AEMO (2020*d*),

[55]The ISP methodology is thoroughly presented in AEMO (2021*n*) (pages 8-59).

page 5). Both use the Supervisory Control and Data Acquisition (SCADA) telemetry (see Table 3.1) and the submitted PASA energy availability of the generator units.[56] Moreover, MT PASA may rely on the GELF resource limit declarations (AEMO (2020*d*), page 8). Another difference is that the MT PASA allocates resource (energy) constrained capacities that have fuel stockpile or water storage limitations to high demand periods over weekly blocks whereas the ST PASA uses the daily-resolution submission data for this allocation (AEMO (2015*b*), page 15).[57] Finally, in addition to the unit-specified plant limit information and the long-run ESOO load, AEMO prepares the Unconstrained Intermittent Generation Forecasts (UIGF) for wind and solar generation in the dedicated Australian Wind Energy Forecasting System (AWEFS) and Australian Solar Energy Forecasting System (ASEFS) (see Table 3.1) as inputs to the MT PASA (AEMO (2020*d*), page 9).

The main MT PASA objective is then to calculate the anticipated USE in the medium term, and indicate the timing and location of any expected breaches as per 3.7.2 in the Rules. This includes the days at the highest risk of security shortfalls and the Low Reserve Condition (LRC) status (AEMO (2020*d*), pages 11-12). These tasks require medium-term demand forecasts as discussed in AEMO (2020*d*) (pages 21-26). The MT PASA process signals the violating network constraints in view of the Network Outage Scheduler (NOS) and the Monte Carlo simulated ambient forced outage landscape (AEMO (2020*d*), pages 12-19; AEMO (2018), pages 9-10). Conversely, the medium-term LRC output also helps participants schedule outages in the NOS.

Closer to the time of dispatch, the ST PASA subsequently publishes the final LRC and the Lack of Reserve (LOR) statuses for the trade interval under 3.7.3 of the Rules (AEMO (2012*b*), page 15). As explained in AEMO (2012*b*) (page 11), the LOR1, LOR2 and LOR3 are the largest contingency-linked explicit benchmark triggers for the AEMO to enable intervention procedures such as constraint relaxation, load shedding, and reserve trader bids (see Section 3.3.6). This also requires a load forecast considering reserve sharing between the regions (AEMO (2012*b*), page 7). The last step of the ST PASA cycle feeds the calculated

[56] See the PASAAVAILABILITY field in the plant commitment data of AEMO (2022*i*), where "PASA availability includes the generating capacity in service as well as the generating capacity that can be delivered with 24 hours' notice" (AEMO (2020*d*), page 8).

[57] See the DAILYENERGYCONSTRAINT field in the AEMO (2022*i*) data.

short-term capacity and the forward-looking assessment of the most likely reserve requirements to the Pre-dispatch protocol as in AEMO (2010*b*) (pages 56-57).

During Pre-dispatch NEMDE publishes the dispatch and price forecasts in a security-constrained LP routine in Pre-dispatch mode, at two timescales; there is a day-ahead run with 30-minute resolution and an overlapping hour-ahead run with 5-minute resolution (AEMO (2021*q*), pages 6-7). Note, however, the main differences between Pre-dispatch and Dispatch.

Pre-dispatch lacks the following four features of Dispatch (AEMO (2010*b*), page 7). First, Pre-dispatch used to omit Fast Start Inflexibility Profiles (see Section 3.3.5.1).[58] Second, Pre-dispatch does not calculate Unit Economic Participation Factors for apportioning aggregate transmission node losses to unit level. Furthermore, Pre-dispatch does not consider intervention scenarios (see Section 3.3.6) or communicate with the AGC remote control activation system (see Section 3.3.5.2) besides the SCADA metering (AEMO (2021*q*), page 9).

On the other hand, Dispatch lacks two functions that are available in Pre-dispatch (AEMO (2010*b*), page 7). First, Unit Daily Energy Constraints are used from the bid submissions similar to PASA for energy constrained units in Pre-dispatch.[59] Second, spot price sensitivities, the expected changes to the published price results over changes to the demand and scheduled generation forecasts, are posted as part of Pre-dispatch as in AEMO (2021*r*) (page 3), but not for the actual Dispatch.

This concludes the reliability assessments undertaken by AEMO and takes us to the start of the 5-minute dispatch and trade interval.

3.3 Dispatch

The Dispatch mode of the main LP run of the NEMDE algorithm is dedicated to update the security-constrained least-cost MW targets in the market, as per 3.8.1 in the Rules, while maximising the value of trade as well as to determine the spot price. This is achieved using a cost minimising objective function subject to system constraints. Ex-post price settlement then

[58] This has, however, been subject to a rule change, as having these profiles in Pre-dispatch is more helpful for 5-minute settlement than it had previously been for the 30-minute trade intervals (AEMC (2019*b*), pages 9-11; AEMO (2021*q*), page 8).

[59] See the DAILYENERGYCONSTRAINT field of the AEMO (2022*i*) data.

obtains the marginal value of demand, or the marginal price, from the solution of this dispatch process, in line with 3.1.4 (a.4) in the Rules.

3.3.1 5-minute cycle of dispatch and price settlement

In accordance with the NEM timetable in AEMO (2021*s*) (page 8), as per 3.4.3 in the Rules, the 5-minute cycle for dispatch and price settlement can be reconstructed as six steps. The timeline of the 7:05 AM price run is posited as follows.

1. Before 7:00 AM, the NEMDE is running in Pre-dispatch mode for two overlapping timescales in parallel to issue price and target forecasts 5 and 30 minutes ahead as per 3.2.2 (b) in the Rules (AEMO (2021*s*), page 8). Nearing 7:00 AM, the forecasts are made available in EMMS to inform bid revisions until 7:00 AM.

2. At 7:00 AM, the NEMDE receives a snapshot of the electric system in SCADA. These initial MW values are compared with the MW targets from the previous cycle to verify the units' conformance (see Section 3.3.2).

3. At 7:00 AM, the NEMDE in Dispatch mode collects the forward-looking demand, outage (AEMO (2021*g*), page 29), and constraint information from the most recent 5-minute Pre-dispatch run.

4. Immediately after 7:00 AM, the NEMDE runs in Dispatch mode (AEMO (2021*s*), page 8), including a cascading series of re-runs (see Section 3.3.6), to schedule the MW quantities and set the price.

5. Immediately before 7:05 AM, the AEMO sends out the dispatch instructions including the MW target quantities and either the required times of completion or the linear ramp rates to be used through AGC or EMMS at 7:05 AM (AEMO (2021*g*), page 9).

6. Immediately after that, the prices for 7:05 AM are calculated ex-post (see Section 3.4) and published in EMMS.

3.3.2 Bid-eligible unit classification and conformance

The NEMDE uses the initial assumption that all bid-eligible units are conforming with the dispatch targets received in the previous time period. However, the devoirs associated with re-

ceiving a target are not the same for every bid-eligible unit. Market service providers with a Dispatchable Unit Identifier (DUID) are classed as scheduled, semi-scheduled or non-scheduled. However, only the scheduled and semi-scheduled units are bid-eligible as per 3.8.2 (a) in the Rules.[60]

The vast majority of the large-sized $\geq$30 MW generation and load units are scheduled (AEMO (2022*b*), page 2). They receive dispatch instructions in the form of point targets that they must neither exceed nor fall short of.

In comparison, the small-sized $\leq$30 MW units are mostly non-scheduled units (AEMO (2022*b*), page 2). They typically neiter bid nor receive any dispatch targets. Non-scheduled units are unrestricted in their output, which is forecast by AEMO for a demand adjustment (AEMO (2021*f*), pages 13-15). As price takers, non-scheduled units have a negligible impact on the energy spot price.

In between are the large-sized $\geq$30 MW semi-scheduled units, i.e. the wind and solar farms, which merit an additional category owing to their characteristically intermittent nature (AEMO (2022*b*), page 2). The NEMDE relies on the AWEFS and the ASEFS for the UIGF output from semi-scheduled plants as per 3.7B in the Rules and AEMO (2023*c*) (page 12). These systems integrate technical plant specifications using plant-level conversion models and various aspects of the expected ambient weather conditions using SCADA.[61] One may argue that these models have improved significantly over time.

Indeed, before a recent rule change semi-scheduled units received cap targets[62] in place of a currently much stricter obligation to follow their resource availability as point targets (AEMC (2021*e*), page ii). The cap targets were only allotted during the semi-dispatch interval when certain trigger conditions were met;[63] otherwise, the semi-scheduled plants acted as price takers. So-called semi-dispatch caps (SDC) were issued at every trade interval to notify the units whether they were given a target like scheduled units (capped, $SDC = 1$), or they were permitted to operate without limits similar to non-scheduled units (not capped, $SDC = 0$) (AEMO

[60] For the Classification and DUID information, see the Generators and Scheduled Loads tab in AEMO (2022*f*).

[61] The model inputs of the UIGF metric are detailed in AEMO (2022*a*) (page 9-12), AEMO (2022*d*) (page 5-8), and AEMO (2021*g*) (page 42).

[62] They could fall short of their targets but they must not have exceeded them.

[63] See 'semi-dispatch interval' in the Glossary in the Rules in AEMC (2021*c*).

(2021*g*), page 10). The main reasons for a $SDC = 1$ flag, i.e. for a semi-dispatch interval, were uneconomic bids and constraint-driven transmission bottlenecks. However, units were able to bid exclusively at the market price floor to receive an $SDC = 0$ and only later decide whether or not to inject any energy into the grid. Depending on the expected market price, they could avoid negative prices and still be conforming with $SDC = 0$.[64] This avoidable source of intermittency by arbitrary ceases of dispatch carried system stability implications. For this and further price quality reasons, a recent rule change requires semi-scheduled plants to dispatch at the level of their resource availability under a $SDC = 0$ flag and at the level lower of their resource availability and cap target under a $SDC = 1$ flag (AEMC (2021*e*), pages ii, 10-11).

Given the classification-specific targets, an error tolerance system is used to regulate when plants reach non-conformance. This employs two error counts, a large and a small error count, based on which the plants maintain a compliance status throughout the trade intervals, as discussed in AEMO (2021*g*) (page 10, 32-41). Starting from the normal status, increasing error counts cause plants to go off-target, and then to gradually worsen to non-responding, NC-pending or non-conforming (AEMO (2021*g*), pages 32-41). As a direct consequence of this status, non-conforming units cannot set the spot price as per 3.8.23 in the Rules.

3.3.3 Energy demand elasticity

First, we refer to Barlow (2002) for the mainstream argument that electricity demand is mostly inelastic. As technological advances allow new freedoms in consumption planning, however, optimised consumption patterns via, for example, smart systems, bilateral agreements, demand response, storage fuel activity and distributed energy solutions, also start to factor into electricity demand both in households and in industrial production. These quantities are conditional on the price of electricity and pose a fundamental challenge to the theoretical inelastic demand assumption.

Electricity is being withdrawn at wholesale, retail, and non-market locations simultaneously. Based on AEMO (2021*a*) (pages 22-25), for unravelling wholesale demand elasticity in the NEMDE must first consolidate all relevant consumption planning practises to specify en-

[64] Unless a system constraint reason materialised for them to receive a target $SDC = 1$ while bidding at very low prices.

ergy demand. As retail participants are becoming increasingly responsive to prices by means of distributed energy resources – for example, by installing solar panels[65] and small-scale batteries, by scheduling energy intensive tasks overnight, and more indirectly via power purchase agreements – retail consumption decreases with greater price elasticity and wholesale demand follows. Only after these adjustments, retail demand and wholesale demand are virtually indistinguishable in the absence of wholesale storage activity and demand response units, such as aluminium smelters.

This wholesale energy demand excluding wholesale storage uptake and demand response is predicted by the market operator for every 5-minute trade interval in advance. The demand forecast with 50% probability of exceedance (POE) minus the projected non-scheduled generation and minor adjustment terms for the regional reference nodes (RRNs), is the scheduled demand currently used as energy demand in the Dispatch run for price settlement (AEMO (2021*f*), pages 10-11, 13, 16). After the predicted demand measure enters the automated NEMDE auction the only sources of price elasticity are wholesale storage uptake and demand response.[66]

3.3.4 Objective function in Dispatch mode

Dispatch minimises the whole-of-the-market costs of energy and FCAS simultaneously as per 3.8.1 in the Rules. The objective function can be expressed as

$$\begin{aligned} min \sum_{r}\sum_{b}\sum_{s}\sum_{d}\sum_{i=1}^{m} \mathsf{bid\_price}_{r,b,s,d,i} \times \mathsf{bid\_qty}_{r,b,s,d,i} + \\ + \sum_{n}\sum_{j} \mathsf{violation\_degree}_{n,j} \times \mathsf{cvp}_{n} \times \mathsf{mpc} \\ s.t. \text{ constraints} \end{aligned} \tag{3.3.1}$$

where by r we denote the price region (NSW, QLD, VIC, SA, or TAS), by b the bid type (energy, FCAS, or MNSP), by s the service type, by d the dispatchable unit ID (DUID) of the bid, and by m the number of tranches where i is the ith tranche. For energy, s distinguishes generation from

[65] The NEM is leading the way in integrating distributed generation, particularly rooftop solar, according to AER (2021) (page 33).

[66] Apart from the numerical example in Section 2.3.2 (see Table 2.2), the price elasticity of the demand is not quantified in this chapter. Total energy demand is assumed to be mostly but not perfectly inelastic.

loading, and there are eight different FCAS types s for ancillary services (see Section 3.3.5.2). Then, $\mathsf{bid\_price}_{r,b,s,d,i}$ captures the as-bid prices for the $\mathsf{bid\_qty}_{r,b,s,d,i}$ decision variables (in MW). Note that $\mathsf{bid\_qty}_{r,b,s,d,i}$ is only negative for $b = energy$ and $s = loading$ as in AEMO (2010*c*) (page 13). Furthermore, $\mathsf{violation\_degree}_{n,j}$ is the jth slack/deficit variable in the nth constraint denoting the MW difference between the left hand side (LHS) and the right hand side (RHS) of a given constraint (AEMO (2011), page 9). Then cvp_n gives the constraint penalty factor associated with the set of the constraint. An exhaustive summary of the constraint sets is shown in Table 3.3, with the set-level penalty cvp_n values shown for all sets (AEMO (2023*d*), pages 5-27). Finally, mpc stands for the market price cap at the time (indexed to inflation) in dollar terms, and $\sum_n \mathsf{violation\_degree}_n \times \mathsf{cvp}_n \times \mathsf{mpc}$ captures the violation costs associated with the physical constraints. The objective function (3.3.1) turns these penalties into dollar amounts so that the conjoint effect of the as-bid cost of supply and the constraint-invoked penalty costs can be simultaneously minimised.

A binding constraint is any constraint that has LHS = RHS with $\sum_n \mathsf{violation\_degree}_n = 0$. In contrast, any violating constraint would see LHS different from the RHS and a non-zero penalty of $\sum_n \mathsf{violation\_degree}_n > 0$. In the absence of binding or violating constraints, $\sum_n \mathsf{violation\_degree}_n = 0$, equation (3.3.1) collapses to $\sum_r \sum_b \sum_s \sum_{i=1}^{m} \mathsf{bid\_price}_{r,b,s,d,i} \times \mathsf{bid\_qty}_{r,b,s,d,i}$. But that is not equivalent to only minimising $\sum_r \sum_b \sum_s \sum_{i=1}^{m} \mathsf{bid\_price}_{r,b,s,d,i} \times \mathsf{bid\_qty}_{r,b,s,d,i}$ to start with. Optimum bid selection purposely absorbs the violation costs associated with physical constraints while establishing a constraint hierarchy – that is, allowing "conflicting constraints to be violated in a pre-determined priority order based on their relative CVP prices" (AEMO (2011), page 6). Last, the as-bid costs with an implicit $\mathsf{cvp}_{bid} \leq 1$ tend to have a lower priority than a constraint violation with $\mathsf{cvp}_n > 1$ for the same MW quantity.

3.3.5 Constraints in Dispatch mode

Most constraints in the NEMDE are generic constraints[67] formulated as linear equations in the form of

[67] In fact, pursuant to Mackenzie et al. (2020) (page 24), "most changes to the dispatch optimisation process have been done via generic constraints rather than through explicit modifications to the formulation of the NEMDE optimisation". This is also revealed in the way more recent system requirements have found their way into the NEMDE, e.g., system strength shortfalls in SA have been resolved using a new class of generic constraints for system strength according to AEMO (2020*c*) (page 30). See also the Binding Impact tab in the NEM constraint report (AEMO (2020*e*)).

Table 3.3 : **Constraint sets in the NEM**

The table shows the system constraints recognised by the main price run of the NEMDE engine as in AEMO (2023*d*) (pages 5-27), including the usual constraint sets under normal system state and outage events. In particular, this table excludes the constraint sets used by the NEMDE only in What-If and Outturn intervention pricing modes. Note that every listed constraint set holds a multitude of exact linear constraint equations (see the Binding Impact tab in AEMO (2020*e*)). Source: AEMO (2023*d*) (pages 5-27); however the presented information draws on other AEMO publications too listed in the References. *constraint set item 38 has a variable penalty factor.

Constraint set	cvp_i	Source of RHS	Item #
Operational plant limitations, see Section 3.3.5.1			
Unit Zero	1160	AEMO (NOS/SCADA)	1
Unit Dispatch Conformance	1160	AEMO (SCADA)	2
Unit Ramp Rate	1155	Bid submission	3
Fast Start Inflexible Profile (T1, T2, T3, T4)	1130	Bid submission	4
Unit Direction System Security	755	AEMO (control room)	5
Unconstrained Intermittent Generation Forecast (UIGF)	385	AEMO (AWEFS/ASEFS)	6
Energy Inflexible Offer (Fixed Loading)	380	Bid submission	7
Unit MaxAvail	370	Bid submission	8
Joint constraints (FCAS), see Section 3.3.5.2			
FCAS MaxAvail	155	Bid submission	9
FCAS Joint Ramping	155	AEMO (formula)	10
FCAS EnablementMin and EnablementMax	70	Bid submission	11
FCAS Regulation Raise (R5RE)	10	AEMO	12
FCAS Regulation Lower (L5RE)	10	AEMO	13
FCAS Contingency Very Fast Lower 1 second	9	AEMO	–
FCAS Contingency Very Fast Raise 1 second	9	AEMO	–
FCAS Contingency Fast Raise 6 second (R6SE)	8	AEMO	14
FCAS Contingency Fast Lower 6 second (L6SE)	8	AEMO	15
FCAS Contingency Slow Raise 60 second (R60S)	6	AEMO	16
FCAS Contingency Slow Lower 60 second (L60S)	6	AEMO	17
FCAS Contingency Delayed Raise 5-minute (R5MI)	4	AEMO	18
FCAS Contingency Delayed Lower 5-minute (L5MI)	4	AEMO	19
System conditions, see Section 3.3.5.3			
Interconnector Zero	1160	AEMO (NOS/SCADA)	20
Interconnector Dispatch Conformance	1160	AEMO (SCADA)	21
Interconnector Capacity Limit	1150	AEMO (ratings)	22
MNSP Interconnector Ramp Rate	1155	Bid submission	23
MNSP Availability	365	Bid submission	24
MNSP Losses	365	Fixed feature	25
Satisfactory Network Limit	360	AEMO	26
Secure Network Limit Stability and Other	35	AEMO	27
Secure Network Limit Thermal	30	AEMO	28
Interconnector Outage (Hard) Ramping	35	AEMO (NOS/formula)	29
Planned Network Outage (Hard) Ramping	26	AEMO (NOS/formula)	30
Planned Network Outage (Soft) Ramping	<1	AEMO (NOS/formula)	31
Interconnector Outage (Soft) Ramping	<1	AEMO (NOS/formula)	32
Non-Physical Loss Oscillation Control	<1	Fixed feature	33
Market requirements, see Section 3.3.5.4			
Total Band MW Offer	1135	Bid submission	34
Total Band MW Offer MNSP	1135	Bid submission	35
Regional Energy Demand Supply Balance - Load Shedding	150	AEMO (forecast)	36
Regional Energy Demand Supply Balance - Excess Generation	150	AEMO (forecast)	37
Negative Residue Management	2*	Fixed feature	38
Tie-Break	<1	Fixed feature	39

$$\sum_{t}\sum_{i=1}^{c} A_{i,l,k} \times \mathsf{ID\_qty}_i \leq RHS_{pre-calc} + \mathsf{violation\_degree}_k + \mathsf{operating\_margin}_k, \quad (3.3.2)$$

for the kth constraint over link l in price region r over all c connection points, where t denotes the type of each connection point quantity $\mathsf{ID\_qty}_i$ (intra-regional connection point or an interconnector) according to AEMO (2021*d*) (page 5) and AEMO (2017*a*) (pages 9-10). The LHS collects the $\mathsf{ID\_qty}_i$ corresponding to the decision variables $\mathsf{bid\_qty}_{r,b,s,d,i}$ in (3.3.1) but grouped by connection points, which can be optimised. The $A_{i,l,k} \geq 0.07$ terms represent the monitored flow across the network elements for an incremental change at the RRN N, i.e. the constraint coefficients, as per AEMO (2021*d*) (page 9-10) and AEMO (2015*a*) (page 11).[68] Moreover, the RHS hardcodes various system limits of the constraint (AEMO (2021*d*), pages 7-8) in the MW term $RHS_{pre-calc}$, which is pre-calculated using real-time telemetry (see Table 3.1) and pre-processed data from various planning schedules (see Section 3.2.6), and the $\mathsf{operating\_margin}_n$ managing the approximations and errors associated with the limit (AEMO (2010*a*), pages 8-12). The aim is to quantify every constraint RHS such that the dynamic MW values on the LHS can be equated to them.[69] Last, the orientation of the constraint in (3.3.2) is $\leq$; therefore, $\mathsf{violation\_degree}_n > 0$ is a surplus variable (AEMO (2017*a*), page 7), and a positive coefficient $A_{i,l,k}$ means that "a generator may be 'constrained-off' when the constraint binds, while a negative coefficient means a generator is 'constrained-on' " (AER (2012), page 7). Also, the marginal value of the constraint is negative, as "by constraining off the Left Hand Side (LHS) terms these lower the objective function" (AEMO (2021*e*)). While $\leq$- and $\geq$-type constraints are both fairly common, the $=$ orientation is largely avoided in security constraints (AEMO (2015*a*), page 7)).

The requirement that the decision variables in the objective function $\mathsf{bid\_qty}_{r,b,s,d,i}$ sum to the r, b, s demand types over all $m \leq 10$ bids by the dispatchable units d in each demand type in the optimal solution is facilitated by the regional energy demand balance constraints for

[68] According to AEMO (2021*d*) (page 7), "The constraint equation decides the optimal balance of supply from the various [competing] contributors, while providing a high degree of confidence that the network limit is not violated." It follows that a high $A_{i,l,k}$ in a '$\leq$'-type equation is a competitive disadvantage.

[69] For reference, see AEMO (2021*e*), AEMO (2015*a*) (pages 7-8), AEMO (2021*d*) (page 16) and AEMO (2021*d*) (page 5).

$b \neq FCAS$ and a particular region $r = A$ (AEMO (2023*d*), pages 13-14). This constraint can be written as

$$min \sum_{b} \sum_{s} \sum_{DUID} \sum_{i=1}^{m} \mathsf{bid\_qty}_{r=A,b,s,d,i} - \mathsf{net\_exports} + \mathsf{losses} = \\ = RHS_{pre-calc} + \mathsf{violation\_degree}_{k}, \tag{3.3.3}$$

introducing two new variables, net_exports and losses, and using the notation of (3.3.1) and (3.3.2). First, $\mathsf{net\_exports} = \sum_{IC} \mathsf{interconnector\_flow}_{IC=IC_A}$ captures the sum of the relevant interconnector flows at the regional boundary points (AEMO (2009), page 3) as net export from the direction of region A. This variable is computed using the decision variables $\mathsf{bid\_qty}_{r,b,s,d,i}$ for $r \neq A$. Second, as per Gorman (2023), $\mathsf{losses} = \sum_{IC} \mathsf{loss}_{IC}$ is defined as the sum of every $\mathsf{loss}_{IC} = \mathsf{interconnector\_flow}_{IC} \times \mathsf{avg\_loss} \times \mathsf{proportioning\_factor}$ for the relevant interconnectors with a non-nil proportioning_factor for region A. Note that avg_loss is computed using Special Ordered Set 2 (SOS2) from a quadratic function detailed in AEMO (2009) (page 14-16).

As of 2020, there are 13,127 constraint equations in the NEM, split across multiple constraint sets, shown in Table 3.3.[70] Many originate in the limit equations calculated by the transmission and distribution service providers and some in the plant-specific models developed by AEMO (Mackenzie et al. (2020), page 25; AEMO (2021*d*), page 13; Mountain and Percy (2020), page 36). In line with AEMO (2021*d*) (page 8), an important feature of this fundamental equation set and the way the constraint equations based on this equation set interlink is their overall applicability regardless of whether the system is in a normal operating state or in a heavily constrained outage mode. Moreover, most equations are static, with the exception of the dynamic feedback equations shown in AEMO (2021*d*) (page 16).

The AEMO must further ensure that the constraint formulation is neither overly restrictive (over conservative) nor too slack (under conservative) (AEMO (2021*g*), pages 30-31). The former causes concerns from a market efficiency perspective and the latter exacerbates the ex-

[70] See the Constraint Changes tab in AEMO (2020*e*) and AEMO (2021*d*) (page 8).

posure to safety hazards. However, throughout the 5-minute Dispatch cycles, the AEMO can also relax the over conservative constraint equations, use variable constraint violation penalties or enact additional quick constraints ad hoc.[71] The freedom of discretionary constraint overrides does not, however, extend to stability constraints (AEMO (2021*g*), page 28).

Last, the NEMDE is an LP solver with only two binary modules. One is related to loss allocation "at connection points where one MLF [marginal loss factor] does not satisfactorily represent active power generation and consumption" (AEMO (2022*e*), page 75): dual MLFs are needed for generators versus loads or for different flow directions over an interconnector, as in AEMO (2012*c*) (page 29). The other handles the calculation of average losses using SOS2 equations (AEMO (2021*g*), page 41).[72] Note that none of these cases directly relate to plant-level unit commitment. As a consequence, the unit bid stacks are convex,[73] and while the onus is on the units to bid in a way to be able to conform with the received targets, there are additional workarounds for lumpy unit requirements apart from the fast-start flexibility unit commitment profiles (see Section 3.3.5.1). For example, the solver heavily relies on negative price bids for self-commitment from slow-start units (see Section 3.3.5.1), and it must take two switch runs to evaluate the on/off status of the Basslink interconnector in each dispatch interval (see Section 3.3.6).

3.3.5.1 Technical plant limitations

Next, we show the plant-level operational constraints regulating scheduled generation and uptake from the first segment of Table 3.3 (items 1–8). The standard bid submission template for all scheduled and semi-scheduled units requires the units to not only specify their terms of trade using ten price–quantity bid pairs but also indicate some other (non-price[74]) availability

[71] AEMO's use of discretionary constraints is mentioned in AEMO (2017*a*) (pages 9-11), AEMO (2021*d*) (page 12), AEMO (2021*g*) (pages 27-28) and AEMO (2013) (page 8).

[72] Personal communications with Nicholas Gorman Oct 4, 2022.

[73] Adding almost always convex virtual bids into the bid pool is an effective way of increasing the convexity of the pool for a better optimum schedule approximation according to Cramton (2017). Nonetheless, there are no virtual bids in the NEM.

[74] Disorderly bidding can be an implication of the fact that the price-quantity offer tranches are the only priced bid components: "Thermal generators in particular tend to face 'lumpy' [non-linear] unit start-up costs, minimum generation levels and ramp rate constraints. This means that a generator's bid may need to reflect its judgement as to how long it may be dispatched, to what extent and at what price." (AER (2017), page 26).

parameters for the period, as per 3.8.6, 3.8.7 and 3.8.19 in the Rules, depending on whether is it a fast-start unit or not (AEMO (2021*j*), page 2).[75] These inform the NEMDE's constraint RHS values about the physically feasible plant-level unit capacity.

First, all units report the minimum and maximum MW capacity limits they might have in their normal operation using the MINIMUMLOAD and MAXAVAIL fields, respectively (as per 3.8.4 in the Rules). They also need to advise AEMO about their ramp rates using the ROCUP and ROCDOWN fields (as per 3.8.3A in the Rules).

Second, every fast-start unit can submit information to opt in to submit a dispatch capability profile – that is, a Fast Start Inflexible Profile (FSIP). This involves four time parameters, T1, T2, T3, and T4 (in minutes) about re-start and ramping. T1 indicates "the time to synchronise" (T1 field definition, AEMO (2022*i*)) or start up from nil output for a generator unit. For example, a thermal plant with a 'hot banking' furnace is faster than a cold one.[76] T2 gives the time to speed up to the Minimum Load MW level as specified by the plant. T3 is the number of minutes a unit can stay on within its feasible output bounds while it is still lower-bounded (AEMO (2021*j*), page 6). T4 indicates the time it takes for the unit to shut down.

In addition, the rule around self-commitment states that given the inflexibility parameters as above, "the sum (T1 + T2) must be less than or equal to 30 minutes" (3.8.19 (e.6) in the Rules) and the sum T1 + T2 + T3 + T4 less than 60 minutes (AEMO (2021*j*), page 5). If not, units "must self-commit to be eligible for dispatch" (see 3.8.17 (a-b) in the Rules) until they notify AEMO about their "intention to self-decommit" (3.8.18 (c) in the Rules)" at least 2 days in advance of dispatch" (3.8.18 (b) in the Rules). Then, "a scheduled generating unit is self-committing if it has a self-dispatch level of greater than 0 MW, where the self-dispatch level equals the sum of all energy bid in offloading (negatively priced) price bands in its dispatch offer" (AEMO (2021*g*), page 15). In other words, fast-start units may have to bid at negative prices to set their binary unit commitment variable to one (see Section 3.3.6).

Finally, the daily energy constraint is only populated by units with resource-constrained operations (see Section 3.2.6), such as hydro generators.

---

[75] These are shown as MINIMUMLOAD, MAXAVAIL, ROCUP, ROCDOWN, T1, T2, T3, T4 and DAILYENERGYCONSTRAINT in the AEMO (2022*i*) data.

[76] Personal communications with Bill Jackson (ElectraNet) Oct 28, 2021.

Focusing on the plant-level constraints from the dispatch engine's perspective, the top priority constraint set[77] is Unit Zero (item 1 in Table 3.3). This coordinates the rate of change adjustments related to shutting individual units in the engine representation of the grid, owing to a forced or planned outage. The second most important constraint set is Unit Dispatch Conformance (item 2 in Table 3.3), for which the rationale is that non-conformance with the issued targets (see Section 3.3.2) outside the acceptable operating margins (AEMO (2010*a*), pages 9-10) carries undesirable consequences for optimum planning; detecting issues around overloaded network elements is difficult. This constraint forces NEMDE to correct any disconnect between the previous MW dispatch target and the real-time SCADA MW before many other aspects in the optimisation. Most of the remaining constraint sets (items 3–4 and 6–8) are used to stay within the technical and availability requests of the units given their bid submission inputs, whereas Unit Direction System Security (item 5) puts a handle on directing individual unit output arbitrarily as and when needed for network security purposes.

3.3.5.2 Joint capacity requirements (FCAS)

Reserves service provision is also present in the NEM, both in the form of co-optimised market-based frequency balancing (FCAS) and as auxiliary non-market contracts (AEMO (2021*k*), pages 8-12; AEMO (2012*a*), page 6)). The NEM is a co-optimised market because the energy and FCAS targets are evaluated concurrently in the objective function. The FCAS-registered units first indicate their preference profiles for energy and FCAS provision; then, the task of a physically constrained minimum price optimum target co-allocation falls to the joint capacity engine constraints in the second segment of Table 3.3 (items 9–19).

Table 3.4 shows the standard ancillary service contract types in the NEM under the broader categories of market and non-market services. Market services only include FCAS, whereas non-market provision involves System Restart (SRAS) and Network Support and Control Ancillary Services (NSCAS). As opposed to market services, non-market enablement is not part of the co-optimisation. Therefore, these have no direct effect on the energy spot price.[78] NSCAS

[77] The constraint set with the highest constraint violation penalty cvp_i factor has top priority.

[78] Note, however, that "Where applicable, AEMO will apply constraint equations to reflect the network support agreement between the service providers and the generators, so that the market dispatch is consistent with operation under those agreements." (AEMO (2021*d*), page 11).

Table 3.4 : **Ancillary services**

The table shows the different ancillary service types in the NEM as per 3.11 in the Rules including both the market-based FCAS specifications and several standard bilateral non-market Network Support Agreements as per AEMO (2021*k*) (pages 8, 13) and AEMO (2023*b*) (page 7).

Service	Category	Function
FCAS Regulation Raise (R5RE)	Market	Continuing response over AGC to even out minor frequency drops.
FCAS Regulation Lower (L5RE)	Market	Continuing response over AGC to taper minor frequency hikes.
FCAS Contingency Very Fast Raise 1 second	Market	1 second frequency response after a credible contingency.
FCAS Contingency Very Fast Lower 1 second	Market	1 second frequency response after a credible contingency.
FCAS Contingency Fast Raise 6 seconds (R6SE)	Market	6 second frequency response after a credible contingency.
FCAS Contingency Fast Lower 6 seconds (L6SE)	Market	6 second frequency response after a credible contingency.
FCAS Contingency Slow Raise 60 seconds (R60S)	Market	60 second frequency response after a credible contingency.
FCAS Contingency Slow Lower 60 seconds (L60S)	Market	60 second frequency response after a credible contingency.
FCAS Contingency Delayed Raise 5 minutes (R5MI)	Market	5-minute frequency response after a credible contingency.
FCAS Contingency Delayed Lower 5 minutes (L5MI)	Market	5-minute frequency response after a credible contingency.
NSCAS Network Loading (NLAS)	Non-market	Manual MW load control on interconnectors after a credible contingency.
NSCAS Voltage Control (VCAS)	Non-market	Automatic enablement to absorb or supply reactive power after a credible contingency.
NSCAS Transient & Oscillatory Stability (TOSAS)	Non-market	Monitored fast-regulation of voltage, inertia and load against circuit faults after a credible contingency.
System Restart (SRAS)	Non-market	Instructed system restart after a partial or full system blackout.

are usually only enabled at times of network failures, called credible contingencies, such as generator trips, short-circuiting and insulation faults (AEMC (2021*d*)) and SRAS are only enabled after full or partial system blackouts. These are provided mostly by non-market participants endowed with the required equipment and deemed apt by AEMO on a case-by-case basis as per the pre-existing bilateral contracts in the standard non-market procedures as an example of uplift payments (AEMO (2021*k*), pages 13-14).

FCAS relates to the rotational speed on the network such that "frequency is maintained within the normal operating band of 49.85 Hz [hertz] to 50.15 Hz" (AEMO (2021*k*), page 6). If consumption suddenly drops but generators keep injecting the same MW load, then the frequency of the system will increase towards 50.15 Hz, and FCAS Lower services are necessarily called upon to withdraw quantities for balancing. Analogously, if consumption suddenly spikes but generators keep injecting the same MW load, then the frequency of the system decreases towards 49.85 Hz, and FCAS Raise services are required for system security according to AEMO

(2021*k*) (page 5). As shown in Table 3.4, there are two disparate mechanisms for frequency balancing, regulation and contingency that both incorporate lowering and raising. Contingency services are enabled using remote devices to detect and counteract contingency-event-related frequency breaches at 1 second, 6 second, 60 second, or 5-minute notice according to AEMO (2021*k*) (page 6), AEMO (2023*b*) (page 7), and AEMC (2021*d*). Regulation works through AGC at 4 second frequency (AEMO (2021*g*) (page 10) and AEMO (2021*k*) (page 6)). The requirement has a base value of 120–130 MW and a cap of 250 MW as in AEMO (2015*a*) (page 27). The mainland contingency requirement (demand) depends on the dispatch amount of the largest online generator (largest contingency) minus load relief, whereas in TAS, it also depends on inertia, as per AEMO (2015*a*) (pages 19, 25).

Units bidding in regulation and contingency FCAS use a similar bidding template per FCAS service as that for energy.[79] Apart from the ten price and quantity bands and the same availability-related fields as in the energy bid template, the ancillary submissions must also input the following four FCAS trapezium variables (see Figure 3.1) as per AEMO (2021*k*) (page 10).[80] The first two, ENABLEMENTMIN and ENABLEMENTMAX, correspond to the lowest and highest MW levels of energy dispatch required to provide a particular FCAS. In addition, LOWBREAKPOINT and HIGHBREAKPOINT bound the energy MW levels needed for servicing the stated MAXAVAIL quantity in the particular FCAS. These variables are then further scaled to AGC enablement and UIGF limits within the NEMDE (AEMO (2017*b*), pages 10-13).

The optimum combination of the regulation, contingency and energy targets – that is, the MW thermal loading on the LHS of the joint FCAS constraints in Table 3.3 – are subject to the respective service demand levels (items 12–19) individually and confined to unit-level capacity limitations on the RHS (items 9–11) collectively. The capacity limits of every service are more restrictive than stated in the FCAS trapeziums, as they take into account concurrent dispatch in other services and energy as well. More specifically, "FCAS availability for a unit at a given energy target is the maximum amount of the service that the unit can provide when it is fully delivering the amounts of all other services for which it is enabled at that energy target" (AEMO (2017*b*), page 23). Different kinds of joint ramping constraint equations (under item

[79] See the BIDTYPE field definition in the bid submission data of AEMO (2022*i*).

[80] These are shown as ENABLEMENTMIN, ENABLEMENTMAX, LOWBREAKPOINT and HIGHBREAKPOINT in the AEMO (2022*i*) data.

Figure 3.1 : **FCAS trapezium**

The figure shows an FCAS trapezium for a single service, where the shaded area captures service availability based on the bid submissions. The upwards sloping segment of the trapezium captures a complementary relationship between energy and the particular FCAS service, whereas the downwards slope indicates a trade-off between the two. Source: AEMO (2017*b*).

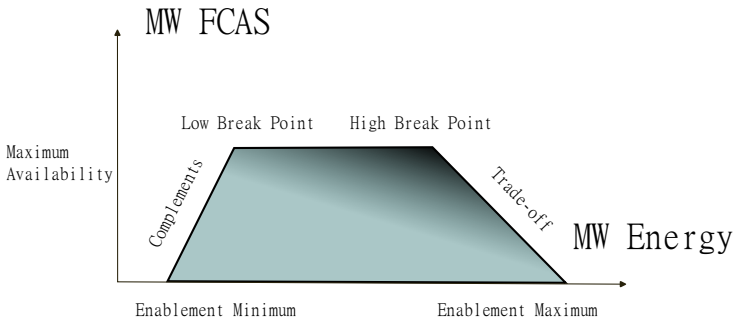

10) are applied to enforce this (AEMO (2017*b*), pages 14-26).

First, the energy and regulating FCAS capacity constraints reinforce the scaled regulation service trapeziums. Second, the joint ramping constraints limit every regulation service trapezium to the area defined by the AGC ramp-up and ramp-down rates. Third, the joint capacity constraints capture the offset between regulation, contingency and energy by shifting the sloped lateral sides of the contingency trapeziums to narrow service availability by the concurrent regulation targets. Finally, the most restrictive of all the above relations emerges as the limiting constraint for each service.

The conjoint nature of FCAS and energy grants that when the co-optimisation constraints bind, they may alter the energy target. In fact, it is not uncommon for a unit to be "trapped within the FCAS trapezium" (AEMO (2017*b*), page 20) – that is, for the NEMDE not to ramp up or ramp down a unit's energy dispatch while supporting regulation or contingency provision.

3.3.5.3 Secure and reliable system conditions (excluding FCAS)

We now turn to the main body of non-plant constraints that aim to avoid equipment damage and safety hazards in general to lend reliability to the operation of the complex electric network as a whole. The third segment of Table 3.3 (items 20–33) showcases interconnector operations, network stability, thermal capacity limits and outage management as the most important non-plant aspects to system security.

First, Interconnector Zero (item 20) is the highest priority network constraint that handles

both planned and forced outages – that is, the full loss of a directed or MNSP interconnector at any notice – for a minutely accurate representation of the disconnected element in the NEMDE so that power flows avoid black lines (AEMO (2023*d*), pages 5-6). However, interconnector limits also apply absent line disconnections. When interconnectors (including MNSP) are fully operational, the security objective is to ensure they conform to the advised thermal capacity ratings (AEMO (2021*d*), page 8), availability limits and ramp rates as well as to correct non-conformance (see Section 3.3.2) if needed (items 21–24). Moreover, based on AEMO (2023*d*) (page 12), there are minor equations for preventing "non-physical circulating flows in both MNSP flow offer directions at once" (item 25) and managing frequency variation after a rate of change of frequency (ROC) in loading MW on a network element.[81] Note that ROC corrections are also possible by enabling NSCAS Network Loading (NLAS).

The second highest priority in network security is maintaining every Satisfactory Network Limit (item 26), such as no exceedance to line ratings, no transformer overheating and no outage.[82] Provided these are met, an operationally stable network under this set of constraints is in a normal system state (NIL) according to AEMO (2013) (page 8).

Secure Network Limit Stability and Other constraints (item 27) manage voltage, oscillatory and transient stability, including system strength (AEMO (2023*d*), pages 16-17; AEMO (2021*d*), page 8). A large amount of stability is already provided by the network elements, such as the generating plants, over the normal course of operation at no cost. Stability constraints are then used, in addition, to prevent unsafe variances to these limits.[83] Note also that the AEMO has the option to use NSCAS (see Table 3.4) for managing network stability when the marginal value of the binding constraint being offset is greater than the cost of the NSCAS providing the offset (AEMO (2012*a*), pages 7–8).[84]

The last constraint set under NIL is the Secure Network Limit Thermal (item 28), which controls the pre- and post-contingency MW capacity loading (Mackenzie et al. (2020), page 26).

---

[81] See the Binding Impact tab in AEMO's constraint report AEMO (2020*e*).

[82] For a brief summary about this limit refer to AEMO (2015*a*) (page 9), AEMO (2020*f*) (page 6) and AEMO (2023*d*) (page 12).

[83] See the Binding Impact tab in AEMO's constraint report AEMO (2020*e*).

[84] An excellent discussion on the future system strength in the NEM is provided by Mountain and Percy (2020) who review the topic with high renewable energy penetration and electricity storage including grid forming batteries in view.

These constraints are often formulated as feedback equations using the ratings or limit equations provided for each line by its operator to AEMO; the thermal capacity limits are usually written as two bounds around the initial MW flows as measured in SCADA (AEMO (2021*d*), page 16).

Regarding the outage constraints (items 29–32), these are, in principle, very similar to the Zero limits in that they invoke line limitations (i.e. islanding), which tend to cause significant changes in the flow direction, as stated in AEMO (2023*d*) (pages 12, 17–25). Hard and soft ramping distinguishes the constraints applied over different but overlapping timescales to achieve smooth and steady switches, if at all possible, considering phase changes (AEMO (2021*d*), page 22). Finally, Non-Physical Loss Oscillation Control (item 33) is put in place to prevent directional over-oscillation – that is, repeated directional changes in subsequent trading intervals over an interconnector – beyond the degree at which it can no longer be safely managed (AEMO (2023*d*), page 26).

3.3.5.4 Market requirements

The system-level operational constraint sets warranting economic dispatch are shown in the last segment of Table 3.3 (items 34–39). These involve market offers, expected demand, settlement residues and price-ties.

The first constraint set in priority order is Total Band MW Offer (including MNSP) (items 34–35). This ensures that the dispatch targets by the NEMDE correspond to the total band size of the ten bid quantities of the units. The total quantity band, as explained in AEMO (2023*d*) (page 9), "must add up to equal or greater than (as designed) the registered maximum capacity". Therefore, the bid quantities are typically greater than or equal to the nameplate capacity – that is, not all are available. In the context of this chapter, refer to Table 3.5 for a summary of the various capacity measures mentioned so far, which displays the indicators starting with the least restrictive Total Band MW Offer. From there, the onus is on the engine to determine the available target quantities using the sophisticated set of constraint rules from Table 3.3.

Regarding the Regional Energy Demand Supply Balance (items 36–37), the economic objective is to match demand with supply. Nearing the start of every 5-minute trade cycle, the preceding efforts in forecasting the usual patterns of consumption minus distributed generation

Table 3.5 : **Capacity indicators**

The table shows multiple capacity indicators and measures to express the contingent capacity of a unit in decreasing order of magnitude.

Availability	Source	Function
Total Band MW Offer	Bid submission	All bid quantity by the BANDAVAIL1-10 field definition in AEMO (2022*i*).
Rated capacity	Plant survey	Nameplate capacity after seasonal adjustments (AEMO (2021*n*), page 29).
Generator energy limitation	GELF declaration	Stockpile scarcity or water storage–bound daily or weekly maximum capacity as estimated over the long run (AEMO (2014*a*), page 4).
PASA availability	Bid submission	Capacity currently in service or available for service within 24 hours by the PASAAVAILABILITY field definition in AEMO (2022*i*) in line with AEMO (2020*d*) (page 8).
Daily energy constraint	Bid submission	Stockpile scarcity or water storage-bound daily or weekly maximum capacity as indicated by the units in real time by the DAILYENERGYCONSTRAINT field definition in AEMO (2022*i*).
MaxAvail	Bid submission	Maximum availability for the 5-minute trade interval as indicated by the units by the MAXAVAIL field definition in AEMO (2022*i*).
Dispatch targets	NEM Dispatch Engine	NEMDE target outcome (AEMO (2021*g*), page 9).

approximate the value of the total quantity to be cleared (i.e., scheduled), within the 5-minute interval. This enters the engine as the regional Total Demand (AEMO (2021*f*), page 17). Then balancing demand and supply within a narrow but initially symmetric – as the associated penalty factors are the same – headroom is achieved using the two Regional Energy Demand Supply Balance constraint sets shown in Table 3.3 (AEMO (2023*d*), pages 13-14).

The inter-regional residue settlement as per 3.6.5 in the Rules requires constraints for counter-price flows. Negative residues arise when the NEMDE optimum dispatch solution directs counter-price flows through directed (non-MNSP) interconnectors, i.e. when electricity generated in a high price region is consumed in a low price region (AEMO (2021*c*), page 5; AEMC (2013), page i). This is a perfectly legitimate NEMDE outcome as long as it minimises the objective function (3.3.1) but is problematic because AEMO receives less from retailers than it is liable to pay out for wholesale generation, as stated in AEMC (2013) (page 5). The costs are borne by the market customers in the importing region as in AEMC (2014) (page 18). The coordination involved is commonly known as Negative Residue Management (NRM) (AEMO (2021*c*), page 3). The main platform for NRM is the Settlement Residue Auctions (SRA) as per 3.18 in the Rules, where the accumulated negative residues are settled and distributed. The

secondary trading of these cash flows has also been permitted more recently.[85] Relevant to real-time dispatch, the NRM constraint (item 38) with a low constraint violation penalty in Table 3.3 is in fact a dynamic penalty factor that can be raised by AEMO for counter-price flow management.[86] According to AEMO (2021*c*) (page 7), as a general rule, AEMO should 'cease' ['clamp'] the accumulation of negative inter-regional settlement residues in the NEM when this accumulation reaches or exceeds the negative residue accumulation threshold of -$100,000 (as of 1 July 2010)". Congestion and disorderly bidding are the two main drivers of negative residue accumulation, and there is an ongoing discourse between industry reference groups and AEMC to streamline the NRM process to reduce the gaming of the counter-price flows and maximise consumer welfare (AEMC (2013), pages 13-14; AEMC (2014), pages 17-25; AEMC (2020), page 59).[87]

Finally, there is a small but important consideration in managing price-tied dispatch outcomes. Should the kind of NEMDE case solution occur wherein a number of bids, none of which bind or violate any constraints, are equally feasible on a price basis, AEMO then has to allocate targets equitably. The Tie-break constraint set (item 39) with a minimal effective violation penalty is used for this purpose. The quantity targets for the price-tied energy bids are split in proportion to the MW quantities in the relevant bid slots, whereas price-tied FCAS bids are "dispatched randomly" (AEMO (2023*d*), page 27).

3.3.6 Out-of-market operations

The usual functions of the main NEMDE run are not fulfilled until a cascading series of out-of-market operations are also evaluated (AEMO (2021*g*), page 15). These include fast-start unit commitment and alternative network constraint formulations as NEMDE re-runs as per 3.8.10

[85] A detailed overview of SRAs is provided by AEMO (2014*c*) (page 5) and AEMO (2019*c*) (pages 6-22)

[86] Automated counter-price flow management is discussed in AEMC (2013) (page 9) and AEMO (2021*c*) (pages 3-9).

[87] It is alarming from a market power concentration point of view that plants at certain electric locations have access to unilaterally moving the real-time spot price through strategic (disorderly) bidding. Based on participants' submission on issues papers, particularly Macquarie (2013) (page 1), "Remote generators in the higher priced region can bid in ways to relieve NRM constraints on an interconnector that was otherwise "clamped" to limit negatively priced flows", i.e., to relieve the clamp and then to restart it, known as 'cycling'. The increased negative residue that accumulates through cycling is later distributed among the generators in the higher priced region in negative residue auctions. Therefore, cycling is detrimental to consumer welfare in the low-priced region. The same issue may arise in new locations once the new high-voltage alternating current (HVAC) interconnector EnergyConnect is built.

(e) in the Rules as well as price administration under system distress, should such a scenario arise, as per 3.14 in the Rules.

Under the principles of self-scheduling, unit commitment is not centralised in the NEM for units that do not meet the requirements for fast-start classification. However, the FSIP of the fast-start units are considered in a two-pass scheme as outlined in AEMO (2021*j*) (pages 10-11) and Gorman (2023). This involves three steps. In step one, NEMDE is run ignoring the FSIP. In step two, units are committed or decommitted using the targets from step one as well as their plant-level technical limits based on their FSIP. Finally, in step three, NEMDE is re-run with the unit commitment variables fixed for fast-start plants.

Then, the NEMDE is re-run as part of the market methodology for three reasons. Firstly, the Basslink's control system[88] must enforce security rules that are difficult to integrate into the NEMDE using linear constraints according to AEMO (2021*g*) (page 17). In particular, there is a No-Go zone for power flows between $\pm$ 50 MW, and FCAS transfer is not always possible near full capacity.[89] Therefore, there is always a normal NEMDE run in Dispatch mode using the SCADA indicated Basslink status (on/off), as well as a re-run that assumes Basslink to be offline. The lower cost solution of the two is ultimately selected for the dispatch solution (AEMO (2021*g*), page 17).

Second, the automated Over Constrained Dispatch (OCD) process rectifies when the solution of the engine in Dispatch mode still contains constraint violation costs that drive the price results near or beyond the market price thresholds (AEMO (2017*a*), pages 5, 9; AEMO (2021*g*), pages 15-16; AEMO (2011), page 8). Barring any serious distortions requiring a market notice and intervention, such as a significant MW shortfall or a voltage instability, the arising variances can usually be resolved by relaxing the RHSs of the violating constraints iteratively or manually.[90, 91]

Another reason for out-of-market re-formulations is a market intervention. If the ST PASA

[88]The Basslink HVDC undersea cable is a scheduled market interconnector (MNSP) across the Bass Strait between VIC and TAS (AEMO (2022*f*); Basslink Pty Ltd (2022)).

[89]For technical details we refer the reader to AEMO (2021*g*) (pages 17) and AEMO (2021*d*) (pages 18-19).

[90]Figure 1 in AEMO (2021*g*) depicts the OCD flowchart.

[91]The only exception being that price-tied bids (item 39 in Table 3.3) are split out on a pro-rata basis as per 3.8.16 in the Rules, i.e., this constraint is not relaxed during OCD. See the Tbslack entries in the DispatchedMarket field in the PriceSetting tab of AEMO (2021*p*).

routine detects a high risk of supply inadequacy, it communicates the intervention conditions to the real-time Dispatch solver immediately using the dedicated LRC and LOR notices (see Section 3.2.6). These then initiate the following two layers of re-runs. The general requisite is that AEMO seeks to restore the market price outcome to the level that would have prevailed had the intervention scenario not arisen, as per 3.9.3 (b) in the Rules, while making every possible effort to secure non-market quantities to meet the reserve shortfall (AEMO (2021*m*), page 5; AEMO (2019*b*), page 4)).[92] This is usually performed in two re-runs by means of voluntary or involuntary load shedding and non-market reserve contracts.[93] The first re-run is in Outturn mode and it determines the new target quantities using reserve trader (RERT) bids for the non-market quantities, and the direction constraints specific to Outturn (AEMO (2023*d*), pages 5-27; AEMO (2021*g*), page 19; AEMO (2021*m*), page 4). Then the second layer to the intervention policy is another run in What-if mode. This removes the RERT bids and the direction constraints, and seeks to recover the price under the original circumstances (AEMO (2023*d*), pages 7-24); AEMO (2021*g*), page 19; AEMO (2021*m*), page 5). A binary label shows in the solution files whether there had been an intervention during a Dispatch run.[94]

Price administration under system distress involves administered pricing and suspension pricing. First, administered pricing periods realise an inter-temporal limitation on the energy spot price as per 3.14.2 in the Rules. Under the AEMC reliability settings in AEMC (2021*a*), an administered pricing cap (APC) of APC $\approx$ \$300 (as per 3.14.1 (a) in the Rules) is applied to curb the duration of high price periods when the energy spot price is successively high and breaches the effective 7-day cumulative price threshold (CPT). The CPT is \$1,359,100 as at October 2021. In case of a CPT exceedance, the energy spot price is set to the APC until the CPT breach is subdued. Similarly, an administered pricing floor of APF $\approx$ -\$300 applies when

[92] Market price levels that would have arisen from the alternative network formulations are thereby averted, i.e., the spot prices do not reflect the grid economics under scarcity. Instead, market-price-cap-level out-of-market uplift payments are paid out for the non-market demand response and unit commitment quantities that have been used to avoid load shedding. From a price quality perspective, the out-of-market payments pay for providing the emergency loads, but they do not encourage new investments in general that might minimise the scarcity risk to begin with.

[93] Non-market reserve contracts include provisioned arrangements through Clause 4.8.9 directives (AEMO (2014*b*), page 7) using constraints beyond the constraints in Table 3.3 in a pre-set priority flow. Note that the details of the related re-runs are available in AEMO (2023*d*) (pages 7-20), AEMO (2021*m*) (pages 5-10) and AEMO (2019*b*) (pages 4-6).

[94] See the Intervention field in the TraderSolution tab in the NEMDE solution data of AEMO (2021*p*).

prices skew oppositely as per 3.14.1 (b) in the Rules. Second, suspension pricing applies during severe demand deficit, for example, after a voltage collapse as per 3.14.3 in the Rules. The price methodology for a black system or emergency scenarios relies on a market suspension pricing schedule consisting of historical price averages (AEMO (2017*d*), page 4). At these times, non-market ancillary services are predominantly used to re-start parts of the network (AEMO (2012*a*), page 8).

3.4 Price settlement

Ex-post price settlement computes the marginal value of an incremental change in load at the regional reference node (RRN), as per 3.9.2 (d) in the Rules, as the dual variable (shadow price) of the regional energy balance constraint (items 36–37 in Table 3.3) as in Mackenzie et al. (2020) (page 28). In addition, as 3.8.1(c) in the Rules requires the market operator to implement a constraint relaxation routine according to AEMO (2017*a*) (page 5) to pre-empt infeasible dispatch solutions, this involves the assignment of constraint violation penalties to every constraint to establish the priority order of the constraints (AEMO (2017*a*), page 5), as shown in the objective function (3.3.1), as well as the OCD re-runs that relax the violating constraints removing these penalties from the dispatch solution (see Section 3.3.6). The regional original price (ROP) then contains the pre-OCD constraint violation penalty costs, but the regional reference price (RRP) does not, according to AEMO (2016) (page 4). In what follows, we refer to the RRP as the unit price of electricity in the NEM.

This price, determined as the marginal value of an incremental change in load at the RRN, is represented by net 1 MW change in load before losses – that is, $\lambda_N^{c,l}$ in (2.3.2) in Chapter 2. However, the change in load does not always correspond to quantities from a single bidder, let alone quantities from a unique bid slot. Often there are multiple price setter bids. Analysing the price setter data over a 5-day interval starting at 4:05 AM 16 September 2021 (see NEOPoint (2021); AEMO (2021*p*, 2022*i*)) reveals that depending on the region only about 12-45% of the market prices are set by a single energy bid from the focus region with inter-regional loss and ancillary service effects remaining under 2 dollars. The upcoming examples delineate several other scenarios when the quantity-weighted averages of multiple price setter bids establish the

regional electricity prices in a more complicated manner.[95]

Example 3.1. *Continuing Example 2.1 – whilst omitting the security constraint effects explained in Example 2.2 – the targets associated with each bid can be written as in columns (b) and (c) in Table 3.6. Conceptually, the differences in the targets in column (b) at 50 MW minus those in column (a) at 49 MW give the (marginal) quantities for each bid in column (c). The price is then expressed as the sum product of the values in the quantity column (c) and the bid price column (d). In particular,* $1 \times \$1000 = \$1000$ *sets the price.*

Table 3.6 : **Price settlement: An as-bid $\lambda_N^{c,l} := \lambda_i$ setting**

The table shows all bids in the market and identifies the 70 MW at $1000 as the price setter bid behind the incremental change in the market-wide target allocation from 49 to 50 MW given a market demand of 50 MW.

Bid	Bid type	Service type	Target (49 MW) (a)	Target (50 MW) (b)	Quantity (c) = (b) - (a)	Price (d)	(c) × (d)	Comments
10 MW at $10	Energy	Generator	10 MW	10 MW	0 MW	$10	$0	
20 MW at $100	Energy	Generator	20 MW	20 MW	0 MW	$100	$0	
70 MW at $1000	Energy	Generator	19 MW	20 MW	1 MW	$1000	$1000	The only price setter bid is marginal in exactly 1 MW.
35 MW at $2000	Energy	Generator	0 MW	0 MW	0 MW	$2000	$0	
-20 MW at -$10	Energy	Load	0 MW	0 MW	0 MW	-$10	$0	
-10 MW at -$100	Energy	Load	0 MW	0 MW	0 MW	-$100	$0	
-5 MW at $900	Energy	Load	0 MW	0 MW	0 MW	$900	$0	
							Price: $1000	

3.4.1 Reserves

For a greater degree of realism $\lambda_N^{c,l} := \lambda_N^c$, the following example shows FCAS reserves impacting the market price.

Example 3.2. *In Table 3.7, five price setter bids are involved in setting the price: one energy bid and four FCAS bids. One generation bid by unit POAT220, a gravity hydro generator located in TAS, sees the complete marginal target increase of 1 MW. At the same time, POAT220 no longer provides 5-minute raise regulation FCAS (-0.67 MW) or 60 second raise contingency FCAS (-0.12 MW) due to the trade-off it apparently has between energy and reserves provision. These services are recovered by enabling units MP2 and MP1 in the same amounts instead,*

[95] See the PriceSetting tab of the AEMO (2021*p*) data.

Table 3.7 : **Price settlement: FCAS effects in a $\lambda_N^{c,l} := \lambda_N^c$ setting**

The table shows the price setter bids behind the incremental change in volume for TAS as at 5:05 AM on 15 July 2021. Source: NEOPoint (2021); AEMO (2021*p*).

Unit ID	State	Bid type	Service type	Quantity (1)	Price (2)	(1) × (2)	Comments
POAT220	TAS	Energy	Generation	1	$25.36	$25.36	The only price setter bid that is marginal in exactly 1 MW.
POAT220	TAS	FCAS	R5RE	-0.67	$5.5	-$3.67	
POAT220	TAS	FCAS	R60S	-0.12	$0.61	-$0.07	
MP2	NSW	FCAS	R5RE	-0.67	$7.99	$5.33	
MP1	NSW	FCAS	R60S	-0.12	$2.01	$0.24	
						Price: $27.19	

respectively, but this afflicts higher prices. We also see that these net to 0 MW and have no role in impacting the marginal change in energy. Although the FCAS target variation sums to zero, the FCAS price increase $-0.67 \times \$5.5 + -0.12 \times \$0.61 + 0.67 \times \$7.99 + 0.12 \times \$2.01 = \$1.83$ *is reflected in the energy spot price. The price is the marginal quantity weighted average of the energy bid prices plus the ancillary service distortion as an additive cost* $1 \times \$25.36 + \$1.83 = \$27.19$.

3.4.2 Losses

For the $\lambda_N^{c,l} := \lambda_N^l$ setting, the marginal MW change is adjusted for intra- and inter-regional losses, owing to the fact that almost all network elements, including lines, are imperfect conductors (AEMO (2012*c*), page 5). Under marginal pricing, the zonal design of the NEM approximates nodal LMP in using marginal loss factors (MLFs) as per AEMO (2012*c*) (pages 10-11), which represent marginal losses, i.e., "the incremental change in total losses for each incremental [1 MW] unit of electricity" (AEMO (2020*b*), page 5; AEMO (2012*c*), page 15). MLFs are forward-looking estimates (AEMO (2020*b*), page 5), note however that average losses are typically lower than marginal losses as in AEMO (2012*c*) (page 10).

There are two kinds of MLFs in the NEM. Intra-regional MLFs are static loss factors within the regions under 3.6.2 in the Rules. These MLFs are the volume-weighted average changes in load at the RRN (swing bus) for changes in injection at the unit connection points, calculated from historical network flow data using TPRICE, as in AEMO (2012*c*) (pages 5, 11, 20) and AEMO (2020*b*) (page 14). The static MLF is then applied as the divisor of the as-bid price at

the source to obtain the (typically higher) intra-regional MLF–adjusted bid price at the RRN of the region.

In contrast, inter-regional (interconnector) MLFs are dynamic loss factors between the regions updated every dispatch interval using a number of system variables, mainly demand and interconnector transfers, in loss factor equations as per 3.6.1 in the Rules. These equations "describe the variation in loss factor at one RRN with respect to an adjacent RRN" (AEMO (2022*e*), page 48), which also come from the load flow calculations in TPRICE, as in AEMO (2020*b*) (page 15). The MLF equation coefficients for demand and interconnector transfers are estimated using linear regression. The MLF estimated dynamically using this inter-regional MLF equation is then applied as an RRP multiplier to obtain the spot price at the RRN of the focus region (AEMO (2012*c*), page 22).

We can also establish the trade directions from the inter-regional MLFs in general while observing the DUID-level marginal quantity values.[96] We have the following relations for a 1 MW change in the focus region's generation. If the DUID-level marginal quantity is less than 1 MW and positive, e.g. 0.95 MW, then the focus region is exporting 1 MW less and some DUID in the other region is recovering the lost amount after inter-regional line losses by increasing its own generation by 0.95 MW. Similarly, if the DUID-level marginal quantity is greater than -1 MW and negative, e.g. -0.95 MW, then the focus region is exporting 1 MW more and some DUID in the other region is matching the incoming amount after inter-regional line losses by decreasing its own generation by 0.95 MW. However, if the DUID-level marginal quantity equals 1 MW exactly, then the focus region is increasing its own generation by 1 MW. Analogously, if the DUID-level marginal quantity is greater than 1 MW, e.g. 1.05 MW, then the focus region is importing 1 MW more from the DUID in another region, which has to increase dispatch by 1.05 MW to account for the increased demand before inter-regional line losses. Similarly, if the DUID-level marginal quantity is less than -1 MW, e.g. -1.05 MW, then the focus region is importing 1 MW less from the DUID in another region, which has to decrease dispatch by 1.05 MW to account for the decreased demand before inter-regional line losses. In contrast, if the DUID-level marginal quantity equals -1 MW exactly, then the focus region

[96] Which correspond to the Increase field values in the PriceSetting tab of the AEMO (2021*p*) data, particularly the energy offer (ENOF) attributes. The load offers (LDOF) have the opposite signs.

is decreasing its own generation by 1 MW. We use these results to construct the upcoming examples.

The following example recreates and, for exposition purposes, refashions the conditions in Example 3.2 to show the price effects of intra- and inter-regional losses.

Table 3.8 : **Price settlement: Loss effects in a $\lambda_N^{c,l} := \lambda_N^l$ setting**

The table shows the price setter bid(s) contributing to the incremental change in the energy demand for TAS in two hypothetical scenarios. One is where the price is fully set by bid(s) from the region (above), and another is where there are additional unit(s) supplying from another region (below).

Price for TAS with intra-regional line losses:

Unit ID	State	Bid type	Service type	Quantity (1)	Price (2)	As-bid price	(1) × (2)	Comments
Unit A	TAS	Energy	Generation	1	$25.36	$24.58	$25.36	Intra-regional loss adjustment is reflected in the price.
						Price: $25.36		

Price for TAS with both intra-regional and inter-regional line losses:

Unit ID	State	Bid type	Service type	Quantity (1)	Price (2)	As-bid price	(1) × (2)	Comments
Unit A	TAS	Energy	Generation	0.60	$25.36	$24.58	$15.22	
Unit B	VIC	Energy	Generation	0.50	$26.00	$23.00	$13.00	Note the additional inter-regional effect.
						Price: $28.22		

Example 3.3. *Focusing on the top segment of Table 3.8, the bid price at the RRN ($25.36) would be equal to the as-bid price ($24.58) without intra-regional line losses. However, as in 3.8.6 (h) in the Rules, we must account for the intra-regional MLF too. The as-bid price, the price placed by unit A in its bid submission, is $24.58. Only after dividing that by the intra-regional MLF can we see the additive intra-regional loss adjustment of 78 cents (as $24.58 + $0.78 = $25.36). In both segments of Table 3.8, the price setter bid price of the unit A hydro plant is $25.36 after intra-regional MLF, as measured at the RRN. Furthermore, the single price setter bid by unit A is only subject to intra-regional losses. There are no inter-regional losses, as it is located in the focus region, TAS. This is also revealed from the fact that marginal quantity is at exactly 1 MW. The TAS price is then* $1 \times \$25.36 = \$25.36$.

In the bottom segment of Table 3.8, however, there are two different price setter bids. One by unit A located in TAS and another by unit B located in VIC. The as-bid price is $24.58 and the intra-regional loss is 78 cents on unit A, as before. In comparison, the as-bid price is $23.00 and the intra-regional loss is 300 cents on unit B.[97] *This is a scenario where the marginal MW*

[97] From the higher dollar loss, we infer that unit B is electrically further away from the reference node within its own region.

is met by local generation (0.60 *MW) and partly by generation increase elsewhere (in VIC). We also know that TAS is importing from VIC, because the generation increase in VIC is more than the difference of 1 and* 0.60 *MW. VIC has to increase generation by more than* 0.40 *before line losses to deliver exactly* 0.40 *to TAS. The TAS price is then* $0.6 \times \$25.36 + 0.5 \times \$26 = \$28.22$.

3.4.3 Loads

The examples have so far only looked at instances when a generator incrementally increased output to arrive at the marginal 1 MW change. We now look at a case with a change in loading (storage uptake).

Example 3.4. *In Table 3.9, a single bid by the HPRL1 battery load unit sets the price. Load in the system increases by decreasing the target of the load unit. The price is the marginal quantity weighted average of the energy bid prices,* $-1.18 \times -\$56.74 = \$66.81$.

Table 3.9 : **Price settlement: marginal load in a $\lambda_N^{c,l} := \lambda_i$ setting**

The table shows the price setter bid behind the incremental change in volume for NSW as at 5:45 AM on 16 September 2021. Source: NEOPoint (2021); AEMO (2021*p*).

Unit ID	State	Bid type	Service type	Quantity (1)	Price (2)	(1) × (2)	Comments
HPRL1	SA	Energy	Load	-1.18	-$56.74	$66.81	NSW imports 1 MW more (after losses) from SA, where loading (storage uptake) at -$56.74 decreases by 1.18 MW.
					Price: $66.81		

3.4.4 Real-world examples with binding constraints

Whenever a plant, FCAS, thermal, stability, or economic constraint is binding over the incremental MW increase, congestion is concomitant. Constraint equations from the constraint sets from all segments of Table 3.3 might invoke line closures and resource trade-offs as per 3.6.4 (a1) in the Rules. This typically complicates price settlement and induces detectable price effects.[98] Below, we present three not atypical real-world examples in the full $\lambda_N^{c,l} := \lambda_N^{c,l}$ setting with reserves, losses, and loads and with one or more binding security constraints.

[98] From a price quality aspect, prices should keep to grid economics, i.e., they should rise at times of scarcity and drop otherwise to return the true costs of capacity investments. However, when constraints equations bind the prices tend to rise and drop irrespective of the overall scarcity level.

Example 3.5. *For price settlement in NSW, the incremental increase in energy requires a marginal quantity increase by the brown coal units LYA1, LYA2, LYA3 and LYA4 in VIC, whereas the local, nominally lower priced solar farm LIMOSF21 (NSW) sees a marginal quantity decrease of 0.11, as in Table 3.10.*[99] *That is because a congested network element (e.g. a line) requires the backing off of cheaper quantities so that load can be increased by injecting more expensive quantities elsewhere on the grid. More specifically, the N^^N_NIL_3 voltage stability constraint, which is a less than or equal to constraint and features LIMOSF21 with a coefficient of 1 and the VIC1–NSW1 interconnector (at the boundary) with a coefficient of 0.093 at the LHS, is binding.*[100] *Given an inter-regional MLF of 1.077 over VIC1-NSW1 (AEMO (2021p)) and a proportioning of 34.38% of the losses to VIC, the extra flow at the boundary due to losses is 1.077/1.027 = 1.0497 MW per 1 MW increase in flow at the boundary, as in AEMO (2009) (page 5), times a quantity multiplier of 1.104, as 1.104×1.077 = 1.19 gives back the change in VIC – that is a change in flow at the boundary of 1.0497×1.104=1.159, which in turn creates a constraint LHS increase of 1.159×0.093 = 0.11. This amount is offset by changing the target of LIMOSF21 by -0.11, as shown in Table 3.10. As a result, the NSW price can be written as the sum product* $1.19 \times -\$31.05 - 0.11 \times -\$1000 = \$71.12$*, which, quite extraordinarily, gives a positive price using solely negative marginal bids (*$-\$1000$ *and* $-\$31.05$*).*

Table 3.10 : **Price settlement: High price in a $\lambda_N^{c,l} := \lambda_N^{c,l}$ setting**

The table shows the price setter bids behind the incremental change in volume using the actual engine outcomes for NSW as at 2:55 PM 15 on July 2021. Source: NEOPoint (2021); AEMO (2021*p*).

				Price for NSW:			
Unit ID	State	Bid type	Service type	Quantity (1)	Price (2)	(1) × (2)	Comments
LYA1, LYA2, LYA3, LYA4	VIC	Energy	Generation	1.19	-$31.05	-$37.08	NSW imports 1.19 MW more quantities (before losses) generated in VIC for -$31.05.
LIMOSF21	NSW	Energy	Generation	-0.11	-$1000	$108.20	NSW generates 0.11 less at -$1000.
						Price: $71.12	

Example 3.6. *Overall, more than ten price setter bids are involved in setting the price in the focus region SA in Table 3.11. The marginal increase in energy in SA requires flow modifications*

[99] There is also a tie-break and associated costs in the order of magnitude of 1e-4 for LIMOSF21 as in AEMO (2021*p*).

[100] The binding constraint information and the proportioning factors are obtained using Nempy, as in Gorman et al. (2022), with default data settings for the dispatch interval.

over the V-S-MNSP1 (Murraylink) and the VIC1-NSW1 interconnectors and therefore dispatch target changes in NSW and VIC but, interestingly, not in the focus region SA. The following dynamic unfolds. First, SA is importing from VIC through Murraylink to meet the 1 MW increase in load in SA, where this is met by a -0.961 MW flow at the boundary, a value obtained using the inter-regional MLF of 0.872 over V-S-MNSP1 (AEMO (2021p)), a proportioning of 72.31% of the losses to VIC to calculate 0.872/(1+(0.872-1)×0.7231) = 0.961, as in AEMO (2009) (page 5), and a negative sign as it is an easterly flow.[101] *Then, after rounding, the change on the VIC side of Murraylink is 0.872 MW and on the SA side is 1 MW, as computed as the at the boundary flow 0.961 plus incremental losses 0.961×(0.872-1)×0.7231=-0.088 (from region), 0.961-0.088=0.872, and as the at the boundary flow minus incremental losses 0.961×(0.872-1)×(1-0.7231)=-0.034 (to region), 0.961+0.034≈1.*

At the same time one of the voltage stability constraints, N^^N_NIL_3, which is a less than or equal to constraint, is binding.[102] *The LHS of this constraint includes V-S-MNSP1 with a -0.5197 coefficient and VIC1-NSW1 with 0.09287. Therefore, as the additional -0.961 MW negative flow at the boundary of V-S-MNSP1 increased the LHS of the constraint, the VIC1-NSW1 flow must increase in the northern direction by -0.961×(-0.5197/0.09287)=5.378 MW at the boundary to neutralise the LHS increase.*

Then, with an inter-regional MLF of 1.147 (AEMO (2021p)) and a proportioning of 34.38% of the losses to VIC, the change on the VIC side of VIC1-NSW1 is approximately 5.6 MW and on the NSW side after rounding it is 4.9 MW, computed as the at the boundary flow 5.378 plus incremental losses 5.378×(1.147-1)×0.3448=0.271 (from region): 5.378+0.271≈5.6, and as the at the boundary flow minus incremental losses 5.378×(1.147-1)×(1-0.3448)=0.517 (to region): 5.378-0.517≈4.9.

Then, the 6.5 MW increase in dispatch in VIC by the units LYA1, LYA2, LYA3 and LYA4 at -$31.05 is the sum of the flows sent through the two different interconnectors, 0.872+5.6≈6.5, as shown in Table 3.11. Also, the 4.9 MW decrease at the other end of VIC1-NSW1 in NSW is met by the higher cost ($43.60) black coal units ER01, ER03 and ER04.

[101] Note that any positive interconnector flow travels northwards or westwards as in AEMO (2023*a*).

[102] The binding constraint information and the proportioning factors are obtained using Nempy as in Gorman et al. (2022) with default data settings for the dispatch interval.

Regarding the related update in ancillary services, the units ER01, ER03 and ER04 are impelled to lower their 5-minute regulatory FCAS provision after decreasing their energy output, and the next least expensive service provider LOYYB2 must step in at a higher price. Even after some losses in value on FCAS, however, the engine has realised considerable value, as the price result for SA is $-\$348.86$ *despite using much higher priced marginal bids for energy (*$-\$31.05$ *and* $\$43.60$*).*[103]

Table 3.11 : **Price settlement: Low price in a $\lambda_N^{c,l} := \lambda_N^{c,l}$ setting**

The table shows the price setter bids behind the incremental change in volume using the actual engine outcomes for SA as at 12:40 PM on 15 July 2021. Source: NEOPoint (2021); AEMO (2021*p*)

				Price for SA:			
Unit ID	State	Bid type	Service type	Quantity (1)	Price (2)	(1) × (2)	Comments
LYA1, LYA2, LYA3, LYA4	VIC	Energy	Generation	6.51	-$31.05	-$202.25	SA reduces exports to VIC by 1 MW. 6.51 MW more quantities are generated in VIC for -$31.05, of which 4.92 MW arrive at NSW.
ER01, ER03, ER04	NSW	Energy	Generation	-4.92	$43.60	-$214.50	Imports into NSW replace 4.92 MW $43.6 dispatch in NSW.
ER01, ER03, ER04	NSW	FCAS	L5RE	-4.92	$0.00	$0.00	With 4.92 MW NSW-generated energy being replaced by imports there is 4.92 MW less capacity in NSW to provide L5RE FCAS.
LOYYB2	VIC	FCAS	L5RE	4.92	$13.80	$67.89	The next least expensive L5RE FCAS provider.
					Price: -$348.86		

There is one further remark to Table 3.11 containing information about SA. At the time of this data, system strength directives under the Rules state that "the minimum requirement in South Australia drops to two synchronous units online, mainly for system security reasons rather than to address the system strength shortfall. This requirement remains until the commissioning of Project EnergyConnect (if built)" (AEMO (2020c), page 30). The input bid data and the cleared target output data in the NEMDE solution files of AEMO (2021p) indeed confirm that two synchronous units were kept online despite bidding at prices near the market price thresholds, which is an example of constrained-on bids that are implicit but not directly observable in the price setter bid selection.

[103] Based on personal communications with Allan O'Neil in the second half of November 2022.

Example 3.7. *A price outcome is shown for NSW wherein changes in the Basslink market interconnector come into play, as per Table 3.12. To meet the incremental increase in load, the ER02 local unit is directed to increase generation by 1 MW for* $55.01 *in NSW, as the flow through the VIC-NSW interconnector is blocked by the binding voltage stability constraint V^^N_DPWG_X5_1. The increase in energy dispatch also allows the ER02 unit to raise its FCAS lowering service enablement over two response time categories, 60-second and 5-minute, for* $1.03*. These FCAS increases do, in turn, lead to increases on the LHSs of a binding loss of Basslink (F_MAIN++NIL_BL_L60) and loss of a potline mainland constraints (F_MAIN++APD_TL_L5), respectively.*[104]

In both equations, there is increase in the mainland enablement of L60S and L5MI, where ER02 has a constraint coefficient of 1, as part of the regional coefficients for NSW1 L60S and NSW1 L5MI; thus the Basslink interconnector flow TVMNSP1 is positive in the northern direction. Therefore, the engine is able to offset the increase caused by ER02 by decreasing the TVMNSP1 by 1 MW, for trade value maximisation. Decreasing the northern flow is achieved by increasing the southern flow, i.e., by sending an additional 1 MW to TAS without increasing the LHSs of the constraints by more than 1 MW after losses. This is satisfied by increasing the target for the NUMURSF unit in VIC by 1.06 MW after losses and decreasing it for TUNGATIN in TAS by 1 MW. Notice also the price effect of the market interconnector; should the bid price of T-V-MNSP1 be different from $0.0*, one would see an additive price impact.*

Due to this increase on the LHSs of the binding mainland constraints, however, it is no longer possible to decrease the L60S and L5MI FCAS targets back to net nil from the mainland. Any such change in FCAS would have to come from TAS. Accordingly, TUNGATIN (TAS) decreases the L5MI service by 1 MW, but neither TUNGATIN, nor any other unit would be able to decrease L60S back to net nil because of a binding local L60S constraint in TAS, F_T+NIL_ML_L60. Considering all these changes over the last 1 MW, the NSW price result is $37.78.[105]

Summarising Examples 3.1–3.7, the energy spot price is the cost of the marginal increase

[104] The binding constraint information and the proportioning factors are obtained using Nempy, as in Gorman et al. (2022), with default data settings for the dispatch interval.

[105] Based on personal communications with Allan O'Neil on 4 November 2022.

Table 3.12 : **Price settlement: Mid price in a $\lambda_N^{c,l} := \lambda_N^{c,l}$ setting**

The table shows the price setter bids behind the incremental change in volume using the actual engine outcomes for NSW as at 11:25 AM 17 Sep 2021. Source: NEOPoint (2021); AEMO (2021*p*).

Price for NSW:

Unit ID	State	Bid type	Service type	Quantity (1)	Price (2)	(1) × (2)	Comments
ER02	NSW	Energy	Generation	1.00	$55.01	$55.01	1 MW energy increase in the focus region as the VIC-NSW interconnector is blocked by a binding voltage stability constraint.
ER02	NSW	FCAS	L60S	1.00	$1.03	$1.03	1 MW L60S FCAS increase provided by ER02 more economically than by mainland competitors.
ER02	NSW	FCAS	L5MI	1.00	$1.03	$1.03	1 MW L5MI FCAS increase provided by ER02 more economically than by mainland competitors.
T-V-MNSP1	TAS	-	Interconnector	1.00	$0.00	$0.00	TAS is sending 1 MW less through Basslink.
NUMURSF1	VIC	Energy	Generation	1.06	-$18.90	-$19.98	On the mainland end of Basslink generation increases for -$18.90.
TUNGATIN	TAS	Energy	Generation	-1.00	-$0.87	$0.87	On the TAS end of Basslink generation decreases for -$0.87.
TUNGATIN	TAS	FCAS	L5MI	-1.00	$0.18	-$0.18	The L5MI FCAS increase is offset by a decrease in TAS that does not affect any binding constraints.
						Price: $37.78	

in supply at the RRN, discretised as 1 MW, but with several security constraint factors at play. First, as emphasised in Section 2.3.4 in Chapter 2, the curtailed (constrained-off) and must-run (constrained-on) quantities influence the price outcome most indirectly by changing the supply pool of bids. More directly, FCAS reserves, losses, and binding security constraints change the price calculation in a way that is irreproducible using the usual merit order rules, i.e. such that the 1 MW change in power takes rearranging more than 1 MW of resources. In effect, security-constrained least-cost pricing comes down to pricing the MW changes that the NEMDE deems as the most economic way of delivering an extra unit of demand at the RRN. It follows that price replication in a traditional bid stack type model framework using historical data under the NEM assumptions is mostly only practicable when the price is not susceptible to these effects. Collating the market bid stack, adjusting it for the constrained-off quantities, adjusting the demand for the constrained-on quantities and letting the inelastic demand line intersect the bid stack gives only the price *before* various non-bid effects. Furthermore, we can decompose the price with non-bid effects and put the pieces back together, as shown in Examples 3.5–3.7,

but it is relatively challenging to predict some of the multiplicative components in a bid stack price model setting, which highlights the limitations of the traditional bid stack price modelling approach.

3.4.5 Outlook

The NEM market clearing process aims to dispatch wholesale electricity at minimum cost. It is not straightforward, however, whether the described mechanism indeed warrants affordability by setting the regional wholesale prices at true marginal costs. The problem is twofold. First, price setting is complicated by a number of factors related to the physical feasibility of dispatch. These include line losses, inter-regional trade, ancillary service co-optimisation, as well as network constraints for system safety. The price of wholesale electricity often fails to correspond to the price of the last used bid in merit order from the focus region (frequently regarded as "the" marginal cost). The above effects obfuscate marginal cost–based price settlement and make the semi-structural modelling of the electricity price more challenging. The novel market model we propose in the upcoming chapter, extending the work of Carmona et al. (2013), is motivated by these findings, in that it captures the mentioned factors to reveal the way they affect price formation in the NEM.

Second, there is some doubt as to whether the bid-in costs reflect the true marginal costs of the units in the NEM. This is because potentially disorderly price-based bidding is allowed in the NEM as opposed to a stricter cost-based regime. This, and other aspects of the current NEM market design that distinguish it from market designs in North America and Europe are more comprehensively evaluated on their welfare impacts in Chapter 5.

3.5 Conclusion

In the broader context of sustainability in worldwide electricity markets, the NEM is an innovative leader in integrating renewable fuels and battery solutions despite of the operative challenges involved. Inverter-based power resources cannot provide inertia; therefore, new system strength constraints had to be introduced, causing some renewable capacities to be constrained-off. In addition, rapid frequency balancing has become important now more than ever to stabilize the hertz equilibrium of the system in the presence of intermittent capacities,

which sometimes causes additive FCAS price components to arise. Also, given the market interconnectness, we see that low-bidding renewables can impact the price outcome in multiple regions because the NEMDE is a market-wide trade value maximisation routine. Evidently, these solutions also induce observable price effects in the continuing transitional shift to clean energy.

Understanding reliability planning and security-constrained real-time dispatch scheduling is key to thoroughly decipher ex-post price settlement in the NEM. Target allocation is preceded by years of reliability planning to ensure that the resources from which the engine is scheduling gives an adequate solution. Then, the objective function of the real-time dispatch underpinning price settlement ensures that the trade value maximising optimal dispatch schedule is physically viable given the security constraints. Finally, price settlement is performed by valuing the marginal unit of demand.

This valuation is rather complex taking real-time physical system limitations into consideration. Understanding how the NEM operates enables the identification of the key factors that impact price formation. These include multi-regional interconnectedness, network losses, wholesale load activity, co-optimised ancillary services, and constrained-on/off effects. Considering these factors, as they are highly relevant to pricing, the present chapter builds a deep understanding of the NEM market design for an improved price hypothesis over the extended equilibrium framework presented in Chapter 2. Moreover, an important contribution of the presented survey is the finding that not all of the above factors can economic bid stack–type market modelling frameworks be easily adapted to.

Chapter 4

A hyperbolic supply function approach to price modelling[106]

4.1 Introduction

The application of the standard equilibrium argument to electricity markets is common across bid stack models (Barlow (2002); Howison and Coulon (2009); Aid et al. (2009); Carmona et al. (2013); Aid et al. (2013); Carmona and Coulon (2014); Ware (2019)). However, this type of price modelling omits fixed cost bids. In addition, the engineering optimisations used in some real-world markets that admit nodal LMPs incorporate the marginal values of the binding security constraints. The applicability of most bid aggregation mechanisms is restricted for market designs with these features. However, as the NEM operates with single-part marginal cost bids and no congestion component in the price, it lends itself readily to bid stack–type modelling.

The implicit assumptions of bid stack models in the literature often mimic a given market design. For example, the non-overlapping fuel merit order principle in Aid et al. (2009) reflects a particular approach to market clearing in the presence of nuclear generation. In contrast, Carmona et al. (2013) use overlapping fuel curves. Another, more direct assumption is the functional form of the market supply curve. Originally, Barlow (2002) suggest a power law supply function, but quantile function (Howison and Coulon (2009)), exponential function (Carmona et al. (2013); Carmona and Coulon (2014)) and polynomial formulations (Ware (2019)) are also present in the literature. Most of these assume a 'hockey stick' shape for the supply curve while ignoring the possibility of negative price bids. The contribution of this study is a market model formulation on bid stack principles wherein price negativity arises in a structural manner.

This chapter presents a novel market model that adapts the economic equilibrium interpre-

[106]This chapter is based on the published article by Katona et al. (2023*a*).

tation of Carmona et al. (2013) to the bid stack extensions developed in Chapter 2 and the insights provided into the market design of the NEM in Chapter 3. The resulting bid aggregation mechanism constructs an increasing hyperbolic supply function that is intersected by a perfectly price inelastic demand quantity[107] to obtain the price considering a number of key factors in the assumptions. The proposed model allows for five interconnected regions where bidding is price-based, renewable technology penetration is high, battery storage is an increasingly integral part of the daily operation, network constraints apply and plants have capacity limits. Moreover, due to its modular structure, the model can easily be adapted to other market designs with similar features.

A trade specification is built on the assumption that the as-bid price at the marginal regional dispatch amount sets the price. This treats the demand before adjustments as the net local generation in the region (net of storage loading), which is the sum of end-user consumption and trade, i.e. export–import flows. The specification estimates the sum with a deterministic function with intra-week and diurnal changes. The size and direction of the trade flow between any two regions can be inferred from this sum as well. Randomness comes from the stochastic constrained-on/off demand adjustment in this case.

The inclusion of renewable fuels is achieved by a departure from modelling the intertemporal changes in the generator and load fuel bid stack (inverse supply) functions in connection to the input fuel, such as gas and coal prices. Shifting the fuel supply curves by some fuel-specific quantities that follow seasonal and diurnal patterns is recommended to capture the strategic bidding behaviour for the different fuels regardless of the input fuel prices.

With regards to model evaluation, a multi-regional implementation study using the Wasserstein metric shows that the proposed framework is sufficiently accurate in its distributional fit for most regions in the NEM. One exception is the SA region, where the model hypothesis fails to capture significant changes in the bid curves over time owing to strategic bidding. This implies that the dynamics of the bidding behaviour are just as important for modelling price formation as correctly capturing the bid aggregation mechanism.

The chapter is organised as follows. Section 4.2 provides an overview of the proposed

[107] See Section 3.3.3 for a discussion on this assumption.

electricity price model and shows the formulation of the core map and input processes. Section 4.3 discusses the implementation of the new model, and the findings are presented in Section 4.4. Section 4.5 concludes the chapter.

4.2 Description of the hyperbolic electricity price model

4.2.1 Model design

4.2.1.1 Bid aggregation

The proposed method captures supply and demand in the wholesale market to recover the electricity price as the equilibrium solution of the assumed market structure. The supply representation combines the supply from a multitude of power plants fuelled by various generator fuels, e.g. coal, solar, hydro, etc., through time-dependent fuel bid stack functions. These express the supply contributed by each fuel over a range of price levels, as implied by the bid data of the plants using the fuel. Demand is expressed as a combination of end-user demand from the consumers, both industrial and household, in the region, export–import, and demand from the load leg of the two-way fuels, such as pumped hydro and battery. End-user consumption plus trade (net generation loads) is assumed to be perfectly inelastic, and it is subject to a number of adjustments in the model. Formulating it as a diffusion process is generally sufficient for the model to admit a price sequence with spikes. In addition, we propose load fuel bid stack functions to capture the uptake demand by each two-way fuel over a range of price levels, usually with a degree of price elasticity, using the respective plant commitment (bid) data.

A market bid stack function is then built based on the fuel bid stack functions considering that every fuel bid stack equation is fundamentally dependent on the typical availability variation of the particular fuel. This temporal variation can be linked to a factor that is physically induced or to a factor that is both physically induced and arises out of the market mechanism. For example, the quantity of solar supply relies on the rate of solar irradiance, an entirely physical component that puts an upper bound on the available quantity domain of the solar bid stack function. In contrast, the quantity of the coal supply usually relies on the ramp rates, a factor that is both physical and economic. The ramp-down and ramp-up rates pose a lower and an upper bound, respectively, on the available quantity domain of the coal bid stack function. It

is a physical factor, as the supply quantity range around the initial output level is based on the technical ramping specifications of the plants using the fuel. Further, it is an economic factor because the initial output level is the output quantity dictated by the equilibrium solution of the preceding time interval. In summary, the different fuel bid stack functions are defined based on different quantity domains, as determined by the appropriate availability factors, prior to being aggregated in the market bid stack function.

The resulting market bid stack function is a time-dependent price map that transforms the expected value of the inelastic demand quantity into the expected value of the electricity price. Visually, the market bid stack function gives the price at the quantity where the inelastic demand, a vertical line, intersects the market supply curve, which is an increasing function over higher quantities. This is consistent with the merit order principles, as end-user demand is first matched with least-cost supply.

4.2.1.2 Equilibrium mechanism

The volumes of electricity the fuels generate and uptake to meet end-user demand to realise the price result (dispatch quantities) are a consequence of the equilibrium solution, which highlights that compliance with the dispatch targets is what makes the scheduled units of a fuel compatible with the proposed framework. In the NEM, using the dispatch quantities at the end of the previous trade interval, the engine determines the optimal dispatch schedule and accordingly issues quantity targets for the next interval (AEMO (2021*g*)): that is, the targets correspond to the dispatch quantities at the end of the current time interval provided that the plants change their dispatch precisely as prescribed. To orchestrate this, the engine possesses timely technical information about the physical limitations of the plants for all fuel types. Using this information and other network data, it performs congestion and contingency planning to find the most optimal schedule for the interval and to provide the plants with viable targets. In addition, to ensure a well met congestion and contingency protocol, the market operator enables ancillary response services (reserves) to maintain the operational frequency of the electric system between 49.85 and 50.15 Hz at all times (AEMO (2021*o*)). Ancillary balancing is necessary when the units of a fuel type are unable to change their dispatch quantities precisely as planned. However, the need for ancillary balancing seldom arises under the simplifying assumptions of the proposed

hyperbolic price model. The available quantity domains of the fuel bid stack functions are presumed fully feasible – that is, the fuels, which are the aggregate of all unit-level bids within a fuel type, are modelled such that they are always able (and willing) to change their generation and uptake to any value within the available quantity domains of their bid stack functions. This is achieved by introducing fuel-level capacity limitations in summary of the unit-level available capacity limits as well as constraint-driven capacity limitations that capture the network-wide infeasibilities of some quantities, for example, for thermal overload, stability thresholds, tie-breaks, etc., subsumed under the constrained-on/off variable. These settings are designed to promote the accuracy of the available quantity domain in the model. Then, the fuels' compliance, i.e., whether the units in the fuels in fact alter their dispatch as needed to realise the price result, is immediate under the model assumptions. Therefore, unit of a fuel type that do not alter their generation and uptake at economic command cannot be modelled through fuel bid stack functions in the proposed approach.

Moreover, the units for a fuel type may forgo bidding but supply or demand smaller quantities. However, this only occurs either when the plants are given a non-scheduled status at registration, or when they use fixed bids to act as price takers to secure trade with no price conditions. The model accommodates this activity using fixed bid quantity variables.

The most important aspect of the equilibrium solution is the merit order dynamic. Three steps are involved in matching end-user demand with the least-cost supply, insofar as the availability and feasibility factors as well as the fixed bid quantities permit, and thus prepare our discussion of the merit order dynamic. The first step is to calculate the inelastic demand for the scheduled fuels to fill. For that, we take the net of the expected value of the inelastic demand term, the fixed bid quantities and the constrained-on/off variable. The second step is to categorise the scheduled fuels as low-priced, mid-priced or high-priced for the following purpose. The low-priced generator fuels and high-priced load fuels are granted complete dispatch and are netted against demand, similar to how the fixed bid quantities had been in step one. Then, the high-priced generator fuels and the low-priced load fuels with an available quantity lower bound at nil are taken out – that is, their bids are removed from the merit order – as these quantities are uneconomic. If, however, the available quantity lower bound of a high-priced (uneconomic) generator fuel is not zero, i.e., the fuel is physically unable to shut down, then it is labelled an

online fuel (a scheduled fuel that must be kept online). It remains dispatched in its lower bound quantity and gets netted from the demand at this time. There might be one or more online generator fuels simultaneously. That leaves the remaining mid-priced fuels as marginal to set the price at the adjusted inelastic demand, the demand for the marginal fuels to fill. The third step is to express the market bid stack function that returns the price at the adjusted inelastic demand in closed form.

4.2.1.3 Assumed market dynamics

The three steps in combination realise a market merit order dynamic that retains the core mathematical apparatus and the overlapping and dynamic properties of the model by Carmona et al. (2013) but also introduces three new price effects, which are the load effect, the online fuel effect and the network constraint effect. The overlapping property allows the different bid stack functions to overlap on price. For example, solar may bid at prices between -$10 and $10 and coal between $0 and $100, and the fact that these overlap between $0 and $10 is perfectly acceptable. The dynamic property allows the fuel bid stack functions to be time-dependent, which is desirable for modelling the variability in the bid curves owing to strategic bidding. The load effect is then the price effect that arises out of the two-way fuels entering with both a generator bid stack and a load bid stack at the same time. The online fuel effect ensures that fuels with a minimum operating level that cannot shut down are represented accordingly in the model. Lastly, the network constraint effect uses the constrained-on/off variable as a demand offset to avoid using quantities subject to curtailment and ensure the use of must-run quantities.

The regional market merit order dynamic that determines the dispatch quantities and marginal price in the model is also subject to the influence of export–import between the regions in multi-regional markets. In real life, NEMDE determines the price as the cost of the incremental 1 MW change in supply in the focus region by the end of the next 5-minute trade interval, including the costs of the marginal energy targets and the consequential marginal frequency balancing target re-arrangements as per AEMO (2010*b*), which involves interconnector availability as follows. When there is free interconnector capacity for price regions that have undispatched bids at lower prices, the engine allows for trade, and the regional prices are set at a similar level. In the absence of interconnector flow capabilities, however, the price is set within each focus

region such that the prices of the different islanded regions are remarkably different. The model accommodates these export–import assumptions by carefully estimating the trade quantities between different regions within the respective interconnector capacity bounds that then enter as adjustments to the inelastic demand level.

The model generally maps well to other electricity markets that meet the following criteria. First, in regional markets, the dual variables of the physical constraints should not be components of the marginal price. Moreover, the auction scheme of the market must be sufficiently similar to that of the assumed market structure, i.e. to the liberalised regional markets where the participants engage in price-based bidding. Whether bidding is price-based or cost-based in a market can impact the suitability of the model when capturing the price levels and temporal changes in the fuel bid stack functions. The diurnal and seasonal shift variable of the proposed model is only concerned with strategic bidding, as is arguably appropriate in the price-based NEM; however, this may not be the recommended approach in cost-based markets, for example, input fuel price–based overlays might be needed for certain fuels. Moreover, sufficient historical non-price data must be available for the model to be accurately calibrated to ensure the physical feasibility of the projected equilibrium solutions over time.

Thus, the new model returns the electricity price as the equilibrium solution of the assumed market structure as described. Note that the proposed hyperbolic model can also be helpful for market analysis, as it does not detach from the production activity dictated by the auction scheme of the assumed market structure.

4.2.2 Model formulation

The model functions as a transformation map that takes inelastic demand D_t as an input and produces price p_t as an output at time t.

4.2.2.1 Fuel bid stack functions

We denote with $I = (1, ...n)$ the scheduled generator fuel set of a price region, with $L = (1, ...m)$ the scheduled load fuel set of the same price region, and with $U = (I, L)$ the complete scheduled fuel set of the region. Let fuel $i \in I$ be a generator fuel and fuel $l \in L$ be a load fuel. We provide two distinct fuel bid stack functions; one for the n generator fuels and another

one for the m load fuels. Both have fuel-, region-, and time-dependent parameters. We also introduce the price taker fuel set $F = (1, ...f)$ for the f fuels that make small, price-independent quantity commitments.

Consider $t \in (t_0, T]$ as the time that partitions the pricing period from time t_0 until times T into 5-minute time intervals starting at t_1.

At time t, the maximum registered capacity of generation fuel i is represented by $\bar{c}_{i,t}$, and the maximum registered capacity of load fuel l by $\bar{c}_{l,t}$, both measured in MW. Then, the maximum scheduled generation capacity $\bar{c}_t$ of the region (in MW) is computed as the sum of the maximum scheduled registered generation capacities in the region – that is, $\bar{c}_t = \sum_{i=1}^{n} \bar{c}_{i,t}$. The full capacity range of generation fuel i is $[0, \bar{c}_{i,t}]$ and the full capacity range of load fuel l is $[0, \bar{c}_{l,t}]$, respectively. When proportionate to the maximum generation capacity $\bar{c}_t$ of the region, the scaled full capacity range of generation fuel i is given by $[0, \frac{\bar{c}_{i,t}}{\bar{c}_t}]$ (in unit amounts), and the scaled full capacity range of load fuel l is given by $[0, \frac{\bar{c}_{l,t}}{\bar{c}_t}]$ (in unit amounts). The bid stack functions are fitted to data on these scaled full capacity ranges.

If the lower and upper availability generation bounds are $c_{i,t,lower}$ and $c_{i,t,upper}$ (in MW), respectively, then the available capacity range of generation fuel i would be $(c_{i,t,lower}, c_{i,t,upper}]$. Similarly, if the lower and upper availability load bounds are $c_{l,t,lower}$ and $c_{l,t,upper}$ (in MW), then the available capacity range of load fuel l would be $[c_{l,t,lower}, c_{l,t,upper})$. When proportionate to the maximum generation capacity in the region $\bar{c}_t$, the scaled available capacity range of generation fuel i would be $(\frac{c_{i,t,lower}}{\bar{c}_t}, \frac{c_{i,t,upper}}{\bar{c}_t}]$ (in unit amounts), and the scaled available capacity range of load fuel l would be $[\frac{c_{l,t,lower}}{\bar{c}_t}, \frac{c_{l,t,upper}}{\bar{c}_t})$ (in unit amounts). The bid stack functions are restricted to these scaled available capacity ranges after the available capacity truncation.

Further, we introduce the regulatory price thresholds P_{floor} for the market price floor, which is usually negative (at around -$1,000), and P_{cap} for the market price cap (at around $15,000 indexed to inflation) in AUD. When proportionate to the market price cap, P_{cap} at time t, the scaled price range between the regulatory thresholds would be $[\frac{P_{floor}}{P_{cap}}, \frac{P_{cap}}{P_{cap}}]$ or equivalently $[\frac{P_{floor}}{P_{cap}}, 1]$ (in unit amounts).

Let the generator fuel bid stack function be the map from the scaled available capacity range of generation fuel i (the quantity x fuel i is able to trade) in unit amounts, to the price range of

generation fuel i (the price y fuel i receives per MW after scaling) in unit amounts, as $\mathbb{R}^+ : x \in (\frac{c_{i,t,lower}}{\bar{c}_t}, \frac{c_{i,t,upper}}{\bar{c}_t}] \to \mathbb{R} : y$. While price y on the real codomain is a monotonically increasing function of quantity x, price y is not necessarily within the scaled regulatory thresholds. The economic interpretation of the map identifies it as an inverse supply curve, or as an implied inverse supply curve, when fitted to data.

Let the load fuel bid stack function be the map from the scaled available capacity range of load fuel l (the quantity x fuel l is able to trade) in unit amounts, to the price range of load fuel l (the price y fuel l pays per MW after scaling) in unit amounts as $\mathbb{R}^+ : x \in [\frac{c_{l,t,lower}}{\bar{c}_t}, \frac{c_{l,t,upper}}{\bar{c}_t}) \to \mathbb{R} : y$. While price y on the real codomain is a monotonically decreasing function of quantity x, price y is not necessarily within the scaled regulatory thresholds. The economic interpretation of the map identifies it as an inverse demand curve, or as an implied inverse demand curve, when fitted to data.

In this setting, we give two separate fuel bid stack functions, one for the generator fuels and another one for the load fuels.

First, we express the bid stack function for every generator fuel $i \in I$ as a strictly increasing hyperbolic map from quantity $x \in \mathbb{R}$ in unit amounts to price $y \in \mathbb{R}$ in unit amounts, $x \to y : b_{\bar{G},i,t}(x)$ as

$$b_{\bar{G},i,t}(x) = \alpha_{t_0} \sinh(\beta_{i,t_0} x - \gamma_{i,t} \beta_{i,t_0}), \tag{4.2.1}$$

with $\alpha_{t_0}, \beta_{i,t_0} > 0$ at time t.

Then for a left-continuous fuel bid stack map $x \to y : b_{G,i,t}(x)$ focusing only on the available capacity in the fuel, we define $b_{G,i,t}(x) := b_{\bar{G},i,t}(x)$ on the scaled available capacity quantity range $\mathbb{R}^+ : x \in (\frac{c_{i,t,lower}}{\bar{c}_t}, \frac{c_{i,t,upper}}{\bar{c}_t}]$ of fuel i in most cases, except when the lower availability generation bound $c_{i,t,lower} = 0$ of the fuel is nil. In this circumstance, we define the map on $\mathbb{R}^+ : x \in [\frac{c_{i,t,lower}}{\bar{c}_t}, \frac{c_{i,t,upper}}{\bar{c}_t}]$.

Furthermore, we introduce the bid stack function for every load fuel $l \in L$ as a strictly decreasing hyperbolic map from quantity $x \in \mathbb{R}$ in unit amounts to price $y \in \mathbb{R}$ in unit amounts, $x \to y : b_{\bar{L},l,t}(x)$ as

$$b_{\bar{L},l,t}(x) = -\alpha_{t_0} \sinh(\beta_{l,t_0} x - \gamma_{l,t} \beta_{l,t_0}), \tag{4.2.2}$$

with $\alpha_{t_0}, \beta_{l,t_0} > 0$ and at time t.

Then for a right-continuous fuel bid stack map $x \to y : b_{L,l,t}(x)$ focusing only on the available capacity in the fuel, we define $b_{L,l,t}(x) := b_{\bar{L},l,t}(x)$ on the scaled available capacity quantity range $\mathbb{R}^+ : x \in [\frac{c_{l,t,lower}}{\bar{c}_t}, \frac{c_{l,t,upper}}{\bar{c}_t})$ of fuel l.

In comparison, Carmona et al. (2013) use exponential fuel bid stack functions only on the positive real codomain for generation fuels, making no assumptions about fuel availability.

Finally, the fuel bid curve equations for generator (4.2.1) and load fuels (4.2.2) are inherently symmetric. Before the availability truncation, the regional alpha α_{t_0} captures the price elasticity (positive relationship) and the fuel beta $\beta_{\cdot,t_0}$ the width (negative relationship) of the mid-range of the symmetric fuel curves. The regional alpha α_{t_0} parameter is the same for all generator fuels i and load fuels l in the price region[108]. The beta $\beta_{\cdot,t_0}$ parameter, i.e. β_{i,t_0} for generator fuels and β_{l,t_0} for load fuels, is specified for every fuel independently. However, the symmetry of the fuel bid stack equations is limited by the scope of the scaled full capacity range of generator fuel i on which its bid stack curve will have been fitted to the data $[0, \frac{\bar{c}_{i,t}}{\bar{c}_t}]$, and also by the available capacity truncation.

4.2.2.2 Inverse fuel bid stack functions

We also propose inverse fuel curves, first in the spirit of Carmona et al. (2013) in general form, and then using the hyperbolic formulae to specify them.[109]

Let the inverse fuel bid curve for fuel $i \in I$ be the strictly increasing, left-continuous hyperbolic map $b^{-1}_{G,i,t}(y)$ from price y in unit amounts, to quantity x, on the scaled available capacity range, as[110] $y \to \mathbb{R}^+ : x \in (\frac{c_{i,t,lower}}{\bar{c}_t}, \frac{c_{i,t,upper}}{\bar{c}_t}] : b^{-1}_{\bar{G},i,t}(y)$ giving the lowest quantity x with

[108] The alpha and beta $(\alpha_{t_0}, \beta_{\cdot,t_0})$ parameters are estimated by least-squares from data at time t_0. Note, however, that one should evaluate whether the quality of the fit would suffer significantly by this restriction on alpha, and if so, it may be worth opting for different values for alpha per fuel per region and a numerical solution in place of a closed-form solution.

[109] For graphs, we refer the reader to Carmona et al. (2013), who readily provide those for the exponential (rather than the hyperbolic) specification.

[110] Or on $\mathbb{R}^+ : x \in [\frac{c_{i,t,lower}}{\bar{c}_t}, \frac{c_{i,t,upper}}{\bar{c}_t}]$ when the lower availability generation bound $c_{i,t,lower} = 0$ of the fuel

$b_{\bar{G},i,t}(x)$ at or above price y, if such exists, or giving the scaled available capacity upper bound $\frac{c_{i,t,upper}}{\bar{c}_t}$ otherwise as

$$b^{-1}_{G,i,t}(y) = \frac{c_{i,t,upper}}{\bar{c}_t} \wedge \inf\left\{x : b_{\bar{G},i,t}(x) \geq y\right\}, \tag{4.2.3}$$

as $\inf \emptyset = +\infty$ (see Carmona et al. (2013)).

We express the inverse of the fuel bid stack function (4.2.1) for generator fuel i as

$$b^{-1}_{\bar{G},i,t}(y) = \frac{\sinh^{-1}\left(\frac{y}{\alpha_{t_0}}\right) + \beta_{i,t_0}\gamma_{i,t}}{\beta_{i,t_0}}. \tag{4.2.4}$$

Analogously, let the inverse fuel bid stack function for fuel $l \in L$ be the strictly decreasing, right-continuous hyperbolic map $b^{-1}_{L,l,t}(y)$ from price y in unit amounts, to quantity x on the scaled available capacity range, as $y \to \mathbb{R}^+ : x \in [\frac{c_{l,t,lower}}{\bar{c}_t}, \frac{c_{i,t,upper}}{\bar{c}_t}) : b^{-1}_{\bar{L},l,t}(y)$ giving the highest quantity x with $b_{\bar{L},l,t}(x)$ at or above price y, if such exists, or else giving the scaled available capacity lower bound $\frac{c_{l,t,lower}}{\bar{c}_t}$ as

$$b^{-1}_{L,l,t}(y) = \frac{c_{l,t,lower}}{\bar{c}_t} \vee \sup\left\{x : b_{\bar{L},l,t}(x) \geq y\right\}, \tag{4.2.5}$$

as $\sup \emptyset = -\infty$.

We give the inverse of the fuel bid stack (4.2.2) for load fuel l as

$$b^{-1}_{\bar{L},l,t}(y) = \frac{-\sinh^{-1}\left(\frac{y}{\alpha_{t_0}}\right) + \beta_{l,t_0}\gamma_{l,t}}{\beta_{l,t_0}}. \tag{4.2.6}$$

4.2.2.3 Fuel subset definition

The fuel subsets help distinguish the type of quantity commitment made by each scheduled fuel within U. Two strands of quantity commitment are considered: constant and formulaic, for both generator and load fuels. Scheduled fuels are categorised as low-priced, mid-priced or high-priced, and the type they are allotted determines the way they usually fill demand D_t

---

is nil.

and set the price – that is, they might enter as price-constant amounts or with price-dependent quantity formulae.

More specifically, every generator fuel can be C_I completely dispatched (low-priced, constant), M_I marginal (mid-priced, formulaic), O_I online or Z_I unused (high-priced, constant). In contrast, the load fuels can be C_L completely dispatched (high-priced, constant), M_L marginal (mid-priced, formulaic), or Z_L unused (low-priced, constant), i.e., C_I, M_I, O_I, Z_I and C_L, M_L, Z_L are the only legal subsets loosely following Carmona et al. (2013).

Then, every generator fuel $i \in I$ is allocated to one of the following four disjoint subsets, $(C_I, M_I, O_I, Z_I) \subseteq I$, as

$$C_I := \{i \in I : \text{generators in fuel } i \text{ are completely dispatched at } c_{i,t,upper}\},$$

$$M_I := \{i \in I : \text{generators in fuel } i \text{ are partially dispatched}\},$$

$$O_I := \{i \in I : \text{generators in fuel } i \text{ are kept online at } c_{i,t,lower} \neq 0\},$$

$$Z_I := \{i \in I : \text{generators in fuel } i \text{ are not used at } c_{i,t,lower} = 0\}.$$

Every load fuel $l \in L$ is allocated to one of the following three disjoint subsets, $(C_L, M_L, Z_L) \subseteq L$, as

$$C_L := \{l \in L : \text{loads in fuel } l \text{ are completely dispatched at } c_{l,t,upper}\},$$

$$M_L := \{l \in L : \text{loads in fuel } l \text{ are partially dispatched}\},$$

$$Z_L := \{l \in L : \text{loads in fuel } l \text{ are not used}\}.$$

Furthermore, let $b_{(M_I,M_L)_{q*},t}(x)$ be the market bid stack function that aggregates the fuel bid stack functions in (M_I, M_L), assuming that only the fuels in (M_I, M_L) contribute formulaically to the market bid stack and that the fuels in the remaining subsets $(C_I, Z_I, O_I, C_L, Z_L)$ contribute to the demand quantity with price-constant quantity adjustments. From above, the

(M_I, M_L) set is the union of the marginal generator fuel M_I set and the marginal load fuel M_L set. Then the function $b_{(M_I,M_L)_{q*},t}(x)$ solves for the market price at the adjusted demand quantity x such that the value of the applied demand adjustment is linked to the subset specification U_{q*}.[111] This adjusts demand D_t by a term encapsulating the price-constant supply contribution of the fuels in $(C_I, Z_I, O_I, C_L, Z_L)$, which gives $x = D_t - \sum_{k \in C_I} \frac{c_{k,t,upper}}{\bar{c}_t} - \sum_{i \in O_I} \frac{c_{i,t,lower}}{\bar{c}_t} + \sum_{k \in C_L} \frac{c_{k,t,upper}}{\bar{c}_t}$. Thus, the value of x is not equal to D_t, unless the supply contribution of the excluded fuels equals zero.

Denoting the upper price in generation fuel i at time t with $\bar{b}_{G,i,t} := b_{G,i,t}(\frac{c_{i,t,upper}}{\bar{c}_t})$ and the lower price with $\underline{b}_{G,i,t} := b_{G,i,t}(\frac{c_{i,t,lower}}{\bar{c}_t})$, the merit order rule for generation gives that $\max(\bar{b}_{G,k \in C_I,t}) < \min(\underline{b}_{G,a \in M_I,t})$ the highest price in any completely dispatched generator fuel $k \in C_I$ is always lower than the lowest price in any marginal generator fuel $a \in M_I$. Also, $\max(\bar{b}_{G,a \in M_I,t}) < \min(\underline{b}_{G,o \in O_I, z \in Z_I,t})$ the highest price in any marginal generator fuel $a \in M_I$ is always lower than the lowest price in any online or unused generator fuel $o \in O_I, z \in Z_I$. Then, for n generator fuels on four subsets[112] the following fuel categorisation defines the elements of C_I (low-priced), M_I (mid-priced) and O_I, Z_I (high-priced):

- $\{i \in C_I | b_{(M_I,M_L)_{q*},t}(x) > \max(\bar{b}_{G,i \in C_I,t})\}$, generator fuel i is in subset C_I, if the price from the market bid stack function $b_{(M_I,M_L)_{q*},t}(x)$[113] at quantity $x = D_t - \sum_{i \in C_I} \frac{c_{i,t,upper}}{\bar{c}_t} - \sum_{o \in O_I} \frac{c_{o,t,lower}}{\bar{c}_t} + \sum_{k \in C_L} \frac{c_{k,t,upper}}{\bar{c}_t}$, demand net of the quantity supplied by fuels $\forall i \in C_I, \forall o \in O_I, \forall l \in C_L$, is greater than the highest price by any completely dispatched generator fuel $\forall i \in C_I$,

- $\{i \in O_I | b_{(M_I,M_L)_{q*},t}(x) < \min(\underline{b}_{G,i \in O_I, z \in Z_I,t}) \; and \; c_{i,t,lower} > 0\}$ generator fuel i is in subset O_I, if the price from the market bid stack function $b_{(M_I,M_L)_{q*},t}(x)$ at quantity $x = D_t - \sum_{k \in C_I} \frac{c_{k,t,upper}}{\bar{c}_t} - \sum_{i \in O_I} \frac{c_{i,t,lower}}{\bar{c}_t} + \sum_{k \in C_L} \frac{c_{k,t,upper}}{\bar{c}_t}$, demand net of the quantity supplied by fuels $\forall k \in C_I, \forall i \in O_I, \forall l \in C_L$, is lower than the lowest price by any online and unused fuel $\forall i \in O_I, \forall z \in Z_I$, and if the lower capacity bound $c_{i,t,lower}$ of fuel i is greater than 0,

[111] Note that the allocation of the fuels into fuel subsets U_{q*} is anterior to the market bid stack function.

[112] For the two-fuel case on three subsets see Table 1 in Carmona et al. (2013).

[113] Using the market bid stack formula as specified in the upcoming Section 4.2.2.4.

- $\{i \in Z_I | b_{(M_I,M_L)_{q*},t}(x) < \min(\underline{b}_{G,i\in Z_I,o\in O_I,t})\ and\ c_{i,t,lower} = 0\}$ generator fuel i is in subset Z_I, if the price from the market bid stack function $b_{(M_I,M_L)_{q*},t}(x)$ at quantity $x = D_t - \sum_{k\in C_I} \frac{c_{k,t,upper}}{\bar{c}_t} - \sum_{o\in O_I} \frac{c_{o,t,lower}}{\bar{c}_t} + \sum_{k\in C_L} \frac{c_{k,t,upper}}{\bar{c}_t}$, demand net of the quantity supplied by fuels $\forall k \in C_I, \forall o \in O_I, \forall l \in C_L$, is lower than the lowest price by any online or unused fuel $\forall o \in O_I, \forall z \in Z_I$, and if the lower capacity bound $c_{i,t,lower}$ of fuel i equals 0,
- $i \in M_I$ otherwise.

To explain these conditions for one fuel $i \in I$ at a time, first consider a setting where the market price is known in advance. Given the upper $\bar{b}_{G,i,t}$ and the lower $\underline{b}_{G,i,t}$ price of fuel i, it can be assigned to a subset by arranging $\bar{b}_{G,i,t}, \underline{b}_{G,i,t}$, and the market price in ascending order. If the market price is greater than $\bar{b}_{G,i,t}$, then $i \in C_I$ is completely dispatched. Or, if the market price is lower than $\underline{b}_{G,i,t}$, then $i \in (O_I, Z_I)$ is online or unused, depending on the lower capacity bound $c_{i,t,lower}$. Otherwise, $i \in M_I$ is marginal. But because $b_{(M_I,M_L)_{q*},t}(x)$ solves for the market price using the preexisting subset allocation on U_{q*}, one cannot determine the market price until $\forall i \in I \subseteq U$ are assigned to the correct subset, i.e. the market price is typically not yet known. One can, however, show, that i always behaves online or unused on the price range $[\frac{P_{floor}}{P_{cap}}, \underline{b}_{G,i,t})$, marginal on the price range $[\underline{b}_{G,i,t}, \bar{b}_{G,i,t}]$ and completely dispatched on the price range $(\bar{b}_{G,i,t}, 1]$ from the given upper $\bar{b}_{G,i,t}$ and the lower $\underline{b}_{G,i,t}$ price of fuel i and the inverse bid stack formula in (4.2.3). By partitioning the entire price range $[\frac{P_{floor}}{P_{cap}}, 1]$ at the upper $\bar{b}_{G,i,t}$ and the lower $\underline{b}_{G,i,t}$ price of every fuel $i \in I$, one can obtain a string of smaller price segments[114], and each segment then has a well-defined subset configuration U_{q*} associated with it, which is the same for all quantities within the segment, but may or may not be the same for two adjacent segments. The two price points defining each segment can be used to obtain the correct subset allocation U_{q*} by replacing "the market price" by the two price points and arranging $\bar{b}_{G,i,t}, \underline{b}_{G,i,t}$, and the two prices in ascending order. If the two price points are both greater than $\bar{b}_{G,i,t}$, then $i \in C_I$ is completely dispatched. Else, if the two prices are both lower than $\underline{b}_{G,i,t}$, then $i \in (O_I, Z_I)$ is online or unused. Otherwise, $i \in M_I$ is marginal.

[114]The present discussion ignores load fuels $l \in L$, but the subset and price algorithm in the example in Section 4.2.2.5 does not. Where then more generally, the string of smaller price segments (the extended partitioning) is obtained by dissecting the price range $[\frac{P_{floor}}{P_{cap}}, 1]$ at the upper $\bar{b}_{G,i,t}, \bar{b}_{L,l,t}$ and the lower prices $\underline{b}_{G,i,t}, \underline{b}_{L,l,t}$ of every fuel $\forall i, \forall l$ on $U = (I, L)$.

Next, considering load fuels, let us denote the upper price in load fuel l with $\bar{b}_{L,l,t} := b_{L,l,t}(\frac{c_{l,t,lower}}{\bar{c}_t})$ and the lower price with $\underline{b}_{L,l,t} := b_{L,l,t}(\frac{c_{l,t,upper}}{\bar{c}_t})$ at time t. Using the merit order rules for load uptake, whereby $\min(\underline{b}_{L,k\in C_L,t}) > \max(\bar{b}_{L,a\in M_L,t})$ the lowest price in any completely dispatched load fuel $k \in C_L$ is always greater than the highest price in any marginal load fuel $a \in M_L$, and $\min(\underline{b}_{L,a\in M_L,t}) > \max(\bar{b}_{L,z\in Z_L,t})$ the lowest price in any marginal load fuel $a \in M_L$ is always greater than the highest price in any unused load fuel $z \in Z_L$, the following are the fuel category conditions for m generator fuels on three subsets, C_L (high-priced), M_L (mid-priced) and Z_L (low-priced):

- $\{l \in C_L | b_{(M_I,M_L)_{q*},t}(x) < \min(\underline{b}_{L,l\in C_L,t})\}$, generator fuel l is in subset C_L, if the price from the market bid stack function $b_{(M_I,M_L)_{q*},t}(x)$ at quantity $x = D_t - \sum_{k\in C_I} \frac{c_{k,t,upper}}{\bar{c}_t} - \sum_{o\in O_I} \frac{c_{o,t,lower}}{\bar{c}_t} + \sum_{k\in C_L} \frac{c_{k,t,upper}}{\bar{c}_t}$, demand net of the quantity supplied by fuels $\forall k \in C_I, \forall o \in O_I, \forall l \in C_L$, is lower than the lowest price by any completely dispatched load fuel $\forall l \in C_L$,
- $\{l \in Z_L | b_{(M_I,M_L)_{q*},t}(x) > \max(\bar{b}_{L,z\in Z_L,t})\}$, generator fuel l is in subset Z_L, if the price from the market bid stack function $b_{(M_I,M_L)_{q*},t}(x)$ at quantity $x = D_t - \sum_{k\in C_I} \frac{c_{k,t,upper}}{\bar{c}_t} - \sum_{o\in O_I} \frac{c_{o,t,lower}}{\bar{c}_t} + \sum_{k\in C_L} \frac{c_{k,t,upper}}{\bar{c}_t}$, demand net of the quantity supplied by fuels $\forall k \in C_I, \forall o \in O_I, \forall l \in C_L$, is greater than the lowest price by any unused load fuel $\forall l \in C_L$.
- $l \in M_L$ otherwise.

These conditions are perhaps more intuitive considering that a single fuel $l \in L$ is always completely dispatched on the price range $[\frac{P_{floor}}{P_{cap}}, \underline{b}_{L,l,t})$, marginal on the price range $[\underline{b}_{L,l,t}, \bar{b}_{L,l,t}]$ and unused on the price range $(\bar{b}_{L,l,t}, 1]$, as from the inverse bid stack formula in (4.2.5). By partitioning the entire price range $[\frac{P_{floor}}{P_{cap}}, 1]$ at the upper $\bar{b}_{G,i,t}$, $\bar{b}_{L,l,t}$ and the lower prices $\underline{b}_{G,i,t}$, $\underline{b}_{L,l,t}$ of every fuel $i \in I$ and $l \in L$, one obtains a string of smaller price segments, such that each segment has a particular subset configuration U_{q*} associated with it. The subset of fuel l can then be found using the above observation and the previously described subset process with this extended partitioning, as opposed to a more direct application of the subset rules.

In conclusion, the subsets of the fuels determine their role in filling the adjusted inelastic demand D_t and consequently in price formation, i.e., in the market bid stack formula

$b_{(M_I,M_L)_{q*},t}(x)$ that solves for the market price. The completely dispatched fuels in C_I, C_L generate or uptake in the quantity at their upper capacity bound $c_{i,t,upper}$ or $c_{l,t,upper}$, which are constant in the sense that they do not depend on the exact price level beyond what is already known about the possible range of the price level that assigned them to C_I, C_L in the first place. Similarly, the online fuels in O_I generate in the quantity at their lower capacity bound $c_{i,t,lower}$, which is also constant in that sense. Moreover, the unused fuels in Z_I, Z_L do not generate or uptake any quantity. In contrast, the marginal fuels in M_I, M_L generate or uptake in some quantity within their capacity bounds, but the quantity has not been determined by the subset as such. Thus, from the perspective of the market bid stack formula $b_{(M_I,M_L)_{q*},t}(x)$, the type of quantity commitment the fuels must make due to being allocated to one particular subset and not to another, polarises the subsets into constant dispatch and formulaic (marginal) dispatch subsets. The generation or uptake quantity in any fuel in the constant dispatch subsets C_I, C_L, O_I, Z_I, Z_L is determined outside $b_{(M_I,M_L)_{q*},t}(x)$ and enters $b_{(M_I,M_L)_{q*},t}(x)$ as part of an additive term, i.e. as a demand adjustment. Whereas the dispatch quantity in any fuel in the marginal dispatch subsets M_I, M_L is determined by the market bid stack formula $b_{(M_I,M_L)_{q*},t}(x)$.

4.2.2.4 Market bid stack formula

Let $b_{(M_I,M_L)_{q*},t}(x)$ be the market bid stack function that aggregates every fuel bid curve on the complete regional fuel set under the appropriate subset allocation U_{q*} in merit order to evaluate the market price at quantity x. To that effect, first, it distinguishes the constant dispatch fuels (in C_I, C_L, O_I, Z_I, Z_L) from the formulaic – marginal or price setter – fuels (in M_I, M_L).

The contribution of the former is captured in the constant term h that adds up the constant supply sum in the generator fuels $\forall i \in (C_I, O_I, Z_I)$ with a negative sign and the constant demand sum in the load fuels $\forall l \in (C_L, Z_L)$ with a positive sign as

$$h = -\sum_{i \in C_I} \frac{c_{i,t,upper}}{\bar{c}_t} - \sum_{i \in O_I} \frac{c_{i,t,lower}}{\bar{c}_t} + \sum_{l \in C_L} \frac{c_{l,t,upper}}{\bar{c}_t}. \tag{4.2.7}$$

To move these quantities to the inelastic demand side of the equilibrium, the demand quantity for the marginal fuels to fill can be expressed as $D_t + h$.

In contrast, every marginal fuel in M_I, M_L is represented by the inverse bid stack function of

the fuel. The strictly increasing left-continuous market bid stack function $b_{(M_I,M_L)_{q*},t}(x)$ maps the adjusted demand quantity $x = D_t + h$ to the highest price p_t, such that the corresponding quantity over all inverse fuel bid stack functions $\sum_{i\in M_I} b^{-1}_{\bar{G},i,t}(p_t) - \sum_{l\in M_L} b^{-1}_{\bar{L},l,t}(p_t)$ is still below the cleared quantity $D_t + h$, provided that there is at least one marginal generator fuel $|M_I| \geq 1$ in the region. Then the main structural components of the market bid stack, the constant term h and the aggregate of the inverse fuel curves, give the price solution of the function as

$$p_t = b_{(M_I,M_L)_{q*},t}(D_t) = \sup\left\{p_t \in \mathbb{R} : \sum_{i\in M_I} b^{-1}_{\bar{G},i,t}(p_t) - \sum_{l\in M_L} b^{-1}_{\bar{L},l,t}(p_t) < D_t + h\right\}. \tag{4.2.8}$$

in general form, extending the market merit order dynamic of Carmona et al. (2013) (see Proposition 1 in Carmona et al. (2013)) to a new generator fuel subset O_I and load fuels.

Then the hyperbolic specification of (4.2.8) is expressed as

$$\begin{aligned} p_t =& b_{(M_I,M_L)_{q*},t}(D_t) \\ =& \alpha_{t_0} \sinh\left(\frac{\left(D_t + h - \sum_{i=1}^{a}\gamma_{i,t} + \sum_{l=1}^{b}\gamma_{l,t}\right)\prod_{i=1}^{a}\beta_{i,t_0}\prod_{l=1}^{b}\beta_{l,t_0}}{\sum_{i=1}^{a}\left(\prod_{j=1}^{a}\beta_{j\neq i,t_0}\prod_{l=1}^{b}\beta_{l,t_0}\right) + \sum_{l=1}^{b}\left(\prod_{i}^{a}\beta_{i,t_0}\prod_{j=1}^{b}\beta_{j\neq l,t+0}\right)}\right). \end{aligned} \tag{4.2.9}$$

Example 4.1. *To demonstrate the proposed method, we consider a price region at time t with four generator and two load fuels, where the bid stack parameters $\alpha_{t_0}, \beta_{t,i}, \beta_{t,l}, \gamma_{t,i}, \gamma_{t,l}$ and the adjusted inelastic demand quantity D_t are already known, but remain unspecified. By careful arrangement,*[115] *the subset configuration U_{q*} is also given. We know that $|C_I| = 1$ of the generator fuels is completely dispatched, $|O_I| = 1$ is online and $|M_I| = 2$ are marginal. Then there is also $|C_L| = 1$ completely dispatched and $|M_L| = 1$ marginal load fuel.*

We can then express h as

$$h = -\frac{c_{i\in C_I,t,upper}}{\bar{c}_t} - \frac{c_{i\in O_I,t,lower}}{\bar{c}_t} + \frac{c_{l\in C_L,t,upper}}{\bar{c}_t},$$

[115] Using the subset and price algorithm as in the example in Section 4.2.2.5.

and denote the inverse fuel bid stack functions of the two marginal generator fuels with $b^{-1}_{\bar{G},1,t}(p_t)$ *and* $b^{-1}_{\bar{G},2,t}(p_t)$*, and the inverse fuel bid stack function of the marginal load fuel with* $b^{-1}_{\bar{L},3,t}(p_t)$.

We evaluate price p_t *inside the supremum in (4.2.8) as*

$$b^{-1}_{\bar{G},1,t}(p_t) + b^{-1}_{\bar{G},2,t}(p_t) = D_t + h + b^{-1}_{\bar{L},3,t}(p_t),$$

$$\frac{\sinh^{-1}\left(\frac{p_t}{\alpha_{t_0}}\right) + \beta_{t,1}\gamma_{t,1}}{\beta_{t,1}} + \frac{\sinh^{-1}\left(\frac{p_t}{\alpha_{t_0}}\right) + \beta_{t,2}\gamma_{t,2}}{\beta_{t,2}} = D_t + h + \frac{-\sinh^{-1}\left(\frac{p_t}{\alpha_{t_0}}\right) + \beta_{t,3}\gamma_{t,3}}{\beta_{t,3}},$$

then

$$\sinh^{-1}\left(\frac{p_t}{\alpha_{t_0}}\right) = \frac{\left(D_t + h - \gamma_{t,1} - \gamma_{t,2} + \gamma_{t,3}\right)\beta_{t,1}\beta_{t,2}\beta_{t,3}}{\beta_{t,2}\beta_{t,3} + \beta_{t,1}\beta_{t,3} + \beta_{t,1}\beta_{t,2}},$$

and for the hyperbolic equilibrium formulation from (4.2.9)

$$p_t = \alpha_{t_0}\sinh\left(\frac{\left(D_t + h - \gamma_{t,1} - \gamma_{t,2} + \gamma_{t,3}\right)\beta_{t,1}\beta_{t,2}\beta_{t,3}}{\beta_{t,2}\beta_{t,3} + \beta_{t,1}\beta_{t,3} + \beta_{t,1}\beta_{t,2}}\right).$$

4.2.2.5 Price formula

The market bid stack function (4.2.9) solves for the market price under the so-called normal market assumption. The value of demand D_t implies this normal market assumption when it is between the lowest $S^1_t \leq D_t \leq S^2_t$ and the highest available generation quantity in the market.[116] The market price can then be written as $p_t(D_t)\mathbb{1}_{[S^1_t, S^2_t]}$. Conversely, should the market have either a demand deficit $D_t < S^1_t$ or a supply deficit $S^2_t < D_t$, it is then in a system-tied state, and the corresponding prices are $p_t(D_t)\mathbb{1}_{[-\infty, S^1_t)} = \max(\underline{b}_{G,i\in O_I,t}, \frac{P_{floor}}{P_{cap}}) = \underline{b_t}$ and $p_t(D_t)\mathbb{1}_{S^2_t,,\infty]} = \frac{P_{cap}}{P_{cap}} = 1$, respectively. In general, we can express the market price as

[116] The values of S^1_t and S^2_t are specified shortly.

$$p_t \ = p_t(D_t)\mathbb{1}_{[-\infty,\infty]} = p_t(D_t)\mathbb{1}_{[-\infty,S_t^1)} + p_t(D_t)\mathbb{1}_{[S_t^1,S_t^2]} + p_t(D_t)\mathbb{1}_{(S_t^2,\infty]}, \tag{4.2.10}$$

the price in any state of the system.

To find the price in a normal market, let us partition the demand domain of the normal state $[S_t^1, S_t^2]$ into a string of quantity segments, such that one particular subset configuration U_{q*} holds for any level of demand D_t within each segment. Finding the boundary points of the segments involves a corresponding string of price segments as well, as the quantity domain and the price codomain are bijective, since the fuel bid stack functions in (4.2.1) and (4.2.2) are strictly monotonic.

The boundary points of the price segments with the property can be given by the upper $\bar{b}_{G,i,t}$, $\bar{b}_{L,l,t}$ and the lower $\underline{b}_{G,i,t}$, $\underline{b}_{L,l,t}$ price points in all generation and load fuels in U. Let $(y_1, y_2, ..., y_j..., y_{2(n+m)})$ denote these prices in increasing order.

Let then for every price y_j quantity x_j be the quantity that sums the generation sum from the left-continuous inverse fuel maps $b_{G,i,t}^{-1}(y_j)$ in (4.2.3) with a positive sign, the uptake sum from the right-continuous inverse fuel maps $b_{L,l,t}^{-1}(y_j)$ in (4.2.5) with a negative sign, and the constant quantities h in (4.2.7) with a negative sign, as

$$x_j(y_j) = \sum_{i=1}^{n} b_{G,i,t}^{-1}(y_j) - \sum_{i=1}^{m} b_{L,l,t}^{-1}(y_j) - h, \tag{4.2.11}$$

giving the boundary points of the respective quantities $(x_1, x_2, ..., x_j, ..., x_{2(n+m)})$ also in increasing order.

Then, $S_t^1 := x_1$ and $S_t^2 := x_{2(n+m)}$. Additionally, every segment of the partitioned quantity domain $[S_t^1, x_2]$, $(x_2, x_3]$, $(x_3, x_4]$, ..., $(x_{2(n+m)-1}, S_t^2]$, has a well-defined fuel subset combination U_{q*} associated with it that holds for any level of demand D_t within the segment. The market bid stack function $b_{(M_I,M_L)_{q*},t}(D_t + h)$ in (4.2.9) gives the price using the subset combination $q*$, which can be represented by q_1* for segment $[S_t, x_2]$, by q_2* for segment $(x_2, x_3]$, by q_3* for $(x_3, x_4]$, and so on. For the same fuel set U, the appropriate fuel subset configuration U_{q*} changes over the different quantity segments. As a result, the market bid stack

formula $b_{(M_I,M_L)_{q*},t}(D_t+h)$ also has a segment-wise formulation, owing to its dependence on the segment-wise different U_{q*}.

Loosely following Carmona et al. (2013), we can then express price p as a segment-wise relation extending (4.2.10) as

$$\begin{aligned} p_t = {} & p_t(D_t)\mathbb{1}_{[-\infty,S_t^1)} \\ & + p_t(D_t)\mathbb{1}_{[S_t^1,x_2]} + p_t(D_t)\mathbb{1}_{(x_2,x_3]} + p_t(D_t)\mathbb{1}_{(x_3,x_4]} + \ldots + p_t(D_t)\mathbb{1}_{(x_{2(n+m)-1},S_t^2]} \\ & + p_t(D_t)\mathbb{1}_{(S_t^2,\infty]}, \end{aligned} \tag{4.2.12}$$

where

$$\begin{aligned} & p_t(D_t)\mathbb{1}_{[-\infty,S_t^1)} = \underline{b_t} \\ & p_t(D_t)\mathbb{1}_{[S_t^1,x_2]} = b_{(M_I,M_L)_{q_1*},t}(D_t+h) \\ & p_t(D_t)\mathbb{1}_{(x_2,x_3]} = b_{(M_I,M_L)_{q_2*},t}(D_t+h) \\ & p_t(D_t)\mathbb{1}_{(x_3,x_4]} = b_{(M_I,M_L)_{q_3*},t}(D_t+h) \\ & \vdots \\ & p_t(D_t)\mathbb{1}_{(x_{2(n+m)-1},S_t^2]} = b_{(M_I,M_L)_{q_{2(n+m)-1}*},t}(D_t+h) \\ & p_t(D_t)\mathbb{1}_{(S_t^2,\infty]} = 1. \end{aligned} \tag{4.2.13}$$

Lastly, we recover the market price P_t in AUD from the price p_t in (4.2.12) in unit amounts. To get P_t, the price p_t is first multiplied by the market price cap P_{cap}. The result is projected to the regulatory price floor P_{floor} or cap P_{cap}, if it is exceeding either of the two. The reason why the threshold restriction has been delayed until now is that tracing the fuel dispatch quantities over time, i.e. computing the generation and the uptake quantities from the inverse fuel curves based on p_t, requires strictly monotonic fuel bid stack formulations, which an untimely threshold projection could potentially impair.

Example 4.2. *We suggest an efficient algorithm for finding the appropriate fuel subset configurations on all segments of the partitioned demand domain and executing pricing using (4.2.12).*

To see how this computation works, we consider a price region with five generator and two load fuels, where the bid stack parameters $\alpha_{t_0}, \beta_{t,i}, \beta_{t,l}, \gamma_{t,i}, \gamma_{t,l}$ and the demand quantity D_t are already known. The scaled available capacity ranges $(\frac{c_{i,t,lower}}{\bar{c}_t}, \frac{c_{i,t,upper}}{\bar{c}_t}]$ and $[\frac{c_{l,t,lower}}{\bar{c}_t}, \frac{c_{l,t,upper}}{\bar{c}_t})$ and the fixed net generation quantity $c_{t,fixed}$ (if any) are also already specified at the start of the algorithm as shown in Table 4.1.

Table 4.1 : **The fuels in the example**

The table shows the fuels of both the regional scheduled U fuel set and the regional price taker F fuel set by type, economic classification, parameters, and quantity (in MW) and bid price (in AUD) range. The region in this example has a maximum registered generation capacity of $\bar{c}_t = 155$. The parameters α_{t_0} and $\gamma\cdot, t$ are rounded to two decimal places and the $\beta_{\cdot,t_0}$ to integers for every fuel $i, j \in U$. The market in the example has a market price floor of $P_{floor} = -4$ and a price cap of $P_{cap} = 14$, but bids may appear outside that range, e.g., in fuel G4 we see the upper price at $15.

Fuel type			Parameters		
			α_{t_0}	$\beta_{\cdot,t_0}$	$\gamma\cdot, t$
Generator fuels					
G1	Coal	Scheduled	0.001	12.4	0.192
G2	Hydro	Scheduled	0.001	47.4	0.002
G3	Solar	Scheduled	0.001	150.3	0.043
G4	Gas	Scheduled	0.001	131.9	-0.041
G5	Biomass	Price taker	-	-	-
Load fuels					
L1	Battery	Scheduled	-0.001	48.9	0.000
L2	Hydro	Scheduled	-0.001	77.1	0.089

Fuel type			Quantity range		Price range	
			$c_{\cdot,t,lower}$	$c_{\cdot,t,upper}$	$\underline{b}_{\cdot,\cdot,t} * P_{cap}$	$\bar{b}_{\cdot,\cdot,t} * P_{cap}$
Generator fuels						
G1	Coal	Scheduled	30 MW	120 MW	$0	$10
G2	Hydro	Scheduled	0 MW	25 MW	$0	$14
G3	Solar	Scheduled	0 MW	7 MW	-$3	$0
G4	Gas	Scheduled	0 MW	3 MW	$2	$15
G5	Biomass	Price taker	$c_{i,t,fixed} = 1.5$ MW		-	-
Load fuels						
L1	Battery	Scheduled	0 MW	20 MW	-$4	$0
L2	Hydro	Scheduled	0 MW	25 MW	-$2	$0

Table 4.1 shows the four scheduled generator fuels (G1-G4), the one price taker generator fuel (G5), and the two scheduled load fuels (L1-L2) in this example. First by fuel type, which identifies the fuel source and places the six scheduled fuels in set $U = (I, L)$ and the one price taker fuel in set F. It then gives the bid stack parameters of the fuels. In the third column, the

table specifies the available capacity ranges of the fuels in MW, which is subsequently scaled by the maximum registered generation capacity $\bar{c}_t = 155$. *This value appears to coincide with the total available (scheduled) generation capacity* $\sum_{i\in I} \frac{c_{i,t,upper}}{\bar{c}_t} = \frac{120}{155} + \frac{25}{155} + \frac{7}{155} + \frac{3}{155} = \frac{155}{155}$ *in the region. In addition, the lowest available generation capacity in the region is* $S_t = \sum_{i\in I} \frac{c_{i,t,lower}}{\bar{c}_t} = \frac{30}{155} + 0 + 0 + 0 = \frac{30}{155}$[117]. *The fourth column shows the price ranges of the fuels, which have been calculated using the bid stack parameters, the quantity ranges, and the maximum registered generation capacity. Finally, it is also stated that the region has a regulatory market price floor of* $P_{floor} = -4$ *and a cap of* $P_{cap} = 14$.

Table 4.2 : **Market view**

The table gives a tabulated view of the market showing the contribution of each scheduled fuels to the net market quantity (bottom line) at any price level. As the price increases, the generator fuels are contributing more and the load fuels are demanding less. For a more concise view, the price range (in AUD) has been discretised to integers and the quantity amounts (in MW) have been rounded to integers as well. The quantities shown in bold are obtained from the inverse fuel bid stack functions (4.2.4) and (4.2.6). The remaining (not bold) quantities are constants, as these are either below the available quantity lower bound $c_{\cdot,t,lower}$, or above the available quantity upper bound $c_{\cdot,t,upper}$ in the given fuel as per Table 4.1.

Price	-$5	-$4	-$3	-$2	-$1	$0	$1	$2	$3	$4	$5	$6	$7	$8	$9	$10	$11	$12	$13	$14	$15
Generation quantity																					
G1	30	30	30	30	30	**30**	**91**	**100**	**105**	**109**	**111**	**114**	**116**	**117**	**119**	**120**	120	120	120	120	120
G2	0	0	0	0	0	**0**	**16**	**19**	**20**	**21**	**22**	**22**	**23**	**23**	**23**	**24**	**24**	**24**	**25**	**25**	25
G3	0	0	**0**	**1**	**2**	**7**	7	7	7	7	7	7	7	7	7	7	7	7	7	7	7
G4	0	0	0	0	0	0	0	**0**	**1**	**1**	**1**	**1**	**2**	**2**	**2**	**2**	**2**	**2**	**2**	**2**	**3**
Total	30	30	30	31	32	37	114	126	132	137	141	144	147	149	151	153	153	154	154	154	155
Load uptake quantity																					
L1	20	**20**	**19**	**18**	**16**	**0**	0	0	0	0	0	0	0	0	0	0	0	0	0	0	0
L2	25	25	25	**25**	**24**	**14**	**4**	**3**	**2**	**1**	**1**	**0**	0	0	0	0	0	0	0	0	0
Total	45	45	44	43	39	14	4	3	2	1	1	0	0	0	0	0	0	0	0	0	0
Net market quantity (generation minus load uptake)																					
Total	-15	-15	-13	-12	-7	23	110	123	130	136	140	144	147	149	151	153	153	154	154	154	155

Then, Table 4.2 carries the main operations of the algorithm:

1. *Get the lower and the upper available capacity bound quantities from the third column in Table 4.1, i.e. every* $c_{i,t,lower}$, $c_{l,t,lower}$, $c_{i,t,upper}$ *and* $c_{l,t,upper}$ *in MW. Scale (divide) these*

[117] The fact that S_t does not include the load fuels (therefore always non-negative $S_t \geq 0$) is acceptable, because the electric system is always a net generator, but not without drawbacks, as it sometimes leads to underestimating the must-run price, see demand between 23 and 30 in Table 4.2.

by the maximum registered generation capacity $\bar{c}_t = 155$. *Then, use the fuel bid stack functions in (4.2.1) and (4.2.2) to find the corresponding prices, i.e., the upper* $\bar{b}_{G,i,t}$, $\bar{b}_{L,l,t}$ *and the lower* $\underline{b}_{G,i,t}$, $\underline{b}_{L,l,t}$ *price points, as shown in column four in Table 4.1, e.g., \$0 and \$10 for G1, \$0 and \$14 for G2, etc. When scaled by* P_{cap} = *\$14 and in increasing order, these prices correspond to* $(y_1, y_2, ..., y_j..., y_{2(n+m)}) = (\frac{-4}{14}, \frac{-3}{14}, \frac{-2}{14}, 0, \frac{2}{14}, \frac{10}{14}, \frac{14}{14}, \frac{15}{14})$. *For exposition purposes, Table 4.2 (unscaled view) also fills the price interval with additional prices for an evenly spaced price interval between -\$5 and \$15 (first row). Also notice that the prices are not yet projected to the regulatory price thresholds -\$4 and \$14.*

2. *Fill the table with the constant quantities (not bold) at the prices outside the price ranges of the fuels, i.e. with* $c_{i,t,lower}, c_{l,t,lower}, c_{i,t,upper}$ *and* $c_{l,t,upper}$. *See lines G1, G2, G3, G4 and L1, L2 in Table 4.2. Notice how the G1 line lists 30 MW at every price level up to \$0. In this way, if the market price ends up below price \$0 (and G1 is online in* O_I*), it would still be accounted for and dispatched in 30 MW.*

3. *Fill the table with the formulaic quantities (bold) at the prices inside the price ranges of the fuels using the inverse fuel bid stack functions (4.2.4) and (4.2.6). See rows G1, G2, G3, G4 and L1, L2 in Table 4.2.*

4. *Sum the quantities in rows G1, G2, G3, G4 vertically at every price for the generation quantity total. Similarly, sum the quantities in the L1, L2 lines for the load uptake quantity total. Take away the load uptake total from the generation total to get the net market Total at every price (last row), which is equivalent to the* $(x_1, x_2, ..., x_j, ..., x_{2(n+m)})$ *interval plus* h *(unscaled view in Table 4.2).*

5. *Assume the constrained-on/off adjustment* $X_t = 0$ *(in MW). Get the inelastic end-user demand proxied by net generation* G_t *(in MW), the fixed net generation quantity of the price taker fuels* $c_{t,fixed}$ = *1.5 MW (see Table 4.1), and the maximum generation* $\bar{c}_t$ = *155 MW in the region. Then the adjusted inelastic demand* D_t *is computed as* $D_t = \frac{G_t - X_t - c_{t,fixed}}{\bar{c}_t} = \frac{G_t - 0 - 1.5}{155}$. *We are going to look at two different demand levels. First,* $D_t = \frac{31-1.5}{155} = \frac{29.5}{155}$ *when* G_t = *31 MW. Second,* $D_t = \frac{115-1.5}{155} = \frac{113.5}{155}$ *when* G_t = *115 MW.*

6. *Establish the state of the market, i.e. whether* $S_t \leq D_t \leq \sum_{i \in I} \frac{c_{i,t,upper}}{\bar{c}_t}$ *holds. From*

earlier, $S_t = \frac{30}{155}$ *and* $\sum_{i \in I} \frac{c_{i,t,upper}}{\bar{c}_t} = \frac{115}{155}$. *Thereby the market has a demand deficit at* $G_t = 31$ *and it is in a normal state at* $G_t = 115$.

7. *If the market has a demand deficit, every scheduled fuel is* S_I *or* S_L *and the price* p_t *(in unit amounts) is set by* $p(D_t)\mathbb{1}_{[-\infty, S_t)} = \underline{b_t}$. *This value may then be multiplied by* P_{cap} *and projected to the regulatory thresholds to get the market price* P_t *in AUD — this is the end of the algorithm.*

8. *In a normal market, get the two quantity points (last row) nearest to* D_t *and get the corresponding two price points too (first row). We have that* $D_t \bar{c}_t = 113.5$ *falls within 110 and 123 (last row), and price $1 and $2. Using the two prices, we can assign every fuel to a subset using simple rules.*

9. *For generator fuels G1, G2, G3, G4, if the two prices $1 and $2 are both greater than* $\bar{b}_{G,i,t} P_{cap}$, *then fuel* $i \in C_I$ *is completely dispatched. Or if the two prices are both lower than* $\underline{b}_{G,i,t} P_{cap}$, *then fuel* $i \in (O_I, Z_I)$ *is online or unused. Otherwise, fuel* $i \in M_I$ *is marginal.*

10. *For load fuels L1, L2, if the two prices $1 and $2 are both lower than* $\bar{b}_{L,l,t} P_{cap}$, *then fuel* $l \in C_L$ *is completely dispatched. Or if the two prices are both greater than* $\underline{b}_{L,l,t} P_{cap}$, *then fuel* $l \in (Z_L)$ *is unused. Otherwise, fuel* $l \in M_L$ *is marginal.*

11. *Get price* p_t *(in unit amounts) from the market bid stack function*

$$b_{(M_I, M_L)_{q*}, t}(D_t + h)$$

in (4.2.9) using the subset configuration on U_{q*} *from above. Back out the current dispatch quantity in each fuel. Then* p_t *may be multiplied by* P_{cap} *and projected to the regulatory thresholds to get the market price* P_t *in AUD — this is the end of the algorithm.*

Table 4.3 : **Subset result**

The table shows the appropriate subset configuration U_{q*} in demand deficit scenario with end-user demand at $G_t = 31$ MW (first column) and in a normal market with $G_t = 115$ MW (second column). At $G_t = 31$ MW, all generator and load fuels are in S_I and S_L, respectively, and their dispatch quantities are all shown to be constants. The Total dispatch quantity also overshoots to 31.5 MW. At $G_t = 115$ MW, the table shows which fuels are marginal (coal G1, hydro G2 and hydro L2) and which fuels are contributing to the constant term for the demand adjustment (solar G3), and the Total dispatch quantity is exactly 115 MW. The price taker fuel (biomass G5) enjoys complete dispatch in both cases.

			$G_t = 31$ MW		$G_t = 115$ MW	
	Fuel type		Subset	Dispatch quantity	Subset	Dispatch quantity
Generator fuels						
G1	Coal	Scheduled	S_I	$c_{i,t,lower} = 30$ MW	M_I	$b^{-1}_{G,i,t}(p_t)$
G2	Hydro	Scheduled	S_I	$c_{i,t,lower} = 0$ MW	M_I	$b^{-1}_{G,i,t}(p_t)$
G3	Solar	Scheduled	S_I	$c_{i,t,lower} = 0$ MW	C_I	$c_{i,t,upper} = 7$ MW
G4	Gas	Scheduled	S_I	$c_{i,t,lower} = 0$ MW	Z_I	0 MW
G5	Biomass	Price taker	-	$c_{i,t,fixed} = 1.5$ MW	-	$c_{i,t,fixed} = 1.5$ MW
Load fuels						
L1	Battery	Scheduled	S_L	-	Z_I	0 MW
L2	Hydro	Scheduled	S_L	-	M_I	$b^{-1}_{L,l,t}(p_t)$
				Total: 31.5 MW		Total: 115 MW

Finally, Table 4.3 displays the subset solutions of the algorithm for the two different demand levels, $G_t = 31$ and $G_t = 115$, discussed in the example. For $G_t = 31$, the price is equal to $p_t = \max(\underline{b}_{G,i\in O_I,t}, \frac{P_{floor}}{P_{cap}}) = \underline{\underline{b}}_t$ in unit amounts. Whereas for $G_t = 115$, the price can be found computing $b_{(M_I,M_L)_{q*},t}(D_t + h)$ using (4.2.9).

4.2.3 Input processes

The market price formula (4.2.12) requires several input processes including the formulaic bid stack function parameter that captures strategic bidding over time, fuel-specific processes of available capacity truncation, fixed capacity input, constrained-on/off quantity process that encompasses network feasibility, and pre-adjustment demand term, which we decompose into regional consumption and export–import.

4.2.3.1 *Fuel gamma*

The formulaic fuel gamma $\mathbb{R} : \gamma_{\cdot,t} := \gamma_{\cdot,(t_{day},t_{time})}$, i.e. $\gamma_{i,t}$ for generator fuels and $\gamma_{l,t}$ for load fuels, expresses what proportion of the maximum fuel capacity is being offered at negative prices in a given fuel at time t. More precisely, $\gamma_{i,t}$ is the inflection point of the fuel bid curve (4.2.1) for generator fuel i and $(1 - \gamma_{l,t})$ is the inflection point of the formulaic load bid stack (4.2.2) for load fuel l. The fact that these are time-dependent assumes that bidding activity changes over time, i.e., the bid stack functions shift horizontally, as gamma changes over time.

For any time $t \in (t_0, T]$ in the pricing period, we can give $t = (t_{day}, t_{time})$ the day and the time can be identified precisely. Let $t_{day} \in \mathbb{N} : [1, 366]$ be the day of year, assuming leap years. Then we denote with $t_{time} \in \mathbb{N} : [1, 366\tilde{n}]$ the time of year for $\tilde{n}$ time points per day, i.e. $(t_{time} \bmod \tilde{n})$ is the time of day. For example, for $\tilde{n} = 288$, t_{time} has 5-minute increments. Further, let $\tilde{t}_{time}$ be a shifted time of day parameter

$$\tilde{t}_{time} = 10(t_{time} \bmod \tilde{n})\frac{1}{\tilde{n}} - 5.$$

Further, $\gamma_{\cdot,t} := \gamma_{\cdot,(t_{day},t_{time})}$ is a sinusoidal function that captures both yearly seasonality for the day of year t_{day} through parameters s_1, s_2, s_3, s_4 and diurnal variation for the time of day $\tilde{t}_{time}$ using $d_1, d_2, d_3, d_4, d_5, d_6$.

For a generator fuel i, we express $\gamma_{i,t} := \gamma_{i,(t_{day},\tilde{t}_{time})}$ as

$$\gamma_{i,(t_{day},\tilde{t}_{time})} = s_1 + s_2 \sin\big(\frac{t_{day} + s_3}{s_4}\big) + d_1 e^{-d_5(\tilde{t}_{time} - d_3)^2} + d_2 e^{-d_6(\tilde{t}_{time} - d_4)^2}. \tag{4.2.14}$$

For a load fuel l, we give $\gamma_{l,t} := \gamma_{l,(t_{day},\tilde{t}_{time})}$ as

$$\gamma_{l,(t_{day},\tilde{t}_{time})} = 1 - s_1 - s_2 \sin\big(\frac{t_{day} + s_3}{s_4}\big) - d_1 e^{-d_5(\tilde{t}_{time} - d_3)^2} - d_2 e^{-d_6(\tilde{t}_{time} - d_4)^2}. \tag{4.2.15}$$

Note that the gamma $\gamma_{\cdot,t}$ parameters of the fuel bid curves can take the formulaic form $\gamma_{\cdot,t} = \gamma_{\cdot,(t_{day},\tilde{t}_{time})}$ directly from (4.2.14) and (4.2.15) at time t.

An alternative to that would be estimating the initial gamma $\gamma_{\cdot,t_0}$ parameters together with the initial alpha and beta $(\alpha_{t_0}, \beta_{\cdot,t_0})$ parameters of the fuel bid curves in the least-squares method. Then, over time, updating the gamma parameter by the cyclical change $\Delta\gamma_{\cdot,(t_{day},\tilde{t}_{time})} = \gamma_{\cdot,(t_{day},\tilde{t}_{time})} - \gamma_{\cdot,(t-1_{day},\tilde{t-1}_{time})}$ in the formulaic form, while retaining its estimated level from t_0, we would have

$$\gamma_{\cdot,t} := \gamma_{\cdot,t-1} + \Delta\gamma_{\cdot,(t_{day},\tilde{t}_{time})}. \tag{4.2.16}$$

4.2.3.2 Available capacity

Available capacity truncation involves restricting $b_{\bar{G},i,t}(x)$ in (4.2.1) for generator fuel i to quantity x on to the scaled available capacity range $x \in (\frac{c_{i,t,lower}}{\bar{c}_t}, \frac{c_{i,t,upper}}{\bar{c}_t}]$ in unit amounts. Also, we let $b_{\bar{L},l,t}(x)$ in (4.2.2) for load fuel l take quantity x on the scaled available capacity range $x \in [\frac{c_{l,t,lower}}{\bar{c}_t}, \frac{c_{l,t,upper}}{\bar{c}_t})$ in unit amounts for all fuels.

From a non-stop power system point of view, the available capacity range is the range around the initial dispatch quantity at time t_n that bounds the dispatch quantity at time t_{n+1}.

A non-zero lower capacity bound $\frac{c_{\cdot,t,lower}}{\bar{c}_t}$ is necessary, whenever a fuel – that is, the individual units in a fuel collectively – is unable to shut down immediately. Regardless of the economic value of their activity, the units in this position are usually given appropriate non-zero targets in the central dispatch optimisation (AEMO (2010*b*)). In the model, we have an analogous treatment for the fuels with inflexible ramping profiles and minimum loading requirements e.g., black and brown coal, in anticipation of this problem, using non-zero lower capacity bounds and the online fuel category O_I.

In addition, different upper bounds arise as full availability up to the maximum registered capacity $c_{\cdot,t,upper} = \bar{c}_{\cdot,t}$ rarely holds in most fuels. First, given the ramp rate specifications and the length of the scheduling intervals, the units in the fuel might be too slow to ramp up to a higher, economically feasible capacity region, approaching the maximum registered fuel capacity $\bar{c}_{\cdot,t}$, at time t_n by the start of next interval at t_{n+1}. Second, the units in particular fuels are often unwilling or unable to produce at their full capacity due to external factors, such as existing ancillary commitments, planned outages, or more commonly, weather effects.

Third, there are two-way fuels that trade both sides of the market, i.e., act as generators or loads interchangeably over time. As any load unit e.g. pumped hydro or battery, would need to charge up in order to "produce" electricity, load units are usually registered in both categories and bid in both categories as well, to participate accordingly (AEMC (2021*c*)). In this sense, we refer to them as two-way fuels. Two-way fuels are actively balancing a storage level, which usually determines their remaining capacity for load uptake and generator dispatch at the same time.

Moreover, the model can capture the permanent changes in the maximum registered fuel capacity $\bar{c}_{.,t}$ of the regional fuel mix for some time ahead, e.g., at the anticipated commissioning or decommissioning of units. The available capacity truncation is then a subsequent layer of capacity reduction.

Let c_{i,t_n} be the dispatch quantity in generator fuel i and c_{l,t_n} be the dispatch quantity in load fuel l, at time t_n, in unit amounts. After we have the market price p_{t_n} at time t_n from (4.2.12), we can obtain the current dispatch quantity $c_{.,t_n}$ of a fuel by passing p_{t_n} in the inverse fuel bid stack function of the fuel $p_{t_n} \rightarrow c_{i,t_n} : b^{-1}_{G,i,t_n}(p_{t_n})$ in (4.2.4) for a generator fuel i and $p_{t_n} \rightarrow c_{l,t_n} : b^{-1}_{L,l,t_n}(p_{t_n})$ in (4.2.6) for a load fuel l. We then give the available capacity bounds $c_{i,t_{n+1},lower} < c_{i,t_n} \leq c_{i,t_{n+1},upper}$ and $c_{l,t_{n+1},lower} \leq c_{l,t_n} < c_{l,t_{n+1},upper}$ at time t_{n+1} around the dispatch level $c_{.,t_n}$ at the end of the previous time t_n interval in a fuel specific manner.

4.2.3.2.1 Base case

Let r^{up}_i, r^{down}_i denote the ramp-up and ramp-down rates in MW per 5-minutes for every generator fuel i and r^{up}_l, r^{down}_l the ramp up and ramp down rates in MW per 5-minutes for every load fuel l. Furthermore, let m denote the regional ramp rate multiplier. This multiplier makes an allowance for the distortions arising out of the fact that the unit ramp rates are aggregated at fuel level to obtain the fuel-level ramp rates instead of applying unit-level ramping directly.

Across all fuels, particularly fossil fuels, e.g., coal, gas, etc., as a base case solution we can specify the available capacity bounds in MW using these fuel-specific ramp-up and ramp-down rates as follows. Let the lower availability bound $c_{.,t_{n+1},lower}$ of fuel i or l at time t_{n+1} be the higher of the dispatch quantity in the previous period minus the ramp-down rate $c_{.,t_n} - mr^{down}_{.}$ and 0 as

$$c_{\cdot,t_{n+1},lower} = \max\left(c_{\cdot,t_n} - mr_{\cdot}^{down}, 0\right). \tag{4.2.17}$$

Let then the upper availability bound $c_{\cdot,t_{n+1},upper}$ of fuel i or l at time t_{n+1} be the lower of the dispatch quantity in the previous period plus the ramp-up rate $c_{\cdot,t_n} + mr_{\cdot}^{up}$ and full as-bid fuel capacity $\bar{c}_{\cdot,t}$

$$c_{\cdot,t_{n+1},upper} = \min\left(c_{\cdot,t_n} + mr_{\cdot}^{up}, \bar{c}_{\cdot,t}\right). \tag{4.2.18}$$

Assuming that the ramp rate specifications are time and dispatch level invariant, we write these as averages and estimate them from the historical ramp rate data for the different fuels, ensuring that the MW per minutes raw ramp rate data is interpreted correctly[118].

4.2.3.2.2 Intermittent fuels

Across renewable fuels, such as solar and wind, as an intermittent case solution, we can give the available capacity upper bounds in MW using fuel-specific available capacity forecasts. This assumes either the direct or the indirect availability of some renewable generation forecast measures via prediction models or predictive indicators. We opt for two very simple forecast processes for the upper availability bounds of solar and wind generation.

Let the lower availability bound $c_{i,t_{n+1},lower}$ of intermittent fuel i at time t_{n+1} be zero $c_{\cdot,t,lower} = 0$. This is a reasonable approximation as the ramp down rates are generally quite high and not restrictive in renewable generation.

Let the upper availability bound $c_{i,t,upper}$ of solar energy i at time t be estimated by a deterministic sinusoidal intraday generation function specified as

$$c_{solar,t,upper} = \min(\max(\sin\left(a(\tilde{\tilde{t}}_{time} + c) + e\right) + \sin\left(b(\tilde{\tilde{t}}_{time} + d) + f\right), 0), g)), \tag{4.2.19}$$

where $\tilde{\tilde{t}}_{time} = (t_{time} \bmod \tilde{n})$ is the time of day for $\tilde{n}$ observations per day. In this formula, the

[118] Multiplied by 5 for the 5-minute ramping limits.

sum of two shifted sine functions is evaluated for generation between 0 and an upper bound g.

Finally, let the upper availability bound $c_{wind,t,upper}$ of wind generation at time t be estimated by a scaled Brownian motion discretised as

$$\Delta c_{wind,t,upper} \sim \mathcal{N}(0, \sigma^2 \Delta t) \tag{4.2.20}$$

such that $c_{wind,t,upper} = \min(\max(c_{wind,t-1} + \Delta c_{wind,t,upper}, \psi \bar{c}_{wind,t}), \bar{\psi} \bar{c}_{wind,t})$ where we denote with $\Delta t = 1$ the time increment and with ψ and $\bar{\psi}$ the allowed thresholds of wind output.

4.2.3.2.3 Two-way fuels

Two-way fuels, such as hydro plants and batteries, actively balance a storage level k over time. Generator dispatch is $k\bar{c}_{i,t}$ at time t and the remaining capacity for load uptake is $(1 - k)$ times the maximum capacity in the fuel $\bar{c}_{i,t}$.

An interesting outcome of the proposed hyperbolic market bid stack method is that the implied storage level k can be inferred from the modelled dispatch solution at the end of each interval when leaving the storage level unrestricted $0 \leq k \leq 1$ at the beginning of the interval.

4.2.3.2.4 Minimum capacity criterion

Fuels that are slow to start-up often have operational capacity minima in the price settlement and scheduling process of the market operator, such as minimum load amounts. We represent this in the model for all affected generator fuel i via the lower bound criterion $c_{i,lo}$ in unit amounts, such that the available capacity lower bound $c_{i,t,lower}$ of the fuel is always at or above this criterion $c_{i,lo} \leq c_{i,t,lower}$.[119]

4.2.3.3 Net fixed generation by price takers

Apart from the basic bid types used in compulsory bidding, fixed bids are optional for both generators and loads in the NEM (AEMC (2021*c*)). In a fixed bid, the bidder opts to trade a

[119] Data for the minimum load amounts are not used in the present model implementation.

predetermined amount at the regional market price as price taker. At time t_n, we denote the fixed bid quantity in generator fuel $i \in F$ with $c_{i,t_n,fixed}$ and the fixed bid quantity in load fuel $l \in F$ $c_{l,t_n,fixed}$, both measured in MW.

We also introduce $c_{t_n,non-scheduled}$ for the net non-scheduled generation quantity in the region (in MW) at time t_n, to capture the quantity flows of the small-scale units excluded from bidding (AEMC (2021*c*)).

Then we express the fixed net generation quantity $c_{t_n,fixed}$ as

$$c_{t_n,fixed} = \sum_{i=1}^{n} c_{i,t_n,fixed} - \sum_{l=1}^{m} c_{l,t_n,fixed} + c_{t_n,non-scheduled}, \tag{4.2.21}$$

at time t_n.

The price taker quantities enter the pricing mechanism in two ways. First, the fixed net generation quantity $c_{t_n,fixed}$ (in MW) is subtracted from the end-user demand as an adjustment when we calculate the demand for the scheduled fuels to fill.

Second, if a generator fuel i or load fuel l has both a bid stack function and a non-zero fixed bid quantity at time t_n, i.e. $i \in I \cap F$ or $l \in L \cap F$ respectively, then the time t_n dispatch quantity of that fuel would have to be revised accordingly. In case of a generator fuel i that is both a scheduled and a price taker at the same time $i \in I \cap F$, the fixed bid quantity $c_{i,t_n,fixed} \neq 0$ would have to be added to the dispatch quantity c_{i,t_n} at the end of the t_n time interval for $c_{i,t_n} \leftarrow c_{i,t_n} + c_{i,t_n,fixed}$. Similarly, in such a load fuel $l \in L \cap F$ the fixed bid quantity $c_{l,t_n,fixed} \neq$ would have to be added to the dispatch quantity c_{l,t_n} for $c_{l,t_n} \leftarrow c_{l,t_n} + c_{l,t_n,fixed}$. In principle, this can impact the available capacity bounds of the particular fuel at time t_{n+1}.

4.2.3.4 Demand

The demand term D_t incorporates trade (inter-regional export–import) as follows. Let G_t represent the input process for net regional generation, $\bar{c}_t$ the maximum scheduled generation, $c_{t,fixed}$ the fixed net generation of the price taker fuels, and X_t the input process for the net constrained-on/off quantity in the price region at time t. The quantity D_t can then be computed as $D_t := \frac{G_t - c_{t,fixed} - X_t}{\bar{c}_t}$ in unit amounts, where G_t can be expressed as a deterministic func-

tion with yearly seasonality for the day of year t_{day} through parameters s_1, s_2, s_3, s_4 and diurnal variation for the time of day $\tilde{t}_{time}$ using $d_1, d_2, d_3, d_4, d_5, d_6$

$$G_t = s_1 + s_2 \sin\left(\frac{t_{day} + s_3}{s_4}\right) + d_1 e^{-d_5(\tilde{t}_{time} - d_3)^2} + d_2 e^{-d_6(\tilde{t}_{time} - d_4)^2}, \tag{4.2.22}$$

and $c_{t,fixed}$ is from (4.2.21) and X_t is introduced in Section 4.2.3.5.

4.2.3.5 Constrained-on/off quantity

In practice, price settlement is performed by an LP engine subject to thousands of security constraints. Often, the binding constraints force the dispatch of some bid quantities and prevent the dispatch of some others. These are the constrained-on and constrained-off quantities, respectively.

Let $X_{I,on,t}$ denote the constrained-on (must-run) generator quantity sum in the region. This is the quantity extent to which the generators are dispatched in the bids offered at prices above the realised market price, i.e., the generators in the region collectively receive higher targets by $X_{I,on,t}$ that what is expected on a price basis. Taking into account the effect of using these expensive bids when parsing the supply data in merit order can be achieved by reducing end-user demand by $X_{I,on,t}$. Note that this term refers to all must-run generator quantities in the system, which is broader than the ramp-rate–implied must-run quantity $\sum \frac{c_{o \in O_I,t,lower}}{\bar{c}_t}$ over all fuels in set O_I. More specifically, $X_{I,on,t} = \sum \frac{c_{o \in O_I,t,lower}}{\bar{c}_t} + X^{-}_{I,on,t}$.

Let $X_{I,off,t}$ denote the constrained-off (curtailed) generator quantity sum in the region. This is the quantity extent to which the generators are not fully dispatched in the bids offered at prices below the realised market price, i.e., the generators in the region collectively receive lower targets by $X_{I,off,t}$ that what is expected on a price basis. Skipping over these unused inexpensive bids when parsing the supply data in merit order can be achieved by incrementing end-user demand by $X_{I,off,t}$.

Let $X_{L,on,t}$ denote the constrained-on (must-run) load quantity sum in the region. This is the quantity extent to which the loads are dispatched in the bids offered at prices below the realised market price, i.e., the loads in the region collectively receive higher targets by $X_{L,on,t}$ that what is expected on a price basis. Taking into account the effect of exceedingly high targets for the

price when parsing the supply data in merit order can be achieved by incrementing end-user demand by $X_{L,on,t}$.

Let $X_{L,off,t}$ denote the constrained-off (curtailed) load quantity sum in the region. This is the quantity extent to which the loads are not fully dispatched in the bids offered at prices above the realised market price, i.e., the loads in the region collectively receive lower targets by $X_{L,off,t}$ that what is expected on a price basis. Skipping these missed expensive load bids when parsing the supply data in merit order can be achieved by reducing end-user demand by $X_{L,off,t}$.

It follows that the constrained-on/off quantity is the sum of the above introduced variables

$$X_t = X^{-}_{I,on,t} - X_{I,off,t} - X_{L,on,t} + X_{L,off,t}, \tag{4.2.23}$$

it is expressed stochastically as

$$dX_t = -\kappa X_t dt + \sigma dZ, \tag{4.2.24}$$

and it is subtracted from demand before adjustments.

4.3 Model implementation

The implementation of the proposed approach is now described. The results are from three 31-day intervals between t_0 4:00 AM 1 January 2022 and T 4:00 AM 1 February 2022, t_0 4:00 AM 1 May 2022 and T 4:00 AM 1 June 2022, and t_0 4:00 AM 1 October 2022 and T 4:00 AM 1 November 2022 for 5-minute time intervals $t \in (t_0, T]$ (8928 observations each period).

The implementation begins by obtaining the fuels on the regional fuel set U in full capacity $\bar{c}_{\cdot,t}$[120], and initialising the ramp rates $r^{up}_{\cdot}$, $r^{down}_{\cdot}$ and the fixed bid quantities $c_{\cdot,t_n,fixed}$. The hyperbolic fuel bid stack formulae are then fitted to the stacked fuel bid data to acquire the fuel bid curve parameters $\alpha_{\cdot,t_0}, \beta_{\cdot,t_0}, \gamma_{\cdot,t_0}$ at time t_0.

The time-dependent input processes are initialised for $t \in (t_0, T]$. First, strategic bidding is

[120]The bid data is truncated to the maximum availability of the units, i.e., the full registered capacity of the fuel $\bar{c}_{\cdot,t}$ is proxied by the maximum available capacity in it, as indicated by the units at the time.

Table 4.4 : **Input data**

The table shows the source of the input data together with the parametric interpretation of each field in the price algorithm.

Model parameter/variable	Source (File)	Source (Field)	Data as of	Type
$\alpha_{\cdot,t_0}, \beta_{\cdot,t_0}$ in (4.2.1-4.2.2)	AEMO (2022*i*)	PRICEBAND1-10, BANDAVAIL1-10	See Table 4.5-4.7	Fitted
$\gamma_{\cdot,t}$ in (4.2.1-4.2.2) from (4.2.14 - 4.2.16)	AEMO (2022*i*)	PRICEBAND1-10, BANDAVAIL1-10	5 working days before t_0	Fitted
$r_{\cdot}^{up}, r_{\cdot}^{down}$ in (4.2.17-4.2.18)	AEMO (2022*i*)	ROCUP, ROCDOWN	t_0 (t_{-288} in May)	Read off
m in (4.2.17-4.2.18)	-	-	-	Arbitrary
$\bar{c}_{\cdot,t}$ in (4.2.18)	AEMO (2022*i*)	MAXAVAIL, reg. cap.*	t_0 (t_{-288} in May)	Read off
$c_{solar,t,upper}$ from (4.2.19)	AEMO (2022*g*)	EnergyTarget	5 working days before t_0	Randomly generated
$c_{wind,t,upper}$ from (4.2.20)	AEMO (2022*g*)	EnergyTarget	5 working days before t_0	Randomly generated
$c_{t_n,fixed}$ from (4.2.21)	AEMO (2022*i*)	FIXEDLOAD	t_0 (t_{-288} in May)	Read off
X_t from (4.2.23)	AEMO (2022*g*)	Price, Bids, EnergyTarget	5 working days before t_0	Computed, fitted
G_t from (4.2.22)	NEOPoint (2022)	Dispatchable Gen	31 days a year earlier	Fitted

*This is calculated as the minimum of the maximum availability (MAXAVAIL in AEMO (2022*i*)) and the registered capacity (as in AEMO (2022*f*)) of all scheduled DUIDs in the fuel.

captured by altering the value of the intercept variable of every fuel bid curve $\gamma_{\cdot,t}$, i.e., by shifting the bid curves over time. Moreover, available capacity truncation is executed to restrict the fuel bid stack functions to their available capacity quantity domains defined between a lower $c_{\cdot,t,lower}$ and an upper capacity threshold $c_{\cdot,t,upper}$ each trading interval. The upper capacity bounds of the renewable fuels follow formulaic relations and ramp rates are applied around the initial dispatch quantity in other fuels to obtain both the lower and the upper bound. Furthermore, the physical feasibility of the fuels overall under the binding network constraints is also time-dependent. This enters the model via the constrained-on/off variable X_t, which adjusts demand over time. Then, demand given as generation G_t is also updated using the applicable time-dependent formulae.

The fuel set allocation and price calculation are performed as in Example 4.2, noting that because the wind availability $c_{wind,t,upper}$ and the constrained-on/off variable X_t are stochastic, one must also iterate the model a number of times for every time point. The current implementation takes 25 iterations before averaging those for the model result.

4.3.1 Data source

A source summary of the data used to estimate the input process (4.2.14 - 4.2.22) parameters is shown in Table 4.4.

4.3.2 Fuel summary

All plants present within the Bidmove Complete file (AEMO (2022*i*)) with a DUID at time t_0[121] are mapped to fuel types using the market operator's mapping in AEMO (2022*f*) to retrieve the regional fuel sets. Each fuel type with a non-zero full bid capacity $\bar{c}_{\cdot,t}$ is included[122] as shown in Table 4.5–4.7.

[121] Or at time t_{-288} in case of the May sample where the last day of the previous month falls on a weekend.

[122] In addition, if only the zero maximum availability of a load fuel prevents it from being included then that load fuel is included in 20 MW full capacity.

Table 4.5 : **Regional fuel sets – January 2022**

The table shows the scheduled fuel set of each of the five NEM regions for January.

Fuel			Full bid capacity	Ramp speed, multiplier			Fixed bids	Fitting date, range
			$\bar{c}_{\cdot,t}$	$r_{\cdot}^{up}$	$r_{\cdot}^{down}$	m	$c_{\cdot,t,fixed}$	
NSW								
G1	Black coal	Slow-start	6340 MW	0.05	0.05	4	-	t_{-144}, [$0,$500]
G2	Gravity hydro	Quick-start	2553 MW	0.80	0.80	4	65 MW	t_{-144}, full range
G3	Natural gas	Quick-start	1085 MW	0.62	0.62	4	-	t_{-144}, full range
G4	Pumped hydro	Two-way	160 MW	-	-	-	-	t_{-144}, full range
G5	Battery	Two-way	49 MW	-	-	-	-	t_{-144}, full range
L1	Battery	Two-way	46 MW	-	-	-	-	t_{-144}, full range
G6	Solar	Intermittent	2382 MW	-	-	-	-	t_{-144}, full range
G7	Wind	Intermittent	2237 MW	-	-	-	-	t_{-144}, full range
QLD								
G1	Black coal	Slow-start	6472 MW	0.07	0.07	4	-	t_{-144}, [$0,$500]
G2	Coal seam gas	Quick-start	1034 MW	0.30	0.30	4	-	t_{-144}, [$0,$500]
G3	Kerosene	Quick-start	395 MW	0.41	0.41	4	-	t_{-144}, full range
G4	Natural gas	Quick-start	697 MW	0.53	0.53	4	-	t_{-144}, full range
G5	Run of hydro	Quick-start	154 MW	0.91	0.91	4	-	t_{-144}, [$0,$500]
G6	Pumped hydro	Two-way	570 MW	-	-	-	-	t_{-144}, full range
G7	Solar	Intermittent	1692 MW	-	-	-	-	t_{-144}, full range
G8	Wind	Intermittent	509 MW	-	-	-	-	t_{-144}, full range
VIC								
G1	Brown coal	Slow-start	3825 MW	0.07	0.07	4	-	t_{-144}, [$0,$500]
G2	Gravity hydro	Quick-start	2165 MW	0.62	0.62	4	-	t_{-144}, [$0,$500]
G3	Natural gas	Quick-start	1758 MW	0.48	0.48	4	-	t_{-144}, full range
G4	Battery	Two-way	33 MW	-	-	-	-	t_{-144}, full range
L1	Battery	Two-way	80 MW	-	-	-	-	t_{-144}, full range
G5	Solar	Intermittent	973 MW	-	-	-	-	t_{-144}, full range
G6	Wind	Intermittent	3271 MW	-	-	-	-	t_{-144}, full range
SA								
G1	Diesel oil	Quick-start	253 MW	1.44	1.44	1	-	t_{-144}, [$0,$500]
G2	Natural gas	Quick-start	1029 MW	1.05	1.05	1	-	t_{-144}, [$0,$500]
G3	Oil products	Quick-start	553 MW	0.32	0.32	1	-	t_{-144}, [$0,$500]
G4	Battery	Two-way	135 MW	-	-	-	-	t_{-144}, full range
L1	Battery	Two-way	112 MW	-	-	-	-	t_{-144}, full range
G5	Solar	Intermittent	365 MW	-	-	-	-	t_{-144}, full range
G6	Wind	Intermittent	1923 MW	-	-	-	-	t_{-144}, full range
TAS								
G1	Gravity hydro	Quick-start	2008 MW	1.13	1.13	1	-	t_{-144}, [$0,$500]
G2	Natural gas	Quick-start	30 MW	5.50	5.50	1	-	t_{-144}, full range
G3	Wind	Intermittent	422 MW	-	-	-	-	t_{-144}, full range

Table 4.6 : **Regional fuel sets – May 2022**

The table shows the scheduled fuel set of each of the five NEM regions for May.

Fuel			Full bid capacity	Ramp speed, multiplier			Fixed bids	Fitting date, range
			$\bar{c}_{\cdot,t}$	$r_{\cdot}^{up}$	$r_{\cdot}^{down}$	m	$c_{\cdot,t,fixed}$	
NSW								
G1	Black coal	Slow-start	5360 MW	0.05	0.05	4	-	t_{-432}, [$0,$500]
G2	Gravity hydro	Quick-start	2454 MW	0.82	0.82	4	49 MW	t_{-432}, [$0,$500]
G3	Natural gas	Quick-start	1099 MW	0.61	0.61	4	-	t_{-432}, full range
L1	Pumped hydro	Two-way	160 MW	-	-	-	-	t_{-288}, full range
G4	Battery	Two-way	49 MW	-	-	-	-	t_{-432}, full range
L2	Battery	Two-way	46 MW	-	-	-	-	t_{-432}, full range
G5	Solar	Intermittent	2502 MW	-	-	-	-	t_{-432}, full range
G6	Wind	Intermittent	2225 MW	-	-	-	-	t_{-432}, full range
QLD								
G1	Black coal	Slow-start	5823 MW	0.07	0.07	4	-	t_{-432}, [$0,$500]
G2	Coal seam gas	Quick-start	870 MW	0.36	0.36	4	-	t_{-432}, [$0,$500]
G3	Kerosene	Quick-start	396 MW	0.40	0.40	4	-	t_{-432}, full range
G4	Natural gas	Quick-start	719 MW	0.51	0.51	4	-	t_{-432}, full range
G5	Run of hydro	Quick-start	132 MW	1.06	1.06	4	-	t_{-432}, full range
G6	Pumped hydro	Two-way	285 MW	-	-	-	-	t_{-432}, full range
L1	Pumped hydro	Two-way	244 MW	-	-	-	-	t_{-288}, full range
G7	Solar	Intermittent	1739 MW	-	-	-	-	t_{-432}, full range
G8	Wind	Intermittent	549 MW	-	-	-	-	t_{-432}, full range
VIC								
G1	Brown coal	Slow-start	3058 MW	0.08	0.08	4	-	t_{-432}, [$0,$500]
G2	Gravity hydro	Quick-start	1584 MW	0.85	0.85	4	-	t_{-432}, [$0,$500]
G3	Natural gas	Quick-start	1813 MW	0.47	0.47	4	-	t_{-432}, full range
G4	Battery	Two-way	240 MW	-	-	-	-	t_{-432}, full range
L1	Battery	Two-way	268 MW	-	-	-	-	t_{-432}, full range
G5	Solar	Intermittent	1001 MW	-	-	-	-	t_{-432}, full range
G6	Wind	Intermittent	2874 MW	-	-	-	-	t_{-432}, full range
SA								
G1	Diesel oil	Quick-start	269 MW	1.36	1.36	1	-	t_{-432}, full range
G2	Natural gas	Quick-start	773 MW	0.97	0.97	1	-	t_{-432}, full range
G3	Oil products	Quick-start	537 MW	0.33	0.33	1	-	t_{-432}, full range
G4	Battery	Two-way	98 MW	-	-	-	-	t_{-432}, full range
L1	Battery	Two-way	112 MW	-	-	-	-	t_{-432}, full range
G5	Solar	Intermittent	381 MW	-	-	-	-	t_{-432}, full range
G6	Wind	Intermittent	2152 MW	-	-	-	-	t_{-432}, full range
TAS								
G1	Gravity hydro	Quick-start	2044 MW	1.02	1.02	1	-	t_{-432}, [$0,$500]
G2	Natural gas	Quick-start	92 MW	1.79	1.79	1	-	t_{-432}, [$0,$500]
L1	Battery	Two-way	16 MW	-	-	-	-	t_{-432}, full range
G3	Wind	Intermittent	422 MW	-	-	-	-	t_{-432}, full range

Table 4.7 : **Regional fuel sets – October 2022**

The table shows the scheduled fuel set of each of the five NEM regions for October.

Fuel			Full bid capacity	Ramp speed, multiplier			Fixed bids	Fitting date, range
			$\bar{c}_{.,t}$	$r_{.}^{up}$	$r_{.}^{down}$	m	$c_{.,t,fixed}$	
NSW								
G1	Black coal	Slow-start	6365 MW	0.04	0.04	4	-	t_{-144}, [$0,$500]
G2	Gravity hydro	Quick-start	2449 MW	0.82	0.82	4	58 MW	t_{-144}, [$0,$500]
G3	Natural gas	Quick-start	712 MW	0.94	0.94	4	-	t_{-144}, full range
G4	Pumped hydro	Two-way	240 MW	-	-	-	-	t_{-144}, full range
L1	Pumped hydro	Two-way	20 MW	-	-	-	-	t_{-144}, full range
G5	Battery	Two-way	50 MW	-	-	-	-	t_{-144}, full range
L2	Battery	Two-way	51 MW	-	-	-	-	t_{-144}, full range
G6	Solar	Intermittent	2617 MW	-	-	-	-	t_{-144}, full range
G7	Wind	Intermittent	2221 MW	-	-	-	-	t_{-144}, full range
QLD								
G1	Black coal	Slow-start	5858 MW	0.07	0.07	4	-	t_{-144}, [$0,$500]
G2	Coal seam gas	Quick-start	712 MW	0.44	0.44	4	-	t_{-144}, full range
G3	Kerosene	Quick-start	276 MW	0.58	0.58	4	-	t_{0}, full range
G4	Natural gas	Quick-start	702 MW	0.52	0.52	4	-	t_{-144}, full range
G5	Run of hydro	Quick-start	132 MW	1.06	1.06	4	-	t_{-144}, full range
G6	Pumped hydro	Two-way	524 MW	-	-	-	-	t_{-144}, full range
G7	Battery	Two-way	20 MW	-	-	-	-	t_{-144}, full range
L1	Battery	Two-way	75 MW	-	-	-	-	t_{-144}, full range
G8	Solar	Intermittent	2294 MW	-	-	-	-	t_{-144}, full range
G9	Wind	Intermittent	661 MW	-	-	-	-	t_{-144}, full range
VIC								
G1	Brown coal	Slow-start	3615 MW	0.07	0.07	4	-	t_{-144}, [$0,$500]
G2	Gravity hydro	Quick-start	1792 MW	0.75	0.75	4	-	t_{-144}, [$0,$500]
G3	Natural gas	Quick-start	1204 MW	0.70	0.70	4	-	t_{-144}, full range
G4	Battery	Two-way	295 MW	-	-	-	-	t_{-144}, full range
L1	Battery	Two-way	285 MW	-	-	-	-	t_{-144}, full range
G5	Solar	Intermittent	1015 MW	-	-	-	-	t_{-144}, full range
G6	Wind	Intermittent	3124 MW	-	-	-	-	t_{-144}, full range
SA								
G1	Diesel oil	Quick-start	204 MW	1.18	1.18	1	-	t_{-144}, full range
G2	Natural gas	Quick-start	822 MW	0.91	0.91	1	-	t_{-144}, full range
G3	Oil products	Quick-start	40 MW	3.75	3.75	1	-	t_{-144}, full range
G4	Battery	Two-way	117 MW	-	-	-	-	t_{-144}, full range
L1	Battery	Two-way	130 MW	-	-	-	-	t_{-144}, full range
G5	Solar	Intermittent	386 MW	-	-	-	-	t_{-144}, full range
G6	Wind	Intermittent	2294 MW	-	-	-	-	t_{-144}, full range
TAS								
G1	Gravity hydro	Quick-start	2044 MW	1.08	1.08	1	-	t_{-144}, [$0,$500]
G2	Natural gas	Quick-start	148 MW	1.11	1.11	1	-	t_{-144}, full range
G3	Wind	Intermittent	422 MW	-	-	-	-	t_{-144}, full range

4.3.3 Fuel bid curves

The fuel bid stack functions are then fitted to the bid data as of t_{-144} or t_0 (or t_{-432} or t_{-288} as for the May sample where the last day of the previous month falls on a weekend) as shown in the last column of Table 4.5-4.7.[123] First, the parameters $(\alpha_{t_0}, \beta_{i,t_0}, \gamma_{i,t_0})$ and $(-\alpha_{t_0}, \beta_{l,t_0}, \gamma_{l,t_0})$ are estimated using a squared error cost function with a number of tweaks.[124] The fitted function is projected to the regulatory maximum and minimum price levels when it would otherwise exceed those. Also, underestimation is penalised five times as much as overestimation.[125] Furthermore, only an arbitrarily chosen price interval of the bid data is fitted, usually the mid-range prices, as also shown in the last column of Table 4.5–4.7.[126] Finally, to have the same α_{t_0} in all fuels in a region a helper function is used to calculate what value of α_{t_0} minimises the fitting error in all fuels at time t_0 when fitting the bid data. Then, $(\beta_{i,t_0}, \gamma_{i,t_0})$ and $(\beta_{l,t_0}, \gamma_{l,t_0})$ are estimated keeping $|\alpha_{t_0}|$ fixed. Table 4.8 (left side) shows the parameter results.

[123] Note that $\alpha_{t_{-144}} = \alpha_{t_0}, \beta_{i,t_{-144}} = \beta_{i,t_0}$ and we detail the approach for $\gamma_{i,t_{-144}} \neq \gamma_{i,t_0}$ in Section 4.3.4.

[124] The data is scaled before fitting, i.e., the prices are divided by the regulatory price cap at $\$15,000$ and the MW amounts by $44,000$ MW, which is an approximation of the full bid capacity sum of every generation fuel in the NEM.

[125] Note that because prices exceeding the market price thresholds are projected to these thresholds, in cases with sparse data, the fit is prone to default to a near-vertical line (fixed at a given quantity, defaulting to values at the two thresholds). Penalising underestimation more than overestimation effectively counters this. In addition, the accuracy of the fit is more relevant at the lower end of the merit order, since it is evaluated at higher levels of demand as well, whereas the high end of the merit order is only factored into prices at high levels of demand.

[126] More precisely, the slow-start and quick start fuels are sought to be fitted on the [$0,$500] price range only. However, if there is fewer than two bid points within that range then the fuel is fitted on the full price range instead.

Table 4.8 : **Fuel bid curve parameters**

The table shows the fuel bid stack function parameters ($\alpha_{t_0}, \beta_{\cdot,t_0}, \gamma_{\cdot,t_0}$) given a regional $|\alpha_{t_0}|$ in a NEM-wide breakdown.

	January			**May**			**October**		
	α_{t_0}	$\beta_{\cdot,t_0}$	$\gamma_{\cdot,t_0}$	α_{t_0}	$\beta_{\cdot,t_0}$	$\gamma_{\cdot,t_0}$	α_{t_0}	$\beta_{\cdot,t_0}$	$\gamma_{\cdot,t_0}$
NSW									
NSWBlack coalGENERATOR	1.99999	0.1	0.08379	0.35548	0.92	0.07641	1.09017	0.22	0.08624
NSWNatural gasGENERATOR	1.99999	159.79	0.0068	0.35548	1.44	-0.00553	1.09017	244.67	0.00125
NSWPumped hydroGENERATOR	1.99999	333.12	-0.00127	0.35548	19.86	-0.08223	1.09017	981.21	-0.00003
NSWPumped hydroLOAD	—	—	—	0.35548	2367.99	0.00371	-1.09017	0.02	1
NSWSolarGENERATOR	1.99999	1851.45	0.05241	0.35548	1497.17	0.05159	1.09017	2285.51	0.05873
NSWWindGENERATOR	1.99999	185.48	0.04655	0.35548	434.47	0.04547	1.09017	1090.43	0.04805
NSWGravity hydroGENERATOR	1.99999	18.66	0.00239	0.35548	1.55	-0.01212	1.09017	0.33	-0.04448
NSWBatteryGENERATOR	1.99999	476.4	-0.00003	0.35548	2136.83	-0.00004	1.09017	570.82	-0.00026
NSWBatteryLOAD	-1.99999	0	1	0.35548	0.16	0.98906	-1.09017	1915.19	0.24422
QLD									
QLDBlack coalGENERATOR	0.614	0.9	0.10642	0.54915	1.48	0.09741	1.73724	0.48	0.09323
QLDCoal seam gasGENERATOR	0.614	8.42	0.00036	0.54915	5.73	-0.00122	1.73724	1679.01	0.00745
QLDNatural gasGENERATOR	0.614	285.07	0.01253	0.54915	787.26	0.01101	1.73724	201.29	0.00711
QLDRun of hydroGENERATOR	0.614	17.09	-0.00003	0.54915	983.36	0.00163	1.73724	4358.63	0.00215
QLDSolarGENERATOR	0.614	1875.17	0.03681	0.54915	3827.84	0.03899	1.73724	405.74	0.04834
QLDKeroseneGENERATOR	0.614	12.41	-0.0884	0.54915	130.63	-0.00104	1.73724	9.07	-0.05116
QLDPumped hydroGENERATOR	0.614	189.77	0.00631	0.54915	321.04	0.00343	1.73724	151.03	-0.0003
QLDPumped hydroLOAD	—	—	—	0.54915	1915.19	0.24422	—	—	—
QLDWindGENERATOR	0.614	181.07	0.00463	0.54915	194.75	0.00520	1.73724	1736.17	0.0138
QLDBatteryGENERATOR	—	—	—	—	—	—	1.73724	2300.41	-0.0002
QLDBatteryLOAD	—	—	—	—	—	—	-1.73724	1915.19	0.24422
VIC									
VICBatteryGENERATOR	0.37907	2032.06	-0.00004	1.30902	341.47	0.00357	0.38197	421.3	0.00209
VICBatteryLOAD	-0.37907	5.26	0.03187	1.30902	12.59	0.01019	-0.38197	0.05	1
VICBrown coalGENERATOR	0.37907	0.09	0.07338	1.30902	0.44	0.05840	0.38197	1.08	0.06282
VICNatural gasGENERATOR	0.37907	682.82	0.01303	1.30902	0.30	-0.00715	0.38197	8.67	-0.19373
VICSolarGENERATOR	0.37907	1775.27	0.01987	1.30902	482.08	0.02075	0.38197	752.42	0.02082
VICWindGENERATOR	0.37907	1039.12	0.06728	1.30902	441.68	0.05243	0.38197	364.33	0.06292
VICGravity hydroGENERATOR	0.37907	1.33	0.00041	1.30902	2.73	0.00090	0.38197	4.22	-0.00066
SA									
SABatteryGENERATOR	0.32016	550.24	-0.00023	0.21425	779.41	0.00019	3.29586	95.13	-0.00017
SABatteryLOAD	-0.32016	0.13	1	0.21425	0.22	1.00000	-3.29586	0.01	-1
SADiesel oilGENERATOR	0.32016	8.29	-0.0072	0.21425	8.05	-0.01433	3.29586	266.18	-0.00035
SANatural gasGENERATOR	0.32016	6.13	0.01037	0.21425	23.68	0.00489	3.29586	81.33	0.00391
SAOil productsGENERATOR	0.32016	17.42	0.00426	0.21425	306.95	0.00261	3.29586	88.88	0.00081
SAWindGENERATOR	0.32016	823.46	0.03962	0.21425	387.09	0.04007	3.29586	208.4	0.05053
SASolarGENERATOR	0.32016	5428.98	0.00787	0.21425	9997.15	0.00843	3.29586	1852.37	0.00855
TAS									
TASNatural gasGENERATOR	5.377e-07	6176.97	-0.00188	1.32753	865.44	0.00188	18.66066	90.66	0.00276
TASWindGENERATOR	5.377e-07	2690.81	0.00397	1.32753	205.33	0.00624	18.66066	169.04	0.00623
TASGravity hydroGENERATOR	5.377e-07	169.49	-0.0254	1.32753	0.58	0.00571	18.66066	0.09	0.00849
TASBatteryLOAD	—	—	—	1.32753	0.01	-0.99899	—	—	—

4.3.4 Strategic bidding

It is assumed that some fuels bid following a particular dynamic bidding strategy rather than bidding the same strategy (bid curve) all the time, i.e., some bid curves are not time-constant. This strategy involves a reallocation of all quantities onto more (less) expensive prices along the bid curve that is achieved by shifting the fuel bid stack to the left (right) along the quantity axis. The shift is achieved by changing the value of the fuel bid curve intercept $\gamma_{\cdot,t}$.

In this implementation we take the $\gamma_{i,t_{-144}}$ value from the parameter estimation via least squares fitting and apply an initial update of $+(\gamma_{\cdot,(t_{0_{day}},t_{0_{time}})} - \gamma_{\cdot,(t_{-144_{day}},t_{-144_{time}})})$ to reflect the time differential and obtain γ_{i,t_0}. After that the value of the intercept changes according to formula (4.2.16).[127]

By fitting the formulae (4.2.14) and (4.2.15) for (4.2.16), some proportion of the full bid capacity of the particular fuel $\bar{c}_{\cdot,t}$ is returned (on $[0,1]$) for $\gamma_{\cdot,t}$. This value is then multiplied by $\bar{c}_{\cdot,t}$ and divided by $44,000$ MW, the approximate full bid capacity sum of every generation fuel in the NEM, to recover $\gamma_{\cdot,t}$ on the correct scale. The parameters of the fit are shown in Table 4.9–4.11.

[127] Note, however, that the intra-year seasonality of gamma is ignored as the fitting interval is only 5-days long.

Table 4.9 : **Gamma $\gamma_{\cdot,t}$ formula inputs – January 2022**

The table shows the inputs of the intra-day gamma variation formulae (4.2.14)–(4.2.16) that capture the intercept of the fuel bid curves for all fuels in the NEM.

Fuel	s_1	d_1	d_2	d_3	d_4	d_5	$-d_6$	R^2
NSW								
NSWBlack coalGENERATOR	0.70	0.18	-0.13	-0.84	-0.86	0.05	-4.84	0.17
NSWNatural gasGENERATOR	0.19	-0.19	-0.10	0.29	-1.85	0.15	-1.64	0.49
NSWPumped hydroGENERATOR	-	-	-	-	-	-	-	-
NSWSolarGENERATOR	-	-	-	-	-	-	-	-
NSWWindGENERATOR	-	-	-	-	-	-	-	-
NSWGravity hydroGENERATOR	0.01	0.10	0.13	3.76	2.37	0.37	-6.00	0.27
NSWBatteryGENERATOR	-	-	-	-	-	-	-	-
NSWBatteryLOAD	-	-	-	-	-	-	-	-
QLD								
QLDBlack coalGENERATOR	0.89	0.02	0.02	-0.78	2.81	0.38	-1.44	0.28
QLDCoal seam gasGENERATOR	-	-	-	-	-	-	-	-
QLDNatural gasGENERATOR	0.36	-0.34	-0.29	-1.00	-3.86	0.17	-0.98	0.68
QLDRun of hydroGENERATOR	0.01	0.44	0.30	2.55	1.48	2.47	-6.00	0.27
QLDSolarGENERATOR	-	-	-	-	-	-	-	-
QLDKeroseneGENERATOR	-	-	-	-	-	-	-	-
QLDPumped hydroGENERATOR	-	-	-	-	-	-	-	-
QLDWindGENERATOR	0.35	-0.43	0.43	-3.40	-3.41	3.00	-3.10	0.16
VIC								
VICBatteryGENERATOR	-	-	-	-	-	-	-	-
VICBatteryLOAD	0.01	0.39	0.42	0.71	-0.29	3.00	-3.49	0.35
VICBrown coalGENERATOR	0.76	1.04	-1.11	-2.20	-2.06	0.14	-0.13	0.38
VICNatural gasGENERATOR	0.00	-1.27	1.33	2.95	2.95	1.24	-1.16	0.24
VICSolarGENERATOR	1.00	-0.10	-0.04	0.88	-1.77	0.24	-4.24	0.51
VICWindGENERATOR	-	-	-	-	-	-	-	-
VICGravity hydroGENERATOR	0.04	0.07	-0.05	3.25	0.91	1.14	-0.02	0.24
SA								
SABatteryGENERATOR	0.00	0.01	-0.01	0.09	-1.06	0.46	-4.73	0.01
SABatteryLOAD	0.02	0.52	-0.39	-0.56	-0.32	1.19	-6.00	0.16
SADiesel oilGENERATOR	0.00	0.06	-0.05	0.90	0.97	2.47	-3.99	0.32
SANatural gasGENERATOR	0.22	0.08	-0.20	2.77	-1.31	0.28	-0.24	0.21
SAOil productsGENERATOR	0.00	0.35	0.23	1.01	3.00	1.20	-0.92	0.26
SAWindGENERATOR	-0.20	1.20	-0.03	3.82	2.19	0.00	-5.81	0.13
SASolarGENERATOR	-	-	-	-	-	-	-	-
TAS								
TASNatural gasGENERATOR	-	-	-	-	-	-	-	-
TASWindGENERATOR	0.66	0.00	-0.01	0.90	1.19	1.92	-5.23	0.01
TASGravity hydroGENERATOR	0.58	-0.20	-0.09	0.91	-1.12	1.49	-0.43	0.20

Table 4.10 : **Gamma $\gamma_{\cdot,t}$ formula inputs – May 2022**

The table shows the inputs of the intra-day gamma variation formulae (4.2.14)–(4.2.16) that capture the intercept of the fuel bid curves for all fuels in the NEM.

Fuel	s_1	d_1	d_2	d_3	d_4	d_5	$-d_6$	R^2
NSW								
NSWBlack coalGENERATOR	0.7	-0.06	0.09	-1.38	-3.93	0.9	-1.26	0.23
NSWNatural gasGENERATOR	0.04	0.21	0.42	-4	2.49	1.46	-1.3	0.19
NSWPumped hydroGENERATOR	-	-	-	-	-	-	-	-
NSWPumped hydroLOAD	-	-	-	-	-	-	-	-
NSWSolarGENERATOR	-0.86	0	1.83	-2.6	2.42	0.95	0	0.08
NSWWindGENERATOR	0.99	-0.09	-0.02	4	-2.61	0	-3.53	0.13
NSWGravity hydroGENERATOR	-0.24	-1.93	2.21	-2.16	-2.65	0.04	-0.02	0.12
NSWBatteryGENERATOR	-	-	-	-	-	-	-	-
NSWBatteryLOAD	0.02	0.23	0.2	-0.34	-4	2.37	-0.63	0.12
QLD								
QLDBlack coalGENERATOR	0.76	0.13	-0.16	-2.67	-2.32	0.11	-0.74	0.32
QLDCoal seam gasGENERATOR	-	-	-	-	-	-	-	-
QLDNatural gasGENERATOR	0.51	-0.31	-0.25	-1.98	0.72	0.32	-5.1	0.21
QLDRun of hydroGENERATOR	-0.95	0.03	1.51	-1.49	2.35	1.24	0	0.02
QLDSolarGENERATOR	0.92	-0.03	-0.02	2.76	-2.51	0.07	-1.31	0.12
QLDKeroseneGENERATOR	-0.29	-1.75	2.08	-2.23	-2.81	0.04	-0.02	0.13
QLDPumped hydroGENERATOR	-	-	-	-	-	-	-	-
QLDWindGENERATOR	0.32	0.15	-0.11	-4	-2.81	0.34	-2.22	0.16
QLDBatteryGENERATOR	-	-	-	-	-	-	-	-
QLDBatteryLOAD	-	-	-	-	-	-	-	-
VIC								
VICBatteryGENERATOR	0	0.23	-0.14	-4	-2.87	0.42	-2.36	0.16
VICBatteryLOAD	-	-	-	-	-	-	-	-
VICBrown coalGENERATOR	-0.14	0.86	0.08	0.16	-3.93	0	-2.19	0.14
VICNatural gasGENERATOR	0.3	0.27	0	2.33	0.31	0.52	0.19	0.12
VICSolarGENERATOR	-0.84	0.01	1.75	-4	0.79	1.6	0	0.17
VICWindGENERATOR	-0.98	-0.01	1.85	1.73	1.22	2.07	0	0.12
VICGravity hydroGENERATOR	1	-1.03	0.29	1.26	2.62	0.01	-1.74	0.13
SA								
SABatteryGENERATOR	0.5	-1.51	1.03	1.57	1.6	0.04	-0.06	0.14
SABatteryLOAD	1	-0.99	-0.11	1.66	-2.31	0.01	-1.56	0.11
SADiesel oilGENERATOR	1	-1.01	-0.12	2.39	-2.31	0.01	-0.81	0.15
SANatural gasGENERATOR	-	-	-	-	-	-	-	-
SAOil productsGENERATOR	1.00	-0.88	-0.18	1.50	-2.90	0.00	-4.14	0.05
SAWindGENERATOR	0.88	0.12	-0.12	-1.89	-2.10	0.11	-0.23	0.11
SASolarGENERATOR	-0.96	1.94	-0.10	-2.13	0.13	0.00	-6.00	0.16
TAS								
TASNatural gasGENERATOR	-	-	-	-	-	-	-	-
TASWindGENERATOR	0.65	-0.01	0.08	-2.06	-4.00	0.22	-0.94	0.14
TASGravity hydroGENERATOR	0.17	0.15	-0.16	-4.00	-2.85	0.45	-2.63	0.10
TASBatteryLOAD	-	-	-	-	-	-	-	-

Table 4.11 : **Gamma $\gamma_{\cdot,t}$ formula inputs – October 2022**

The table shows the inputs of the intra-day gamma variation formulae (4.2.14)–(4.2.16) that capture the intercept of the fuel bid curves for all fuels in the NEM.

Fuel	s_1	d_1	d_2	d_3	d_4	d_5	$-d_6$	R^2
NSW								
NSWBlack coalGENERATOR	-0.65	1.28	0.10	0.21	2.26	0.00	-0.71	0.31
NSWNatural gasGENERATOR	0.54	-0.55	0.05	-0.73	2.60	0.01	-4.61	0.36
NSWPumped hydroGENERATOR	-	-	-	-	-	-	-	-
NSWPumped hydroLOAD	-	-	-	-	-	-	-	-
NSWSolarGENERATOR	-	-	-	-	-	-	-	-
NSWWindGENERATOR	-	-	-	-	-	-	-	-
NSWGravity hydroGENERATOR	0.07	0.04	0.06	-3.92	0.06	1.04	-0.27	0.37
NSWBatteryGENERATOR	0.00	-0.17	0.31	2.62	2.62	3.00	-6.00	0.24
NSWBatteryLOAD	0.00	0.02	0.09	-0.83	-0.09	1.88	-6.00	0.09
QLD								
QLDBlack coalGENERATOR	0.73	-0.04	-0.05	0.49	-1.00	1.64	-1.86	0.36
QLDCoal seam gasGENERATOR	0.00	0.14	0.27	4.00	2.84	0.44	-1.94	0.61
QLDNatural gasGENERATOR	0.40	-0.37	-0.30	-2.83	0.56	0.15	-1.33	0.42
QLDRun of hydroGENERATOR	0.68	-0.79	-0.75	-4.00	-0.15	0.71	-0.52	0.74
QLDSolarGENERATOR	-	-	-	-	-	-	-	-
QLDKeroseneGENERATOR	-	-	-	-	-	-	-	-
QLDPumped hydroGENERATOR	-	-	-	-	-	-	-	-
QLDWindGENERATOR	0.93	-1.27	1.08	-0.42	-0.44	1.05	-0.97	0.47
VIC								
VICBatteryGENERATOR	0.00	0.00	0.00	0.41	1.74	2.47	-5.20	0.04
VICBatteryLOAD	0.00	0.17	0.18	0.19	-3.55	1.06	-2.04	0.21
VICBrown coalGENERATOR	0.77	0.06	0.06	0.72	-0.56	0.64	-2.93	0.11
VICNatural gasGENERATOR	0.01	2.25	-2.06	2.30	2.19	0.43	-0.45	0.65
VICSolarGENERATOR	-	-	-	-	-	-	-	-
VICWindGENERATOR	-	-	-	-	-	-	-	-
VICGravity hydroGENERATOR	-0.35	-0.30	0.99	1.88	0.17	0.74	-0.02	0.20
SA								
SABatteryGENERATOR	-0.72	-1.62	2.34	-3.17	-3.81	0.00	0.00	0.02
SABatteryLOAD	0.01	0.07	0.09	-3.23	1.04	2.60	-0.89	0.12
SADiesel oilGENERATOR	0.00	0.04	0.03	1.00	-0.62	3.00	-6.00	0.25
SANatural gasGENERATOR	0.20	-3.00	2.79	1.02	1.13	0.25	-0.20	0.62
SAOil productsGENERATOR	-	-	-	-	-	-	-	-
SAWindGENERATOR	-	-	-	-	-	-	-	-
SASolarGENERATOR	-	-	-	-	-	-	-	-
TAS								
TASNatural gasGENERATOR	0.25	-0.21	0.13	-3.04	-0.01	0.34	-1.03	0.14
TASWindGENERATOR	0.65	-0.01	0.01	1.43	1.62	2.02	-5.26	0.01
TASGravity hydroGENERATOR	0.49	0.04	-0.07	-0.24	2.93	0.32	-0.54	0.32

4.3.5 Fuel availability updates

4.3.5.1 Ramp rates

Restrictive ramp rates apply to slow-start and quick-start fuels to determine their lower and upper capacity bounds around the starting dispatch level in the trade interval. For example, a ramp rate of 0.05 in the case of black coal in NSW signifies a MW amount equal to 5% of the full bid capacity of the fuel $\bar{c}_{\cdot,t}$. These are shown in Table 4.5-4.7, where we see that the ramp rates of the slow-start fuels are typically much lower, and therefore more restrictive than those of the quick-start fuels.

4.3.5.2 Renewable fuels

By contrast, only the upper availability bounds are calculated for renewable fuels as their lower bounds are kept at nil. Table 4.12 shows the parameter estimation for the upper threshold of solar generation $c_{solar,t,upper}$ in (4.2.19).[128] The function parameters are not very dissimilar for the fuels across time periods, except for the value of g which is somewhat lower in May for NSW and QLD.

[128]The generation data is divided by 2300 MW in all five regions before fitting for a more tractable scale.

Table 4.12 : **Solar availability formula inputs**

The table shows the solar generation upper bound quantity (4.2.19) inputs of the relevant NEM regions.

Jan 2022							
Region	a	b	c	d	e	f	g
NSW	0.0000	0.0150	-1.0000	-0.9920	0.0000	-0.5818	0.8
QLD	-0.0007	0.0152	-0.5354	-0.3525	-0.1253	-0.5746	0.5
VIC	-3.18e-04	1.78e-02	1.16e-01	-5.36e-01	-4.73e-02	-8.92e-01	0.2
SA	-0.0020	0.0119	-0.0184	0.1870	-0.2785	-0.1330	0.1

May 2022							
Region	a	b	c	d	e	f	g
NSW	-1.35e-05	1.55e-02	1.81e-01	-9.57e-01	-1.95e-01	-2.49e-01	0.5
QLD	-0.0008	0.0152	-0.2712	-0.1369	-0.1450	-0.5905	0.35
VIC	-4.10e-04	1.86e-02	4.36e-01	-4.02e-01	-6.09e-02	-8.61e-01	0.15
SA	-0.0021	0.0058	0.4605	-0.3066	-0.2906	-0.1429	0.1

Oct 2022							
Region	a	b	c	d	e	f	g
NSW	-5.00e-04	1.55e-02	-9.99e-01	-9.99e-01	-4.36e-06	-9.99e-01	0.75
QLD	-4.67e-04	1.53e-02	-3.19e-01	-9.49e-02	-3.55e-06	-4.58e-21	0.6
VIC	-3.76e-04	1.83e-02	3.15e-01	-4.53e-01	-5.57e-02	-8.73e-01	0.2
SA	-0.0020	0.0119	-0.2359	0.0365	-0.2785	-0.1078	0.125

Next, Table 4.13 shows the parameter estimation for the upper threshold of wind generation $c_{wind,t,upper}$ in (4.2.20). While the σ parameters are relatively close regardless of the fitting period, the $\bar{\psi}$ and the ψ thresholds are maintained at the exact same level in all of them.

Table 4.13 : **Wind availability formula inputs**

The table shows the wind generation upper bound quantity (4.2.20) inputs of the five NEM regions.

	Jan 2022			May 2022			Oct 2022		
Region	σ	$\bar{\psi}$	ψ	σ	$\bar{\psi}$	ψ	σ	$\bar{\psi}$	ψ
NSW	18.205	0.6	0.2	14.964	0.6	0.2	20.404	0.6	0.2
QLD	11.288	0.6	0.2	11.466	0.6	0.2	13.872	0.6	0.2
VIC	42.212	0.6	0.2	25.255	0.6	0.2	30.155	0.6	0.2
SA	21.921	0.4	0.2	25.077	0.4	0.2	21.354	0.4	0.2
TAS	6.162	0.6	0.2	7.687	0.6	0.2	6.027	0.6	0.2

4.3.6 Demand process

The modelled price paths P_t are considered under a generation-based process for demand $D_t = \frac{G_t - c_{t,fixed} - X_t}{\bar{c}_t}$. This requires the Ornstein-Uhlenbeck process for the feasibility adjustment X_t, and the deterministic formulae with intra-week and intra-day variation for generation G_t as inputs.

4.3.6.1 Feasibility adjustment

The constrained-on/off quantity X_t in (4.2.24) constitutes the feasibility adjustment in the model. It is computed as the sum of the unused low-price (constrained-off) and the used high-price (constrained-on) bid quantities. The path of this process can be drawn from a distribution with mean zero and variance $\frac{\sigma^2}{2\kappa}(1 - e^{-2\kappa t})$, where the values of the drift and diffusion coefficients κ and σ are estimated from the data. Table 4.14 shows these values for the three sample intervals.

Table 4.14 : **Constrained-on/off X_t formula inputs**

The table shows the inputs of the constrained-on/off quantity X_t in (4.2.24) over the three periods for the five NEM regions.

	Jan 2022		May 2022		Oct 2022	
Region	κ	σ	κ	σ	κ	σ
NSW	0.1	4.60	0.1	5.68	0.1	7.11
QLD	0.1	5.25	0.1	5.43	0.1	5.30
VIC	0.25	9.84	0.25	3.02	0.25	3.17
SA	0.1	1.20	0.1	0.65	0.1	0.79
TAS	0.25	4.68	0.25	3.80	0.25	7.00

As in Table 4.14, the κ values are stable for all regions, but there is some slight variation in the σ values.

4.3.6.2 Deterministic component

The formulae for generation G_t is given by the sinusoidal function (4.2.22) that captures both weekly and diurnal variation. This is fitted to the data to recover the function parameters as in Table 4.15. The quantity data is divided by 7000 MW in all five regions before fitting for a more tractable scale. Note the variation in the fitted generation function parameters between the different data windows.

Table 4.15 : **Generation G_t formula inputs**

The table shows the inputs of the generation quantity G_t in (4.2.22) over the three periods for the five NEM regions.

Jan 2022

Fuel	s_1	s_2	s_3	s_4	d_1	d_2	d_3	d_4	d_5	$-d_6$	R^2
NSW	0.83	-0.06	0.64	1.10	0.48	-0.25	1.65	0.76	0.13	-0.43	0.53
QLD	0.88	-0.03	0.56	1.14	0.26	0.00	2.62	0.87	0.24	1.43	0.75
VIC	0.74	-0.02	1.46	1.19	0.15	-0.01	2.81	1.09	0.53	-0.91	0.26
SA	0.14	-0.01	1.02	1.04	0.06	0.00	3.02	0.78	0.56	1.05	0.22
TAS	0.09	0.00	1.01	1.14	0.05	0.00	3.01	0.78	0.68	1.05	0.22

May 2022

Fuel	s_1	s_2	s_3	s_4	d_1	d_2	d_3	d_4	d_5	$-d_6$	R^2
NSW	0.90	-0.05	-10.78	1.16	0.61	-0.54	1.28	0.77	0.12	-0.43	0.56
QLD	0.84	0.03	-2.39	1.13	0.24	0.00	2.88	0.82	0.59	1.27	0.55
VIC	0.72	0.04	-2.43	1.13	0.19	0.00	2.90	0.91	0.83	1.02	0.42
SA	0.16	-0.01	1.01	1.28	0.09	0.00	3.02	0.78	0.97	1.05	0.32
TAS	0.16	-0.02	1.01	1.27	0.10	0.00	2.94	0.78	0.59	1.05	0.37

Oct 2022

Fuel	s_1	s_2	s_3	s_4	d_1	d_2	d_3	d_4	d_5	$-d_6$	R^2
NSW	0.82	-0.06	-27.91	1.15	0.57	-0.57	1.30	0.65	0.15	-0.31	0.59
QLD	0.80	0.03	1.49	1.17	0.25	0.00	2.82	0.85	0.47	1.38	0.69
VIC	0.67	0.03	-13.05	1.11	0.16	-0.11	3.00	0.34	1.08	-0.58	0.57
SA	0.14	-0.02	1.01	1.27	0.02	0.00	3.18	0.78	1.01	1.05	0.09
TAS	0.16	0.01	1.01	1.27	0.08	0.00	3.18	0.78	0.88	1.05	0.24

4.4 Model results

The model result analysis starts with the hyperbolic map before turning to assess the full model.

4.4.1 An assessment of the hyperbolic map

The hyperbolic map is dynamic in that it captures the changes in the strategic bidding activity, fuel availability and fuel feasibility at every 5-minutes interval for $t \in (t_0, T]$. These features unequivocally improve the model's performance, although their execution is susceptible to slight inaccuracies.

First, strategic bidding is modelled with diurnal variation only. This presumes that the units of the fuels allocate their MW quantities mostly on the same price domain during the day[129] but that they are shifting their quantities onto the next more (less) expensive price points every 5-minutes as the day progresses. More precisely, the bid curves slide to the right (left) due to strategic bidding in a pattern that repeats every day in the same way. Nevertheless, this is a rather restrictive way of bidding, and the actual bidding profiles are somewhat more changeable in the NEM in comparison.[130] Therefore, the model is prone to errors when the fuels shift their quantities more or less aggressively than anticipated. This is indicated by the imperfect R^2 scores for the fit of the dynamic intercept $\gamma_{i,t}$ in Tables 4.9-4.11.

Second, regarding the fuel availability features, the fact that their focus is inherently fuel-specific also poses some problems. Amassing the available quantities in the different units within a fuel for fuel-level availability sometimes misrepresents what unit bids correspond to the available fuel quantities, for example, when the ramp rate–based availability truncation deems extremely priced bids unavailable before deeming those priced closer to the current price level so. The lowest-price quantities are then erroneously filled first in merit order even if those were not in fact available, for example, because the high ramp rates correspond to higher priced quantities falsely tagged unavailable in the model or due to locational differences in generation in the case of renewables, which are physical factors independent from the merit order principle.

[129] It is a market requirement that they use the same ten price buckets over the same trading day as observed in AEMO (2022*i*).

[130] The modelled shifts are more regular and restrictive than what actual strategic bidding might look like, which is currently the main limitation of the proposed model.

If one such misrepresented fuel receives higher targets at falsely deemed-available lower prices than it would have received in real life, then another fuel is receiving lower targets than it would have in the actual, real-life run. Then, a sharp increase in price may occur if the other low-target fuel subsequently cannot ramp up to – that is, its fuel curve is cut off too low to be able to ramp up to – a higher target in the next round, and a remaining quantity has to be filled by the next, considerably more expensive fuel in merit order. This erroneous mid-price spike effect could be mitigated using ramp rate multipliers.

Third, related to the previous argument, negative spikes also arise when a slow-start fuel receives relatively low targets and it operates at its lower capacity bound as a must-run fuel. In this case, the remaining flexible demand sets the price, but because this demand is lower than it would have been in the absence of the lower bound, the price is also lower, causing the negative spikes. This effect is, too, mitigated by the ramp rate multiplier $m > 1$.

Furthermore, there is an overlap between the constrained-on and must-run quantities. The former are forced on due to physical constraints disallowing their disuse, whereas the latter must stay online due to the supply side availability truncation. However, the constrained-on/off data ultimately also encapsulates the must-run quantity data. The unavailable sum can be removed by running the map a few times at different levels of demand and computing the average $\sum \frac{c_{o \in O_I, t, lower}}{\bar{c}_t}$, but this has been omitted from the current implementation. The possible consequences of such double counting include a suppressed price level and an increased proportion of fuels in subset O_I, as the constrained-on/off variable is overestimated.

4.4.2 An assessment of the full model

The main difference between the transformation map and the full model is that the map is agnostic to the way demand is defined. Indeed, a keystone assumption of the proposed approach is that modelling regional net generation might be a more appropriate input for the price map than modelling regional consumption. That is because net generation (net of storage load) assimilates trade between the regions, after which the post-trade price level can be determined from the market bid stack function at that quantity level, which is congruent with the trade assumption. In practice, too, the marginal quantity being priced is understood to be the post-trade quantity.

Therefore, the generation-based formulation takes the post-trade quantity as the demand to be fed into the transformation map to obtain the modelled price. Fitting the generation data for the process G_t gives back the historical quantity of export–import over time. This estimation is error-prone to the extent the historical generation quantities, on which G_t is based, might deviate from the current ones, and to the extent of the general imprecision of the fit.

4.4.3 Evaluation metric

The distributional fit by the model is evaluated using the Wasserstein metric, which represents the similarity between the actual and modelled price distribution in that it measures the 'work' required to transform one into the other. This 'distance to model' is then benchmarked against the distributional variation in the actual price data measured as the Wasserstein distances between the three different samples pairwise. Based on the comparison of the distributional inaccuracy of the model with the magnitude of the ex ante uncertainty in the actual price data, if the distance to model is approximately the same or less than the distances between the empirical distributions, then representing the electricity price risk using the model is reasonably accurate – that is, the distributional fit by the model is adequate. The rationale for this is that the model distribution is no further (in the Wasserstein sense) from the empirical distribution than the empirical distributions themselves vary over time. Table 4.16 shows these results.

Table 4.16 : **Wasserstein distances**

The table shows the Wasserstein distances between the actual price series (first column) and between the modelled price averages of 25 iterations and the actual price series.

	Actual prices			Modelled prices		
Region	January–May	May–October	January–October	January	May	October
NSW	243.6	169.4	81.6	**153.5**	**115.0**	**92.4**
QLD	211.3	194.0	79.7	**132.7**	**183.4**	571.7
VIC	189.7	135.5	68.9	**56.4**	**122.9**	**80.1**
SA	223.8	219.4	74.7	251.5	913.6	1089.6
TAS	154.1	104.9	71.6	**59.0**	**41.4**	231.9

Figure 4.1 : **Modelled paths: A full-range view**

The figure shows the path-wise differences for the complete price range between the average of the simulated 5-minute prices (red) with α_{t_0} and the sample (black) of the five NEM regions for the three sample periods: January, May and October (left to right).

-

NSW: 153.5, 115.0, 92.4

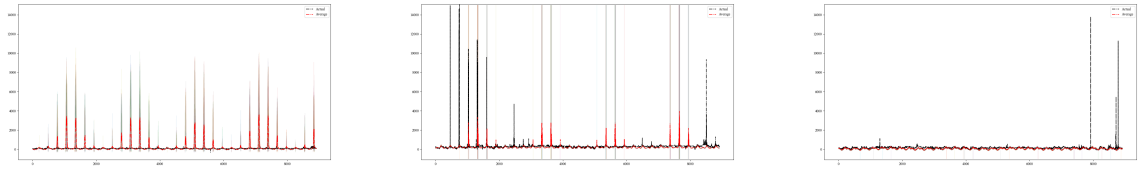

QLD: 132.7, 183.4 , 571.7

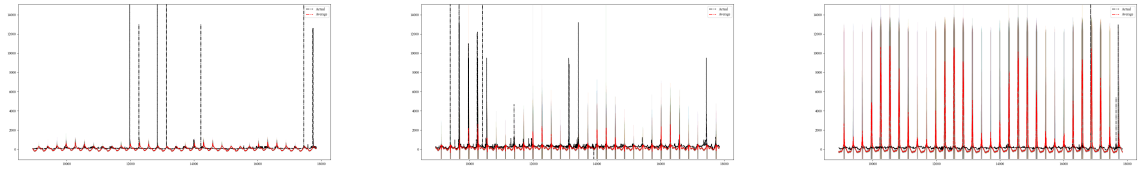

VIC: 56.4, 122.9, 80.1

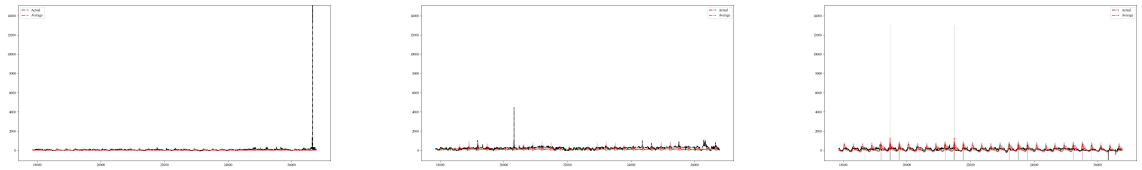

SA: 251.5, 913.6, 1089.6

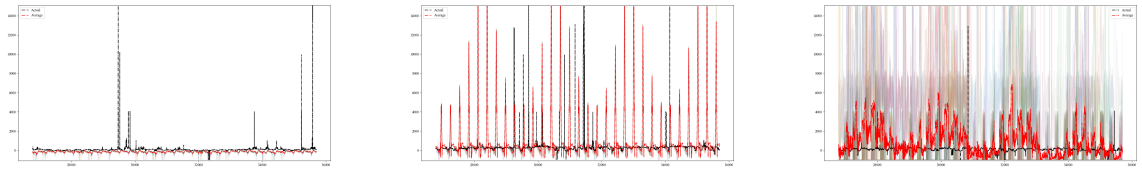

TAS: 59.0, 41.4, 231.9

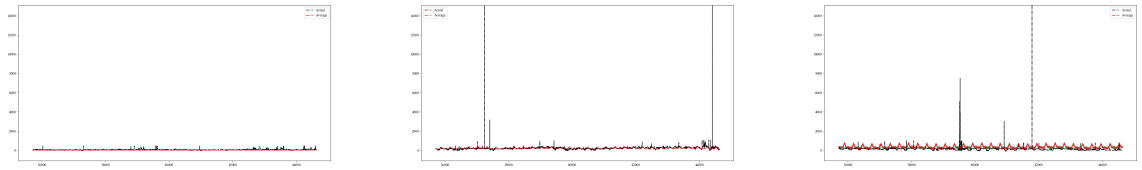

4.4.4 Results

In each of the five modelled NEM price regions the price path obtained using the generation-based demand measure can, to some degree, be characterised to display the required empirical properties, including price negativity and price spikes. Figure 4.1 shows the full view of the average price path result (between the regulatory price thresholds), whereas Figure 4.2 displays the distributional accuracy of the average results over the mid-range prices only. In addition,

we refer to the overall distributional distance to model via the numerical values in Table 4.16.

The NSW region has a relatively good mid-range fit and correct diurnal patterns most of the time. However, the modelled price series (red) over-delivers on mid-range price spikes in January, as these spikes are too frequent, which also drives a higher Wasserstein metric in May than in January. In contrast, the modelled prices for October do not exhibit any spikes, contrary to the fact that the sample does have a couple of large spikes. In terms of price negativity, the average results omit negative prices, which is problematic in October, but the individual iterations allow for them.

The modelled prices (red) in QLD are, to a lesser extent, also reasonably close to the actual price path (black) distributionally. The Wasserstein distance is below the benchmark for January and May. During these months, the main issue is an over-emphasis on near-nil prices, which can be traced back to inadequate bid curve shifts. Nevertheless, the intra-day pattern is largely correct. Regarding the large spikes present in the actual price sample, the model does not emulate them in January, but does in May and October, although with a slight overemphasis in October, which drives the high distance to model in that period. Price negativity is rare and the model sufficiently replicates this aspect of the price.

With the best Wasserstein metrics amongst the regions, the modelled price paths (red) in VIC reflect the actual price distribution (black) reasonably well, although issues remain around suppressed price volatility in the modelled sample in January and May.

The fit is overall not good in SA, with ballooned Wasserstein metrics in May and October, due to excessive volatility in the modelled paths (red) – that is with the exception of January, when the modelled price path is more limited owing to the [$0,$500] fit of the bid curves of multiple quick fuels. However, in this instance, the actual spikes (black) are not captured at all.

The modelled price paths (red) for TAS struggle to maintain the correct price levels (black) in January and October, as seen in the mid-range distributions. However, because price spikes are infrequent and the model does not produce them at all, the Wasserstein distance to model remains moderate. Furthermore, the diurnal patterns are mostly correct.

Figure 4.2 : **Distributional results: A mid-range view**

The figure shows the mid-range distributional differences between -$1000 and $1000 of the average of the simulated 5-minute prices (red) and the sample prices (black) for the three sample periods: January, May and October (left to right).

NSW: 153.5, 115.0, 92.4

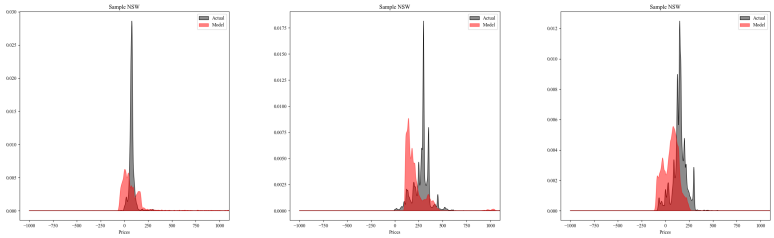

QLD: 132.7, 183.4 , 571.7

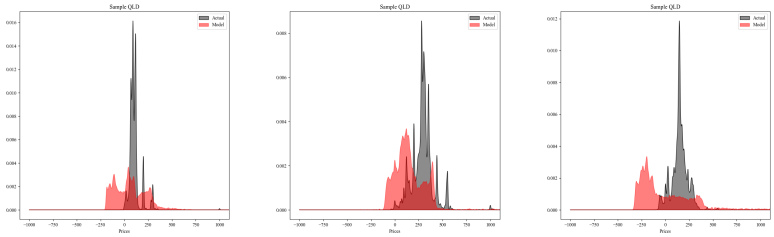

VIC: 56.4, 122.9, 80.1

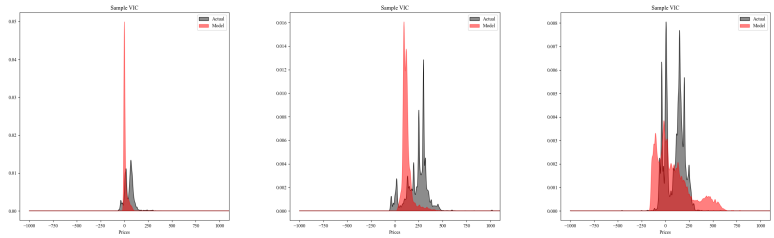

SA: 251.5, 913.6, 1089.6

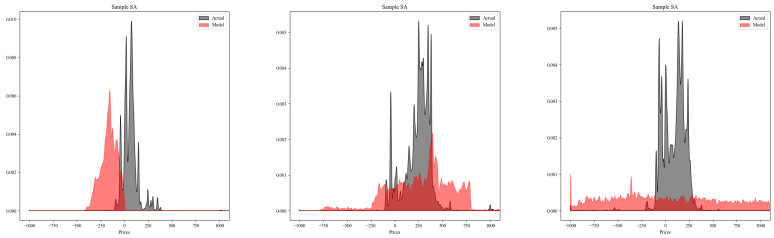

TAS: 59.0, 41.4, 231.9

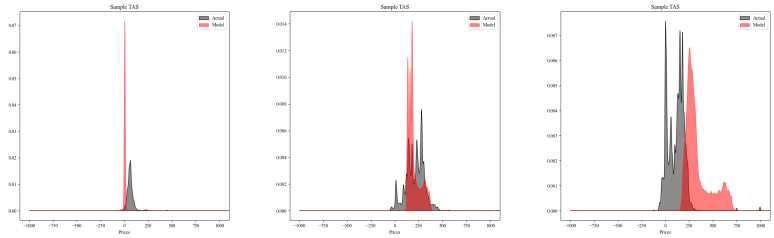

4.5 Conclusion

This chapter proposes a novel parametric price model retaining the mathematical core of the model by Carmona et al. (2013) with overlapping and dynamic merit order properties. Our approach has primarily been developed to match the features of the multi-regional Australian NEM for improved accuracy over existing electricity price models. The already high and increasing renewable fuel penetration, the ongoing storage fuel expansion, the price effects of binding network constraints, multi-regional trade, fuel availability, the negative price floor and disorderly bidding are all part of the proposed price hypothesis.

Accounting for these power market characteristics in a parametric setup, the model transforms demand after adjustments into a stochastic price process that allows for negativity and extreme values, i.e. price spikes. Capturing negative electricity prices in a structural manner is the key contribution of this chapter to the electricity price modelling literature.

A multi-regional implementation study using the Wasserstein metric is used for model evaluation. This assessment shows that the proposed framework is sufficiently accurate in its distributional fit for most regions in the NEM. The SA region is an exception, however, as the model hypothesis fails to capture active strategic bidding by renewable and gas units in SA. This underpins our finding that bidding behaviour is just as important for modelling price formation as correctly capturing the bid aggregation mechanism.

Finally, in terms of limitations, it is important to emphasise that the effects of ancillary service co-optimisation and network losses are noises to the proposed model and more generally, to most semi-structural (bid stack) model hypotheses as well.

Chapter 5

Supply function non-monotonicity and welfare under different market designs

5.1 Introduction

The equilibrium argument central to economic theory posits that price is determined at the intersection of demand and supply (Parkin and Bade (2016)). Demand is often considered perfectly price inelastic in electricity markets. Supply in price is typically assumed to be monotonically increasing in that marginal costs increase along the supply curve as quantity increases. Monotonicity of supply in price is an assumption that is so standard throughout economic theory that it is almost axiomatic. This chapter questions the validity of this assumption for electricity markets.

The bid aggregation mechanics assumed for bid stack–type modelling in Chapter 4 retrieve the supply curve presuming that the price is set by a single marginal bid and ignoring ancillary service co-optimisation and network losses. However, the recovery of price formation using data from a central dispatch engine solution in Chapter 3 reveals that serving the marginal unit of demand sometimes involves multiple marginal bids and omitted market design factors. Therefore, a more exhaustive bid aggregation method is preferred for constructing the supply curve for closer analysis.

The objective of the present study is to validate the violation of supply monotonicity. Monotonicity is examined across three major market designs, the Pennsylvania-New Jersey-Maryland Interconnection (PJM) in the United States, the Balancing Market (BM) in Great Britain and the NEM in Australia. Therefore, the assumed mechanics of bid aggregation closely follow market clearing. In integrated pool markets, this involves deciphering the engineering models used for dispatch and pricing. Exchange trading as well as physical balancing are regarded jointly in exchange-based settings. The three focus markets span both paradigms and many different aspects of market design. Their implied supply curves are recovered by formulating

these multi-stage processes in mathematical detail based on the available information.[131]

Table 5.1 : **Specifications in the real-time electricity supply curve**

The table shows various aspects of the focus markets that determine the assumptions for recovering their supply curves. Many of these are specific to certain markets. Consequently, the supply curves retain a large degree of dependency on differences in market design.

Market design feature			Supply function representation
BM	**PJM**	**NEM**	
Day-ahead and intra-day exchanges	Day-ahead settlement	–	The real-time supply curves make some assumptions about these sub-markets.
Balancing bids and offers	Multi-part bids	Price–quantity pairs	Bid language is often different from just using marginal price-quantity pairs.
Bid convexification, bid shading	-	Bid 'convexification', disorderly bidding	Bidding behaviours are present.
Emissions Trading Scheme (ETS)	Carbon pricing	Large-scale generation certificates (LGCs)	Green certificates trading may also influence bidding behaviour.
Pay-as-bid balancing	Uniform prices	Uniform prices	Prices are not always uniform. The supply curve cannot be obtained under the pay-as-bid rules of the BM.
Balancing costs	Uplift payments	Directions payments	Out-of-market payments are a social cost to welfare, but not part of the supply curve.
Self-dispatch	Central dispatch	Self-scheduling	The baseline approach to scheduling most volumes in the market.
Unit commitment changes as part of balancing override self-dispatch	Unit commitment being updated throughout the day-ahead period	Real-time unit commitment for fast-start plants only	The way unit commitment (on/off decision) is integrated in the dispatch solution plays a role in how non-monotonicities appear.
–	Integer relaxation for fast-start plants	–	Marginal cost may correspond to costs by constrained-on units.
Day-ahead solution: last MW sets the price	Solver: next MW sets the price	Solver: last MW sets the price	This determines the marginal cost calculation in edge cases.
–	Congestion is priced	Trade-offs on the demand constraint's LHS due to binding constraints	Congestion and constraint trade-offs influence prices along the constructed supply curve.
Load-dependent constraints	Load-dependent constraints	Load-dependent constraints	These depend on demand at the end of the previous dispatch interval, which is fixed for all levels of demand and does not impact the supply curve in one-shot pricing.
Frequency balancing service providers can also provide energy	Frequency balancing is co-optimised with energy	Frequency balancing is co-optimised with energy	Frequency balancing may have an indirect capacity withdrawal impact or a direct energy price impact depending on the level of co-integration.
Static interconnector losses	Static interconnector losses	Dynamic interconnector losses	Dynamic interconnector losses imply load-dependent costs, which may lead to non-monotonicities in the supply curve.
National	Nodal	Regional	Supply curve resolution is different.

Table 5.1 summarises the features influencing the set of assumptions used to recover electricity supply curves in real-time markets across the three market designs. First, real-time markets are commonly complemented by so-called sub-markets for energy, such as day-ahead and intra-day markets. These are usually material enough to affect the construction of the real-time supply curve. Second, the bid language and usual bidding behaviours are non-identical, which also impact the constructed supply curves. In addition, prices are not always uniform

[131] See, for example, Gorman et al. (2022), Elexon (2020), PJM (2022*a*) and many more academic resources and industry publications referenced within the text.

due to pay-as-bid pricing or due to out-of-market payments, although the latter are typically not reflected in the supply curves.[132] Indeed, the baseline approach to dispatching most volumes in the market can be as different as self-dispatch across exchanges and bilaterally, central dispatch following algorithmically assigned targets, or self-scheduling akin to central dispatch but placing the responsibility of compliance onto the units more fully. Therefore, the way unit commitment – and in some cases its relaxation – occurs is also vastly different. In addition, solver settings can vary between those using the last MW and those using the next MW of energy as marginal amounts, which affects the construction of edge cases along the supply curve. Moreover, sometimes congestion and constraint trade-offs are reflected in the prices along the supply curve depending on the exact market design. However, because we consider one-shot pricing[133] load-dependent constraints have no effect along the supply curves. Nevertheless, the co-optimisation of energy and frequency balancing services as well as a dynamic calculation of interconnector losses can have important price effects. Last, the scope of the supply curve is different – national, regional or nodal – under the three different market designs.

In this chapter, a small-scale case study is presented that approximates dispatch and pricing algorithmically by emulating market clearing in the three focus markets as closely as possible while keeping the physical and cost assumptions identical within the comparative setting. Supply curves are obtained by running the multi-stage market algorithms that take demand as input and yield price as output for a range of demand levels. The welfare results are displayed in a breakdown that separately presents consumer surplus, producer surplus and social surplus. Centrally optimised market models such as the PJM and NEM outperform the market clearing process in Great Britain on self-dispatch principles in terms of consumer surplus. However, the BM in Great Britain leads in producer surplus. Surprisingly, the social surplus outcomes are relatively similar across the three market designs albeit with a clear primacy of the PJM market design.

As mentioned in Hogan and Ring (2003); Bjørndal and Jörnsten (2008); Ruiz et al. (2012);

[132] The use of discretionary pricing including out-of-market payments and the presence of day-ahead markets as part of the market design cast doubt on the applicability of the economic equilibrium argument. This is because a single real-time supply function cannot embody these market features. Although in most cases it is still possible to discern a real-time supply curve but it is key to take the broader dispatch and pricing process into consideration too to evaluate welfare.

[133] We consider pricing in a single trade interval and not in multiple consecutive intervals in this article.

Gribik et al. (2007); Byers and Hug (2023), fixed costs as part of multi-part bidding and minimum loading requirements cause non-monotonicity of supply. This study shows new evidence that dynamic interconnector losses and ancillary service co-optimisation may result in non-monotonicity. These findings have important implications for incentive compatibility within particular market designs as well as for market modelling on equilibrium principles.

The market design lessons drawn from this analysis concern small, practical details. The fact that prices drop due to constrained-on units coming online with a sufficiently high minimum loading level appears to be a case when producers should perhaps either receive a make-whole compensation in the NEM or be able to trade at prices that reflect the bid-in cost by the constrained-on unit. Fast-start integer relaxation was introduced to a similar effect in the PJM. In the PJM, however, it is not clear when the last unit commitment run takes place and whether it incorporates the latest information from the bidders. Bidding until gate closure 5 minutes ahead of the trade interval might be good practice to learn from the NEM to allow the most recent cost information to be factored in. Last, for the BM, the units make conspicuously excessive bids and offers as part of bid shading, which might require a data-driven investigation into how bid shading works in reality as perhaps part of firmer regulatory oversight.

The remainder of this chapter is organised as follows. Section 5.2 describes the simplified mathematical formulations of dispatch and price optimisation under three different real-world market designs. Section 5.3 discusses supply function non-monotonicities in the literature due to indivisibilities in energy and provides new evidence concerning dynamic interconnector losses. Section 5.4 presents a case study that compares supply non-monotonicity and welfare under different market designs using the simplified mathematical formulations. Section 5.6 concludes the chapter.

5.2 Algorithms for price and welfare

5.2.1 Generic formulation

We first express the dispatch optimisation in a somewhat market design–neutral form loosely based on LMP and fixed configuration pricing (FCP) principles described in Wood et al. (2013), Biggar and Hesamzadeh (2014) and Byers and Hug (2023). There is no day-ahead or intra-day market or a separate unit commitment run in this formulation. Moreover, the resulting real-time

nodal prices are all uniform.

The notation can be set up as follows. Let $i \in N_j$ be a generator unit where N_j denotes the set of generators located at node $j \in J$. We assume that there is a single generator at every node such that $|N_j| = 1$; therefore $i = j$ for all j.

Let $w_i \in \{0, 1\}$ denote the online/offline status (i.e. on-off state) of unit i. Let Q_i^S denote the quantities supplied by generator unit i, and let Q_j^B denote the quantities bought at node j, which we take to be constant values based on the inelastic demand assumption. In particular, $\sum_{j=1}^{|J|} Q_j^B = D$, where D denotes demand. We assume no two-way fuels (storage fuels) in this formulation. Then, every generator i has capacity limits $0 \leq Q_i^S \leq w_i \bar{Q}_i^S$ and minimum loading $w_i \underline{Q}_i^S \leq Q_i^S$.

Moreover, let Z_j be the net injection at node j. In other words, Z_j is the difference of all quantities sold $\sum_{i \in N_j} w_i Q_i^S$ by online generators minus all quantities bought Q_j^B at node j, assuming sufficient reactive power as

$$Z_j = \sum_{i \in N_j} w_i Q_i^S - Q_j^B. \tag{5.2.1}$$

Let F_l denote the power flow over the unidirectional link $l \in U$, and let K_l be the physical limit of the power flow over link l such that $F_l \leq K_l$. Then, the power flow F_l is a linear function of net injections Z_j as $F_l = \sum^{\forall j} H_{lj} Z_j$, where H_{lj} is an element of the size $U \times J$ matrix of power transfer distribution factors $\mathbf{H}$. We consider $\mathbf{Z}$ as the net injection vector of size $J \times 1$, and $\mathbf{K}$ as the physical limit vector of size $U \times 1$, from which $\mathbf{HZ} \leq \mathbf{K}$ or $\forall l \in U, \sum^{\forall j} H_{lj} Z_j \leq K_l$.

Let losses be denoted by $L(\mathbf{Z})$ as a function of all net injections on the grid. Our present formulation assumes $L(\mathbf{Z}) = 0$.

Let the cost function be

$$C_i(Q_i^S, w_i) = \sum_{d=1}^{D_i} c_{i,d} x_{i,d} | \sum_{d=1}^{D_i} x_{i,d} = w_i Q_i^S, \tag{5.2.2}$$

where D_i denotes the number of bid slots used by unit i in its bidding.

More succinctly, the optimisation reads as

$$\min_{\forall i Q_i^S, w_i} \sum^{\forall i} C_i(Q_i^S, w_i) \tag{5.2.3}$$

subject to the demand balance constraint

$$\sum_{j=1}^{|J|} -Z_j + L(\mathbf{Z}) = 0 (\leftrightarrow \lambda), \tag{5.2.4}$$

network constraints

$$\sum_{j=1}^{|J|} H_{lj} Z_j - K_l \leq 0 (\leftrightarrow \mu_l), \tag{5.2.5}$$

plant capacity constraints

$$Q_i^S - w_i \bar{Q}_i^S \leq 0 (\leftrightarrow \beta_i), \tag{5.2.6}$$

and minimum loading requirements

$$w_i \underline{Q}_i^S - Q_i^S \leq 0 (\leftrightarrow \gamma_i), \tag{5.2.7}$$

with the duals in round brackets.

However, due to unit commitment in the formulation, namely that $w_i \in \{0, 1\}$ for all $i \in N$, the full dispatch algorithm reads as follows:

1. Solve an MIP for (5.2.3) given (5.2.4)-(5.2.7) to find w_i^* in $w_i^* \in \{0, 1\}$.
2. Solve an LP for (5.2.3) given (5.2.4)-(5.2.7) fixing $w_i = w_i^*$ to find Q_i^{S*} for all i.

The pricing formula can then be obtained for the LP by forming the Lagrange function as

$$\mathcal{L} = \sum_{i=1}^{N} C_i(Q_i^{S*}, w_i^*) + \lambda\big(\sum_{j=1}^{|J|} -Z_j + L(\mathbf{Z})\big) + \sum_{l=1}^{|U|} \mu_l \big(\sum_{j=1}^{|J|} H_{lj} Z_j - K_l\big) + \beta_i(Q_i^S - w_i^* \bar{Q}_i^S) + \gamma_i(w_i^* \underline{Q}_i^S - Q_i^S) \tag{5.2.8}$$

and by applying the four KKT conditions as in Wood et al. (2013). The first condition can be stated as (recall that $i = j$)

$$\frac{\partial \mathcal{L}}{\partial Q_i^S} = C_i'(Q_i^{S*}, w_i^*) - \lambda + \sum_{l=1}^{|U|} \mu_l (H_{lj} Z_j) + \beta_i + \gamma_i = 0,$$

noting that $L(\mathbf{Z}) = 0$. The second and third conditions ensure that the equality and inequality constraints hold. Then, the fourth condition states that for the inequality constraints, the dual is greater than or equal to zero, and the inequality constraint acts as an equality constraint. More specifically, $\mu_l \geq 0$ and $\mu_l(\sum_{j=1}^{|J|} H_{lj} Z_j - K_l) = 0$ for all l. This forces $\mu_l = 0$ if the constraint is not binding, i.e., if $\sum_{j=1}^{|J|} H_{lj} Z_j - K_l > 0$. The same applies for β_i and γ_i.

Thus, assuming that generator i at node j is operating neither at minimum loading nor at maximum output but that a network constraint binds over link $l = 1$, we can express the price at node P_j as the marginal cost of unit i at the optimum

$$P_j = C_i'(Q_i^{S*}, w_i^*) = \lambda - \sum_{l=1}^{|U|} \mu_1 \Big(\sum_{j=1}^{|J|} H_{1j} Z_j \Big), \tag{5.2.9}$$

that is, as a function of marginal values of different constraints, which is a well-known result for LMP (see, for example, Wood et al. (2013)).

5.2.2 PJM in the United States

In the PJM, wholesale scheduling takes place through a centrally orchestrated day-ahead market and the Reliability Assessment and Commitment (RAC) process bridging day-ahead and real-time dispatch, whereas real-time dispatch uses multi-part bids and fast-start integer relaxation (PJM (2023); Hui et al. (2009)). Assuming that the mathematical details of day-ahead settlement and RAC put forward in FERC (2012) are still up-to-date, we note that unit commitment is performed in a constrained formulation. This is relevant to the emergence of supply non-monotonicities due to minimum loading in the absence of full integer relaxation. Furthermore, the multi-part bid format includes marginal cost, start-up cost, and no-load cost bids, as well as operational information. According to PJM (2021), no-load cost bids refer to the hourly costs of generating units to output zero MW energy. Under fast-start integer relaxation, the start-up and no-load costs of fast-start units are incorporated into their marginal bid prices as

well (PJM (2018)). For the real-time electricity supply curve, we interpret that this supply curve is composed of the adjusted marginal prices for fast-start units and the unadjusted marginal cost bids for all other units at every level of demand above the sum of all day-ahead volumes.

The real-time PJM solver is assumed to reference the marginal cost bid of the incremental unit of load approximated by the next 1 MW of load, which should mostly be served by units that are already online (EPRI (2019)). Note, however, that referencing of the marginal cost bid is not yet reflective of the marginal congestion and the marginal loss components of real-time prices in the spirit of LMP, as per Ott (2003). For simplicity, we assume that these price components have a dollar value of zero. Moreover, discretionary uplift is being paid under certain conditions to prevent firms from running at a loss (Monitoring Analytics (2023)).

Electricity prices are nodal in the PJM (Ott (2003)) and the market is also assumed to be connected to other markets through interconnectors. The interconnector losses are presumed to be static, and therefore not dependent on throughput. Under these definitions, nodal prices and supply (marginal cost) curves are not dependent on interconnector activity.

In addition, so-called spinning reserves and regulation reserves are procured and co-optimised with energy to provide hertz-level frequency balancing (PJM (2023)). These services may exert some influence on the real-time electricity supply curve.

Drawing from PJM (2017), Hung-po (2019), Hytowitz et al. (2020), PJM (2022*a*), Tongxin et al. (2018), FERC (2012) and FERC (2019), we then recover the price at every level of load in part by applying the notations and initial assumptions from the generic case (see Section 5.2.1) as follows. Regarding the notations, let $u_i \in \{0, 1\}$ be set to $u_i = 0$ if unit i is turned off and to $u_i = 1$ if unit i is turned on (start-up decision). We extend the binary variable for the online/offline status with a time dimension as $w_{i,t}$ for time t. Then the start-up cost is denoted by c_i^{SU} and the no-load cost by c_i^{NL} for each unit i. Also, let Y denote the set of fast-start units such that $i \notin Y$ are the slow-start units. Last, let $f_{i,d}$ denote the bid-in price and Q_i^F the bid-in quantity for spinning reserves that are co-optimised with energy.

To review the generic assumptions, first, let m be the proportion of every unit's total supply quantity (assumed $m < 1$) being exchanged day-ahead and in the reliability run(s).[134] Sec-

[134] We assume a single reliability run in our simplified formulation.

ond, let k be the proportion of total load (assumed $k < 1$) being settled day-ahead and in the reliability run. Finally, we assume $m = k$.

We introduce a new objective function for day-ahead and real-time dispatch that reflects multi-part bidding and frequency balancing service costs

$$\min_{Q_i^S, Q_i^F, u_i, w_{i,t}} \sum_{i=1}^{N} C_i(Q_i^S, w_{i,t}) + u_i c_i^{SU} + w_{i,t} c_i^{NL} + F_i(Q_i^F, w_{i,t}), \tag{5.2.10}$$

where $F_i(Q_i^F, w_{i,t}) = f_{i,d} w_i Q_i^F$, and the corresponding binary constraint

$$w_{i,t} - w_{i,t-1} \leq u_i, \tag{5.2.11}$$

with $u_i, w_{i,t} \in \{0, 1\}$.

In addition, the loss function in the load balance constraint (5.2.4) is modified for interconnector losses as

$$L(\mathbf{Z}) = \frac{\bar{m}}{2} Q_i^S, \tag{5.2.12}$$

for mid-point loss factor $\bar{m}$ and node i located in another market.

Then for the reliability run the objective function becomes

$$\min_{Q_i^F . u_i, w_{i,t}} u_i c_i^{SU} + w_{i,t} c_i^{NL} + F_i(Q_i^F, w_{i,t}), \tag{5.2.13}$$

roughly as in FERC (2012), with the addition of $F_i(Q_i^F, w_{i,t}) = f_{i,d} w_i Q_i^F$, given that

$$Q_i^S + Q_i^F \leq w_i \bar{Q}_i^S, \tag{5.2.14}$$

i.e. the quantity served in energy and spinning reserves cannot exceed the maximum capacity of any unit i.

Furthermore, for dispatch in the pricing run, (5.2.10) remains the objective function, but the binary constraint is removed for fast-start plants. The start-up and status variables are relaxed

for fast-start plants $u_i, w_{i,t} \in [0,1]$ for $i \in Y$.

In addition, pricing is performed under partial integer relaxation but separately from the pricing run for dispatch. First, the integer-relaxed fast-start units use amortised prices as

$$p_{i,d} = c_{i,d} + \frac{c_i^{SU}}{\bar{Q}_i^S} + \frac{c_i^{NL}}{\bar{Q}_i^S}, \tag{5.2.15}$$

(see PJM (2018), pages 8-9). Second, offline units cannot participate in pricing. Third, slow-start units are evaluated on the convexity condition – namely, on whether they are dispatched exactly at their minimum loading level. If they are, then they cannot set the price. Then, a merit order is assembled, and the next 1 MW is priced by the first least expensive viable unit to obtain P^* (PJM (2018)).

Moreover, the settlement dispatch run has the following objective function using the price outcome P^*:

$$\max_{\forall i Q_i^S, u_i, w_{i,t}} \sum_{i=1}^{N} P_i^* Q_i^S - C_i(Q_i^S, w_{i,t}) - u_i c_i^{SU} - w_{i,t} c_i^{NL} - F_i(Q_i^F, w_{i,t}). \tag{5.2.16}$$

It is solved to find $u_i^{**}, w_i^{**}, Q_i^{S**}$ and Q_i^{F**}.

The profit Π_i for unit i is calculated using

$$\Pi_i(u_i, w_i, Q_i^S, Q_i^F, P_i) = P_i Q_i^S - C_i(Q_i^S, w_{i,t}) - u_i c_i^{SU} - w_{i,t} c_i^{NL} - F_i(Q_i^F, w_{i,t}), \tag{5.2.17}$$

which then gives the formula for uplift U_i as

$$U_i = \Pi_i^{**} - \Pi_i^*. \tag{5.2.18}$$

Finally, for simplicity, the must-run requirements for system strength and minimum loading are introduced via setting variable $w_i = 1$ for any given unit i.

The full algorithm reads as follows.

1. An MILP is solved for (5.2.10) given (5.2.4)-(5.2.7), (5.2.11) and (5.2.12) to find the optimum level of the binary variables $u_i^*, w_i^* \in \{0,1\}$ and dispatch target variables Q_i^{S*}. An LP is also solved for the same problem by fixing $w_i = w_i^*$ to get the day-ahead prices $P_j^{day-ahead}$ for every node j.

2. An MILP is solved for (5.2.13) given (5.2.4)–(5.2.7), (5.2.11) and (5.2.12) to update the optimum values of u_i^* and w_i^*. Decommitments are not allowed.

3. An LP is solved for (5.2.10) given (5.2.4)–(5.2.7) and (5.2.12) in the real-time dispatch run to find the dispatch target variables Q_i^{S*}, keeping the binary variables $u_i^*, w_i^* \in \{0,1\}$ fixed.

4. An LP is solved for (5.2.10) given (5.2.4)–(5.2.7) and (5.2.12) in the pricing run with fast-start integer variables relaxed. The obtained online, convex quantities are arranged in merit order to compute the price P^* using amortised costs for fast-start units.

5. Profit $\Pi_i^*(u_i^*, w_i^*, Q_i^{S*}, Q_i^{F*}, P_i^*)$ at the dispatch solution is determined using (5.2.17).

6. A MILP is solved for (5.2.16) in the settlement run given (5.2.4)–(5.2.7) and (5.2.12) using P_i^* to find u_i^{**}, w_i^{**} and Q_i^{S**}. Profit $\Pi_i^{**}(u_i^{**}, w_i^{**}, Q_i^{S**}, Q_i^{F**}, P_i^*)$ at the settlement solution is determined using (5.2.17).

7. Uplift is calculated from (5.2.18).

5.2.3 NEM in Australia

In the NEM, electricity dispatch takes place in a real-time (5 minute) market only (no day-ahead market), as per AEMO (2021*i*). The real-time market uses simple bids and mostly self-scheduling with the exception of fast-start unit commitment. The bid language comprises 10 price–quantity pairs, no fixed cost bids, and some operational specifications (AEMO (2022*i*)). Fast-start unit commitment is a two-step process wherein the units that can start up and shut down within 60 minutes are centrally scheduled. The fast-start unit commitment decision is first evaluated in a dispatch run ignoring flexibility constraints that finds the optimal commitment

quantities (step 1). Next, the engine is re-run such that relevant constraints are imposed to keep the committed quantities fixed at or above the required levels (step 2) (AEMO (2021*j*)). Apart from fast-start scheduling, the NEM is organised on self-scheduling principles. The units are placing marginal cost bids at prices they see fit based on private information available to them at the time. These marginal cost bids are considered disorderly when they fail to reflect true marginal costs. Disorderly bids might instead compensate for or 'convexify'[135] the fixed costs incurred by the units placing them (AER (2017)). The real-time supply curve is composed of these simple and potentially disorderly bids at every level of demand.

The NEM solver is assumed to reference the supply cost of the incremental unit of load approximated by the last 1 MW of load. Importantly, the NEM price methodology does not leave any LMP-style congestion or loss components in the price (AEMC (2021*c*)). Due to network constraints, however, some quantities are must-run and others are curtailed, which pre-empts the use of the standard bid stack approach for supply curve construction. In addition, the incremental net 1 MW change might involve a bid reallocation that calls for both positive and negative changes in the bid target differentials – that is, volumes above 1 MW might be moved around as part of serving the last 1 MW – in the presence of binding constraints. This is due to trade-offs on the LHS of the binding constraint equations as observable in the full dispatch data (AEMO (2022*g*)).

Regarding out-of-market payments, directed participants are eligible for compensation under the directions framework set out in Clause 4.8.9 in the NER (AEMC (2021*c*)). However, constrained-on (not directed) units are not entitled to out-of-market compensation (see Clause 3.9.7(b) in the NER).[136]

Furthermore, prices are regional in the NEM, and interconnectors are used to connect the different regions. Owing to the sheer magnitude of geographical distances in Australia, these interconnectors have relatively large losses. These losses are dynamically calculated, which

[135]The term 'convexification' refers to the apportioning of lumpy costs such as start-up and shut-down costs into bid slots for marginal costs (price–quantity pairs) at unit level.

[136]Note that the constraints associated with the directed and constrained-on (not directed) units are equal-to constraints. Participants may bid their capacity as unavailable if they think they are going to be behind a constraint, i.e., they are going to be constrained-on without compensation (and their bids thrown out of the solver). In turn, the market operator may invoke the directions framework to tell the affected units to operate at a given level of output.

means that their level depends on the amount of interconnector throughput (AEMO (2022*k*)). According to AEMO (2021*g*), SOS2 are used in the NEM to handle dynamic losses through integer constraints. The SOS2 constraints for every interconnector r can be laid out as follows. Let $\underline{K}_r \leq 0$ be the lower limit of the interconnector flow in a specific direction and $\bar{K}_r \geq 0$ be the upper limit. Let the $[\underline{K}_r, \bar{K}_r]$ segment be split into $n-1$ sub-segments on breakpoints $i = 1, 2, ..., n$ such that $F_{r,i}$ are the values taken at the breakpoints. Also, let $\forall i, z_i \in [0, 1]$ denote the binary variables, given that $\sum^{\forall i} z_i \leq 2$, and let $\forall w_i, w_i \in \mathbf{R}^+, w_i \leq z_i$ denote the weight variables at breakpoint i such that the breakpoints i, j with $z_i = 1, z_j = 1$ are adjacent: $\forall i, \forall j \in [i+2, ..., n], z_i + z_j \leq 1$. Then, the function $L^r(F_r)$ is evaluated by finding the values of all z_i, w_i such that $\sum^{\forall i} w_i F_{r,i} = F_r$ and $\sum^{\forall i} w_i L^r(F_{r,i}) = L^r(F_r)$.

Finally, FCAS manage frequency balancing in the market. These reserve services are co-optimised with energy through so-called FCAS trapeziums in a way that FCAS can influence the energy price and regional supply curves (AEMO (2017*b*, 2021*k*)). There is a separate FCAS trapezium for all ten types of FCAS in the NEM that a unit can provide. Five of these types of services are contracts to raise the frequency of the system and five are to lower it, noting that "contingency raise requirements are set to manage the loss of the largest generator on the system" (AEMO (2021*k*)). Additionally, every unit that wishes to provide FCAS must submit a bid comprising up to 10 price–quantity pairs and technical parameters (AEMO (2022*i*)). Then, the FCAS trapeziums are defined from the bid-in information as follows. The x-axis records the amount dispatched in energy and the y-axis records the dispatch volume in the FCAS. Then, the four corner points of the trapezium are – from left to right – the enablement minimum, low break point, high break point and enablement maximum (see Figure 3.1 in Chapter 3). The enablement minima and maxima determine the energy bounds within which a unit can provide FCAS, and the break points signal the start and end of FCAS provision in maximum FCAS capacity in terms of energy output (AEMO (2021*k*)).

We recover the price at every level of load based on the following optimisation routine (for more detail, see Chapter 3 or more directly Gorman (2023)).

1. Solve for optimal dispatch values whilst ignoring fast-start flexibility constraints.

2. Identify fast-start quantities. Fix the fast-start unit targets for all demand levels D given

on the outcome of the previous step and the inflexibility profiles.

3. Re-run the co-optimisation to allocate targets using the fixed unit commitment configurations.

4. Perform the necessary re-runs as outlined in Section 3.3.6 in Chapter 3.

5. Evaluate the total cost for D and $D-1$ for all demand levels taking dynamic losses into consideration.

6. Calculate price as the change in total cost as demand levels incrementally increase from $D-1$ to D for every level of demand D to build the supply curve.

5.2.4 BM in Great Britain

In Great Britain, the most volumes of wholesale dispatch are conferred on exchange-based markets (self-dispatch) preceding the BM. After that, the BM organises real-time (30 minutes) balancing with a unique bid language, a relatively complex constraint mechanism, and pay-as-bid settlement (Elexon (2019, 2020)). The 'bids' submitted to the BM comprise bid and offer price–quantity pairs for volumes incremental and decremental to the self-dispatched final physical notification (FPN) quantities and operational details. The bids propose decreasing generation or increasing load, and the offers refer to increasing generation or decreasing load. There is no fixed cost component in the bid language. The market operator is responsible for selecting which bids and offers to fulfill in addition to the FPN quantities to balance the grid in line with the physical constraints (Elexon (2019, 2020)). The bid selection process and unit commitment overrides are currently not automated. Moreover, the selected bids are remunerated on a discriminatory pay-as-bid (or pay-your-bid) basis, meaning that at a given point in time, there are different prices for different transactions, based on the bid-in prices rather than on one market clearing price (Krishna (2009); Elexon (2019, 2020)). In addition, a single market price is computed by the settlement agent as an average of various self-dispatch transactions based on information provided by the exchanges arranging those transactions, which is mainly used as an index for financial contracts and has but a very weak link to the real-time balancing market (Elexon (2020)).

In the absence of uniform real-time pricing, backing out a real-time supply curve would be difficult even under very restrictive assumptions. Therefore, we omit the question of supply monotonicity and focus on computing welfare. This we undertake given the following assumption. First, the gap between the volumes traded before real-time balancing (the FPN level) and the real-time demand should be the same at all levels of demand. We assume that this gap is 1 MW for simplicity: the aggregate self-dispatch volume tends to match all but the last 1 MW of real-time demand (which is a 'positive market' according to Ocker, Ehrhart and Belica (2018)). We assume that there is only one day-ahead exchange and no other bilateral or intraday trading. Furthermore, a proportion m of their total supply quantity (assumed $m < 1$) is being exchanged on the day-ahead exchange by each unit.

In principle, the day-ahead price from this exchange should be an unbiased predictor of every BM bid and offer price, assuming nil bid–offer spreads at all levels of demand; otherwise, arbitrage would be possible. However, noting that the BM mechanism rearranges $x \geq 0$ MW quantities to obtain a physically feasible outcome and that the money paid to certain units for increasing output by $1 + x$ MW (x MW after bridging the FPN to real-time demand) and others for decreasing their output by x MW are calculated on a pay-as-bid basis,[137] we introduce seller heterogeneity as follows. All generators are assumed to bid at their cost level subject to bid shading in the BM. This bidding behaviour is typical for pay-as-bid auction settings (Ocker, Ehrhart and Belica (2018)).

Bid shading involves buyers bidding below cost and sellers bidding above cost as per Krishna (2009) and Ocker, Ehrhart and Belica (2018). To quantify these amounts, we apply Equation (9) from Ocker, Ehrhart and Ott (2018) in a positive market. This formula expresses the amount of bid shading by sellers as a function of the perceived position in the merit order $x(p^S_{i,d})$ given the optimally bid shaved offer price $p^S_{i,d} \in [P_{min}, P_{max}]$ within the lowest P_{min} and highest P_{max} offer prices envisaged in the market, demand in the market D, and the acceptance (demand) probability $n(x(p^S_{i,d}))$ these infer. Under very simple linear assumptions, let $x(p) := (p - P_{min})\frac{D}{P_{max}-P_{min}}$ and $n(x(p)) := 0.5 - x(p)\frac{0.5}{D}$. Then, Equation (9) from Ocker, Ehrhart and Ott (2018) states that

[137] We found no reference to make-whole payments other than these balancing payments.

$$p_{i,d} = c_{i,d} - \frac{n(x(p_{i,d}))}{n'(x(p_{i,d}))x'(p_{i,d})},$$

where $c_{i,d}$ denotes the cost associated with the bid slot d (see Section 5.2.1). A simplified form can be obtained as

$$p^S_{i,d} = c_{i,d} - \frac{0.5 - ((p^S_{i,d} - P_{min})\frac{D}{P_{max}-P_{min}})\frac{0.5}{D}}{(-\frac{0.5}{D})(\frac{D}{P_{max}-P_{min}})} = c_{i,d} + P_{max} - p^S_{i,d},$$

from where we obtain

$$p^S_{i,d} = \frac{c_{i,d} + P_{max}}{2}. \tag{5.2.19}$$

For negative markets, let $x(p) := D - (p - P_{min})\frac{D}{P_{max}-P_{min}}$, whereas $n(x(p))$ remains unchanged, which gives

$$p^B_{i,d} = c_{i,d} - \frac{0.5 - (D - (p^B_{i,d} - P_{min})\frac{D}{P_{max}-P_{min}})\frac{0.5}{D}}{(-\frac{0.5}{D})(-\frac{D}{P_{max}-P_{min}})} = c_{i,d} - p^B_{i,d} + P_{min},$$

from where we obtain

$$p^B_{i,d} = \frac{c_{i,d} + P_{min}}{2}. \tag{5.2.20}$$

The spread for unit i equals

$$\frac{c_{i,d} + P_{max}}{2} - \frac{c_{i,d} + P_{min}}{2} = \frac{P_{max} - P_{min}}{2}$$

regardless of the value of $c_{i,d}$.

Moreover, although the BM takes place at a national level, considering the fact that it does not operate in isolation but is coupled with other countries' markets through interconnectors, the loss properties of the interconnectors involved are of interest. Most importantly, the interconnector loss factors are typically static mid-point loss factors that are not dependent on the level of load throughput (Nemo Link (2022)).

Frequency balancing (reserves) service provision is also present, complementing the BM mechanism. The "response provided within 30 seconds and sustained until 30 minutes following the point at which the frequency trigger was reached" is called Static Firm Frequency Response (SFFR) as per ESO (2023). Note that this and a suite of other, partly overlapping frequency balancing services provided alongside the BM are not co-optimised with the BM; hence, they hardly impact the real-time energy supply curve.[138]

We recover the real-time balancing targets and discretionary prices in the BM using the notation provided as part of the generic formulation (see Section 5.2.1) with a few changes.

First, we distinguish between positive balancing costs to supply additional units of energy and negative balancing costs to purchase additional units of energy in addition to the FPN level of a given generator i denoted by Q_i^{S*}. The values of Q_i^{S*} are determined in the day-ahead exchange. Let q_i^S then denote the additional supply target of unit i and let $p_{i,d}^S$ from (5.2.19) denote the optimal cost for these quantities for $d = 1, 2, .., 5$ bid slots. Let q_i^B denote the additional demand target of generator unit i, and $p_{i,d}^B$ from (5.2.20) denote the associated cost after bid shading for $d = 1, 2, .., 5$ bid slots. We can express the net 1 MW the BM mechanism procures as $\sum^{\forall i} q_i^S - q_i^B = 1$ MW.

In addition, we use Boolean variables to decide if a given unit i is providing energy, $b_i^B = 0, b_i^S = 1$, or is loading it $b_i^B = 1, b_i^S = 0$.

Then, the cost function of positive balancing

$$C_i(q_i^S) = \sum_{d=1}^{5} p_{i,d}^S x_{i,d} | \sum_{d=1}^{5} x_{i,d} b_i^S w_i = q_i^S \tag{5.2.21}$$

and that of negative balancing

$$C_i(q_i^B) = \sum_{d=1}^{5} p_{i,d}^B x_{i,d} | \sum_{d=1}^{5} x_{i,d} b_i^B w_i = q_i^B \tag{5.2.22}$$

are separated. We use variables w_i for the online status as earlier and b_i^B, b_i^S for the bid–offer binaries. Note that unit i may be given a positive bid target $q_i^B \geq 0$ (to buy capacity back that

[138] We assume that these services are auctioned prior to the BM and hence deploy the lowest price frequency balancing quantities.

it had sold day-ahead) while being offline $w_i = 0$. However, in the absence of demand side bidding, offline units are always allocated nil balancing offer targets $q_i^S = 0$.

The objective function can be expressed as

$$\min_{\forall i Q_i^S} \sum^{\forall i} C_i(q_i^S) - C_i(q_i^B), \tag{5.2.23}$$

subject to the load balance constraint

$$\sum_{i=1}^{|N_j|} Q_i^{S*} + q_i^S - q_i^B - D - L(q_i^S) - L(q_i^B) = 0 (\leftrightarrow \lambda), \tag{5.2.24}$$

where the loss function can be given as

$$L(q_i) = \frac{\bar{m}}{2}(q_i) \tag{5.2.25}$$

for q_i^B, q_i^S given mid-point loss factor $\bar{m}$ and node i located in another market.

Note that must-run requirements for system strength or minimum loading are introduced via setting variable $w_i = 1$ for any unit i.

We then evaluate the given algorithm by the steps below.

1. For the day-ahead exchange, solve an LP for (5.2.3) subject to (5.2.4) and (5.2.25) while ignoring losses and fixing $w_i = 1$ such that $\sum_{j=1}^{|J|} Q_j^B = D - 1$ to find Q_i^{S*} for all i.[139] Note that the offered supply quantities are proportional to m. The day-ahead price $P^{day-ahead}$ equals the dual value of constraint (5.2.4).

2. For real-time balancing (mimicking the BM), first solve an LP for (5.2.23) given (5.2.4)–(5.2.7) and (5.2.25) where it appears in the formulae to find q_i^{S*}, q_i^{B*}.

3. Then, recover the bid-in costs (pay-as-bid prices) associated with every MW of scheduled balancing quantity q_i^{S*}, q_i^{B*}.

[139] $Q_i^{S*} = 0$ may be obtained for some i even though the corresponding $w_i = 1$.

5.2.5 Welfare calculation

Table 5.1 shows a formulaic specification of the welfare calculation. Taking the 11 steps one-by-one, we first sum the amounts paid by consumers[140] for energy (step 1). These are the amounts paid in both day-ahead and real-time markets in the PJM, only day-ahead exchanges in the BM and only real-time markets in the NEM. In step 2, we quantify interconnector losses in the system and price them at real-time prices. Step 3 merely sums the amounts from steps 1 and 2 to obtain the amounts received by producers for energy. Step 4 computes the amounts paid by frequency balancing services using the price of that service P^F, which is the shadow price of the frequency balancing requirement constraint in the PJM and the NEM and the cost of the highest priced used capacity in the BM. Step 5 calculates VOLL, which is the maximum value that consumers are willing to pay for 1 MWh energy, times the energy they require. Step 6 calculates consumer surplus as the difference of the value obtained in step 5 and that obtained in step 1. In step 7, the costs of the producers are calculated using the same formula. Moreover, out-of-market payments are obtained in steps 8a and 8b, after which producer surplus and social surplus can be obtained via the shown formulas.

Table 5.2 : **Welfare calculation**

The table shows the formulaic specifications for calculating different measures of welfare under the three discussed market designs.

	Generic formulation	**BM formulation**	**PJM formulation**	**NEM formulation**
Steps				
1) Paid by consumers	$\sum^{\forall j} D_j P_j$	$P^{day-ahead}(D-1)$	$\sum^{\forall j} P_j^{day-ahead} kD_j + P_j(1-k)D_j$	PD
2) Costs of losses	–	$C_i(q_i^B)L(q_i^B) + C_i(q_i^S)L(q_i^S)$	$P_{i-1}L(Q_i^S)$	$PL^r(F_r)$
3) Producers receive	1)+2)			
4) Paid for frequency balancing	–	$P^F Q_i^F$		
5) VOLL times demand	VOLL $\times \sum^{\forall j} D_j$	VOLL $\times D$	VOLL $\times \sum^{\forall j} D_j$	VOLL $\times D$
6) Consumer surplus	5)-1)			
7) Costs of producers	$C_i(Q_i^S, w_{i,t}) + u_i c_i^{SU} + w_{i,t} c_i^{NL}$			
8a) Out-of-market payments	–	$\sum^{\forall i} C_i(q_i^S)$	$\sum^{\forall i} \Pi_i^{**} - \Pi_i^*$	–
8b) Out-of-market receipts	–	$\sum^{\forall i} C_i(q_i^B)$	–	–
9) Producer surplus	3)-7)+8a)			
10) System charges	2)+4)+8a)-8b)			
11) Social surplus	6)+9)-10) (or equivalently 5)-4)-7)+8b))			

Note that step 8 is separated into two parts to reflect a distinction of out-of-market payments (step 8a) and receipts (step 8b) in Great Britain. This is required because producer surplus excludes the out-of-market receipts of the grid operator paid by those units that buy quantities as part of the balancing schedule.

[140] Consumers represent wholesale consumers in this context.

5.3 Non-monotonicity of supply

The following supply or marginal cost function non-monotonicities have been recorded in the literature. Hogan and Ring (2003), Bjørndal and Jörnsten (2008) and Ruiz et al. (2012) discuss that 'integer programming' prices (IP prices) from the seminal O'Neill et al. (2005) model are volatile and hardly increase over increasing levels of load. They use Scarf's adapted example (see Scarf (1994) for the original) with minimum output and start-up costs. Gribik et al. (2007) also show that the FCP-style marginal cost curve decreases as quantity increases due to fixed costs. Furthermore, Byers and Hug (2023) confirm that prices may decrease as demand increases due to fixed costs under FCP.

These references all focus on indivisibilities in energy in centrally dispatched markets. They discuss unit commitment with fixed costs and uplift but omit market complexities, such as the co-existence of day-ahead and real-time markets, co-existence of energy markets and frequency balancing markets, as well as price effects of binding constraints, dynamic interconnector losses and integer relaxation. Some of these additional market design elements abate non-monotonicity, whereas others exacerbate it, as we explain after restating the non-monotonicities known from the cited papers.

5.3.1 Non-monotonicities due to fixed costs and minimum loading

The real-time electricity supply function is built from lower quantities to higher quantities. Adding incremental amounts of load usually involves committing new units and may involve shutting down already running units. However, the decisions for start-up and shut-down are binary. Units often have to bear fixed costs or dispatch at a discrete minimum level to start up or shut down. Some of these non-convex features of the dispatch problem are retained in the formulation of the dispatch solution with multi-part bidding and automated pool market settings. Indeed, Byers and Hug (2023) recognise bid-in start-up costs and minimum output requirements in their formulation. They apply FCP principles to extract the price and show supply function non-monotonicity (see Table 1 and Figure 1 in their paper).

Example 5.1. *Byers and Hug (2023) observe the following dynamic due to start-up costs. Assuming two units in a market, unit 1 with $5 marginal cost and $500 start-up cost and unit 2 with $10 marginal cost and no start-up cost, the total cost function is evaluated as the sum*

of these cost components. At lower levels of demand, the total cost is lower if only unit 2 is dispatched, which has no start-up costs. This unit has a marginal bid of \$10. Then, at higher levels of demand, it becomes economical to dispatch unit 1, with a marginal bid at \$5. The breakeven between low and high levels of demand appears at $5x + 500 = 10x$*, where* $x = 100$ *in MW. Because the price is \$10 below 100 MW and \$5 above 100 MW, the supply curve is said to be non-monotonic.*

Byers and Hug (2023) also record that minimum loading leads to discontinuities in the total cost function. Rearranging their example, we show that minimum loading requirements cause the following effect at low levels of demand.[141]

Example 5.2. *Assuming two units in a market, unit 1 with \$5 marginal cost and 100 MW minimum loading and unit 2 with \$10 marginal cost and no minimum loading, the total cost function is evaluated subject to the minimum loading requirement that states that unit 1 cannot be dispatched at below 100 MW. Therefore, unit 2 is dispatched below 100 MW demand at \$10 and unit 1 above 100 MW demand at \$5. Hence, the relationship between price and quantity is not monotonically increasing.*

Example 5.2 can then be extended to the real-world treatment of minimum loading as follows. Assuming that there is a unit 3 at \$0 marginal cost, no minimum loading, and 150 MW maximum capacity, we posit that unit 3 gets dispatched at all levels of demand up to 150 MW. Without minimum loading requirements, an additional 1 MW of unit 1 would typically be dispatched at \$5 for 151 MW demand under most market designs to minimise total cost (maximise trade value). In the minimum loading–constrained case, however, this is not possible. Looking at the three different market designs, at least three target allocation and pricing alternatives are present at 151 MW load.

First, minimum loading requirements in the NEM are only present for fast-start fuels (AEMO (2021*j*)); thus, we assume unit 1 falls into this category. At 151 MW demand, unit 3 may then be turned down to 51 MW (-99 MW change) for unit 1 to come online in 100 MW (+99 MW

[141] Note that this refers to units with minimum loading that – if turned on – can only be committed at or above certain volumes and not must-run units that must be turned on and committed at or above the minimum loading level. The supply function would not be defined at MW levels below the minimum loading level in case of the latter.

change). In this case, the cost of the incremental bid is $0 by unit 3 at 151 MW because the binding minimum loading constraint is not relaxed. This alternative is reflective of the fast-start unit commitment market design of the NEM, where the unit commitment decision is given a non-constrained formulation before taking minimum loading into consideration.

Second, minimum loading limits of fast-start plants vanish in the process of fast-start integer relaxation; therefore, the illustrated indivisibilities only apply to slow-start units that do not participate in that. For exposition purposes, we may then assume that unit 1 is a slow-start plant. To resolve the dispatch allocation and pricing problem at 151 MW demand, unit 3 may be kept at 150 MW and unit 2 may be committed for an additional 1 MW for $10 at 151 MW demand. Then, only at above 250 MW demand would unit 1 be dispatched, setting the price at $5. This alternative yields a lower centrally managed total cost at 151 MW than the first alternative. Therefore, it may be used in markets in the United States, such as in the PJM, where unit commitment is performed in a constrained formulation. The fact that it gives a $0 price at <150 MW, a $10 price at 151 MW and a $5 price at 250 MW implies that the above quoted non-monotonicity due to minimum loading may materialise at any level of demand.

Third, exchange-allocated FPNs in the BM ignore physical constraints, including minimum loading requirements. At 151 MW demand, unit 3 would be dispatched for 150 MW and unit 1 for the additional 1 MW. Then, the balancing algorithm must evaluate whether it is worth keeping unit 1 switched on, which means allocating 99 MW balancing targets to it at its offered price and deallocating 98 MW balancing targets from unit 3 at its bid price, taking bid shaving into consideration or whether it is more economical switching unit 1 off instead and allocating additional 2 MW balancing targets to unit 3 instead. Either way, although it is possible to obtain balancing costs that are decreasing over different levels of demand, we cannot say the same about the supply curve because prices are set out on a pay-as-bid basis. Figure 5.3 provides a summary of these relationships for different market designs.

Table 5.3 : **Supply non-monotonicities due to indivisibilities in energy**

The table shows what sources of non-monotonicity apply under different market designs.

	NEM	PJM	BM
Start-up costs	Not applicable	Applicable for slow-start plants	Not applicable
Minimum loading	Applicable for fast-start plants	Applicable for slow-start plants	Not applicable

5.3.2 Mitigating factors under different market designs

Indivisibilities in energy have been shown to drive supply function non-monotonicities. These inevitably depend on the market-specific rules of price discovery, as already shown. The pre-existing market designs can now be more fully evaluated on the ways they mitigate energy-related non-monotonicities.

5.3.2.1 PJM in the United States

In our supply (marginal cost) curve definitions for the PJM, the prices of real-time electricity are tied to the adjusted or unadjusted marginal cost bids over the next 1 MW electricity supplied. The adjustment applies for fast-start integer relaxation, as per PJM (2023), that also alters the way the above quoted non-monotonicities unfold. To illustrate this, assume that in the above example, unit 1 is a fast-start unit with 300 MW maximum capacity and $0 no-load costs.

The adjusted (integer-relaxed) marginal bid price $p*$ is given by (5.2.15). Substituting the above information for unit 1 into (5.2.15), we get $p_1* = 5 + \frac{500}{300} + \frac{0}{300} = 6.67$. Thus, unit 1 at an adjusted marginal cost bid of $p_1* = 6.67$ is assumed to have been committed in the RAC in a quantity pinned down as the minimum loading requirement, but has its minimum loading constraint relaxed due to integer relaxation.

Example 5.3. *First, returning to the start-up example from earlier, we add unit 2 with $10 marginal cost p_2 and $0 fixed costs, assuming it is a slow-start unit. We no longer need a breakeven calculation to compute the price depending on the level of demand. For the price calculation, the units can be arranged in merit order given $p_1* = 6.67$ and $p_2 = 10$. Then, the price is p_1* up to the maximum capacity of unit 1 until 300 MW demand because $p_1* < p_2$ and p_2 above 300 MW. This ordering retains the monotone property.*

Example 5.4. *Second, the minimum loading example can be changed to better reflect the PJM market design as follows. All unit information remains unchanged, further assuming that unit 3 has $0 fixed costs bid-in. Here, we have $p_1* = 6.67$, $p_2 = 10$ and $p_3 = 0$. At 150 MW demand, unit 3 is dispatched for 150 MW as earlier. At 151 MW demand, however, unit 1 is committed, and the price is set at $p_1* = 6.67$. Later, at 250 MW demand, the price is still $p_1* = 6.67$, as it is within the 300 MW maximum capacity of unit 1. At no level of demand would the supply*

function become non-monotonic because the minimum loading requirement of fast-start unit 1 is being relaxed.

In summary, the monotonic results only occur when unit 1 is a fast-start plant. This is the alleviatory scope of the current PJM market design.

5.3.2.2 NEM in Australia

In our supply curve definitions for the NEM, the prices of real-time electricity are tied to the cost of the last 1 MW energy supplied at all levels of demand. However, because the start-up and no-load cost are 'convexified' into the simple marginal cost bids, the fixed cost–linked non-monotonicity does not appear in the NEM.

However, non-monotonicity due to minimum loading is likely to some extent occur for the following reason. Recall that only fast-start plants are centrally committed by the market operator in the NEM, whereas all other (slow-start) units are self-scheduled via their bids. Related to Example 5.2, we have seen that for fast-start units, the use of minimum loading constraints with bid replacement leads to a relatively low price, if not necessarily non-monotonicity. Had there been another, even lower cost bid being replaced, the price could have dropped to cause non-monotonicity. However, this only occurs for fast-start plants. For slow-start plants, minimum loading requirements are not even formulated beyond what is being signalled by low priced bids. Therefore, those cannot trigger any non-monotonicities either.

Overall, the NEM market design is slightly more effective in controverting non-monotonicities due to indivisibilities in energy than the PJM design without integer relaxation.

5.3.2.3 BM in Great Britain

In our supply (marginal cost) curve definitions for the BM, the prices of real-time electricity are tied to the per MW balancing bid prices received by the units that partake in balancing. The balancing bid prices are proxied by the day-ahead prices at the same levels of demand minus 1 MW. Standard bid stack building is only applicable for the day-ahead price, as neither are there physical constraints involved in computing these exchange-based prices, nor do the day-ahead bids contain any fixed costs. Fitting the real-time supply curve to the day-ahead bid stack

returns a curve that is not susceptible to non-monotonicities due to start-up costs or minimum output constraints.

The BM mechanism's resilience against violations of supply monotonicity in this sense lies in the fact that it is 'convexifying' fixed costs in its bid language. In addition, we assumed that balancing bid prices are considered on a per MW basis, although the cost of balancing at any level of demand may be different from the per MW price due to the uncertain nature of the MW quantity being rearranged for the grid to satisfy its physical constraints x. More specifically, x and therefore the total compensation paid to cater to the rearrangement may be large owing to minimum loading overrides, but this would not be captured as part of the supply curve under our definitions.

5.3.3 Non-monotonicities due to interconnector losses (NEM only)

As opposed to energy-linked violations of non-monotonicity, another, newly discovered source of supply function non-monotonicity is also presented in the context of the Australian market. This is linked to dynamic interconnector losses.

The system-wide allocation of load gives the engine's decision variables (AEMO (2021*g*)). Therefore, these variables, including interconnector flows, are not kept fixed in the implied inverse supply curve. The dynamic losses in the system may change in such a way that quantities at one side of the interconnector must also take an accompanying change in quantity over the marginal net 1 MW change in load that sets the price. If the interconnector flow contracts by withdrawing exports, then there is a connected loss decrease at a given rate. Similarly, if inter-regional transfers occur at a higher MW rate, then there is a commensurate loss increase. These changes in losses are constant as long as the trade flows do not step into a different SOS2 segment over the incremental amount.[142] Otherwise, the marginal MW amount of loss changes over subsequent levels of load impacting the monotonicity of the implied inverse supply curve.

Example 5.5. *A relatively simple example would be the following. Assume that unit 1 is exporting electricity into the focus region through an interconnector with dynamic losses. At lower levels of throughput, say 10 and 11 MW, the losses are only 0.9 and 1 MW, respectively. At 19*

[142]This was first brought to our attention by Allan O'Neil in discussions about the price setter outcome as at 12:40 AM on 15 July, 2021, for NSW.

and 20 MW throughput, however, the losses are 3 and 3.5 MW, respectively. Assuming that the bid-in price of unit 1 is -$20 (this must be negative) and that unit 1 is the only provider in the focus region up to 20 MW demand, we have the following relationships. At 10 MW demand, the total cost is $-20 \times (10 + 0.9) = -218$*. Moreover, at 11 MW demand, the total cost is* $-20 \times (11 + 1) = -240$*. Therefore, serving the last 1 MW of energy at 11 MW demand costs* $-240 - -218 = -22$*, giving a price of -$22. Similarly, at 19 MW demand, the total cost is* $-20 \times (19 + 3) = -440$*, and at 20 MW demand, it is* $-20 \times (20 + 3.5) = -470$*; hence, the price is -$30 at 20 MW demand. Putting it differently, the inter-regional marginal loss factor is* 0.5 *for interconnector transfers above 16 MW, and the respective price paid by the consumers in the importing region is* $-20 \times (1 + 0.5) = -30$ *(O'Neil (2019)). We see that the price–quantity relationship is non-monotonic.*[143]

Example 5.6. *A slightly more complex case can be numerically illustrated via a hypothetical price setter outcome using data and a reference implementation of the Australian NEMDE called Nempy (Gorman et al. (2022)) as of 07:45 on 10 April, 2022, for SA when the N^^N_NIL_3 voltage stability constraint and the V::N_DDSM_V2 thermal constraint are binding. Keeping all except the engine's decision variables, including interconnector flows and the loss-relevant demand quantities, constant, we observe the change in the implied inverse SA supply curve as load changes from 1155 to 1156 MW.*

First, we can identify the bids that are setting the price by running Nempy at 1154, 1155 and 1156 MW and taking the differences in the allotted dispatch targets at unit level. In the present example, LOYYB1 and LOYYB2 (brown coal, VIC), TARONG#1 (black coal, QLD) and WEMENSF1 (solar, VIC) set the price. However, the marginal quantities will be slightly different from the quantities in the solution, because Nempy hardcodes the demand variables of the loss calculations; we cannot update those to reflect the changing level of load in SA.[144] *We can obtain the marginal quantities by reconstructing the interconnector flow values, the losses and the constraint equations.*

[143] In terms of settlements, unit 1 is being compensated at the price in its own region $P_{non-focus}$, which is unspecified in the example, but we might assume it to be $P_{non-focus} = -50$. In addition, the inter-regional residue obtained by the interconnector's transmission network service provider (TNPS) is computed as $P_{focus} \times Import - P_{non-focus} \times Export = -30 \times 20 + 50 \times 23.5 = 575$, as per AEMO (2014*c*). In summary, unit 1 receives $-50 \times 23.5 = -1175$, consumers in the focus region pay $-30 \times 20 = 600$, and the TNSP receives 575, which all sum to nil.

[144] See the _format_regional_demand() function in the source code.

The interconnector flow at the boundary point through VIC1–NSW1 is 728.508 MW at 1154 MW demand towards NSW, as per the Nempy run, and it increases by 0.1082 MW for every MW increase in load. In this way, the flows are 728.508+0.1082=728.616 MW at 1155 MW load and 728.508+2×0.1082=728.724 MW at 1156 MW load. The SOS2 boundary points are at 708 and 755 MW. Similarly, the flow through NSW1–QLD1 is -464.741 MW at 1154 MW demand towards NSW, and it changes by 0.10315 MW (towards QLD) for every MW increase in load. The SOS2 boundary points are at -493 and -459 MW. Third, interconnector transfers over V–SA are 198.902 MW at 1154 MW load towards SA, and they marginally increase by 1.025 MW. The SOS2 boundary points are at 185, 200 and 215 MW.

The interconnector loss factors are computed using the following equations:

$$\begin{aligned} MLF_{I:=VIC1-NSW1} &= c + fF_I + d^I_{NSW} D^{loss}_{NSW} + d^I_{VIC} D^{loss}_{VIC} + d^I_{SA} D^{loss}_{SA}, \\ MLF_{I:=NSW1-QLD1} &= c + fF_I + d^I_{NSW} D^{loss}_{NSW} + d^I_{QLD} D^{loss}_{QLD}, \\ MLF_{I:=V-SA} &= c + fF_I + d^I_{VIC} D^{loss}_{VIC} + d^I_{SA} D^{loss}_{SA}. \end{aligned} \tag{5.3.1}$$

These can be transformed into losses as

$$\int (MLF_I - 1) dF_I = (C_I - 1)F_I + \frac{f}{2} F_I^2 \tag{5.3.2}$$

where C_I sums all the flow-constant terms: $C_{I:=VIC1-NSW1} = c + d^I_{NSW} D^{loss}_{NSW} + d^I_{VIC} D^{loss}_{VIC} + d^I_{SA} D^{loss}_{SA}$, as per AEMO (2022k). These calculations, the segment-wise SOS2 linear relationships and the loss allocations are shown in Table 5.4.

In the last section of Table 5.4, we see that at 1155 MW demand in SA, the VIC region sees an export-driven production increase of 0.100873+1.072634=1.173309 MW and QLD an import-lead production decrease by 0.107170 MW. At 1155 MW demand, these numbers are slightly higher for VIC owing to higher flows and higher losses, but not for QLD.

Furthermore, information about two binding constraints helps find the value split between the units in VIC that collectively deliver the additional 1.173309 MW.

The change on the LHS of N^^N_NIL_3 is given as

Table 5.4 : **Loss factor and loss calculations**

The table shows the coefficients and variables used in the marginal loss factor and dynamic loss calculations as per AEMO (2022*k*).

I	c	f	d^I_{NSW}	d^I_{QLD}	d^I_{VIC}	d^I_{SA}
VIC1-NSW1	1.0629	0.000182	0.000005		0.000009	0.000050
NSW1-QLD1	0.9217	0.000190	0.000001	0.000017		
V-SA	1.0121	0.000355			0.000001	0.000006

I	D_{NSW}	D_{QLD}	D_{VIC}	D_{SA}	D^{loss}_{NSW}	D^{loss}_{QLD}	D^{loss}_{VIC}	D^{loss}_{SA}	F_I
–	6235.30	5204.95	3711.70	1179.34	6556.16	5215.04	3792.56	1229.77	–
VIC1-NSW1	6235.30		3711.70	1154	6556.16		3792.56	1204.43	728.508
VIC1-NSW1	6235.30		3711.70	1155	6556.16		3792.56	1205.43	728.616
VIC1-NSW1	6235.30		3711.70	1156	6556.16		3792.56	1206.43	728.724
NSW1-QLD1	6235.30	5204.95			6556.16	5215.04			-464.741
NSW1-QLD1	6235.30	5204.95			6556.16	5215.04			-464.637
NSW1-QLD1	6235.30	5204.95			6556.16	5215.04			-464.534
V-SA			3711.70	1154			3792.56	1204.43	198.902
V-SA			3711.70	1155			3792.56	1205.43	199.927
V-SA			3711.70	1156			3792.56	1206.43	200.952

I	F_I	x_1	x_2	y_1	y_2	w_1	w_2	$loss$	$\Delta loss$
VIC1-NSW1	728.508	708	755	47.307	53.675	0.5636	0.4364	50.0860	–
VIC1-NSW1	728.616	708	755	47.272	53.638	0.5614	0.4386	50.0644	-0.02155
VIC1-NSW1	728.724	708	755	47.237	53.600	0.5591	0.4409	50.0429	-0.02156
NSW1-QLD1	-464.741	-493	-459	19.409	16.590	0.1688	0.8312	17.0658	–
NSW1-QLD1	-464.637	-493	-459	19.409	16.590	0.1658	0.8342	17.0573	0.00855
NSW1-QLD1	-464.534	-493	-459	19.409	16.590	0.1628	0.8372	17.0487	0.00855
V-SA	198.902	185	200	6.625	7.695	0.0732	0.9268	7.6164	–
V-SA	199.927	185	200	6.625	7.695	0.0049	0.9951	7.6883	0.07187
V-SA	200.952	200	215	7.695	8.842	0.9365	0.0635	7.7652	0.07693

I	D_{SA}	ΔF_I	$\Delta loss$	$from(\%)$	to	$\Delta from$	Δto
VIC1-NSW1	1155	0.1082	-0.02155	VIC(34)	NSW	**0.100873**	0.122424
VIC1-NSW1	1156	0.1082	-0.02156	VIC(34)	NSW	**0.100869**	0.122431
NSW1-QLD1	1155	0.10315	0.00855	NSW(53)	QLD	0.098617	**0.107170**
NSW1-QLD1	1156	0.10315	0.00855	NSW(53)	QLD	0.098617	**0.107170**
V-SA	1155	1.025	0.07187	VIC(66)	SA	**1.072634**	1.000563
V-SA	1156	1.025	0.07693	VIC(66)	SA	**1.075776**	0.998843

$$0.09287 \times \Delta F_{VIC1-NSW1} + 0.4487 \times \Delta WEMENSF1 \leq 0, \tag{5.3.3}$$

whereas the change on the LHS of V::N_DDSM_V2 can be expressed as

$$-0.1039 \times \Delta F_{V-SA} + 0.9461 \times \Delta F_{VIC1-NSW1} - 0.112 \times \Delta WEMENSF1 \leq 0. \tag{5.3.4}$$

From these the $\Delta WEMENSF1$ *that gives the highest possible LHS values is estimated*

to be -0.036 MW. To recover the 1.173309 MW net production increase in VIC, the LOYYB1 and LOYYB2 farms then collectively produce 1.173309-(-0.036)=1.209309 MW at 1155 MW demand. The case for 1156 MW load is analogous, as shown in Table 5.5.

Table 5.5 : **Price calculations**

The table shows the price of the incremental change in load.

At 1155 MW demand:

Unit ID	State	Bid type	Service type	Quantity (1)	Price (2)	(1) × (2)	Comments
LOYYB1, LOYYB2	VIC	Energy	Generation	1.2093	-$19.9508	-$24.1932	Increase in generation by 1.2093 MW before losses.
WEMENSF1	VIC	Energy	Generation	-0.036	-$19.9815	-$0.7193	
TARONG#1	QLD	Energy	Generation	-0.1072	$56.0617	-$6.0081	
						Price: -$29.4155	

At 1156 MW demand:

Unit ID	State	Bid type	Service type	Quantity (1)	Price (2)	(1) × (2)	Comments
LOYYB1, LOYYB2	VIC	Energy	Generation	1.2126	-$19.9508	-$24.1932	Increase in generation by 1.2126 MW before losses.
WEMENSF1	VIC	Energy	Generation	-0.036	-$19.9815	-$0.7193	
TARONG#1	QLD	Energy	Generation	-0.1072	$56.0617	-$6.0081	
						Price: -$29.4821	

The above example highlights that the dollar magnitude of this type of non-monotonicity is not large, yet it is prone to arise every time a constrained trade flow volume switches to the next segment of the piecewise-linear SOS2 loss curve – that is, as many times per supply curve as there are breakpoints on the loss curve.

5.4 Case study

The general idea is to establish three largely identical physical systems (a set of generators in a network) and expose these to three different market design settings closely resembling those of the NEM, PJM and BM. Our objective is then to reconstruct the supply curves, if possible, and compare welfare across these three markets.[145] Similar numerical comparisons have not yet come to our attention.

[145]For simplicity, we remove the inter-temporal dimension when recovering the implied inverse supply curves at a particular point in time (one-shot pricing).

5.4.1 Setting the scene

Table 5.6 provides the starting information set for the numerical example. This includes the most-equivalent layout, network and plant specifications, constraint properties and cost definitions of the three modelled market designs. First, the jurisdiction of interest comprises six busses (nodes 1–6) that are located in the same region in the NEM, the same market in the PJM and in the same country in the BM. In addition, node 7 at the other end of an interconnector is located in a different region in the NEM, a different market relative to the PJM and a different country for the BM. Demand is assumed to be distributed at a single 'artificial' reference node in the NEM and at nodes 1–6 in the PJM and BM. Moreover, interconnector losses are assumed to be dynamic in the NEM and static in the other two markets. These differences aside, the network has a largely identical plant set and network constraints in all three jurisdictions. Concerning the plant specifications, we see in Table 5.6 that there is one generator unit located at every bus on the network, such as Gas A at node 1, Gas B at node 2, etc.[146] There are no load units such as batteries or pumped hydro. Every generator unit has a 100 MW maximum capacity. Some of them have minimum loading criteria. All of these units are either online or offline in the preceding trade interval in line with their minimum run times. Some are fast-start units, whereas others are slow-start units, under the assumption that typically equivalent definitions hold in this respect across all three market designs. Some frequency balancing constraints are also stated from the perspective of the NEM market design. In addition, the following network constraints are included in this numerical example. First, a thermal line limit that states that electric throughput on the unidirectional link from node 1 to 2 cannot exceed 90 MW. Second, a system strength limit that ensures that Gas B is always online at minimum 10 MW rate. Last, capacity limits exist on the interconnector that connects nodes 6 and 7.

For further specifications, we see from Table 5.6 that the trade intervals are 5 minutes long in the NEM and PJM and 30 minutes long in the BM and that there is an 80 MW frequency balancing requirement in one direction – raise service – only with an unspecified response time.[147] In addition, renewable units' receipts for carbon offsets are assumed to be $50 per MWh in all three jurisdictions, which is a simplifying assumption on carbon pricing. Then,

[146] There are neither two-way fuels nor any virtual bids in this case study for simplicity.

[147] This could be extended with one or more lowering service(s) at different resolutions.

Table 5.6 : **Summary of the assumptions**

The table shows the key system, product and cost assumptions behind the presented numerical example.

	Australia (NEM)	**US (PJM)**	**GB (BM)**
System assumptions			
		Layout	
Grid setup	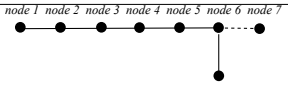	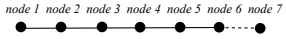	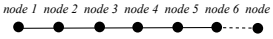
Jurisdiction: nodes 1-6	One regional price	Six nodal prices	One national price
Interconnector to/from	Node 7 in another region	Node 7 in another market	Node 7 in another country
Load location	At node 8 an artificial hub	Evenly split over nodes 1-6	
		Losses	
Across nodes 1-6	No losses		
To/from node 7	Dynamic, non-linear losses $0.001 \times flow^2$ with SOS2	Mid-point loss factor 2.5% Importing value: $flow \times (1 - 0.025/2)$	
		Plant specifications	
Gas A	Max capacity 100 MW, min loading 50 MW, previously offline, min run time 1 trade interval, fast-start, node 1		
Gas B	Max capacity 100 MW, min loading 10 MW, previously online, min run time 1 trade interval, fast-start, node 2		
Gas C	Max capacity 100 MW, no min loading, previously online, min run time 1 trade interval, slow-start, FCAS: 0, 5, 60, 100, node 3		
Coal	Max capacity 100 MW, min loading 30 MW, previously online, min run time 120 min, slow-start, FCAS: 0, 5, 60, 100, node 4		
Hydro	Max capacity 100 MW, no min loading, previously offline, min run time 1 trade interval, slow-start, FCAS: 0, 5, 60, 100, node 5		
Wind A	Max capacity 100 MW, no min loading, previously online, min run time 1 trade interval, fast-start, forecast 100 MW, FCAS: 0, 5, 60, 100, node 6		
Wind B	Residual max capacity 100 MW, no min loading, previously online, min run time 1 trade interval, fast-start, forecast 100 MW, node 7		
		Network constraints	
Line limit	$\leq$ 90 MW constraint on the link from Gas A		
System strength limit	$\geq$ 10 MW constraint on Gas B		
Interconnector limit	≥ -100 MW and $\leq$ 100 MW constraints on the link		
		Market specifications	
Trade interval duration	5 minutes	5 minutes	30 minutes
Freq. balancing req.	80 MW		
Carbon offsets	50 $/MWh		
Demand D	At 1 MW increments between the physically feasible bounds		
Day-ahead demand $\check{D}$	–	90 % of demand	Demand minus 1 MW
Product assumptions			
		Plant portfolio	
Gas A, B, Wind B	100 MW energy	90% offered day-ahead, the rest for real-time only	90% offered day-ahead, the rest for balancing only
Gas C, Coal, Hydro, Wind A	100 MW energy 40 MW 6 sec Raise FCAS	90% offered day-ahead, the rest for real-time only, 40 MW spinning reserve	90% - 40 MW offered day-ahead, the rest for balancing only, 40 MW SFFR
Cost assumptions			
		Energy costs	
Gas A	$50 start-up, $50 no-load, 50 MW @$40, 50 MW @$60		
Gas B	$100 start-up, $75 no-load, 50 MW @$45, 50 MW @$65		
Gas C	$100 start-up, $100 no-load, 50 MW @$50, 50 MW @$70		
Coal	$500 start-up, $100 no-load, 50 MW @$42, 50 MW @$62		
Hydro	$100 start-up, $100 no-load, 50 MW @$25, 50 MW @$55		
Wind A	$0 start-up, $0 no-load, 50 MW @-$50, 50 MW @$0		
Wind B	$0 start-up, $0 no-load, 50 MW @-$49, 50 MW @$1		
		Frequency balancing costs	
Gas C	40 MW @$80		
Coal	40 MW @$62		
Hydro	40 MW @$58		
Wind A	40 MW @$13		

the assumed levels of day-ahead demand and supply are also stated. Last, the plant portfolios,

the energy costs including fixed and variable cost components[148] and the assumed frequency balancing service costs are stated. Note that for a raise service, the headroom[149] is priced including some premia – that is, the frequency balancing price bids take values at or above the second (more expensive) bid slot energy bid prices for each fuel.

Furthermore, Table 5.7 details the assumptions used to 'convexify' the energy cost information into step-wise bid prices. All three markets have methods for this as part of the wider settlement and/or pricing mechanism. For example, Gas A, which is a fast-start plant that is offline in the previous pricing run, has the following costs: \$50 start-up, \$50 no-load, 50 MW @\$40 and 50 MW @\$60 as per Table 5.6. Table 5.7 explains how this translates into the bids Gas A submits in each jurisdiction. For the NEM,[150] we assume that the start-up costs are amortised per maximum capacity (100 MW) per the length of the trading interval (5 minutes) over the minimum run time of the unit (5 minutes). Similarly, no-load costs are amortised per maximum capacity. The same applies for the day-ahead exchange preceding the BM using 30 minutes increments. However, the BM bids are subject to bid shading as well, as outlined in Section 5.2.4. In contrast, we apply the amortisation formula from (5.2.15) for PJM. The 'convexification' of the multi-part bids continues for the rest of the fuels too along the same lines, except for Wind A and B that have no fixed costs and two exceptions in the NEM. Recall that the NEM allows disorderly bids at prices away from true marginal costs. There are two typical manifestations of this, one when slow-start units are securing their minimum loading levels via bids at the price floor (Coal) and the other when units recognise that they are bidding at the highest price among all bidders and decide to push their highest price bid to the market price cap (Gas C) as per Yarrow (2014).

We then implement the market-specific price and welfare algorithms prescribed in Sections 5.2.2, 5.2.3 and 5.2.4, using the above detailed inputs and assumptions. The three market algorithms are as consistent as the different market designs permit. For the NEM, we deploy the reference software called Nempy by Gorman et al. (2022), and we use our own source code for the PJM and the BM. A number of relatively minor assumptions and limitations of the imple-

[148] The same costs are used for day-ahead and real-time bidding in this example.

[149] That is, the remaining available capacity.

[150] We often refer to the small-scale market with rules reflecting the market design of the NEM as 'the NEM'. The same is done for all three markets throughout the chapter only to ease expression.

Table 5.7 : **'Convexifying' the bids**

The table shows the bidding assumptions behind translating the common generation costs into bids submitted to the market operator in each jurisdiction.

	Australia (NEM)	**US (PJM)**	**GB (BM)**
Bidding assumptions			
		Energy bid calculations	
Gas A	Start-up: $50 \times \frac{1}{100} \times \frac{5}{5} = 0.5$ No-load: $50 \times \frac{1}{100} = 0.5$ 50 MW @\$41, 50 MW @\$61	see (5.2.15)	Start-up: $50 \times \frac{1}{100} \times \frac{30}{30} = 0.5$ No-load: $50 \times \frac{1}{100} = 0.5$ 50 MW @\$41, 50 MW @\$61 + bid shading in real time
Gas B	No-load: $75 \times \frac{1}{100} = 0.75$ 50 MW @\$45.75, 50 MW @\$65.75	see (5.2.15)	No-load: $75 \times \frac{1}{100} = 0.75$ 50 MW @\$45.75, 50 MW @\$65.75 + bid shading in real time
Gas C	No-load: $100 \times \frac{1}{100} = 1$ 50 MW @\$51, 50 MW @\$16000	see (5.2.15)	No-load: $100 \times \frac{1}{100} = 1$ 50 MW @\$51, 50 MW @\$71 + bid shading in real time
Coal	No-load: $100 \times \frac{1}{100} = 1$ 30 MW @-\$998, 20 MW @\$43, 50 MW @\$63	see (5.2.15)	No-load: $100 \times \frac{1}{100} = 1$ 50 MW @\$43, 50 MW @\$63 + bid shading in real time
Hydro	Start-up: $100 \times \frac{1}{100} \times \frac{5}{5} = 1$, No-load: $100 \times \frac{1}{100} = 1$ 50 MW @\$27, 50 MW @\$57	see (5.2.15)	Start-up: $100 \times \frac{1}{100} \times \frac{30}{30} = 1$ No-load: $100 \times \frac{1}{100} = 1$ 50 MW @\$27, 50 MW @\$57 + bid shading in real time

mentation must further be highlighted.

First, all monetary values are given in dollars (\$), and the VOLL values are the same constant (VOLL = \$12000) regardless of the depicted jurisdiction. In addition, the upcoming plots showing 'continuous' demand ranges show solutions at levels of demand that are 1 MW apart.

Second, using Nempy for the Australian NEM and the Python MIP package for the BM and PJM, we observe that both solvers take the cost of the next MW as the marginal value of the load balance constraint. This poses a minor discrepancy compared with the intended formulation as per Table 5.1.

Third, trade via interconnectors – that is, the dispatch of Wind B at node 7 – is possible both in the day-ahead exchange in the BM and in day-ahead scheduling the PJM. The BM has only real-time losses and no associated losses in the day-ahead exchange. However, there is a mid-point loss element in PJM's day-ahead dispatch. The costs of the losses in PJM's day-ahead market are assessed alongside real-time losses at real-time prices in the welfare calculation. Note, however, that uplift is not computed in the PJM for Wind B. On a related note, although

inter-regional losses are in this manner included, intra-regional losses are assumed to be nil throughout the case study.

Fourth, the formulation of the line limit constraint over the unidirectional link $l_{1,2}$ between nodes 1 and 2 uses the net injections and power transfer distribution factors for the PJM. However, we do not calculate node-level net injections for the NEM or BM. Nevertheless, we assume that the only flow on link $l_{1,2}$ is from generator Gas A located at node 1 towards node 2. Therefore, an equivalent line limit restricts Gas A to produce 90 MW or less. All other line limits are set at 600 MW. For the system strength constraint, the units are simply forced online via some appropriate constraints.

Fifth, frequency balancing in Great Britain is assumed to take place at auctions independently from the BM. Therefore, the quantities used for frequency balancing are withdrawn from the day-ahead exchange and balancing. These are assumed to replace quantities from the second bid slots (higher bids and higher offers).

Sixth, the minimum run time is specified to be equal to the length of the trading interval for some fuels, which causes minor inconsistencies given that this interval is only 5 minutes in the NEM but 30 minutes in the BM, which we attempted to smooth out in Table 5.7. Both 5 minute and 30 minute prices are per megawatt-hour, but 30 minutes prices are in effect for longer.

Seventh, it is assumed for the BM that units are only able to buy and sell for balancing the self-dispatched amounts as per the FPN amounts – no more and no less – in each bid slot.

Eighth, the minimum run time of the Coal unit is 120 minutes. Although the NEM does not take this metric into consideration as part of dispatch, as Coal is a slow-start unit, it is relevant for the PJM and BM to pin down where the observed trade interval lies relative to this 120 minutes given that we also state that the Coal unit is already online in the preceding interval. In effect, the Coal unit is assumed to have been running for about 40 minutes at the time of the supply curve snapshot, implying that it is unable to shut down in the present interval (embedded unit commitment decision), as it is well within the 120 minutes minimum run time. Furthermore, the bid-in maximum availabilities of all units in the NEM and elsewhere are the same as the maximum capacity.

In addition, the welfare calculation in Table 5.2 assumes that frequency balancing costs

are not included in the amounts paid by consumers. Instead, these are considered a kind of social cost, which leaves the 'person' of the payer unspecified. In future work, this could be differentiated across market designs to better reflect the welfare impact of who is paying for frequency balancing.

Furthermore, interconnector losses in the NEM are fully attributed to the 'from region', i.e. the region exporting the flow, in Nempy (this refers to the value of proportioning_factor in the NEMDE objective function from Section 3.3.5 in Chapter 3).

Four operational modes are distinguished in the fast-start unit commitment run of the NEM as per AEMO (2021*j*), which are also included in this implementation as follows. Units that receive nil targets in the unconstrained run are assigned mode 1 that keeps them offline. Then, previously offline units (e.g., Gas A) operate in mode 3 when given a non-nil target, which prevents their targets to drop below minimum loading. Previously online units (e.g., Gas B) are assigned to mode 4, which does not limit their targets in any way in the absence of ramp rates.

Moreover, loads – those that absorb demand, not storage loads – are assumed not to bid into either of the three markets but act as price takers: there is no demand side bidding in this small-scale example.

Finally, the PJM's integer-relaxed pricing algorithm has the following exception. Convexity and commitment conditions are checked for those prices that perfectly correspond to the amortised bid-in prices, but not for composite prices that arise due to trade-offs in the constraints, most commonly owing to marginal rearrangements across spinning reserves and energy. Therefore, these composite prices may use non-convex or non-online quantities, which is a weakness of the implementation. However, the congestion component is added to these prices where appropriate.

5.4.2 Supply curves

Figure 5.1 shows the resulting real-time fuel mix (in colour) and supply curve. The fuel mix can be read as follows. The x-axis of the plot shows the demand, and the y-axis shows the generation. The sum of the generation by all dispatched fuels would be equal to demand (forming a 45° line) in the absence of any losses. With interconnector losses, however, generation is slightly above demand when Wind B is dispatched. In general, the fuel segment with

a slope other than nil is the marginal fuel. In addition, the sub-plot below the energy demand–generation exhibit shows the frequency balancing service dispatch (y-axis) in comparison with the energy demand (x-axis).

Figure 5.1 : **The NEM fuel mix and supply curve**

The plot shows the NEM fuel mix (in colour) and supply curve (black line).

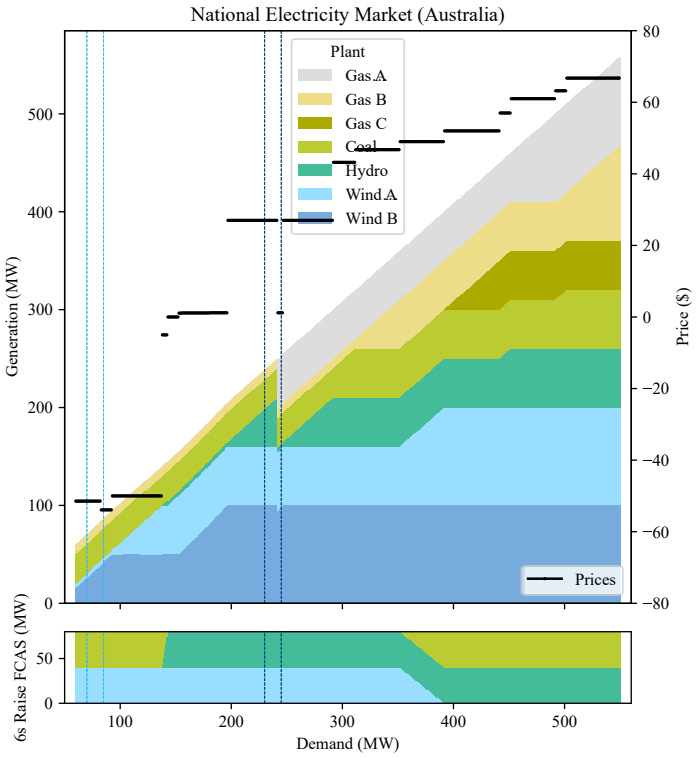

Some interesting price levels are highlighted by vertical blue lines at demand levels 70 and 85 MW (light blue) and 230 and 245 MW (dark blue). First, the price at 70 MW (-$51.45) is higher than that at 85 MW (-$53.9). This non-monotonicity is due to interconnector losses as per Example 5.5. Indeed, looking at the fuel mix at 70 MW versus 85 MW demand, there is no change in the fuel mix other than the increased targets in the marginal fuel Wind B with a bid-in price of -$50. The marginal amounts are being transferred from another region subject to dynamic losses.

In addition, the price drop between 230 and 245 MW demand unfold as follows. At 255 MW load, the price is set at $27 by Hydro, which has a bid-in price of $27. At this level, Gas A has a target quantity of nil, Hydro of 38.51 MW, Wind B of 100 MW and the rest of the fuels

of 100 MW, which sums to 238.51 MW including 8.51 MW losses.[151] FCAS is provided by Hydro and Wind A at 40 MW each. At 245 MW demand, Gas A is dispatched at 50 MW, Hydro only at 5 MW and Wind B at 98.25 MW, with the rest of the fuels remaining at the previous levels. Here, Wind B sets the price at 1.175 × \$1 = \$1.175, where the slope of the average cost approximation at 0.175 takes effect as well.

Figure 5.2 : **The PJM fuel mix and supply curve**

The plot shows the real-time fuel mix (in colour) and an the implied day-ahead (purple) and real-time supply curves (black) for the PJM-style small-scale market in our numerical example.

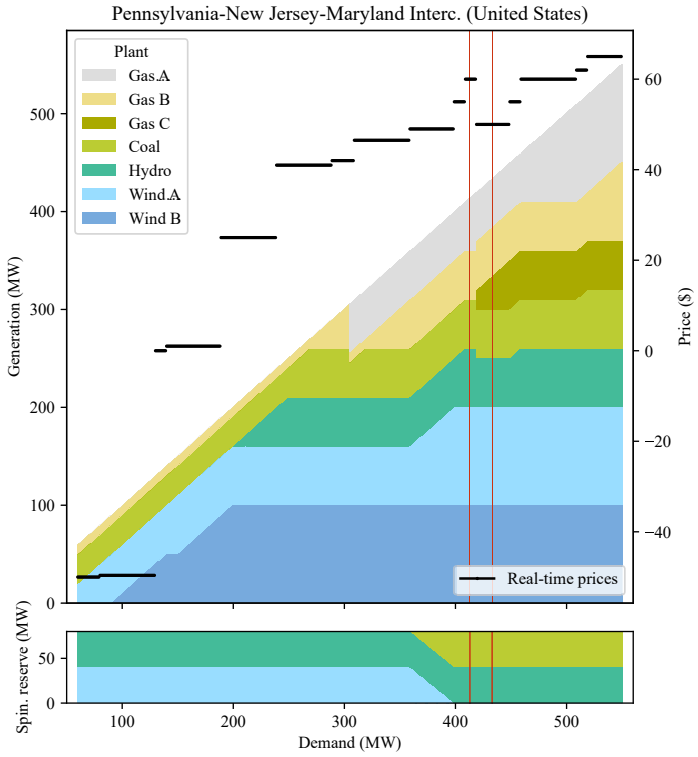

Figure 5.2 shows the supply curve result for the PJM at node 6.[152] A case of non-monotonicity is also highlighted using red vertical lines in this solution. These lines pick up a fixed cost–related non-monotonicity between 413 and 433 MW demand. At 413 MW, the price is set by Gas B at \$61, as it is not economic to switch on Gas C. At a higher level of load, however, the targets allocated to Gas C are non-zero and marginal. It sets the price at \$51.

[151] The value of these losses can be verified as $0.001 * 75^2 + (100 - 8.51 - 75) * 0.175 = 8.51$.

[152] For this supply curve, the price on the secondary y-axis is the price at node 6 for the total demand quantity across all nodes shown on the x-axis.

Figure 5.3 : **The BM fuel mix**

The plot shows the effective fuel mix in the day-ahead exchange and in the BM for the small-scale system based on the market in Great Britain.

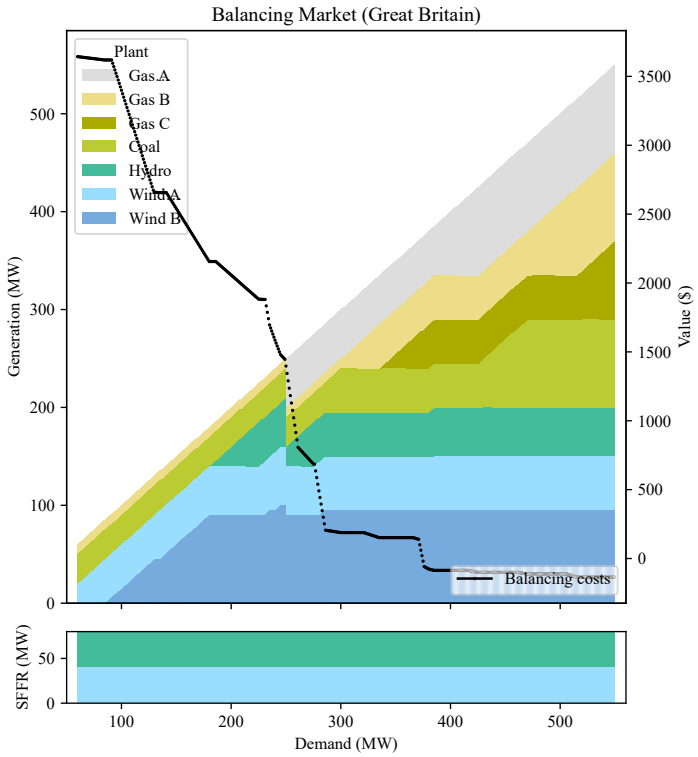

Figure 5.3 depicts the final fuel mix – summing the quantities traded day-ahead and the balancing adjustments – and the balancing cost results for Great Britain. Note that this balancing cost curve is not equivalent to a supply curve.

5.4.3 Welfare results

The welfare results comprise three parts: consumer surplus, producer surplus and social surplus. A broad summary of these is shown in Table 5.8. At first glance, the PJM-style market outperforms both other markets in social surplus at all levels of demand. The NEM market design is highly competitive in terms of consumer surplus, especially at mid-range demand levels. The BM struggles to keep pace with the other two markets, but it outperforms both of those in producer surplus except at high levels of demand.

The level of demand polarises the results. The fact that the fuel mixes and the unit commitment decisions are more homogeneous at low levels of demand can explain the greater degree of

Table 5.8 : **Welfare summary**

The table shows the welfare results of the routine implementation. PJM outperforms the other two markets in terms of social surplus in general.

	NEM	PJM	BM
Consumer surplus	High	High except at mid-range demand	Low
Producer surplus	Low except at high demand	Low except at mid-range demand	High except at high demand
Social surplus	In-between	High	Low

convergence in the welfare results at those levels of demand. Arguably, when certain units are required to run for physical feasibility, there is less room for market-specific unit commitment decisions. This is reflected in the convergence of the welfare results, to some degree, at lower levels of demand.

Figure 5.4 : **Consumer surplus**

The plot shows consumer surplus and its decomposition under the different market designs at different levels of load.

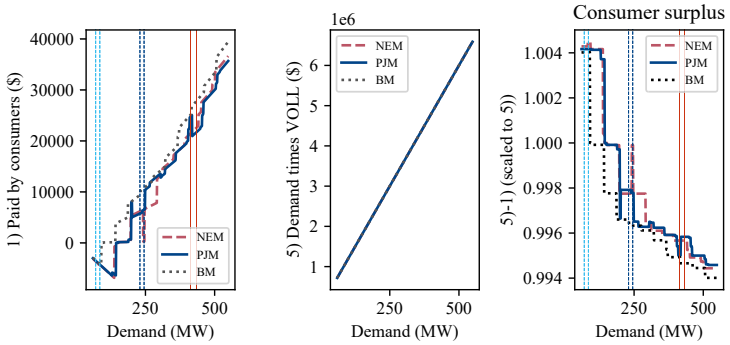

First, consumer surplus is shown in Figure 5.4 as a difference of the estimated maximum value the wholesale consumers are willing to pay (VOLL times demand) and what they pay for energy (see Table 5.2). Note that at monotonically increasing prices, the amounts paid by consumers increase with demand. However, at times of non-monotonicity, these values are decreasing, as shown between the vertical lines in colour. This in turn positively impacts consumer surplus at the highlighted non-monotonicity events. Overall, consumer surplus is typically the highest in the NEM except at very high demand. This is driven by the low amounts paid by consumers for energy.

Second, producer surplus and its components are shown in Figure 5.5. In order of magnitude, the largest component of producer surplus is what is being paid by consumers for energy. This first sub-plot shows that consumers pay less under the NEM design than under other market

Figure 5.5 : **Producer surplus**

The plot shows producer surplus and its decomposition under the different market designs at different levels of load.

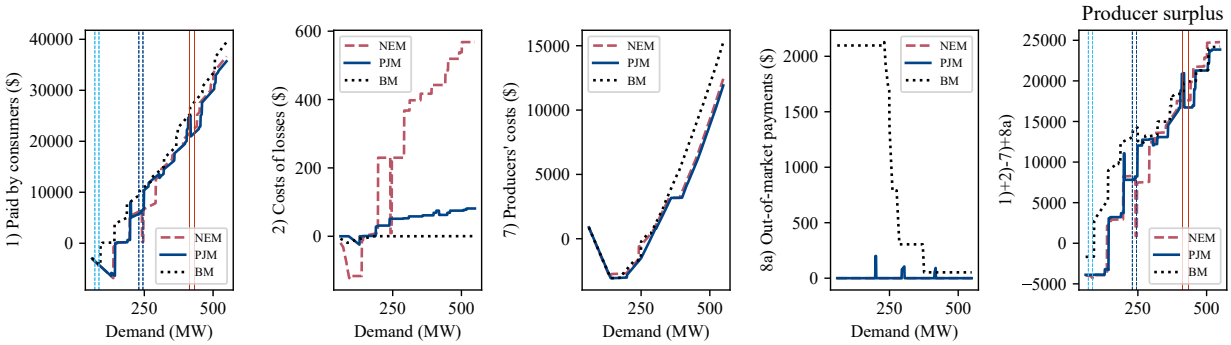

designs. In particular, the BM has the most expensive design by this metric (see discussion in Section 5.4.4.2). The second largest component of producer surplus is producers' costs, which enters with a negative sign. These costs are calculated using the equivalent costs from Table 5.6 and the quantity targets from the market-specific algorithms. The lower this cost, the higher the cost efficiency in energy dispatch excluding frequency balancing. In this respect, the PJM seems to outperform the other two markets. The third largest component of producer surplus is out-of-market payments to producers in some jurisdictions at some levels of demand. This amount is nil in the NEM under the current set of assumptions and possibly positive in the PJM and BM – see discussions in Section 5.4.4.4 and 5.4.4.5. The last and smallest component of producer surplus is the costs of losses, which producers receive. The quantity of losses appears highest in the NEM (see discussion in 5.4.4.6). Costs of losses are immaterial under other market designs. In summary, producer surplus is highest in the BM, with the PJM in second place and the NEM significantly lagging especially at mid-range demand levels.

Third, social surplus is shown for the three market designs in Figure 5.6. Two new components appear in this calculation: the amounts paid for frequency balancing services and the balancing (out-of-market) payments received by the grid operator for selling electricity back to the generators. We see that frequency balancing services are most efficiently procured through prioritisation in the BM (see discussion in Section 5.4.4.2), whereas these services themselves are more expensive in centrally co-optimised markets such as the PJM and NEM. Minor distortions to the robustness of these calculations are put forward in Section 5.4.4.7. In addition,

Figure 5.6 : **Social surplus**

The plot shows social surplus and its decomposition under the different market designs at different levels of load.

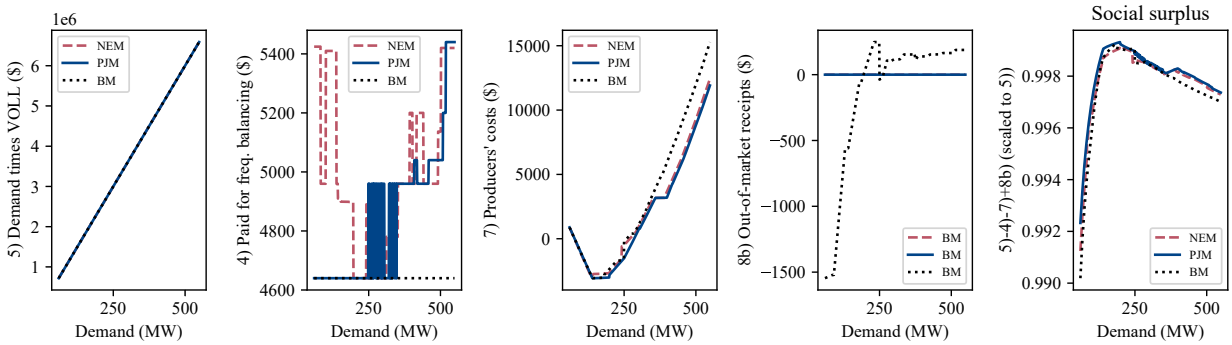

balancing receipts are only relevant for the BM (see Table 5.8). Overall, social surplus is the highest in the PJM.

5.4.4 Analysis of findings

This welfare analysis reveals that although the PJM dominates in social surplus, its advantage is not sizeable. The biggest difference between the markets lies in the fact that the BM allocates significantly more to producer surplus and less to consumer surplus than the other two markets. Further analysis of these findings is presented below.

5.4.4.1 In what way do the different market designs use different fuels as demand increases?

The optimal dispatch outcomes differ across markets based on the final fuel mix. First, Wind B comes online in the NEM at much lower levels of demand than in other markets because interconnector losses are pushing down the related prices – involving negative price marginal bids – non-monotonically. In other words, the negative price bid subject to losses appears to have an even lower cost from the perspective of the NEMDE, as it is multiplied by an MLF factor above one for imports. However, this does not result in a material cost inefficiency as per the middle sub-plot (with 7) on the y-axis) in Figure 5.5.

Second, the NEM is using Coal at $62 for frequency balancing instead of Hydro at $58 at low levels of demand. Hydro is not switched on by the NEMDE's fast-start unit commitment run, as there is already sufficient generation by Wind A and B and the must-run units;

hence, it cannot provide frequency balancing. At the same time, the PJM and BM have no joint constraints preventing Hydro from providing frequency balancing services. This flags an asymmetry of assumptions in that by using FCAS trapeziums for the NEM, we introduce a stricter set of joint constraints on frequency balancing and energy, particularly enablement minima at 5 MW, that are not present in the other markets. Although this seems to have very little effect on relative cost efficiency, future work should detail the equivalent assumptions on joint service constraints for the other markets as well.

Moreover, Gas A gets committed at different levels of demand under different market designs. In the BM, Gas A is switched on once it is cheaper to invoke offered quantities to meet the minimum loading requirement than it is to invoke bid quantities in the fuel to force Gas A offline. This takes place at roughly the same demand level as that at which the NEM's fast-start unit commitment run constrains Gas A on to dispatch. In contrast, PJM's scheduling algorithm starts dispatching Gas B before Gas A as a bridging fuel to reach the minimum loading level in Gas A.[153] Committing Gas A and the fact that it is replacing other fuels adds an observable jump to producers' costs – and a drop in cost efficiency – in the NEM and BM. The same involves a much smoother transition in the PJM, as fixed costs are disclosed in multi-part bidding and optimised centrally.

Finally, the level of demand and the initial dispatch level at which Gas C starts up differs across market designs. The NEM and PJM are reallocating Wind A from frequency balancing towards energy before switching on Gas C. The NEM turns on Gas B at lower levels of demand possibly because these quantities appear relatively cheaper in the NEM at levels below maximum capacity due to bid price amortisation at the maximum capacity level. By contrast, the quantities attract a fixed no-load cost of $100, wherefore they are only dispatched at an 'artificial' minimum loading level bridged by quantities from Gas A. In this way, the addition of Gas C to the fuel mix does not seem to cause material cost inefficiency under either market design.

[153] Owing to the fast-start integer relaxation pricing process Gas B with a higher variable cost is not setting prices at a higher level at lower level of demand before Gas A comes online, whereby lower price fuels would become marginal without integer relaxation.

5.4.4.2 *Why are consumers paying more for exchange-traded energy in Great Britain than for energy including 'balancing' in other jurisdictions?*

Trading energy over exchanges in Europe typically ignores the physical constraints to be adhered to whilst using the electric grid. Therefore, in comparing the amounts paid for exchange-traded energy in Great Britain to those paid by consumers in centrally optimised markets, it is somewhat surprising to find that the former are greater. Two aspects are to be highlighted here.

Figure 5.7 : **Cost of energy and frequency balancing**

The plot shows the amounts paid for energy and frequency balancing separately and in total.

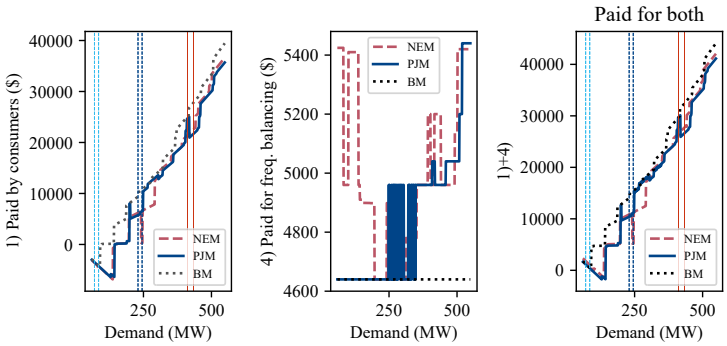

The first sub-plot comparing the amounts paid by consumers for energy in different jurisdictions in Figure 5.4 (with 1) on the y-axis) does not reveal the complete picture. In reality, the same pool of resources are used to provide energy and frequency balancing, and in centrally optimised markets, these two are usually co-optimised. In the BM, however, the auctions for frequency balancing services are assumed to take priority over energy scheduling. Therefore, as the second sub-plot (with 4) on the y-axis) in Figure 5.7 shows, the amounts paid for frequency balancing are the lowest in Great Britain. If, however, the cheapest resources are used towards these reserves, then energy might become more expensive. The sum of the amounts paid for both energy and frequency balancing services are shown in the third sub-plot in Figure 5.7. We might expect that due to a lack of physical constraints in the exchange-based self-scheduling process in Great Britain, the combined costs are still lower in that market than elsewhere.

However, we find that the combined amounts paid are still mostly the highest in Great Britain. There is a further explanation as to why this is the case, which is related to the unused capacity in the system. Earlier we set out that a proportion $m = 0.9$ of all supply capacity

is being offered day-ahead in Great Britain and in the PJM, whereas the NEM works with all capacities being offered real time. In addition, a proportion $k := m$ of demand is being settled day-ahead in the PJM, and more than that, demand minus 1 MW, in Great Britain. We see that relatively higher levels of demand are being met in the day-ahead scheme in Great Britain, which can drive prices up under standard assumptions about supply monotonicity (which hold well in constraint-free settings), especially at low levels of demand; this in part explains the lack of convergence of the BM results to the results in other markets. Note that not all amounts that remain unused from day-ahead are in fact deployed in real time. However, the necessary rearrangements to meet the physical constraints in real time might require larger unused capacities under the BM's market design than in centrally optimized settings, which is reflected in our assumptions about the value of parameter k.

5.4.4.3 Why are producers' costs decreasing with demand at low to mid levels of demand? What drives cost efficiency in different markets?

Producers' costs for energy decrease with demand under all three market designs owing to the negative variable costs of renewable fuels. These fuels are assumed to earn carbon offset income in all three jurisdictions via conceptually largely equivalent certification schemes such as LGCs in the NEM. In addition, these costs – as they only capture the energy costs and not the frequency balancing costs – see a significant drop in the PJM and the NEM when these markets withdraw from using Wind A for frequency balancing and start replacing it by Coal. Wind A can after that be used to provide energy at $0 variable and fixed costs.

5.4.4.4 When is uplift being paid in the PJM?

As mentioned earlier, uplift is being paid to generators in North American markets whenever compliance with targets causes a generator to run at a loss. In theory, the amount of uplift each unit is eligible for is computed as the difference between the profit of the unit using the optimal targets from the settlement run and the profit given the optimal targets as per the dispatch run (see (5.2.18) for the case for the PJM). In our analysis, the fourth sub-plot in Figure 5.5 shows uplift to be relatively rare. We find a few load segments with non-nil uplift between 199 and 201 MW ($200), 295 and 304 MW ($78.75 to $105.75), and 414 and 418 MW ($52.50 to $92.50).

First, between 199 and 201 MW demand, Hydro, which is committed in the reliability run, receives $200 uplift as compensation for its fixed costs. Second, at 295 MW demand, Gas B is replaced by Gas A in the settlement run when price is $P_j^* = 42$ at all nodes. More precisely, the real-time dispatch run schedules 36.25 MW by Gas B, but the subsequent settlement run only schedules 10 MW, which is the minimum loading requirement in this fuel. The bid-in price by Gas B is $45 per MWh for these quantities. Thus, the real-time dispatch run creates a 26 $\times$ (42-45) = -$78.75 negative income, which is compensated by the uplift at 295 MW load. The same pattern continues until 304 MW demand. Last, an inverse dynamic can be observed between 414 and 418 MW load when 15.25 MW by Gas C replaces Gas A and Hydro in the settlement run, implying that it would have been profitable for Gas C to run at this rate at the price of $P_j^* = 60$ despite receiving a nil real-time dispatch target rate. Recall that Gas C has a fixed no-load cost of $100 and a variable cost of $50 for the first 50 MW. Hence, not dispatching 15.25 MW came at the lost opportunity cost of 15.25 $\times$ (60-50) - 100 = $52.50. The same dynamic continues until 418 MW load. In sum, uplifts are paid when the real-time dispatch run overschedules quantities that run at sub-zero profits, taking fixed and variable costs into consideration, as seen in the first two instances, or if it underschedules infra-marginal quantities that could have been generated at a profit given the realised price.

5.4.4.5 What drives extreme positive and negative balancing costs in the BM?

Although the bid–offer spreads of the individual units are typically positive, it is sometimes possible to fulfill the balancing mandate by buying the missing 1 MW load at a relatively low price and rearranging quantities in a profitable manner. More frequently, the rearrangement involves buying high price quantities and disposing off low price quantities, which achieves modest positive balancing costs. However, we also observe extreme positive costs at low levels of demand and negative costs at high levels of demand.

First, extreme positive balancing costs occur at 100 MW demand in the BM implementation, where Gas B and Coal are forced to run at $53.375 and $52.125 at their 10 and 30 MW minimum loading levels, respectively, due to physical constraints. Therefore, 10 $\times$ $53.375 + 30 $\times$ $52.125 = $2097.5 is paid for balancing costs (see the fourth sub-plot with 8a) on the y-axis in Figure 5.5). For full rearrangement, then Wind A buys back 5 MW at -$15 and Wind

B buys back 29.58 MW at -$39.5 and 4 MW at -$14.5, which means an additional negative payment of 5 × -$15 + 29.58 × -$39.5 + 4 × -$14.5 = -$1301.41 (see the fourth sub-plot with 8b) on the y-axis in Figure 5.6), further contributing to the balancing costs shown in Figure 5.3.

Second, negative balancing costs are driven by cases where the amounts paid for balancing (8a) are lower than the amounts received from balancing (8b). Such a case can be observed at around 400 MW demand and above that demand level. At 400 MW, the following actions are taken for balancing. First, the grid operator buys 5 MW from Wind A and 5 MW from Wind B for -$5 and -$5.50 per megawatt-hour, respectively, which leads to a cost of 5 × $5 + 5 × $5.50 = $52.5. In addition, it sells 8.94 MW back to Gas A at $15.50 for a balancing receipt of 8.94 × $15.50 = $138.57. Overall, the balancing cost is negative at $52.5 - $138.57 = -$86.07.

We see that depending on how efficient exchange-based self-dispatch is, which seems to improve at higher rates of demand, the costs of balancing can generate an income or pose significant costs to the grid operator.

5.4.4.6 Why do losses cost more in the NEM than elsewhere?

Achieving equivalence of assumptions across the three market designs in terms of interconnector losses is difficult. Dynamic interconnector costs are greater in the NEM than the static interconnector losses at a mid-point value of 1.125% when Wind B is dispatched at above 35.795 MW, as $0.001 \times (35.795 - 1.125)^2 = 1.125$. Dynamic losses can go up to 8.51 MW at 100 MW targets for Wind B, as $0.001 \times 75^2 + (100 - 75 - 8.51) \times 0.175 = 8.51$ in the NEM. In contrast, losses in the PJM go up to $100 \times 0.0125 = 1.125$ in MW, whereas in the BM, they are dependent on the balancing quantities q_i^S, q_i^B only and not on the self-dispatch values Q_i^{S*}. The higher costs of losses in the NEM are primarily attributable to the higher magnitude of losses in that market setting.

5.4.4.7 Why do the shadow prices for frequency balancing deviate from the expectation?

First, in the NEM, an instability of the shadow price is observed, which drives the amounts paid for frequency balancing (see sub-plot with 4) in the y-axis in Figure 5.6). At lower levels of demand, Wind A and Coal are used for FCAS and the next unused FCAS capacity would be by

Gas C at \$80; nevertheless, we do not see costs at around 80 $\times$ \$80 = \$6400. Similar oscillatory results are observed at higher levels of demand as well probably owing to trade-offs within the binding constraint set.

Similarly, for the PJM, it is unclear why the Python MIP package's solver struggles to settle either at a price of \$58 as per the bid-in price of the last 1 MW used capacity for a total cost of 80 $\times$ \$58 = \$4640 or at a price of \$62 as per the bid-in price of the next 1 MW unused capacity for a total cost of 80 $\times$ \$62 = \$4960 at demand levels where 40 MW spinning reserves are provided by Wind A at \$13 and 40 MW by Hydro at \$58 (see the bottom sub-plot of Figure 5.2).

5.4.4.8 What drives high consumer surplus in the NEM at mid-range demand levels?

Simply put, the way Gas A is brought online over increasing levels of demand pushes real-time prices down in the NEM, which in turn raises consumer surplus. Gas A is introduced as a constrained-on quantity, which typically has a downward merit order effect on the resulting spot price owing to cheaper fuels becoming price setters in the NEM, potentially causing non-monotonicities as in the example too. Note that the non-monotonicity only came about because the 50 MW cheaper fuel capacity had to be replaced, of which 45 MW could be taken from the previously marginal fuel Hydro, but an additional 5 MW was due to be subtracted from the even cheaper Wind B. Had Wind B not entered, the price would have not exhibited any non-monotonicity. We do not observe a similar effect of committing Gas A in other markets due to fast-start integer relaxation pricing in the PJM and pay-as-bid settings in the BM.

5.4.4.9 What market design elements warrant high producer surplus in the BM and what impair it?

At lower levels of demand, the BM is leading in producer surplus. This is attributable to its relatively high exchange-based prices, high balancing payments and competitiveness in cost efficiency. At higher levels of demand, however, the rearranging of much lower quantities for balancing and the fact that it is scheduling low-price frequency balancing services impairs its ability to remain cost competitive in energy dispatch, which then leads to relatively lower producer surplus levels.

5.4.4.10 *What market design elements promote the first place of the PJM in social surplus?*

The PJM is the most cost efficient among all three markets, which is likely because of multi-part bidding and the fact that fixed cost components are part of central optimisation.

5.4.5 Scaling to real-world systems

It is key to highlight some caveats about scaling this small-scale analysis to real-world systems before drawing any meaningful conclusions. Markets in reality are larger in size and physically more complex, they carry out multi-period processes instead of fixing certain assumptions for one-shot pricing, and they tend have more complex pre-dispatch mechanisms and often capacity markets as well. Also, sometimes they operate at extreme demand levels that we truncated for convenience. The role a financial market plays alongside a physical electricity market is also not negligible: for example, in the absence of day-ahead markets, units might seek firmness via forward contracts. These factors are not considered within the scope of the small-scale case study, but it is important to ask whether and how they might impact non-monotonicity and welfare.

In general, increasing the size of the system by adding more generator units increases the number of applicable physical constraints. We identified minimum loading constraints to cause non-monotonicities in the NEM. Therefore, some of the added units are very likely to have this requirement, thus increasing the number of non-monotonicities along the supply curve. However, taking a step back, just adding more previously offline slow-start generators to the system that have positive fixed costs – without any minimum loading constraints involved – increases the chance of non-monotonicity, too, in the PJM.[154]

Moreover, adding more types of frequency balancing services and other ancillary service types to the problem definition introduces new joint constraints to the optimisation problem. In our case study, a change in the initial assumptions as simple as labelling Hydro's frequency balancing cost to be one dollar more, \$63 instead of \$62, can be shown to invoke a trade-off effect in the PJM, where serving the next 1 MW in energy rearranges the fuel mix serving frequency balancing, which is then reflected in the energy price. The NEM is also susceptible

[154]Note that slow-start plants are expected to have longer minimum run times, which means that they are constrained-on longer and perhaps shut down more infrequently to meet the condition of being previously offline.

to such trade-off effects.[155] In combination with non-convex elements, such trade-off effects are potential sources of non-monotonicity. Therefore, we argue that real-world systems with more complex product portfolios and constraint sets are more prone to non-monotonicities than their small-scale counterparts.

It would be interesting to see how adding more physical constraints to a simplified dispatch optimisation problem – until obtaining a very reliable real-world system – would impact welfare under different market designs. The present work has confirmed that balancing cost payments to producers significantly increases producer surplus and that negative balancing cost receipts from units due to negative pay-as-bid prices weaken social surplus results in the BM at low levels of demand when several must-run constraints are binding. When more constraints are added, balancing costs are likely to rise faster in the BM than required to keep pace with other market designs in terms of welfare. The case study could easily be extended to test this hypothesis and capture the welfare effect of adding further constraints under all three market designs.[156]

Another vital aspect of real-world systems is multi-interval planning either by the market operator or by the individual units. For example, in the NEM, bidding its must-run quantities at -$999 is the result of an inter-temporal optimisation for the Coal unit. The Coal unit could have also chosen to withdraw capacities from the market by bidding in a nil maximum availability in the face of a series of low demand intervals where it might be operating at a considerable loss. In that case, the market operator could have stepped in to invoke some intervention framework to constraint the Coal unit on while adhering to plant-level inflexibilities. This response mechanism is particularly relevant at very low levels of demand when reaching an equilibrium is more likely to involve market interventions. Our small-scale numerical example finds that the plausibly intervention-free demand ranges are to some extent – but not fully – overlapping under different market designs and focuses on those entirely. Careful analysis of inter-temporal and one-off interventions is subject to future work.[157]

---

[155] One upshot of this is that negative price bids from outside the pricing region can become marginal (price-relevant) due to trade-offs across several binding constraints at relatively high levels of demand too, implying that non-monotonicities due to dynamic interconnector losses can occur at higher demand levels in the NEM.

[156] Another hypothesis to test would be the welfare effect of fast-start integer relaxation in the PJM.

[157] The role of multi-interval day-ahead, intra-day and real-time demand forecasts, their accuracy, synchrony, and effect of welfare should also be investigated and presented in a more precise and perhaps probabilistic manner when extending the case study to interventions.

Furthermore, the argument put forward in Creative Energy Consulting (2020) is that the efficiency of NEM self-scheduling lies in that the units are allowed to update their bid submission, which might include disorderly bid prices in a way that reflects private information only they are privy to, in the pre-dispatch mechanism continuously until gate closure (see Chapter 3 for details). In contrast, the reliability run in the PJM takes place only a number of times, primarily day-ahead, and may not capture some updates that are private information. Although we have included one reliability run for the PJM in our numerical case study, this alone cannot accurately depict the full-blown pre-dispatch mechanism in the three focus markets.

All three market designs have been shown as if they were energy-only market designs. However, capacity markets do operate in the PJM and BM, which we have so far omitted. Future work should rectify this omission.

Last, the plant-level technical assumptions behind the numerical example emulating the real-world bid submission templates are not sufficiently precise to be equivalent across the three markets. For instance, introducing frequency balancing minima into the markets on both sides of the Atlantic, similar to the FCAS trapezium for the NEM, could bring about interesting developments in terms of both supply non-monotonicity and welfare. Also, the rules around making plant-level decisions on maximum availability, such as on withdrawing from the market in face of a low demand forecast, would be interesting to compare in greater detail.

5.5 Implications

The implications of the above findings for incentive compatibility and economic equilibrium modelling are described below.

5.5.1 Incentives under non-monotonicity

Incentive compatibility is satisfied when actors bid at their true costs as price takers and comply with the central allocation of unit commitment and dispatch, which is assumed to be efficient (Chao (2019)). We argue that incentive compatibility is hindered by supply non-monotonicities in general and discuss the subtleties of this relationship. In addition, we detail the extent to which parties are made whole under different degrees of incentive compatibility under different market designs.

First, in the Australian context, allowing disorderly bids and/or bid convexification is a way to circumvent certain non-convexities in the problem formulation. Thus, incentive compatibility is violated in the process of preventing non-monotonicities through self-scheduling, such as by eliminating fixed costs or ignoring plant-level inflexibility profiles for slow-start plants. Moreover, allowing disorderly bids in the self-schedules gives units not only a degree of discretion in bidding, including the chance to charge premia, but also the legal liability to comply with the central allocation resulting from their bids. Hence, whereas the first part of incentive compatibility might not be met, the second part is actively enforced. To the extent units are unsuccessful in bidding disorderly in a way that turns out to be optimal to them under non-convexities, such as fixed costs, as well as unprevented non-monotonicities, e.g., due to dynamic interconnector losses, they are left without any compensation for disincentives to comply with the targets allocated to them. In our small-scale numerical example, the units are assumed to use a simple cost convexification method without any adjustments for private information and apply no price premium, which resulted in a relatively low producer surplus and a state of the market where units may not have been made whole for their fixed costs. The fact that units may not have been made whole due to non-monotonicity is a weakness of the current NEM market design that should be addressed in the future to promote fairness.

By contrast, a single uniform price is shown to be insufficient to remove the incentive to deviate from the efficient allocation under the non-convex North American formulation. An additional, discriminatory price component for uplift is justified by the arguments in Elmaghraby et al. (2004), Liberopoulos and Andrianesis (2016), Chao (2019) and Wang et al. (2023).[158] It is imperative not to omit uplift payments when focussing on the truthfulness of the bids underpinning non-monotonic supply curves from uniform prices, as any price suppression (non-monotonicity) effect of fixed costs is being compensated through uplifts. Note that non-monotonicity is also less prevalent under the more recently introduced fast-start integer relaxation module. Therefore, the North American design warrants a greater degree of, if not full, incentive compatibility. Full incentive compatibility may not be attainable under this type of market design because units remain privy to information about their true costs, and the standardised bid submission format fails to capture every detail in that respect, again, impairing the

[158] See also references therein.

extent to which parties are made whole.

Additionally, incentives in two connected market facilities are also directly impacted by supply curve non-monotonicities in wholesale electricity. As Byers and Hug (2023) note, these can disturb the efficacy of demand response programs. Furthermore, non-monotonicities adversely impact virtual bidding outcomes (PJM (2017)).

5.5.2 Implications for market modelling

Equilibrium models have become increasingly important in electricity market analysis with wide-spread deregulation. At the core of these models, an equilibrium supply quantity is balanced against an equilibrium demand quantity whose amounts are specified in aggregate supply and demand functions, respectively. In most bid stack models, the market supply curve is exponentially increasing (Carmona et al. (2013)); in most supply function equilibrium models, there is an explicit monotonicity requirement (Day et al. (2002)); and although complementarity-based models seem agnostic to supply curve monotonicity, they do not disprove the need for non-monotonic formulations (Ruiz et al. (2014)). These model classes and their nexus to our main premise are developed next.

5.5.2.1 Market power models

The literature proposes two broad categories of equilibrium models. Models in the first category provide some measure of market power and those in the second generally aim at spot price simulation. More specifically, the first set of models formulates the Nash equilibrium of the market power problem either as an analytical supply function equilibrium (SFE), or as a complementarity-based system. In SFE models, starting with Klemperer and Meyer (1989) and Green and Newbery (1992), the generating companies optimise their continuous supply functions[159] using some parameters of those functions as decision variables.[160] The function

[159] This closely tracks the real-world format of bid-based strategies (bidding) in electricity markets as opposed to 'games in quantity' (Cournot) or 'games in price' (Bertrand) where a firm's decision variable is one-dimensional.

[160] Static candidate solutions are then obtained by solving first-order equilibrium conditions, which can be ordinary differential equations in the simple case or integro-differential equations in networks with loops according to Ruddell (2017), or using numerical techniques for asymmetric firms as in Anderson and Hu (2008) and Holmberg (2009). Unfortunately, SFEs quickly become intractable for large-scale networks with security-constraint considerations (Day et al. (2002)).

space is typically greatly restricted by the initial assumptions to satisfy existence as mentioned in Day et al. (2002). Costs are mostly convex in these types of models as in Liberopoulos and Andrianesis (2016). Importantly, only strictly monotonic unit-level supply curves are considered (monotonicity requirement) through the use of appropriate assumptions (Holmberg et al. (2013)), monotonicity constraints and 'ironing'[161] (Ruddell (2017); Wilson (2008)). As a consequence, prices from these models are expected to be monotonically increasing in demand.

In contrast, in complementarity-based systems, the generating companies optimise their individual cost functions using only quantity (Cournot games) (Cardell et al. (1997)), or the quantity and some parameter of the rivals' conjectured (affine) response function as in Hobbs et al. (2000) and Day et al. (2002), as decision variables. Only the aggregate demand function and not the aggregate supply function is given a functional form.[162] Although there are multiple variations to this type of models in the literature – preeminently mixed complementarity problems (MCP)[163] and mathematical programs with equilibrium conditions (MPEC)[164] – the question of supply non-monotonicity is rarely considered even in the presence of non-convex costs.[165] One notable exception is Cheng et al. (2021) who devise an optimisation method for solving MPECs

[161] As Ruddell (2017) explain, "Succinctly, ironing means that where a supply curve is forced at (perfectly elastic or perfectly inelastic) by the monotonicity constraint, there it must satisfy the first-order optimality condition on average over the whole flat segment.".

[162] Given $f = 1, 2, ..., F$ generating companies (firms) that wish to optimise their decision variables x_f with objective functions and inequality constraints $f_f(x)$ and $g_f(x)$, respectively, each firm's problem is $\min_{x_f} f_f(x)$ such that $g_f(x) \leq 0 : \mu_f$ and $-x_f \leq 0 : \beta_f$, where μ_f and β_f are the duals, and $f_f(x)$ includes the demand function of quantity x for the price, paraphrasing Ruiz et al. (2014). As long as $f_f(x)$ and $g_f(x)$ are continuously differentiable and convex, a system of KKT equilibrium conditions are both necessary and sufficient to give an equivalent solution of the optimisation problem (Ruiz et al. (2014)), although the convexity assumption is in reality incorrect for $g_f(x)$ due to unit commitment-type binary decisions in the KKT constraints, as in Day et al. (2002).

[163] Mixed complementarity problems (MCP) include both equality and complementarity conditions and the problem is square if the number of endogenous decision variables equals the number of individual KKT conditions (Ruiz et al. (2014)). This usually breaks down when a complementarity condition simultaneously links the feasible regions of the different firms, resulting in infinitely many equilibria, since it adds as many decision variables as there are firms for a single condition, unless the associated dual variables are restricted to the same value for all firms (Ruiz et al. (2014)). This restriction often assumes that firms are price-takers in transmission prices and do not manipulate their outputs to benefit from congestion or decongestion as in Hobbs and Helman (2003).

[164] In game theory, the leader firm is the one that determines its strategy first, often by anticipating the follower firms' reactions, and the follower firms only determine their strategy after that. Using these definitions, we can also note that embedding the followers' or the market operator's equilibrium problem, given the actions of the leader firm, into the KKT conditions of the leader firm in a bilevel (Stackelberg) game yields non-convex feasible regions. Therefore, nothing in general can be asserted about the existence and uniqueness of the equilibrium in these problems. MPECs are typically solved using equilibrium programs with equilibrium constraints (EPECs), as explained in Ruiz et al. (2014) and Hobbs and Helman (2003).

[165] It is not well understood if supply aggregation mechanisms that give rise to non-monotonic market supply curves also destabilise certain types of complementarity-based model solutions.

while accommodating non-monotonic unit-level bid curves, e.g., due to deep peak regulation.[166] Furthermore, Yang et al. (2013) suggest a formulation that allows for non-monotonic unit-level incremental cost curves due to valve point loadings.[167]

5.5.2.2 Pricing models

The properties of the inverse supply function are also highly relevant to bid stack–type models that solve for the electricity price by using an inelastic demand quantity as a modelled input variable and formulating the market bid stack function (aggregate inverse supply function) as a parametric map. This map transforms a typically Gaussian process for load into the required non-Gaussian price dynamic with spikes (see Meyer-Brandis and Tankov (2008)). The proposed continuous inverse market supply functions are often calibrated by fitting the bid stack data. Importantly, they are assumed to be exponential (Burger et al. (2004); Aid et al. (2009); Carmona et al. (2013); Kiesel and Kusterman (2016)), a quantile function (Howison and Coulon (2009)), a Box-Cox power transform (Barlow (2002)), a power law function (Aid et al. (2013)) or a (piece-wise) polynomial (Kanamura and Ōhashi (2007); Ware (2019)). The functional forms of the modelled aggregate inverse supply functions or additional elements, such as regime switching, often capture the price effects of system scarcity as a departure from the energy-only bid data. However, the inverse supply curve is considered to be monotonically increasing in all of these functional specifications.

The use of probabilistic layers onto the main market bid stack curve similar to the regime switching solution by Carmona and Coulon (2014) (cf. Carmona et al. (2013)) is a way to part with the perfect monotonicity of supply in the assumptions.

5.6 Conclusion

It is a pervasive assumption in both academia and industry that the price of electricity increases as the demand in the system rises. This chapter cites forerunning literature and lays down new evidence on the topic, weakening the validity of this monotonicity assumption. Mar-

[166] Deep peak regulation of thermal units is used to cope with high wind penetration (Yang et al. (2019)).

[167] As Fraga et al. (2012) write, “Modelling valve point loadings is necessary to capture the losses incurred due to the throttling of partially open valves in electric power generators.”.

ket design–implied inverse supply curves are examined in the context of the PJM in the United States, the NEM in Australia and the BM in Great Britain. First, we find that supply curves do not always exist – for example they do not exist in the context of the BM, where there is discretionary pricing for balancing. Second, there is not always a single-part real-time price, such as in the PJM, that would appropriately outline the values along the inverse supply curve.

Different measures of welfare are compared considering these complicating factors via a numerical example. The core principle of this example is having three physically and economically equivalent small-scale markets with market settings resembling the three examined market designs as closely as possible. This allows an evaluation of these on welfare and the components of welfare, such as cost efficiency. Some elements of market design can then be identified to drive these components; for example, multi-part bidding drives a smooth cost curve (no jumps), which speaks of greater cost efficiency driving better social surplus results. Similarly, high balancing payments are an important part of why the BM outperforms the other markets in producer surplus, and somewhat surprisingly, the same replacement mechanism that can cause supply non-monotonicity in the NEM suppresses prices too, to the point where the NEM leads in consumer surplus.

Even if a single uniform price for electricity can be obtained, this price does not always increase with increasing load in the market due to non-convexities such as fixed costs and minimum loading requirements as well as dynamic interconnector losses. Indeed, Hogan and Ring (2003); Bjørndal and Jörnsten (2008); Ruiz et al. (2012); Gribik et al. (2007); Byers and Hug (2023) have previously found that fixed costs as part of multi-part bidding and minimum loading requirements cause non-monotonicity of supply. In addition, our study shows new evidence that dynamic interconnector losses and ancillary service co-optimisation may also result in non-monotonicity. These contributions have important implications for incentive compatibility within particular market designs as well as for market modelling on equilibrium principles. Therefore, the key idea emerging from the current discussion is that pricing models and analytical heuristics relying on a monotonic supply relationship should be re-evaluated and updated prior to wide-spread use in applications.

Chapter 6

Conclusion

This thesis presents four essays on electricity market design, semi-structural price modelling, supply function non-monotonicity and welfare in electricity markets. The first two essays cover market designs in the integrated pool model in general and the market design of the Australian NEM in particular to better understand the applicability of existing semi-structural market models, with a specific focus on bid stack–type modelling frameworks, to price modelling in the NEM.

Most bid stack models in the literature appear to be built upon market structures reflecting the North American or European standards. These models often lack some required properties under the NEM market design, such as price negativity, load-dependent fuel availability, the inclusion of renewable and storage fuels and network constraint effects, or the use of cleared generation as a proxy for demand. To fill this gap in the literature, the third essay presents our revised price hypothesis in the form of a novel hyperbolic bid stack approach to electricity price modelling. In this bid stack model, much like in any other bid stack model before it, supply is assumed to be monotonically increasing.

The fourth essay explores the applied cases of non-monotonicity in electricity markets. It argues that due to non-convexities or dynamic interconnector flows in the optimisation problem, supply is not always a monotonically increasing function of quantity demanded under certain market design settings. A small-scale numerical study underpins these arguments and compares the implied supply curves and the amount of welfare gained under three real-world market designs. This enables us to draw conclusions about the effectiveness of these market designs.

Upon reflection, this thesis spans a broad topic. Studying any single wholesale electricity market from physical flows – which is the domain of electrical engineering – to how pricing works, whether it efficiently impacts welfare, and how to model it in a semi-structural manner, is an ambitious undertaking. Nevertheless, a comparison of three different market designs is

presented in algorithmic detail, albeit in a simplified setting.

6.1 Limitations and further research

This thesis has a number of limitations. First, the survey of the NEM in Chapter 3 seeks to provide an up-to-date account of market design. However, this is only possible to the extent that the market design remains constant over time, which is hardly the case in electricity markets, as rule changes are frequently being brought forward. Therefore, the presented research undertaken between 2020 and 2023 is already, to some degree, outdated. For example, the Rules version 175 is referenced (AEMC (2021*c*)) instead of version 204 as of December 2023.

Second, in Chapter 5, the conclusions are drawn from a supply monotonicity and welfare analysis that considers a relatively small and physically simple, one-shot market without an elaborate pre-dispatch run or without considering the complete set of ancillary service and other side service markets. Another limitation is the units' equivalence in their slow- or fast-start classification and plant specifications across the three jurisdictions, as different definitions, classifications and bidding formats co-exist worldwide. Moreover, the fuel mixes of the discussed real-world markets are different and therefore the connecting physical constraint sets vary. Acknowledging that there is a limit to the extent to which a physically and economically equivalent assumption set of these markets can be set out, it is also very interesting to see how different market designs distinguish themselves in the way grid extensions are integrated, network constraints are formulated, carbon offsets are factored in and incentive compatibility and informational efficiency are encouraged. Future work aims to execute re-runs of the existing model behind the numerical example that measures the welfare effects of changing single assumptions in each of the three market design frameworks.

Finally, the fourth essay in this thesis that finds the inverse supply curve (or market bid stack curve) in the NEM being non-monotonic affects the hyperbolic market model in Chapter 4. Importantly, the fuel bid curves in Section 4.2.2.1 remain monotonic with the invertibility condition intact, as the bids of the units always take a monotonically increasing form. However, the central bid aggregation process leads to a non-monotonic effect. Forthcoming work should address this development.

Apart from the shortcomings listed above, it is highly plausible that we made further omis-

sions unbeknownst to us simply because the topic at hand is constantly evolving to accommodate regulatory changes, macro-economic conditions and actions to combat the impacts of climate change.

References

AEMC (2013), 'Management of negative inter-regional settlements residues, Issues Paper, 18 April 2013, Sydney'. URL: https://www.aemc.gov.au/sites/default/files/content/24248fd6-739e-4d38-a4b8-9be79d05fcc8/Issues-Paper.PDF.

AEMC (2014), 'Management of negative inter-regional settlements residues, Final Report, 20 February 2014, Sydney'. URL: https://www.aemc.gov.au/sites/default/files/content/c651efa3-ddfc-4a5d-9f75-650fcf5010c2/Final-Report.PDF.

AEMC (2015), 'Bidding in Good Faith, Final Rule Determination, 10 December 2015, Sydney'. URL: https://www.aemc.gov.au/sites/default/files/content/815f277c-a015-47d0-bc13-ce3d5faaf96d/Final-Determination.pdf.

AEMC (2018*a*), 'Congestion Management Review – Final Report, Appendix A: An introduction to congestion in the NEM'. URL: https://www.aemc.gov.au/sites/default/files/content/42a1dfd9-bf32-4bf1-bcc4-81dd8095dfc7/Final-Report-Appendix-A-An-introduction-to-congestion-in-the-NEM.PDF.

AEMC (2018*b*), 'Congestion Management Review – Final Report, Appendix E: Additional background information'. URL: https://www.aemc.gov.au/sites/default/files/content/d8332368-feaf-4a38-b6af-850de3c3df3a/Final-Report-Appendix-E-Additional-background-information.PDF.

AEMC (2019*a*), 'Coordination of Generation and Transmission Investment - Access Reform, Directions paper, 27 June 2019'. URL: https://www.aemc.gov.au/sites/default/files/2019-06/COGATI%20-%20directions%20paper%20-%20for%20publication_0.PDF.

AEMC (2019*b*), 'Five minute settlement and global settlement implementation amendments, Consultation paper, 13 June 2019'. URL: https://www.aemc.gov.au/sites/default/files/2019-06/ERC0267%20Consultation%20paper.PDF.

AEMC (2020), 'Transmission Access Reform (COGATI), 26 March 2020'. URL: https://www.aemc.gov.au/sites/default/files/documents/technical_specifications_report_-_transmission_access_reform_-_march_update.pdf.

AEMC (2021*a*), 'AEMC publishes the schedule of reliability settings for 2021-22'. URL: https://www.aemc.gov.au/news-centre/media-releases/aemc-publishes-schedule-reliability-settings-2021-22#:~:text=The%20Australian%20Energy%20Market%20Commission,to%20the%20national%20electricity%20market., Accessed on 1 October 2021.

AEMC (2021*b*), 'Integrating energy storage systems into the NEM, Draft rule determination, 15 July 2021'. URL: https://obpr.pmc.gov.au/sites/default/files/posts/2021/07/Integrating%20energy%20storage%20systems%20into%20the%20NEM%20-%20ERC0280%20-%20Draft%20determination.pdf.

AEMC (2021*c*), 'National Electricity Rules version 175'. URL: https://energy-rules.aemc.gov.au/ner/356.

AEMC (2021*d*), 'Security'. URL: https://www.aemc.gov.au/energy-system/electricity/electricity-system/security, Accessed on 1 September 2021.

AEMC (2021*e*), 'Semi-scheduled generator dispatch obligations, Rule determination, 11 March 2021'. URL: https://www.aemc.gov.au/sites/default/files/documents/erc0313_-_final_determination_-_for_publication.pdf.

AEMC (2022*a*), 'Electricity supply chain'. URL: https://www.aemc.gov.au/energy-system/electricity/electricity-system/electricity-supply-chain, Accessed on 1 March 2022.

AEMC (2022*b*), 'National energy governance'. URL: https://www.aemc.gov.au/regulation/national-governance, Accessed on 3 March 2022.

AEMC (2023), '2022-23 market price cap now available'. URL: https://www.aemc.gov.au/news-centre/media-releases/2022-23-market-price-cap-now-available, Accessed on 20 August 2023.

AEMO (2009), 'Proportioning inter-regional losses to regions'. URL: https://aemo.com.au/-/media/files/electricity/nem/security_and_reliability/loss_factors_and_regional_boundaries/2009/0170-0003-pdf.pdf.

AEMO (2010*a*), 'ESOPP guide – Confidence levels, offsets & operating margins – Policy'. URL: https://www.aemo.com.au/-/media/files/electricity/nem/security_and_reliability/congestion-information/2016/confidence_levels_offsets_and_operating_margins.pdf.

AEMO (2010*b*), 'Pre-dispatch process description'. URL: https://aemo.com.au/-/media/files/electricity/nem/security_and_reliability/dispatch/policy_and_process/pre-dispatch-process-description.pdf, Accessed on 19 June 2020.

AEMO (2010*c*), 'Treatment of dispatchable loads in the NEM'. URL: https://aemo.com.au/-/media/files/electricity/nem/security_and_reliability/dispatch/policy_and_process/treatment-of-dispatchable-loads-in-the-nem.pdf, Accessed on 19 June 2020.

AEMO (2011), 'Over-Constrained Dispatch Rerun Process document'. URL: https://www.aemo.com.au/-/media/Files/Electricity/NEM/Security_and_Reliability/Congestion-Information/2016/Over-Constrained-Dispatch-Rerun-Process.pdf.

AEMO (2012*a*), 'Non-market ancillary services'. URL: https://aemo.com.au/-/media/files/electricity/nem/security_and_reliability/power_system_ops/procedures/so_op_3708-non-market-ancillary-services.pdf?la=en&hash=DEA7DF4A06ED236BBC52B694569EA929.

AEMO (2012*b*), 'Short Term PASA Process Description'. URL: https://aemo.com.a

u/-/media/Files/Electricity/NEM/Planning_and_Forecasting/Solar-and-Wind/STPASAProcessDescriptionFinalpdf.pdf.

AEMO (2012*c*), 'Treatment of Loss Factors in the National Electricity Market'. URL: https://www.aemo.com.au/-/media/Files/Electricity/NEM/Security_and_Reliability/Loss_Factors_and_Regional_Boundaries/2016/Treatment_of_Loss_Factors_in_the_NEM.pdf.

AEMO (2013), 'Constraint Naming Guidelines'. URL: https://www.aemo.com.au/-/media/files/electricity/nem/security_and_reliability/congestion-information/2016/constraint-naming-guidelines.pdf.

AEMO (2014*a*), 'Guide to Generator Energy Limitation Framework (GELF) Declarations'. URL: https://www.aemo.com.au/-/media/files/market-it-systems/historical/guide_to_gelf_declarations_2014_july.pdf.

AEMO (2014*b*), 'Intervention, Directions and Clause 4.8.9. Instructions'. URL: https://www.aemo.com.au/-/media/archive/files/other/consultations/nem/soop-3707-intervention-direction-and-clause-489-instructions-sept-2014.pdf.

AEMO (2014*c*), 'Methodology for the Allocation and Distribution of Settlements Residue'. URL: https://aemo.com.au/-/media/files/electricity/nem/settlements_and_payments/settlements/methodology_for_the_allocation_and_distribution_of_settlements_residue_july_14.pdf.

AEMO (2015*a*), 'Constraint implementation guidelines'. URL: https://www.aemo.com.au/-/media/files/electricity/nem/security_and_reliability/congestion-information/2016/constraint-implementation-guidelines.pdf.

AEMO (2015*b*), 'Reliability standard implementation guidelines'. URL: https://aemo.com.au/-/media/archive/files/electricity/consultations/2015/reliability-standard-implementation-guidelines-amended-report.pdf.

AEMO (2016), 'Automated procedures for identifying dispatch intervals subject to review'. URL: https://aemo.com.au/-/media/files/stakeholder_consultation/consultations/nem-consultations/2019/dispatch/automated-procedures-for-identifying-dispatch-intervals-subject-to-review---superseded.pdf.

AEMO (2017*a*), 'Constraint relaxation procedure'. URL: https://aemo.com.au/-/media/files/electricity/nem/security_and_reliability/congestion-information/2016/constraint-relaxation-procedure.pdf.

AEMO (2017*b*), 'FCAS model in the NEMDE'. URL: https://nempy.readthedocs.io/en/latest/_downloads/e3c8a21d3084db332a30bd0d564e93c3/FCAS%20Model%20in%20NEMDE.pdf, Accessed on 14 December 2023.

AEMO (2017*c*), 'Guide to Energy and FCAS Offers'. URL: https://www.aemo.com.au/-/media/files/electricity/nem/it-systems-and-change/2018/guide-to-energy-and-fcas-offers.pdf?la=en.

AEMO (2017*d*), 'Guide to the Market Suspension Pricing Schedule'. URL: https://aemo.com.au/-/media/files/stakeholder_consultation/consultations/nem-consultations/2019/dispatch/guide-to-market-suspension-pricing-schedule---suspended.pdf.

AEMO (2017*e*), 'Interconnector Capabilities'. URL: https://www.aemo.com.au/-/media/Files/Electricity/NEM/Security_and_Reliability/Congestion-Information/2017/Interconnector-Capabilities.pdf.

AEMO (2018), 'Congestion information resource guidelines'. URL: https://www.aemo.com.au/-/media/files/electricity/nem/security_and_reliability/congestion-information/2018/congestion_information_resource_guidelines_2018.pdf?la=en.

AEMO (2019*a*), 'Guide to Administered Pricing'. URL: https://aemo.com.au/-/media/files/stakeholder_consultation/consultations/nem-consult

ations/2019/dispatch/guide-to-administered-pricing---final.pdf.

AEMO (2019*b*), 'Guide to Intervention Pricing'. URL: https://aemo.com.au/-/media/files/stakeholder_consultation/consultations/nem-consultations/%E2%80%8C2019/%E2%80%8Cdispatch/guide-to-intervention-pricing.pdf?la=en&hash=4EB7C0EA39AB0103A5674182F58C64B8.

AEMO (2019*c*), 'Guide to the Settlements Residue Auction'. URL: https://aemo.com.au/-/media/files/electricity/nem/settlements_and_payments/settlements/2019/guide-to-the-settlements-residue-auction.pdf?la=en&hash=FF4564280891B22874B65060013A48D0.

AEMO (2020*a*), 'Energy Adequacy Assessment Projection (EAAP) Guidelines'. URL: https://www.aemo.com.au/-/media/files/stakeholder_consultation/consultations/nem-consultations/2020/rsig/final-documents/eaap-guidelines.pdf?la=en.

AEMO (2020*b*), 'Forward-Looking Transmission Loss Factors'. URL: https://aemo.com.au/-/media/files/electricity/nem/security_and_reliability/loss_factors_and_regional_boundaries/forward-looking-loss-factor-methodology.pdf?la=en.

AEMO (2020*c*), 'Market Modelling Methodologies'. URL: https://aemo.com.au/-/media/files/electricity/nem/planning_and_forecasting/inputs-assumptions-methodologies/2020/market-modelling-methodology-paper-jul-20.pdf?la=en#:~:text=AEMO%20generally%20uses%20three%20models,two%20variants%20of%20differing%20granularity.&text=The%20time%2Dsequential%20model.&text=The%20gas%20supply%20model.

AEMO (2020*d*), 'Medium Term PASA Process Description'. URL: https://aemo.com.au/-/media/files/stakeholder_consultation/consultations/nem

-consultations/2020/rsig/final-documents/mt-pasa-process-description.pdf?la=en.

AEMO (2020*e*), 'National Electricity Market Constraint Report 2020'. URL: https://aemo.com.au/-/media/files/electricity/nem/security_and_reliability/congestion-information/2020/nem-constraint-report-2020-summary-data.xlsx.

AEMO (2020*f*), 'Network Support and Control Ancillary Services Description and Quantity Procedure'. URL: https://aemo.com.au/-/media/files/electricity/nem/security_and_reliability/ancillary_services/nscas-description-and-quantity-procedure-v21.pdf.

AEMO (2020*g*), 'Procedure for the Exercise of the Reliability and Emergency Reserve Trader'. URL: https://www.aemo.com.au/-/media/Files/Electricity/NEM/Emergency_Management/RERT/Procedure_for_the_Exercise_of_Reliability_and_Emergency_Reserve_Trader_RERT.pdf.

AEMO (2021*a*), '2021 Electricity Statement of Opportunities'. https://aemo.com.au/-/media/files/electricity/nem/planning_and_forecasting/nem_esoo/2021/2021-nem-esoo.pdf?la=en.

AEMO (2021*b*), '2021 Inputs, Assumptions and Scenarios Report'. URL: https://aemo.com.au/-/media/files/major-publications/isp/2021/2021-inputs-assumptions-and-scenarios-report.pdf?la=en.

AEMO (2021*c*), 'Brief on Automation of Negative Residue Management'. URL: https://www.aemo.com.au/-/media/Files/Electricity/NEM/Security_and_Reliability/Dispatch/Policy_and_Process/2018/Brief-on-Automation-of-Negative-Residue-Management.pdf.

AEMO (2021*d*), 'Constraint Formulation Guidelines'. URL: https://aemo.com.au/-/media/files/stakeholder_consultation/consultations/nem-consultations/2020/wholesale-demand-response/first-stage/constraint-formulation-guidelines.pdf?la=en.

AEMO (2021*e*), 'Constraint Frequently Asked Questions'. URL: https://aemo.com.au/en/energy-systems/electricity/national-electricity-market-nem/system-operations/congestion-information-resource/constraint-faq, Accessed on 1 October 2021.

AEMO (2021*f*), 'Demand Terms in EMMS Data Model'. URL: https://aemo.com.au/-/media/files/electricity/nem/security_and_reliability/dispatch/policy_and_process/demand-terms-in-emms-data-model.pdf?la=en.

AEMO (2021*g*), 'Dispatch'. URL: https://aemo.com.au/-/media/files/electricity/nem/5ms/procedures-workstream/stakeholder-consultation/dispatch-procedures/so_op_3705---dispatch---marked-up.pdf.

AEMO (2021*h*), 'Electricity Data Model'. URL: https://nemweb.com.au/Reports/Current/MMSDataModelReport/Electricity/MMS%20Data%20Model%20Report.htm, Accessed on 1 October 2021.

AEMO (2021*i*), 'Fact Sheet – The National Electricity Market'. URL: https://aemo.com.au/-/media/files/electricity/nem/national-electricity-market-fact-sheet.pdf.

AEMO (2021*j*), 'Fast Start Inflexibility Profile'. URL: https://aemo.com.au/-/media/files/electricity/nem/security_and_reliability/dispatch/policy_and_process/fast-start-unit-inflexibility-profile.pdf.

AEMO (2021*k*), 'Guide to Ancillary Services in the NEM'. URL: https://aemo.com.au/-/media/files/electricity/nem/security_and_reliability/ancillary_services/guide-to-ancillary-services-in-the-national-electricity-market.pdf, Accessed on 2 October 2022.

AEMO (2021*l*), 'Guide to Scheduled Loads'. URL: https://aemo.com.au/-/media/files/stakeholder_consultation/consultations/nem-consultations/2019/5ms-dispatch-non-rules-procedures/guide-to-scheduled

-loads---marked-up.pdf?la=en&hash=9505F2B2FE94CEDC4DF4EBCFA07688B8.

AEMO (2021*m*), 'Intervention Pricing Methodology'. URL: https://aemo.com.au/-/media/files/stakeholder_consultation/consultations/nem-consultations/2020/wholesale-demand-response/final-stage/intervention-pricing-methodology.pdf?la=en.

AEMO (2021*n*), 'ISP Methodology'. URL: https://www.aemo.com.au/-/media/files/major-publications/isp/2021/2021-isp-methodology.pdf?la=en.

AEMO (2021*o*), 'Market ancillary service specification'. URL: https://aemo.com.au/-/media/files/stakeholder_consultation/consultations/nem-consultations/2021/mass/second-stage/reformatted-mass---draft-determination.pdf?la=en.

AEMO (2021*p*), 'NEM SPD Outputs'. URL: https://aemo.com.au/energy-systems/electricity/national-electricity-market-nem/data-nem/market-data-nemweb.

AEMO (2021*q*), 'Pre-dispatch'. URL: https://www.aemo.com.au/-/media/files/electricity/nem/5ms/procedures-workstream/stakeholder-consultation/dispatch-procedures/so_op_3704---predispatch---marked-up.pdf.

AEMO (2021*r*), 'Pre-Dispatch Sensitivities'. URL: https://aemo.com.au/-/media/files/electricity/nem/security_and_reliability/dispatch/policy_and_process/pre-dispatch-sensitivities.pdf.

AEMO (2021*s*), 'Spot Market Operations Timetable'. URL: https://www.aemo.com.au/-/media/Files/Electricity/NEM/Security_and_Reliability/Dispatch/Spot-Market-Operations-Timetable.pdf.

AEMO (2022*a*), 'Australian Wind Energy Forecasting System (AWEFS) and Australian Solar Energy Forecasting System (ASEFS)'. URL: https://www.aemo.com.au/-/medi

a/files/electricity/nem/security_and_reliability/dispatch/policy_and_process/2016/australian-wind-energy-forecasting-system-awefs.pdf.

AEMO (2022*b*), 'Fact Sheet: Visibility of the Power System'. URL: https://aemo.com.au/Electricity/National-Electricity-Market-NEM/Security-and-reliability/-/media/0DE87F5ADD5D42F7B225D7D0799568A8.ashx, Accessed on 12 May 2022.

AEMO (2022*c*), 'Five-Minute Pre-dispatch Reports'. URL: https://nemweb.com.au/Reports/Current/P5_Reports/.

AEMO (2022*d*), 'Guide to Data Requirements for AWEFS and ASEFS'. URL: https://www.aemo.com.au/-/media/files/electricity/nem/security_and_reliability/dispatch/policy_and_process/guide-to-data-requirements-for-awefs-and-asefs.pdf.

AEMO (2022*e*), 'Marginal Loss Factors: Financial Year 2022-23'. URL: https://www.aemo.com.au/-/media/files/electricity/nem/security_and_reliability/loss_factors_and_regional_boundaries/2022-23/marginal-loss-factors-for-the-2022-23-financial-year.pdf?la=en.

AEMO (2022*f*), 'NEM Registration and Exemption list'. URL: https://www.aemo.com.au/-/media/Files/Electricity/NEM/Participant_Information/NEM-Registration-and-Exemption-List.xls, Accessed on 12 June 2022.

AEMO (2022*g*), 'NEM SPD Outputs'. URL: https://aemo.com.au/energy-systems/electricity/national-electricity-market-nem/data-nem/market-data-nemweb.

AEMO (2022*h*), 'NEMWeb'. URL: https://www.aemo.com.au/energy-systems/electricity/national-electricity-market-nem/data-nem/market-data-nemweb, Accessed on 11 May 2022.

AEMO (2022*i*), 'Next Day Bids applied Dispatch report - COMPLETE'. URL: https://nemweb.com.au/Reports/Current/Bidmove_Complete/.

AEMO (2022*j*), 'Pre-Dispatch Reports'. URL: https://nemweb.com.au/Reports/Current/PredispatchIS_Reports/.

AEMO (2022*k*), 'Regions and Marginal Loss Factors: FY 2021-22'. URL: https://aemo.com.au/-/media/files/electricity/nem/security_and_reliability/loss_factors_and_regional_boundaries/2021-22/marginal-loss-factors-for-the-2021-22-financial-year.pdf?la=en.

AEMO (2023*a*), 'Data dashboard'. URL: https://aemo.com.au/en/energy-systems/electricity/national-electricity-market-nem/data-nem/data-dashboard-nem, Accessed on 20 January 2023.

AEMO (2023*b*), 'Guide to Ancillary Services in the NEM'. URL: https://aemo.com.au/-/media/files/electricity/nem/security_and_reliability/ancillary_services/guide-to-ancillary-services-in-the-national-electricity-market.pdf.

AEMO (2023*c*), 'NEM Operational Forecasting and Dispatch Handbook for wind and solar generators'. URL: https://www.aemo.com.au/-/media/files/electricity/nem/security_and_reliability/dispatch/policy_and_process/nem-operational-forecasting-and-dispatch-handbook-for-wind-and-solar-generators.pdf?la=en.

AEMO (2023*d*), 'Schedule of constraint violation penalty factors'. URL: https://www.aemo.com.au/-/media/files/electricity/nem/security_and_reliability/congestion-information/2016/schedule-of-constraint-violation-penalty-factors.pdf.

AEMO (2023*e*), 'WEM Procedure: Dispatch Algorithm Formulation'. URL: https://aemo.com.au/-/media/files/electricity/wem/procedures/2023/dispatch-algorithm-formulation---v10.pdf?la=en&hash=E9BFAD16FE36686E91F187C5A492C4AD.

AEMO (2023*f*), 'Wholesale Electricity Market (WEM)'. URL: https://aemo.com.au/

en/energy-systems/electricity/wholesale-electricity-market-wem, Accessed on 6 December 2023.

AER (2012), 'The impact of congestion on bidding and inter-regional trade in the NEM, Special Report, December 2012'. URL: https://www.aer.gov.au/system/files/Special%20Report%20-%20The%20impact%20of%20congestion%20on%20bidding%20and%20inter-regional%20trade%20in%20the%20NEM.docx.

AER (2017), 'Approach to electricity wholesale market performance monitoring, Discussion paper, August 2017'. URL: https://www.aer.gov.au/system/files/Discussion%20paper%20-%20Approach%20to%20electricity%20wholesale%20market%20performance%20monitoring.PDF.

AER (2021), 'State of the energy market 2021'. URL: https://www.aer.gov.au/system/files/State%20of%20the%20energy%20market%202021%20-%20Full%20report_1.pdf.

Ahlqvist, V., Holmberg, P. and Tangerås, T. (2018), 'Central-versus self-dispatch in electricity markets', *EPRG Working Paper 1902, University of Cambridge* .

Aid, R., Campi, L., Huu, A. N. and Touzi, N. (2009), 'A structural risk-neutral model of electricity prices', *International Journal of Theoretical and Applied Finance* **12**(07), 925–947.

Aid, R., Campi, L. and Langrené, N. (2013), 'A structural risk-neutral model for pricing and hedging power derivatives', *Mathematical Finance* **23**(3), 387–438.

Anderson, E. J. and Hu, X. (2008), 'Finding supply function equilibria with asymmetric firms', *Operations Research* **56**(3), 697–711.

ASX (2020), 'Energy derivatives - Electricity - Key features'. URL: https://www2.asx.com.au/markets/trade-our-derivatives-market/overview/energy-derivatives/electricity, Accessed on 14 October 2020.

Barlow, M. T. (2002), 'A diffusion model for electricity prices', *Mathematical Finance* **12**(4), 287–298.

Basslink Pty Ltd (2022), 'The Basslink Interconnector'. URL: http://www.basslink.com.au/basslink-interconnector/, Accessed on 1 October 2022.

Benth, F. E. and Ibrahim, N. 2017), 'Stochastic modeling of photovoltaic power generation and electricity prices', *Journal of Energy Markets* **10**(3), 1–33.

Beran, P., Pape, C. and Weber, C. (2019), 'Modelling German electricity wholesale spot prices with a parsimonious fundamental model – Validation & application', *Utilities Policy* **58**, 27–39.

Bidwell, M. and Henney, A. (2004), 'Will the new electricity trading arrangements ensure generation adequacy?', *The Electricity Journal* **17**(7), 15–38.

Biggar, D. R. and Hesamzadeh, M. R. (2014), *The economics of electricity markets*, Wiley Blackwell.

Biggar, D. R. and Hesamzadeh, M. R. (2022), 'Do we need to implement multi-interval real-time markets?', *The Energy Journal* **43**(2), 111–131.

Bjørndal, M. and Jörnsten, K. (2008), 'Equilibrium prices supported by dual price functions in markets with non-convexities', *European Journal of Operational Research* **190**(3), 768–789.

Broom, R. (2020), 'Corporate Power Purchase Agreements – The Preferred Route for Corporates to Secure Renewable Energy Supplies in a Decarbonized World', *The National Law Review* . URL: https://www.natlawreview.com/article/corporate-power-purchase-agreements-preferred-route-corporates-to-secure-renewable, Accessed on 14 October 2020.

Burger, M., Klar, B., Muller, A. and Schindlmayr, G. (2004), 'A spot market model for pricing derivatives in electricity markets', *Quantitative Finance* **4**(1), 109–122.

Buzoianu, M., Brockwell, A. and Seppi, D. (2012), 'A Dynamic Supply-Demand Model for Electricity Prices', *Carnegie Mellon University. Journal contribution* . https://doi.org/10.1184/R1/6586331.v1.

Byers, C. and Hug, G. (2023), 'Long-run optimal pricing in electricity markets with non-convex costs', *European Journal of Operational Research* **307**(1), 351–363.

Cardell, J. B., Hitt, C. C. and Hogan, W. W. (1997), 'Market power and strategic interaction in electricity networks', *Resource and Energy Economics* **19**(1-2), 109–137.

Carmona, R. and Coulon, M. (2014), A survey of commodity markets and structural models for electricity prices, *in* 'Quantitative Energy Finance', Springer.

Carmona, R., Coulon, M. and Schwarz, D. (2013), 'Electricity price modeling and asset valuation: a multi-fuel structural approach', *Mathematics and Financial Economics* **7**(2), 167–202.

Cartea, A. and Figueroa, M. G. (2005), 'Pricing in electricity markets: a mean reverting jump diffusion model with seasonality', *Applied Mathematical Finance* **12**(4), 313–335.

Cartea, Á. and Villaplana, P. (2008), 'Spot price modeling and the valuation of electricity forward contracts: The role of demand and capacity', *Journal of Banking & Finance* **32**(12), 2502–2519.

Chao, H.-p. (2019), 'Incentives for efficient pricing mechanism in markets with non-convexities', *Journal of Regulatory Economics* **56**(1), 33–58.

Cheng, L.-M., Bao, Y.-Q. and Chen, C. (2021), 'An improved optimisation method based on augmented constraint for electricity market clearing considering non-increasing stepwise bidding', *IET Energy Systems Integration* **3**(2), 202–212.

Clewlow, L. and Strickland, C. (2000), *Energy derivatives: pricing and risk management*, Lacima Publications.

Coulon, M., Powell, W. B. and Sircar, R. (2013), 'A model for hedging load and price risk in the Texas electricity market', *Energy Economics* **40**, 976–988.

Cramton, P. (2017), 'Electricity market design', *Oxford Review of Economic Policy* **33**(4), 589–612.

Cramton, P., Ockenfels, A. and Stoft, S. (2013), 'Capacity market fundamentals', *Economics of Energy & Environmental Policy* **2**(2), 27–46.

Creative Energy Consulting, P. L. (2020), 'Scheduling and Ahead Markets'. URL: https://www.energycouncil.com.au/media/eginmtjb/20200630-cec-final-report.pdf.

Csereklyei, Z. and Kallies, A. (2022), 'A legal-economic framework of electricity markets: Assessing Australia's transition', *Munich Personal RePEc Archive* (114191). URL: https://mpra.ub.uni-muenchen.de/id/eprint/114191.

Csereklyei, Z., Qu, S. and Ancev, T. (2019), 'The effect of wind and solar power generation on wholesale electricity prices in Australia', *Energy Policy* **131**, 358–369.

Day, C. J., Hobbs, B. F. and Pang, J.-S. (2002), 'Oligopolistic competition in power networks: a conjectured supply function approach', *IEEE Transactions on power systems* **17**(3), 597–607.

De Vries, L. J. (2005), 'Securing the public interest in electricity generation markets: The myths of the invisible hand and the copper plate.'. URL: https://repository.tudelft.nl/islandora/object/uuid:126e09db-29cb-46d8-9302-98bb85793843.

Deng, S.-J. and Oren, S. S. (2006), 'Electricity derivatives and risk management', *Energy* **31**(6-7), 940–953.

Department of Industry, Science, Energy and Resources (2021), 'Australian Energy Statistics, Table O'. URL: https://www.energy.gov.au/publications/australian-energy-update-2021, Accessed on 2 October 2022.

Department of Industry, Science, Energy and Resources (2022), 'Australian Energy Statistics, Table O'. URL: https://www.energy.gov.au/publications/australian-energy-update-2022, Accessed on 2 October 2022.

Deschatre, T. and Veraart, A. E. (2017), A joint model for electricity spot prices and wind penetration with dependence in the extremes, *in* 'Forecasting and Risk Management for Renewable Energy', Springer.

Ela, E. and O'Malley, M. (2015), 'Scheduling and pricing for expected ramp capability in real-time power markets', *IEEE Transactions on Power Systems* **31**(3), 1681–1691.

Eldridge, B., O'Neill, R. and Hobbs, B. F. (2019), 'Near-optimal scheduling in day-ahead markets: pricing models and payment redistribution bounds', *IEEE transactions on power systems* **35**(3), 1684–1694.

ElectraNet (2021), 'ElectraNet confirms Project EnergyConnect will be built'. URL: https://www.electranet.com.au/electranet-confirms-project-energyconnect-will-be-built/, Accessed on 7 November 2021.

Elexon (2019), 'The Electricity Trading Arrangements A Beginner's Guide'. URL: https://bscdocs.elexon.co.uk/guidance-notes/the-electricity-trading-arrangements-a-beginners-guide, Accessed on 15 June 2023.

Elexon (2020), 'Imbalance Pricing Guidance'. URL: https://bscdocs.elexon.co.uk/guidance-notes/imbalance-pricing-guidance, Accessed on 15 June 2023.

Elmaghraby, W., O'Neill, R., Rothkopf, M. and Stewart, W. (2004), 'Pricing and efficiency in "lumpy" energy markets', *The Electricity Journal* **17**(5), 54–64.

EPRI (2019), 'Independent System Operator and Regional Transmission Organization Price Formation Working Group White Paper'. URL: https://www.epri.com/research/products/3002013724.

ESB (2020), 'Post 2025 Market Design Consultation Paper'. URL: https://esb-post2025-market-design.aemc.gov.au/32572/1599208730-final-p2025-market-design-consultation-paper.pdf.

ESO (2023), 'Firm Frequency Response (FFR)'. URL: https://www.nationalgrideso.com/industry-information/balancing-services/frequency-response-services/firm-frequency-response-ffr#Technical-Requirements, Accessed on 16 June 2023.

Eydeland, A. and Wolyniec, K. (2003), *Energy and Power Risk Management: New Developments in Modeling, Pricing, and Hedging*, John Wiley & Sons.

FERC (2012), 'RTO unit commitment test system'. URL: https://citeseerx.ist.psu.edu/document?repid=rep1&type=pdf&doi=8c789c6502ccd701664e4b479ba362e713eaab24.

FERC (2019), 'Order on Paper Hearing (Docket No. EL18-34-000)'. URL: https://cms.ferc.gov/sites/default/files/whats-new/comm-meet/2019/041819/E-3.pdf.

Finon, D. and Pignon, V. (2008), 'Electricity and long-term capacity adequacy: The quest for regulatory mechanism compatible with electricity market', *Utilities Policy* **16**(3), 143–158.

Föllmer, H. and Schweizer, M. (1993), 'A microeconomic approach to diffusion models for stock prices', *Mathematical Finance* **3**(1), 1–23.

Fraga, E. S., Yang, L. and Papageorgiou, L. G. (2012), 'On the modelling of valve point loadings for power electricity dispatch', *Applied Energy* **91**(1), 301–303.

Gianfreda, A. and Bunn, D. (2018), 'A stochastic latent moment model for electricity price formation', *Operations Research* **66**(5), 1189–1203.

Gorman, N. (2023), 'Introduction — nempy 0.0.1 documentation'. URL: https://nempy.readthedocs.io/en/latest/intro.html, Accessed on 4 December 2023.

Gorman, N., Bruce, A. and MacGill, I. (2022), 'Nempy: A Python package for modelling the Australian National Electricity Market dispatch procedure', *Journal of Open Source Software* **7**(70), 3596.

Green, R. J. and Newbery, D. M. (1992), 'Competition in the British electricity spot market', *Journal of Political Economy* **100**(5), 929–953.

Gribik, P. R., Hogan, W. W. and Pope, S. L. (2007), 'Market-clearing electricity prices and energy uplift', *Cambridge, MA* .

Gudkov, N. and Ignatieva, K. (2021), 'Electricity price modelling with stochastic volatility and jumps: An empirical investigation', *Energy Economics* **98**, 105260.

Hinz, J. (2004), 'A revenue-equivalence theorem for electricity auctions', *Journal of Applied Probability* **41**(2), 299–312.

Hirst, E. and Hadley, S. (1999), 'Generation adequacy: Who decides?', *The Electricity Journal* **12**(8), 11–21.

Hobbs, B. F. and Helman, U. (2003), Chapter 3 Complementarity-Based Equilibrium Modeling for Electric Power Markets. URL: https://api.semanticscholar.org/CorpusID:17025800.

Hobbs, B. F., Metzler, C. B. and Pang, J.-S. (2000), 'Strategic gaming analysis for electric power systems: An MPEC approach', *IEEE Transactions on Power Systems* **15**(2), 638–645.

Hogan, W. W. (1999), 'Transmission congestion: the nodal-zonal debate revisited', *Harvard University, John F. Kennedy School of Government, Center for Business and Government* **29**(4).

Hogan, W. W. (2005), 'On an "energy only" electricity market design for resource adequacy'. URL: https://www.lmpmarketdesign.com/papers/Hogan_Energy_Only_092305.pdf.

Hogan, W. W. (2012), 'Multiple market-clearing prices, electricity market design and price manipulation', *The Electricity Journal* **25**(4), 18–32.

Hogan, W. W. (2014), 'Electricity Market Design and Efficient Pricing: Applications for New England and Beyond', *The Electricity Journal* **27**(7), 23–49.

Hogan, W. W. and Ring, B. J. (2003), 'On minimum-uplift pricing for electricity markets', *Electricity Policy Group* . URL: https://lmpmarketdesign.com/papers/Hogan_Ring_minuplift_031903.pdf.

Holmberg, P. (2009), 'Numerical calculation of an asymmetric supply function equilibrium with capacity constraints', *European Journal of Operational Research* **199**(1), 285–295.

Holmberg, P., Newbery, D. and Ralph, D. (2013), 'Supply function equilibria: Step functions and continuous representations', *Journal of Economic Theory* **148**(4), 1509–1551.

Holmberg, P. and Ritz, R. A. (2020), 'Optimal capacity mechanisms for competitive electricity markets', *The Energy Journal* **41**, 33–66.

Howison, S. and Coulon, M. (2009), 'Stochastic behaviour of the electricity bid stack: from fundamental drivers to power prices', *The Journal of Energy Markets* **2**, 29–69.

Hua, B., Schiro, D. A., Zheng, T., Baldick, R. and Litvinov, E. (2019), 'Pricing in multi-interval real-time markets', *IEEE Transactions on Power Systems* **34**(4), 2696–2705.

Hui, H., Yu, C.-N. and Moorty, S. (2009), Reliability unit commitment in the new ERCOT nodal electricity market, *in* '2009 IEEE Power & Energy Society General Meeting', IEEE.

Hung-po, C. (2019), 'Incentives for Efficient Price Formation in Markets with Non-Convexities'. URL: https://www.pjm.com/-/media/library/reports-notices/special-reports/2019/20190621-incentives-for-efficient-price-formation-in-markets-with-non-convexities.ashx.

Hytowitz, R. B., Frew, B., Stephen, G., Ela, E., Singhal, N., Bloom, A. and Lau, J. (2020), Impacts of price formation efforts considering high renewable penetration levels and system resource adequacy targets, Technical report, National Renewable Energy Laboratory (NREL).

Joskow, P. L. (2008), 'Capacity payments in imperfect electricity markets: Need and design', *Utilities Policy* **16**(3), 159–170.

Kanamura, T. and Ōhashi, K. (2007), 'A structural model for electricity prices with spikes: Measurement of spike risk and optimal policies for hydropower plant operation', *Energy Economics* **29**(5), 1010–1032.

Katona, K., Nikitopoulos, C. S. and Schlögl, E. (2023*a*), 'A Hyperbolic Bid Stack Approach to Electricity Price Modelling', *Risks* **11**(8), 147.

Katona, K., Nikitopoulos, C. S. and Schlögl, E. (2023*b*), 'A Price Mechanism Survey of the Australian National Electricity Market', *Available at SSRN: https://ssrn.com/abstract=4428450*.

Kiesel, R. and Kusterman, M. (2016), 'Structural models for coupled electricity markets', *Journal of Commodity Markets* **3**(1), 16–38.

Klemperer, P. D. and Meyer, M. A. (1989), 'Supply function equilibria in oligopoly under uncertainty', *Econometrica: Journal of the Econometric Society* **57**(6).

Krishna, V. (2009), *Auction theory*, Academic press.

Kulakov, S. (2020), 'X-model: Further Development and Possible Modifications', *Forecasting* **2**(1), 20–35.

Leslie, G., Campbell, A. and Gawler, R. (2019), 'COGATI Access and Charging, Consultation Paper Response'. URL: https://www.aemc.gov.au/sites/default/files/2019-05/Monash%20University.PDF.

Liberopoulos, G. and Andrianesis, P. (2016), 'Critical review of pricing schemes in markets with non-convex costs', *Operations Research* **64**(1), 17–31.

Littlechild, S. C. (1992), Spot Pricing of Electricity: An Appraisal of the MIT Model, *in* 'Systems and Management Science by Extremal Methods: Research Honoring Abraham Charnes at Age 70', Springer.

Liu, J., Wang, J. and Cardinal, J. (2022), 'Evolution and reform of UK electricity market', *Renewable and Sustainable Energy Reviews* **161**, 112317.

Lucia, J. J. and Schwartz, E. S. (2002), 'Electricity Prices and Power Derivatives: Evidence from the Nordic Power Exchange', *Review of Derivatives Research* **5**(1), 5–50.

Maciejowska, K. (2020), 'Assessing the impact of renewable energy sources on the electricity price level and variability – A quantile regression approach', *Energy Economics* **85**, 104532.

Mackenzie, H., Thorncraft, S., Vickers, P. and Wallace, S. (2020), 'A preliminary indication of the Information Technology costs of Locational Marginal Pricing'. URL: https://www.aemc.gov.au/sites/default/files/2020-09/IT%20costs%20of%20implementing%20NEM%20locational%20_ng%20-%20Hard%20Software%20-%20Information%20Technology%20costs%20of%20nodal%20pricing%20-%202020_09_07.PDF.

Macquarie, G. (2013), 'Management of Negative Inter-Regional Settlement Residues'. URL: https://www.aemc.gov.au/sites/default/files/content/992d03d4-a6c1-4aaa-869a-3049f117fb4d/Macquarie-Generation.PDF.

Mahler, V., Girard, R., Billeau, S. and Kariniotakis, G. (2019), Simulation of day-ahead electricity market prices using a statistically calibrated structural model, *in* '2019 16th International Conference on the European Energy Market (EEM)', IEEE.

Mayer, K. and Trück, S. (2018), 'Electricity markets around the world', *Journal of Commodity Markets* **9**, 77–100.

Meyer-Brandis, T. and Tankov, P. (2008), 'Multi-factor jump-diffusion models of electricity prices', *International Journal of Theoretical and Applied Finance* **11**(05), 503–528.

Moazeni, S., Coulon, M., Rueda, I. A., Song, B. and Powell, W. B. (2016), 'A non-parametric structural hybrid modeling approach for electricity prices', *Quantitative Finance* **16**(2), 213–230.

Monitoring Analytics (2023), 'State of the Market Report for PJM: 2022 (Vol. 2)'. URL: https://www.monitoringanalytics.com/reports/PJM_State_of_the_Market/2022.shtml.

Mountain, B. R. and Percy, S. (2020), 'Inertia and System Strength in the National Energy Market: A report prepared for The Australia Institute'. URL: https://australiainstitute.org.au/wp-content/uploads/2021/03/VEPC-system-security-report-FINAL.pdf.

Munoz, F. D., Wogrin, S., Oren, S. S. and Hobbs, B. F. (2018), 'Economic inefficiencies of cost-based electricity market designs', *The Energy Journal* **39**(3), 51–68.

Mwampashi, M. M., Nikitopoulos, C. S., Konstandatos, O. and Rai, A. (2021), 'Wind generation and the dynamics of electricity prices in Australia', *Energy Economics* **103**, 105547.

Mwampashi, M. M., Nikitopoulos, C. S., Rai, A. and Konstandatos, O. (2022), 'Large-scale and rooftop solar generation in the NEM: A tale of two renewables strategies', *Energy Economics* **115**, 106372.

Nelson, T., Gilmore, J. and Nolan, T. (2023), 'Be Wary of Paying Wounded Bulls – Capacity Markets in Australia's National Electricity Market', *Economic Papers* **42**(1), 72–91.

Nemo Link, L. (2022), 'Nemo Link's Loss Factor, Rounding and Netting'. URL: https://www.nemolink.co.uk/wp-content/uploads/2022/09/Nemo-Link-Losses-Rounding-and-Netting_effective-from-21-Sep-22.pdf.

NEOPoint (2021), 'NEM Plant Bids in Actual Price Ranges'. URL: http://neopoint.com.au/.

NEOPoint (2022), 'Region Generation and Load Summary 5min ALL'. URL: http://neopoint.com.au/.

NERA (2013), 'Review of Financial Transmission Rights and Comparison with the Proposed OFA Model'. URL: https://www.aemc.gov.au/sites/default/files/content/ba583ab5-fea3-468b-bc0e-8ebfdec2c668/NERA-Review-of-Financial-Transmission-Rights-and-Comparison-with-the-Proposed-OFA-Model-in-Australia.PDF.

NERA (2020), 'Simplified Model of Locational Marginal Pricing - User Guide'. URL: https://www.aemc.gov.au/sites/default/files/2020-09/200911%20Simplified%20Model%20User%20Guide.pdf.

Newbery, D. (2016), 'Missing money and missing markets: Reliability, capacity auctions and interconnectors', *Energy Policy* **94**, 401–410.

Newbery, D., Pollitt, M., Ritz, R. and Strielkowski, W. (2018), 'Market design for a high-renewables European electricity system', *Renewable and Sustainable Energy Reviews* **91**, 695–707.

Ocker, F., Ehrhart, K.-M. and Belica, M. (2018), 'Harmonization of the European balancing power auction: A game-theoretical and empirical investigation', *Energy Economics* **73**, 194–211.

Ocker, F., Ehrhart, K.-M. and Ott, M. (2018), 'Bidding strategies in Austrian and German balancing power auctions', *Wiley Interdisciplinary Reviews: Energy and Environment* **7**(6).

O'Neil, A. (2019), 'Price Setting Concepts – an Explainer'. URL: https://wattclarit

y.com.au/articles/2019/03/price-setting-concepts-an-explainer/, Accessed on 14 December 2023.

O'Neill, R. P., Sotkiewicz, P. M., Hobbs, B. F., Rothkopf, M. H. and Stewart Jr, W. R. (2005), 'Efficient market-clearing prices in markets with nonconvexities', *European Journal of Operational Research* **164**(1), 269–285.

Ott, A. L. (2003), 'Experience with PJM market operation, system design, and implementation', *IEEE Transactions on Power Systems* **18**(2), 528–534.

Pachkova, E. V. (2004), 'Duality in MIP. Generating Dual Price Functions Using Branch-and-Cut', *Linköping Electronic Conference Proceedings* **14**(5). URL: https://ep.liu.se/ecp/014/005/ecp014005.pdf.

Paraschiv, F., Erni, D. and Pietsch, R. (2014), 'The impact of renewable energies on EEX day-ahead electricity prices', *Energy Policy* **73**, 196–210.

Parkin, M. and Bade, R. (2016), *Microeconomics*, Pearson Australia.

Pinhão, M., Fonseca, M. and Covas, R. (2022), 'Electricity spot price forecast by modelling supply and demand curve', *Mathematics* **10**(12).

PJM (2017), 'Proposed Enhancements to Energy Price Formation'. URL: https://www.pjm.com/-/media/library/reports-notices/special-reports/20171115-proposed-enhancements-to-energy-price-formation.ashx#:~:text=Enhancements%20to%20energy%20price%20formation%20will%20improve%20market%20price%20signals,incremental%20costs%20to%20serve%20load.

PJM (2018), 'Single Period Integer Relaxation Examples'. URL: https://pjm.com/-/media/committees-groups/task-forces/epfstf/20180305/20180305-item-10-single-period-integer-relaxation-examples.ashx.

PJM (2021), 'No-Load and Incremental Energy Offer Numerical Examples'. URL: https://www.pjm.com/-/media/committees-groups/subcommittees/cds/20

21/20210316/20210316-item-05-no-load-and-incremental-energy-offer-numerical-examples.ashx.

PJM (2022*a*), 'Energy and Ancillary Service Co-Optimization Formulation'. URL: https://www.pjm.com/-/media/markets-ops/energy/real-time/real-time-energy-and-ancillary-service-co-optimization-formulation.ashx.

PJM (2022*b*), 'LMP Model Information - Pricing Nodes in AEP Zone'. URL: https://www.pjm.com/markets-and-operations/energy/lmp-model-info.

PJM (2023), 'PJM Manual 11: Energy & Ancillary Services Market Operations'. URL: https://www.pjm.com/directory/manuals/m11/index.html.

Pollitt, M. G. and Anaya, K. L. (2016), 'Can current electricity markets cope with high shares of renewables? A comparison of approaches in Germany, the UK and the State of New York', *The Energy Journal* **37**, 69–88.

Rassi, S. and Kanamura, T. (2023), 'Electricity price spike formation and LNG prices effect under gross bidding scheme in JEPX', *Energy Policy* **177**, 113552.

Roques, F. A. (2008), 'Market design for generation adequacy: Healing causes rather than symptoms', *Utilities Policy* **16**(3), 171–183.

Ruddell, K. (2017), Supply function equilibrium in electricity markets, PhD thesis, ResearchSpace@ Auckland.

Ruiz, C., Conejo, A. J., Fuller, J. D., Gabriel, S. A. and Hobbs, B. F. (2014), 'A tutorial review of complementarity models for decision-making in energy markets', *EURO Journal on Decision Processes* **2**(1), 91–120.

Ruiz, C., Conejo, A. J. and Gabriel, S. A. (2012), 'Pricing non-convexities in an electricity pool', *IEEE Transactions on Power Systems* **27**(3), 1334–1342.

Scarf, H. E. (1994), 'The allocation of resources in the presence of indivisibilities', *Journal of Economic Perspectives* **8**(4), 111–128.

Schweppe, F., Tabors, R., Caraminis, M. and Bohn, R. (1988), *Spot pricing of electricity*, Kluwer Academic Publishers, Norwell, MA.

Simshauser, P. (2008), 'The dynamic efficiency gains from introducing capacity payments in the National Electricity Market', *Australian Economic Review* **41**(4), 349–370.

Simshauser, P. (2018), 'On intermittent renewable generation & the stability of Australia's National Electricity Market', *Energy Economics* **72**, 1–19.

Simshauser, P. (2019*a*), 'Missing money, missing policy and resource adequacy in Australia's National Electricity Market', *Utilities Policy* **60**, 100936.

Simshauser, P. (2019*b*), 'On the stability of energy-only markets with government-initiated contracts-for-differences', *Energies* **12**(13), 2566.

Simshauser, P. (2021*a*), Lessons from Australia's National Electricity Market 1998-2018: strengths and weaknesses of the reform experience, *in* 'Handbook on Electricity Markets', Edward Elgar Publishing.

Simshauser, P. (2021*b*), 'Renewable energy zones in Australia's National Electricity Market', *Energy Economics* **101**, 105446.

Simshauser, P. and Gilmore, J. (2020), 'Is the NEM broken? Policy discontinuity and the 2017-2020 investment megacycle', *EPRG Working Paper 2014, University of Cambridge* .

Stoft, S. (2002), *Power system economics: designing markets for electricity*, Vol. 468, IEEE press Piscataway.

Tómasson, E., Hesamzadeh, M. R., Söder, L. and Biggar, D. R. (2020), 'An incentive mechanism for generation capacity investment in a price-capped wholesale power market', *Electric Power Systems Research* **189**, 106708.

Tongxin, Z., Feng, Z., Dane, S. and Eugene, L. (2018), 'The Hidden Properties of Fast Start Pricing'. URL: https://www.ferc.gov/sites/default/files/2020-08/T1-3_Zheng.pdf.

Wang, Y., Yang, Z., Yu, J. and Liu, S. (2023), 'Pricing in non-convex electricity markets with flexible trade-off of pricing properties', *Energy* **274**, 127382.

Ward, K., Green, R. and Staffell, I. (2019), 'Getting prices right in structural electricity market models', *Energy Policy* **129**, 1190–1206.

Ware, T. (2019), 'Polynomial Processes for Power Prices', *Applied Mathematical Finance* **26**(5), 453–474.

Wilson, R. (2008), 'Supply function equilibrium in a constrained transmission system', *Operations Research* **56**(2), 369–382.

Wolak, F. A. (2019), 'The role of efficient pricing in enabling a low-carbon electricity sector', *Economics of Energy & Environmental Policy* **8**(2), 29–52.

Wood, A. J., Wollenberg, B. F. and Sheblé, G. B. (2013), *Power generation, operation, and control*, John Wiley & Sons.

Yang, L., Fraga, E. S. and Papageorgiou, L. G. (2013), 'Mathematical programming formulations for non-smooth and non-convex electricity dispatch problems', *Electric Power Systems Research* **95**, 302–308.

Yang, Y., Qin, C., Zeng, Y. and Wang, C. (2019), 'Interval optimization-based unit commitment for deep peak regulation of thermal units', *Energies* **12**(5), 922.

Yarrow, G. (2014), 'Bidding in energy-only wholesale electricity markets'. URL: https://www.aemc.gov.au/sites/default/files/content/c196404a-e850-46bd-8ae2-41600f8454bb/Professor-George-Yarrow-and-Dr-Chris-Decker-%28RPI%29-Bidding-in-energy-only-wholesale-electricity-markets-Final-report.PDF.

Ziel, F. and Steinert, R. (2016), 'Electricity price forecasting using sale and purchase curves: The X-Model', *Energy Economics* **59**, 435–454.